STUDIES ON SOME METAL COMPLEXES AND SOME HOMOGENEOUSLY CATALYSED REACTIONS

COMPUTERISED

A THESIS

SUBMITTED TO THE

UNIVERSITY OF POONA

FOR THE DEGREE OF

DOCTOR OF PHILOSOPHY

IN CHEMISTRY

NATIONAL CHEMICAL LABORATORY
TH-346
Date...
LIBRARY

BY

SURESH R. PATIL
M. Sc.

546·3:541·49:541·128(043)
PAT

NATIONAL CHEMICAL LABORATORY
POONA-411 008 (INDIA)

1981

CONTENTS

PART-I

		Page
CHAPTER -I -	General Introduction	1-30
CHAPTER -II -	Experimental	31-41
CHAPTER -III -	Mass spectral studies on some ferrcepylidene derivatives of α-N-acyl hydrazines - Results and discussion	42-56
CHAPTER -IV -	Infrared spectral studies : Results and discussion	57-107
CHAPTER-V -	^{1}H NMR studies on tin(IV) complexes of ferrocenyildene derivatives of α-N-acyl hydrazines: Results and discussion	108-125
REFERENCES		126-134

PART - II

CHAPTER - I -	General Introduction	135-156
CHAPTER - II -	Experimantal	157-161
CHAPTER -III -	Hydrogenation of cyclohexene : Results and discussion	162-197
CHAPTER - IV-	Hydrogenation of allylic compounds: Resultsanddiscussion	198-215
REFERENCES		216-219
ACKNOWLEDGEMENT		220

****

PART - I

CHAPTER -1 GENERAL INTRODUCTION

		Page
1.1	Introduction	1
1.2	Literature background	4
1.2.1	Complexes of ferrocene containing ligands	4
1.2.2	Mass-spectra of ferrocenyl compounds	5
1.2.3	Infrared spectral studies	15
1.2.4	^{1}H n.m.r. spectral studies	24
1.2.5	Scope and objective of the present work	29

1.1 Introduction

Ligands which selectively remove excess of some metals from human body without affecting other biometals offer a challenging area of research for bioinorganic chemists[1]. Equally important is the addition of metals to the human body, since as well as excesses, deficiencies of essential metals are known, iron being the most common case. Here the problem is the addition of metals in suitable form with minimum increase in toxicity in order to assist the defence mechanism. One of the major areas of research of bioinorganic chemist is to study, in vitro, chemical criteria which can be used as indicators of biological activity with the eventual aim of designing metal chelates as suitable sources of various trace elements in animal nutrition. In living systems the absorption, secretion and retention of iron are largely controlled by the intestinal mucosa. A specific iron protein, transferrin, exists in the blood serum and serves as a carrier for iron. Another protein, ferritin, functions both in iron absorption from the intestine and in iron storage in the liver, kidney and spleen[2]. The normal iron content of men and women is 50 and 35 mg/kg of body weight respectively giving an approximate total of 2-5 g of iron in the normal adult. When the level of iron falls below these levels, a state of iron deficiency is present. Search for iron complexes which

may help to carry iron through the metabolic channels and insert it into porphorins and other iron containing enzymes and proteins is, therefore, of considerable importance.

Ferrocene is ideal for drug design, because of its low toxicity, bioavailability and ease of substitution[3]. Edward et al.[4] and Rockett and Marr[5] have reported the use of ferrocene as the aromatic nucleus in the antibiotics such as pencillins and cephalosphorins. The introduction of ferrocene molecule in these compounds modifies their two dimensional profile and effects changes in the antibiotic activity and β-lactamic susceptibility. Thus the replacement of phenyl or heteroaromatic group by ferrocene moiety in which the metal atom is in close proximity to the β-lactam ring of the antibiotic leads to high antibiotic activity and these compounds act as β-lactamase inhibitors. On the other hand, N-acyl-hydrazines are known to possess tuberculostatic activity. Their mode of action has been attributed to the formation of stable chelates with transition metals present in the cell; such processes inhibit so many vital enzymatic reactions catalyzed by metal ions.

These results have prompted us to synthesize some ferrocene moiety containing hydrazones with the hope that the dual activity of beneficial components of such compounds may have synergestic drug effect. Although some ferrocene

derivatives have been used in recent years for metal complexation, metal complexes of ferrocenyl derivatives of N-acyl hydrazines have received little attention. Furthermore, it has been claimed that the activity of isonicotinyl hydrazide against M-tuberculosis in vitro as well as vivo is increased by the addition of copper(II)[6]. Therefore, several such heterometallic copper(II) chelates have been prepared in this laboratory. However, these compounds are insoluble except in exotic solvents like THF. Incidentally, THF as solvent has been used for intravenous injection of drugs, although one has to fight against complications that may result from the use of such solvents. However, such work is very much involved, requires expertise and is time-consuming and therefore, the scope of the present work has been restricted to the synthesis and characterization of such compounds only.

Certain organotin compounds, especially the R_2SnCl_2 type, are excellent stabilizers for polyvinyl chloride (PVC), neoprene and other polymers against degradation by light and oxygen and decomposition during hot fabrication. Organotin compounds are also suitable as stabilizers for chlorinated polyethylenes[7], vinyl copolymers[8], silicones[9] and polyamides[10]. On the other hand ferrocene and ferrocene derivatives have been used as stabilizers for

polyethylene against thermal and UV degradation[11]. It is also known that ferrocene and acetyl ferrocenes are used as stabilizers for low pressure polyethylene against degradation by heat, uv and γ-irradiation[12]. So it is worthwhile to synthesize some organotin ferrocenyl compounds which may have the dual properties of ferrocene and organotin compounds. Here again the work reported in this thesis has been restricted to the syntheses and characterization of such compounds only.

1.2 Literature background

Since there are large number of books and reviews on ferrocenyl compounds, no attempt is made here to review this area. However, in this section a short account on complexes of ferrocene-containing ligands and some literature background on mass spectra, IR and ^{1}H n.m.r. studies of some ferrocenyl compounds are included.

1.2.1 Complexes of ferrocene-containing ligands

There are a few reports in the literature on the metal complexes of ferrocene-containing ligands. Omote and coworkers[13] have prepared thiosemicarbazones of acetyl- and diacetyl-ferrocenes by reacting thiosemicarbazide with acetyl and diacetyl ferrocenes and prepared copper(II) complexes of these ligands (Fig.1). Casellato and

coworkers[14] have prepared acetylacetonate type of compounds containing ferrocenyl moiety i.e. 1- and 1,1'-di(1-phenyl-propane-1,3-dione)ferrocene (Fig. 2) and studied uranyl complexes (Fig. 3). Later, Imai and Ota[15] have synthesized several first row transition metal complexes of acetoacetyl-ferrocene. These authors have shown that manganese(II) complex of this ligand is tetrahedral (Fig. 4) while that of copper(II) complex is square-planar in structure (Fig.4). Copper(II) and iron(III) complexes of ferrocenyl acetone have been reported by Shevchic and coworkers[16].

1.2.2 Mass spectra of ferrocenyl compounds

The mass spectral study of organometallic and a large number of inorganic compounds has increased at an accelerating rate over the last two decades. The usefulness of mass-spectrometry in providing accurate molecular weights and formulae and otherwise unobtainable data about gas-phase properties of molecules and ions has come to be recognized by most inorganic and organometallic chemists. Several reviews have appeared in the literature on the mass spectra of organometallic compounds[17-21]. In this section, mass spectra of π-cyclopentadienyl metal compounds, particularly of ferrocenyl compounds are discussed briefly.

Friedman and coworkers[22] have reported the results of a mass spectral study of a new and interesting class of

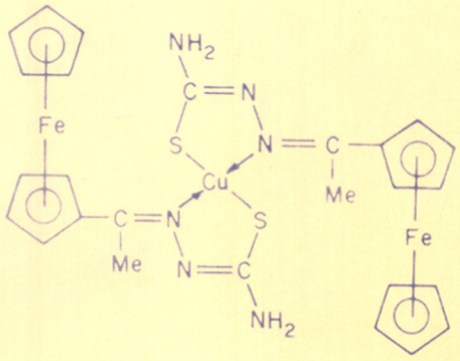

FIG. 1

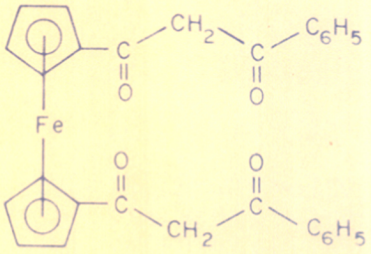

FIG. 2

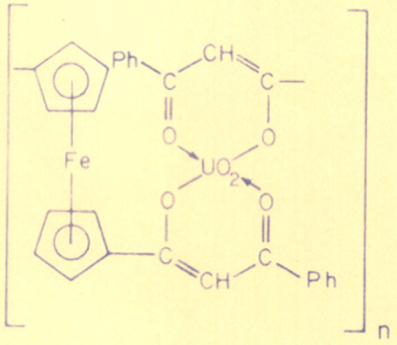

FIG. 3

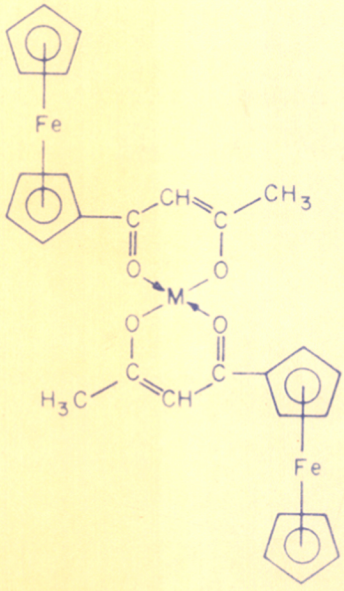

Where M = Mn or Cu

FIG. 4

compounds of formula $M(C_5H_5)_2$ (where M = Fe, Co, Ni, Ru, etc). This study has served to divide the compounds into two types in agreement with their other known physical and chemical properties. The "Sandwich" bonded compounds of V, Cr, Fe, Co, Ni and Ru give rise to spectra in which the parent molecular ions are the most abundant whereas the corresponding ions of Mg and Mn are relatively unstable and undergo a greater degree of fragmentation resulting in higher yields of $C_5H_5M^+$ and M^+. These results are correlated with a higher degree of ionic bonding in the metal to ring bonds of Mg and Mn compounds. The principal ions formed from all the compounds are $(C_5H_5)_n M^+$ (n = 0, 1 or 2) with very little further fragmentation of these ions. Similar fragmentation patterns have been obtained by Muller and D'Or[23] in a much more recent study. A stepwise loss of cyclopentadienyl rings from ferrocene (Scheme 1) has been established by Schumacher and Taubeynest[24] and Denning and Wentworth[25].

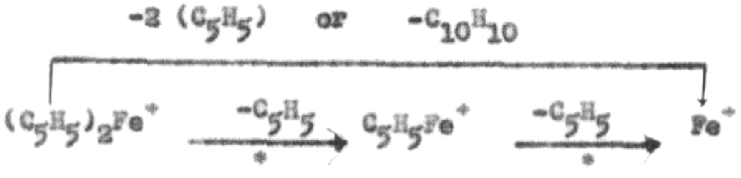

[Scheme 1]

The fragmentation pattern shown in the above scheme is supported by metastable peaks. A metastable transition corresponding to the decomposition process:

$$(C_5H_5)_2Fe \xrightarrow{*} Fe^+ + C_{10}H_{10}$$

which could be caused by the simultaneous expulsion of two discrete C_5H_5 units rather than a $C_{10}H_{10}$ neutral species has been reported by Schumacher and Taubenest[24]. While Mendelbaum and Cais[26] have observed a different process which is again suggested by metastable peaks in the mass spectra of a number of monosubstituted ferrocenes.

$$C_5H_5FeC_5H_4^+ \xrightarrow{*} C_5H_5C_5H_4^+ + Fe$$

The fragment ions corresponding to $C_{10}H_{10}$[27] and $C_{10}H_9$[26,27] have been observed in the spectrum of ferrocene. From these reports it appears that the elimination of iron and cyclopentadienyl rings from ferrocene and combination of cyclopentadienyl ring systems can take place via an unique process under the electron impact. Further fragmentation of a cyclopentadienyl ring has also been observed in the mass spectra of ferrocene[24,25] and nickelocene[24]. Presence of the fragment ions $FeC_3H_3^+$, $FeC_3H_2^+$ and FeC_2H^+ clearly

indicates the fragmentation of cyclopentadienyl ring. Schumacher and Taubenest[24] have shown that the fragmentation process for nickelocene (Scheme 2) is supported by metastable peaks.

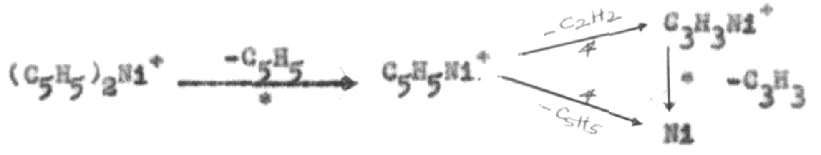

[Scheme 2]

A number of ions $(C_5H_5)_2Fe_2^+$, $(C_5H_5)_2Fe_2C_3H_3^+$, $C_5H_5Fe_2C_3H_3^+$ and $(C_5H_5)_3Fe^+$ have also been observed in low yields in the spectrum of ferrocene[24]. Friedman and coworkers[22] have calculated the metal-ring bond energies for several bis(cyclopentadienyl) metal compounds on the basis of appearance potential measurements. Metal-ring bond energy is weaker in $(C_5H_5)_2Mg$, $(C_5H_5)_2Mn$ and $(C_5H_5)_2Ni$ as compared with the corresponding compounds of Fe, Co, Cr and V.

The mass spectra of various mono-substituted ferrocenes $C_5H_5FeC_5H_4COR$, (where R = CH_3, C_6H_5, p-$CH_3OC_6H_4$, OH, OD, OCH_3 and $NHCH_3$) are reported[26] showing that these compounds follow a number of decomposition paths. One of particular interest (which is not observed when R = CH_3) involves rearrangement of the R group to form the ion

$C_5H_5FeR^+$, which in turn decomposes to FeR^+. The parent molecular ion for all these compounds except where R = OH is most intense in the spectrum. A similar rearrangement is found to occur in the series of ferrocene derivatives

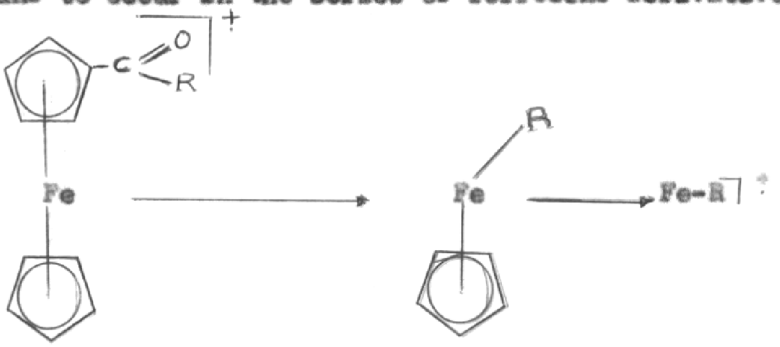

with an alkyl hydroxy side chain and in fact, the fragment

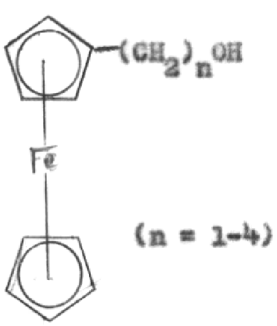

ion $C_5H_5FeOH^+$ is responsible for the base peak in the spectrum of hydroxy methyl ferrocene[28]. Later Cais and coworkers[29,30] have shown the cleavage of the side chain to form the ion $C_5H_5FeC_5H_4CH_2^+$, which rearranged to incorporate a π-benzene ring in a wide range of compounds.

The presence or absence of the ion $C_5H_5Fe^+$ (m/e 121) has been suggested[30] as a more sensitive criteria for distinguishing between homo- and hetero annularly disubstituted ferrocene than the 9-10 μ rule[31]. Imai[32] has studied the mass spectra of several disubstituted ferrocenes and showed that mass spectral technique can be used to distinguish between 1,1'- and 1,2 disubstituted ferrocenes. Fragment ions such as $C_5H_5FeC_5H_4^+$ (m/e 185) $C_5H_5Fe^+$ (m/e 121) are observed only in case of mono-substituted ferrocenes, whereas ions $C_5H_4FeC_5H_4^+$ (m/e 184) and $C_5H_4Fe^+$ (m/e 120) are observed in the spectra of disubstituted ferrocenes.

Seel and Superber[27] and King[33] have studied the mass spectrum of azaferrocene, $C_5H_5FeC_4H_4N$ and a different kind of fragmentation pathway has been suggested (Scheme 3).

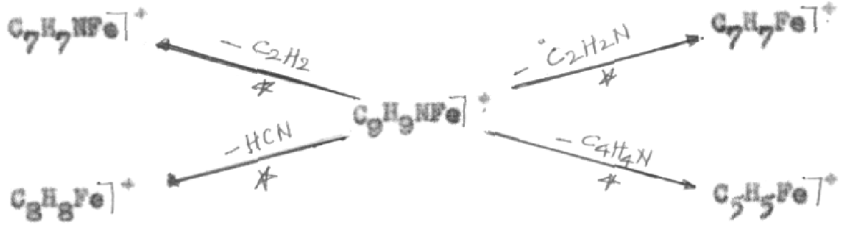

[Scheme 3]

The fragmentation pattern shown in Scheme 3 is supported by metastable peaks. The peak at m/e 131 has been assigned

to the ion $C_9H_9N^+$ by King[33] and to the ion $FeC_6H_3^+$ by Seel and Sperber[27]. The greater intensity of the ion $C_5H_5Fe^+$ than that of the ion $C_4H_4NFe^+$ shows that the ability of the C_4H_4N ring to act as a ligand is lower than that of the cyclopentadienyl ring.

Very recently Nesmeyanov and coworkers[34] have studied several ferrocenyl compounds analogoues to chalcones of the type FeCOCH=CHAr (where Fe = $C_5H_5FeC_5H_4$, Ar = C_6H_5, C_6H_4Br, $C_6H_4OCH_3$) with an objective to investigate the effect of the cyclopentadienyl group π-bonded to the transition metal atom on the chalcone fragmentation, as well as the effect of the ArCH=CHCO and ArCOCH=CH- substituents on the fragmentation of the organometallic moiety. These authors have shown that cleavage of the metal ligand bond under electron impact is the main process and a 'chalcone' mode of fragmentation is not significant in the spectra of ferrocenyl compounds. This observation suggests that the replacement of chalcone phenyl group by ferrocenyl may result in competition for the change between the aromatic and the metal containing fragments of the molecule. In molecular ions of π-complexes the positive charge is preferably localized on the transition metal atom. The intense fragment ions $C_5H_5^+$, $C_5H_5Fe^+$ and Fe^+ are also observed in the spectra of these compounds. In this study, the authors are unable to observe the ion $FeC_2H_2^+$, instead

of this, the rearrangement ions FeC_2H and $FeC_5H_5C_2H$ are observed. Such a change in properties of the aromatic system caused by introducing the organometallic group, can well be interpreted in terms of delocalization of the positive charge in the metal atom[35].

Contrary to the general pattern with a number of ferrocenyl compounds, the molecular ion is not the base peak in the mass spectra of the compounds of the type as shown in Figure 5 and 6. These are synthesized by condensation of ferrocene carboxyhydrazide with 5-nitro-2-furaldehyde, 5-nitro-2-acetyl furan and with ethyl 5-nitro-2-furimidate hydrochloride[36]. The fragmentation path for these compounds seems to be one typical of ferrocene giving rise to fragments such as $C_5H_5Fe^+$, $C_5H_5FeC_5H_4^+$, $C_5H_5.C_5H_5^+$, $C_5H_5.C_5H_4^+$, $C_5H_5^+$, Fe^+, $FeCH{=}CH^+$ and $FeCH = CHCO$. Several other type of ferrocenyl compounds have also been studied with respect to the mass spectra and reviewed in the literature[37-40].

The available literature survey shows that ferrocenyl compounds are sufficiently volatile to be introduced into the direct inlet probe of the mass spectrometry and do not thermally decompose. They can be characterized by mass-spectral fragmentation processes. Strong peaks are observed corresponding to the molecular ions of ferrocenyl

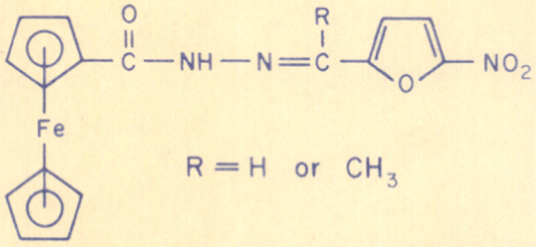

FIG. 5

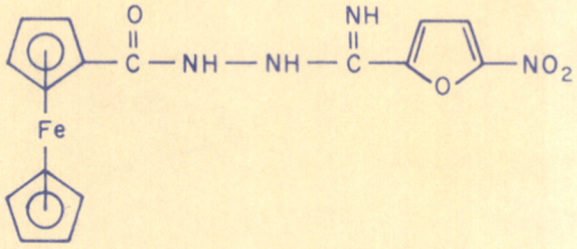

FIG. 6

compounds and the characteristic fragmentation process is the loss of organic ligands from the molecular ion which is supported by the metastable peaks.

1.2.3 Infrared spectral studies

Vibrational spectra originate in the vibrations of the nuclei in a molecule and are observed both as the infrared and the Raman spectra in the frequency region between approximately 10^4 cm^{-1} (1 μ) and 10 cm^{-1} (10^3 μ). The frequencies of the vibrational transitions are determined by the masses of constituent atoms, the molecular geometry (bond distances, bond angles, and angles of internal rotations) and the interatomic forces. The intensities of infrared and Raman spectra are related to the changes in the dipole moment and polarizability respectively, caused by molecular vibration.

For convenience, vibrational spectra of metal chelate compounds can be divided into the high frequency (4000-650 cm^{-1}) or NaCl region, and the low frequency (650-50 cm^{-1}) or far infrared region. In general, vibrations which occur in the high frequency region originate in the ligand itself, whereas those in the low frequency region originate in the metal-ligand coordinate bonds. High frequency vibrations are ligand-sensitive and have already been the subject of a large number of studies

On the other hand, low frequency vibrations are metal-sensitive and relatively less work has been done. The spectra in the low frequency region are more difficult to interpret on an empirical basis than are those in the high frequency region.

Since the basic aspects involved in infrared spectroscopy have been a subject of number of text books and reviews, these are not discussed here. However, the literature background of the infrared spectral studies on ferrocenyl compounds, ferrocenyl Schiff bases, copper-chelates containing Cu-N and Cu-O bonds and organotin(IV) chelates containing Sn-C, Sn-Cl, Sn-O and Sn-N bonds etc. relevant to the present work are presented.

Lippincott and Nelson[41] have studied the infrared spectrum of ferrocene in detail. The results are based on the infrared spectra in dissolved and gaseous states as well as on the Raman-spectrum. Furthermore, these assignments are also used as a basis for single crystal studies and for a comparison of the spectra of a series of cyclopentadienyls of different metals. From Lippincott's assignments one can interpret the nature of the strong bands. The two strong bands at 1408 and 1104 cm^{-1} are assigned to ν C-C as asymmetric and totally symmetric ring breathing modes. The band at 1104 cm^{-1} shows a

NATIONAL CHEMICAL LABORATORY
TH-376
Date.....
LIBRARY.

steady decrease in intensity as the bonding between metal and ring ligand becomes more and more ionic. Thus, in the salt-like alkali metal cyclopentadienyls, it disappears completely. However, this behaviour can be explained by assuming that the deviation from D_{5h} symmetry of the anion to C_{5v} of the covalently bonded ring becomes smaller and smaller when going, for example, from Osmocene, Cp_2Os to potassium cyclopentadiene. With D_{5h} symmetry, this normal vibration is infrared inactive and therefore vanishes.

Rosenblum[42] has made remarkable contribution in the infrared study of ferrocenyl compounds. He has studied the infrared spectra of a number of mono- and disubstituted ferrocenes and correlated them with their structures. This correlation is known as 9, 10 μ rule. Ferrocene derivatives possessing an unsubstituted ring exhibit infrared absorption near 9 and 10 μ, whereas those derivatives in which both the rings are either singly or multiply substituted do not possess such absorption. Rosenblum and Woodward[43] have observed that both mono-acetyl and 1,1'-diacetyl ferrocenes, as well as all the acetyl alkyl ferrocenes in which the acetylated ring is unencumbered by alkyl substituents exhibit two medium intensity bands near 8.97 μ and 11.17 μ. These absorptions are absent in all of those acetyl-alkyl ferrocenes in which an acetyl and an alkyl group are

546.3 : 541.49 : 541.128(043)
PAT

substituted on a single ferrocene ring. However, such substances exhibit medium to weak intensity absorption near 10.85 μ and within this spectral class, those derivatives in which the acetyl- and alkyl substituents occupy 1:3 position on the aromatic ring possess additional absorption near 11.05 μ.

Toma and Perjessy[44] have studied the infrared spectra of several mono- and disubstituted ferrocene derivatives and checked the validity of 9, 10 μ rule. According to these authors, if the acetyl group is one of the substituents in a 1,1'-disubstituted compound, a moderately intense absorption band appears in the 8.98 μ - 8.91 μ region. The presence of this band is a proof of the 1,1'-disubstitution in ferrocene. However, they have found that this band also appears in the case of disubstitution in the same cyclopentadienyl moiety of ferrocene. In such cases 9, 10 μ rule does not distinguish the 1,1'-, 1,2- or 1,3 disposition of a monoacetyl derivative.

Dzoryanstsera and coworkers[45] have studied the infrared spectra of ferrocene derivatives in carbon tetrachloride solutions and discussed the absorption bands of characteristic vibrations of cyclopentadienyl rings. In carbon tetrachloride all the ferrocene derivatives give a C-H band in the 3100 cm^{-1} region except for nitroferrocene.

In the crystalline state this band splits into two or three components in the 3070-3130 cm^{-1} region. Nesmeyanov and coworkers[46] have also studied the infrared spectra of thirtytwo different ferrocene derivatives in order to determine the position of substituents in the ferrocene. Very meagre work has been reported on other ferrocenyl compounds.

Metal-ligand stretching modes such as metal-oxygen, metal-nitrogen, metal-carbon and metal-halogen appear in the far infrared region. These modes are more sensitive to the nature of the metal atom than the ligand and strictly speaking, can be assigned only by carrying out a normal coordinate analysis of the whole chelate ring. Since our study deals mainly with ν (Cu-N), ν (Cu-O), ν(Sn-O), ν(Sn-C), ν(Sn-N) and ν(Sn-Cl) frequencies, the following discussion is restricted to these stretching frequencies only.

Metal-carbon frequencies are found in the range 772-420 cm^{-1} for metal-alkyl and metal-alkenyl bonds. It is known that metal-olefin and metal-allyl stretching frequencies are lower than metal-alkyl frequencies of the same metal and in the same oxidation state and the symmetric stretch may be about 100 cm^{-1} lower. The majority of metal-alkyl compounds for which ν(M-C) data are

available contain the metal atom in four-coordination in a stable oxidation state. Very little is, however, known concerning the effect of change of coordination number, stereochemistry or oxidation state on ν(M-C). However, ν(M-C) stretching mode is sensitive to the changes in ligand. Thus formation of $MeSnCl_3.py_2$ from $MeSnCl_3$ lowers ν(Sn-C) by 34 cm^{-1} but, on the other hand, ν_{as}(C-Sn-C) as in such adducts as Me_2SnCl_2.bipy differs little from that of Me_2SnCl_2[47].

The tin-carbon stretching frequency is dependent on the organic group attached to the tin. The di- and trialkyltin compounds generally show two bands: νas (Sn-C) in the range 600-500 cm^{-1} and νs (Sn-C) in the range 530-470 cm^{-1}. The intensity of these bands vary considerably. Mono-alkyltin compounds are expected to show a single (Sn-C) stretching band. The spectra of longer alkyl chain are more complex. The presence of electronegative halogen atoms gives higher ν(Sn-C) frequencies in methyltin halide due to the greater effective nuclear charge on tin[48]. The position of ν(Sn-C) bands are not particularly sensitive to changes in coordination number. However, the number of bands observed may be affected. Both ν_{as}(Sn-C) and ν_s(Sn-C) bands are observed for tetrahedral $Me_3SnCOOH$ molecule in chloroform

solution, but the ν_s(Sn-C) band slowly disappears by the addition of pyridine. This is because the trimethyltin group assumes planar configuration in 1:1 complex of pyridine. Other tin-carbon skeletal modes include C-Sn-C bending which occur[49] below 250 cm^{-1}.

Metal-oxygen frequencies occur between 1090-250 cm^{-1}. The highest frequencies are clearly associated with double bonds and those below about 600 cm^{-1} with single bonds. Tin-oxygen stretching vibrations occur over a wide range of frequencies depending upon the precise environment of Sn-O group in the molecule. Partial explanations have been advanced in terms of dπ-pπ bonding between oxygen and tin[50], variation in the bond angle at oxygen[51] and the differences in the ionic character of Sn-O bond[52]. Copper-oxygen stretching frequencies appear in a range of 460-250 cm^{-1}. In the i.r. spectra of bis(acetylacetonato)-copper(II) complexes, bands at 455 cm^{-1} and 320 cm^{-1} are assigned for (Cu-O) symmetric and (Cu-O) asymmetric stretching modes[53].

The metal-nitrogen frequency is of particular interest, since it provides direct information about the coordinate bond. Because of the relatively heavy mass of the metal and the low bond order of the coordinate bond, the M-N stretching vibration may appear in the lower frequency region.

Tin-nitrogen frequencies occur over a wide range and are sensitive to changes in environment. Absorption bands of much lower frequency have been assigned to the stretching vibrations of N-Sn coordination bands in compounds in which the nitrogen atom is incorporated into organic ring[54]. Copper-nitrogen stretching frequencies appear[55] in the range 500-400 cm^{-1}.

Much more is known about metal-chlorine frequencies than those associated with the other halogens. A wide range is associated with each metal-halogen stretching frequency. The overall ranges of the tin-halogen stretching frequencies are (Sn-Cl) 385-318 cm^{-1}; (Sn-Br) 264-222 cm^{-1} and (Sn-I) 207-170 cm^{-1}. The tin-halogen frequencies are highly sensitive to changes in coordination number of the tin atom and also vary with the physical state of the compound[56]. The conversion of a four coordinate diorganotindichloride to a six coordinate adduct with Lewis bases causes a reduction in frequency of ν(Sn-Cl) bands by ~ 100 cm^{-1} with respect to the free dichloride[57]. Similar reductions are also observed for six coordinate complexes of other dihalides. The effect is less marked in iodides. The ν(Sn-Cl) absorption band in Me_3SnCl complexes is shifted to below 250 cm^{-1} and in $MeSnCl_3$ complex the corresponding frequencies[58] are found at about 320 cm^{-1} and 280 cm^{-1}.

The structure and bonding of organotin carboxylates have been most extensively investigated and discussed[59] on the basis of i.r. spectroscopy. From the different features of the infrared spectra of various trialkyltin carboxylates in the solid state and in solution and from the result of the temperature dependence of the absorption intensities, Janssen[60] and Cummins and Dunn[61] have concluded that trialkyltin carboxylates are polymeric in the solid state with planar trialkyltin groups and bridging acetoxy groups (Fig. 7a) and are ester-like monomers in dilute solution (Fig. 7b).

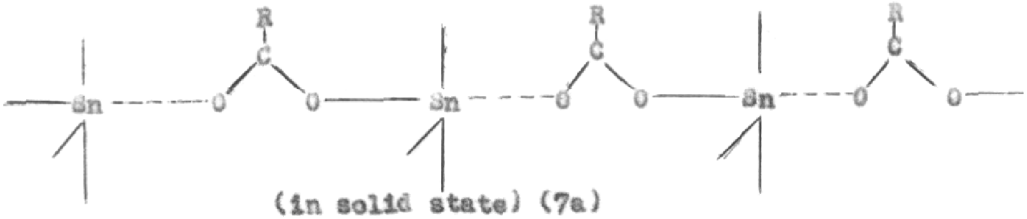

(in solid state) (7a)

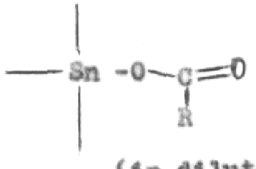

(7b)

(in dilute solution)

Okawara and Ohara[62] have examined the infrared spectra of several organotin carboxylates and assigned the broad absorption around 290 cm^{-1} to the coordination bond and referred to the Sn-O coordinate bond at 300 cm^{-1}

in methyltin formates[63]. Poller[49] has studied a number of phenyltin carboxylate compounds showing that the vibration frequencies due to carboxylate groups appear between 1425-1525 cm^{-1}. He has shown that ν(C-O) symmetric and ν(C-O) asymmetric vibrations appear around 1425 and 1530 cm^{-1} as strong intense bands in the infrared spectrum of triphenyltin acetate. Poller's results are in accordance with that reported by Newman[64] and Okawara and coworkers[65] for a number of methyltin acetate compounds.

1.2.4 ^{1}H NMR spectral studies

A number of investigations have been carried out on various molecular spectra of ferrocene and its derivatives which are of particular interest as source of information concerning the structure and properties of these compounds. However, nuclear magnetic resonance investigations of ferrocene have relatively limited scope[66]. One of the reasons for this is that the protons in each cyclopentadienyl ring comprise a system of five chemically equivalent spins yielding only a single spectral peak. However, in the nmr studies carried out with simple derivatives of ferrocene[67-72], the principal interest appears to be the behaviour of the chemical shifts.

The 2,5- and the 3,4-protons in the substituted cyclopentadienyl ring have been assigned from the analogy

with the effect of substituents on the chemical shifts of the protons in benzene ring. Kamezawa[73] has studied in detail ^{1}H nmr spectra of some ferrocene derivatives with the purpose of finding the convenient procedure for assignments. A gradual deshielding of the cyclopentadienyl ring protons in the metallocene series proceeding from ferrocene to ruthenocene to osmocene has been noted by several investigators[74-76]. Raush and Mark[72] have studied nmr spectra of several mono- and diacyl metallocenes in order to examine the generality of these observations to compare quantitatively the τ values for each set of acylmetallocenes and to obtain information regarding the coupling interaction of acylmetallocene ring protons as a function of the metal.

The presence of both acetyl and benzoyl groups in the metallocene molecule is reflected by a deshielding of not only the hydrogen alpha and beta to the acyl group, but also by a consistent, although smaller deshielding of the non-substituted ring.

The presence of electron-withdrawing substituents on ferrocene leads to pronounced differences in chemical shifts between the 2,5- and 3,4-protons of the substituted cyclopentadienyl ring and both resonances are usually (resonances due to ring protons) shifted to lower field[77]. In certain cases, such as the haloferrocenes, one resonance

appears at lower field and the other at slightly higher field compared to the resonance for ferrocene. Weakly electron-donating substituents, such as alkyl group do not exhibit this chemical shift difference between resonances representing the 2,5- and the 3,4-protons, whereas strongly electron-donating substituents, such as $-NH_2$ and $-OCH_3$ result in substantially larger chemical shift differences between these resonances. The latter fall at higher field than does the resonance for ferrocene[69,78].

The resonances representing the 2,5- and the 3,4-protons in nearly all mono-substituted ferrocene except alkyl derivatives appear as a pair of apparent triplet (line separation ca. 2 Hz) corresponding to an A_2B_2 spin system. Thus in the nmr spectrum of vinyl ferrocene[79] (Fig. 8) unsubstituted C_5H_5 ring appears as singlet at 4.18 τ,

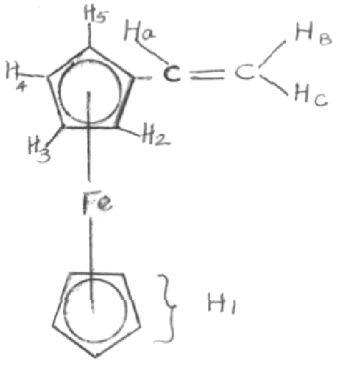

[Fig. 8]

whereas $H_{2,5}$ and $H_{3,4}$ appear as triplets at 4.34 τ and 4.18 τ respectively. The presence of vinyl group in a given metallocene molecule is reflected by a deshielding of both the $\alpha(H_{2,5})$ and $\beta(H_{3,4})$ protons relative to the protons of the parent metallocene. The lower field triplet in each of the vinyl metallocene spectra is assigned to $H_{2,5}$ while the higher field triplet is assigned to $H_{3,4}$. A similar result is observed in the proton nmr spectra of acyl ferrocenes[72].

Nuclear Magnetic Resonance spectroscopy is one of the most popular methods for the study of molecular structure and bonding in organotin compounds. The volume of published data on proton chemical shifts, tin-proton coupling constants and C-H coupling constants in organotin compounds is considerable and comprehensive compilations are available[80-82].

The proton magnetic resonance studies have been predominantly carried out on methyl-tin compounds. The chemical shifts have been shown to be determined by the simultaneous influence of the electronic effect and neighbouring anisotropy. The coupling constants for methyl protons in $Me_3SnC_6H_4X$ (where X = halogen) depend on the electronegativity of X[83]. As the electron withdrawing power of attached group X increases, the

chemical shift decreases. The actual electronegativity of the atom depends upon its environment due to variation in the effective nuclear charge. It is also possible from the proton magnetic resonance measurements to distinguish between the protons of different types of methyl groups[84].

The structures of organotin chelates and acetylacetonate complexes have received considerable attention during recent years. It has been found[85,86] that there is a linear relationship between chemical shifts of gamma protons and those of the methyl protons of acetylacetone. Both values decrease with electron-attracting power of the substituents on the tin atom and this can be correlated with C=O and Sn-O stretching frequencies. These relationships are explained in terms of inductive effect of the substituent on the tin atom. The stereochemistry of $R_2SnCl(acac)_2$ complexes ($R = CH_3$ or C_6H_5; acac = acetylacetone anion) has been investigated by nmr method by Serpone and Hersh[87]. These complexes are predominantly cis in chloroform-D and bromoform solutions.

Attempts to assess the structure of bis(acetyl-acetonato)dimethyltin(IV) in solution by variable temperature nmr technique are not successful. Recently,

the mechanistic studies on configurational rearrangements have also been carried out in dithiocarbamate[88] and tropolonate complexes[89]. The bis(tropolonate) complexes of dimethyltin dichloride[90] may be included in a category of highly distorted octahedral structure. It has been known that the less electronegative methyl groups occupy equatorial positions in their trigonal bipyramidal structures in solid state. From this analogy, dimethyltin halide tropolonate [$(CH_3)_2SnX(T)$ where X = halogene, T = tropolonate] are considered to have a trigonal bipyramidal structure with two methyl groups in equitorial position, although their structures may be more or less distorted.

The long range spin-spin coupling observed between 3-proton and tin in bis(kojato)dihalogenotin(IV) and methyl halogenotin[91] suggests that this coupling occurs more strongly through carbon-oxygen single bond. The configuration of bis(kojato)dimethyl tin has been shown to be a distorted octahedron with trans-methyl groups on the basis of the coupling constants of methyl protons with tin.

Scope and objective

The scope and objective of the present work are therefore as follows:-

(1) Synthesis of ferrocenylidene derivatives of α-N-acyl hydrazines and their mass spectral studies (Chapter III).

Although there have been a number of reports on mass spectral studies of ferrocenyl compounds there is no report on the mass spectral studies of ferrocenylidene derivatives of α-N-acyl hydrazines so far.

(2) Infrared spectral studies of all the compounds prepared are reported in Chapter IV.

(3) Synthesis of dichloro- and organotin(IV) complexes of aroyl ferrocenylidene derivatives of α-N-acyl hydrazines and their proton magnetic resonance spectral studies (Chapter V).

CHAPTER -II

EXPERIMENTAL

		Page
2.	Materials and methods	
2.1	Ferrocene	31
2.2	Acetyl ferrocene	32
2.3	Formyl ferrocene	32
2.4	N-acyl hydrazines	32
2.5	Stannous chloride dihydrate	33
2.6	Dibutyl- and dioctyltin oxides	33
2.7	Triphenyltin acetate	33
2.8	Cupric acetate dihydrate	33
2.9	Solvents	33
2.10	Ferrocenylidene derivatives of N-acyl hydrazines	33
2.11	Copper(II) complexes	34
2.12	Dichlorotin(IV) complexes	34
2.13	Dibutyl- and dioctyltin(IV) complexes	34
2.14	Reactions of triphenyltin acetate with ferrocenylidene ligands	35
2.15	Spectroscopic methods	35

EXPERIMENTAL

2. Materials and methods

2.1. Ferrocene

Ferrocene was prepared following essentially the method given in Inorganic Synthesis[92]. A 500 ml three-necked flask, equipped with a stirrer was charged with 240 ml of tetrahydrofuran and 100 g of KOH powder. While the mixture was slowly stirred and the flask was flushed with nitrogen from one side neck, 22 ml (0.268 mole) of cyclopentadiene was added. The other side neck was fitted with a $CaCl_2$ guard tube and the main neck with a 100 ml dropping funnel. A solution of 26.0 g (0.130 mole) of iron(II) chloride tetrahydrate in 100 ml of dimethyl-sulphoxide was placed in the dropping funnel and solution was added dropwise with stirring during one hour. The stopcock of the funnel was closed and the stirring was continued for another 30 minutes. The nitrogen stream was stopped and the mixture was added to a mixture of 360 ml of 6 M HCl and approximately 400 g ice. The slurry was stirred for 15 minutes and the precipitate was collected on a filter and washed with four 25 ml portions of water. The product was allowed to dry in air overnight. Yield 25.25 g (89%); m.p. 174°C (reported 173-174°C). Found: C, 63.14; H, 5.33; Fe, 30.6%. Calculated for

$C_{10}H_{10}Fe$, C, 63.57; H, 5.42; Fe, 30.02%.

2.2. Acetyl ferrocene

Acetyl ferrocene was prepared essentially according to reported method[93].

To 18.6 g of ferrocene was added 40 ml acetic anhydride and 4 ml of 85% phosphoric acid. The mixture was heated at 100°C for 10 minutes, cooled and poured on 200 g ice. The mixture was allowed to stand overnight. It was neutralized with 40 g of Na_2CO_3 dissolved in 40 ml of water. The resulting pasty mass was solidified by cooling in an ice bath, filtered, washed with water and dried over P_2O_5. The product was recrystallized from petroleum ether. Yield, 14 g (57%), m.p. 85°C (reported 85-86°C). Found: C, 63.23; H, 5.89; Fe, 24.91%. Calculated for $C_{10}H_9COCH_3Fe$: C, 63.17; H, 5.26; Fe, 25.00%.

2.3. Formyl-ferrocene was purchased from Fluka, A.G. Switzerland.

2.4. N-acyl hydrazines

N-acyl hydrazines such as benzoyl-, isonicotinoyl- and salicyloyl hydrazides were prepared following the procedure reported by Struve[94]. p-Chlorobenzoyl- and o-nitrobenzoyl hydrazides from Fluka A.G., Switzerland, were used.

2.5. Stannous chloride dihydrate ($SnCl_2.2H_2O$) was of analytical grade (SD's Chemicals) Bombay.

2.6. Dibutyl- and dioctyltin oxides were obtained from Pisons, Philadelphia, U.S.A.

2.7. Triphenyltin acetate was obtained from Alfa Products (U.K.) and used without further purification.

2.8. Cupric acetate dihydrate was obtained from BDH (Bombay).

2.9. Solvents

Commercially available solvents were used after purification and drying by standard procedures[95].

2.10. Ferrocenylidene derivatives of N-acyl hydrazines

All these ferrocenyl derivatives of N-acyl hydrazines were prepared using a general procedure as given below:

The condensation reactions were carried out by refluxing equimolar quantities of formyl- and acetyl ferrocene respectively with required quantities of N-acyl hydrazines in alcohol for 4 hours. Concentration of the solutions to the appropriate volumes and cooling in refrigerator overnight yielded the products. These were purified by repeated recrystallization from absolute ethanol.

The compounds prepared are listed in Table 1 along with their melting points and elemental analysis.

2.11 Copper(II) complexes

The copper(II) complexes of these ligands were prepared by mixing the respective ligand in ethanol with a hot ethanolic solution of cupric acetate dihydrate (in the molar ratio of 2:1) and heating the solution for half an hour under reflux with constant stirring. The solid that separated out was collected on a filter, washed several times with alcohol and dried. The compounds prepared, along with their melting points and elementary analyses, are listed in Table 2, except the copper(II) complexes of α-N-isonicotinoyl-β-N-(methyl)ferrocenylidenehydrazide, α-N-p-chloro- and α-N-(o)-nitrobenzyl-β-N-ferrocenylidenehydrazide which could not be isolated in pure state.

2.12 Dichlorotin(IV) complexes

To an ethanolic solution of ligand (0.001 mole), a solution of stannous chloride dihydrate (0.0005 mole) was added with vigorous stirring and the mixture was refluxed till the product separated out. The crystalline product was collected on the filter, washed with ethanol repeatedly, dried under vacuum and recrystallized from chloroform.

2.13 Dibutyl- and dioctyltin(IV) complexes

A benzene solution of organotin oxide and ferrocenyl compound (in a ratio of 1:2 moles) was refluxed for about 8 hours. The dark violet coloured solution was then

concentrated, filtered and the filtrate was evaporated to dryness under vacuum. The crude product was recrystallized from either benzene or chloroform. The compounds prepared are listed along with their melting point and elementary analyses in Table 3.

2.14 Reaction of triphenyltin acetate with ferrocenylidene hydrazide ligands

Triphenyltin acetate and ferrocenyl ligand in equimolar ratio were taken in benzene and the solution refluxed for about 8 hours. The hot mixture was filtered to remove the insoluble impurities and the filtrate was concentrated under vacuum at 50°C. The solid product obtained in almost quantitative yield was recrystallized from either benzene or chloroform and dried under vacuum. The compounds prepared, along with their melting points and elemental analysis, are given in Table 4.

2.15 Spectroscopic methods

Mass spectra: were recorded on a double focusing mass spectrometer (CEC 21-110B (USA)) at a voltage of 70 eV and a current of 20 milliamperes.

Infra-red spectra: Infrared spectra were recorded on Perkin-Elmer model 283B spectrophotometer using cesium iodide optics.

^{1}H n.m.r. spectra: were recorded on a Varian Associates Model T-60 using tetramethyl silane as an internal standard.

TABLE 1

FERROCENYLIDENE DERIVATIVES OF α,N-ACYLHYDRAZINES

Fc-C(R)=N-NH-C(=O)-Ar (Fc = Ferrocenyl group)

S.No.	Compound	Composition	Yield %	m.p. °C	Mol.wt.	Elemental analysis (%) C	H	N
1.	α-N-benzoyl-β-N-ferrocenylidene-hydrazide (R=H, Ar=C_6H_5)	$Fe(C_{18}H_{16}N_2O)$	88	158	332	65.66 (65.13)	5.20 (4.86)	8.56 (8.44)
2.	α-N-(p)-Chlorobenzoyl-β-N-ferrocenylidenehydrazide (R=H, Ar=C_6H_4Cl(p)	$Fe(C_{18}H_{15}N_2OCl)$	80	220	366	57.29 (58.96)	4.38 (4.12)	7.53 (7.63)
3.	α-N-(o)-nitrobenzoyl-β-N-ferrocenylidene hydrazide (R=H, Ar=$C_6H_4NO_2$(o))	$Fe(C_{18}H_{15}N_3O_3)$	85	235	377	56.90 (57.30)	4.41 (4.00)	10.46 (11.14)
4.	α-N-Isonicotinoyl-β-N-ferrocenylidenehydrazide (R=H, Ar=C_5H_4N)	$Fe(C_{17}H_{15}N_3O)$	90	213	333	62.85 (61.28)	5.03 (4.54)	12.58 (12.61)
5.	α-N-Salicyloyl-β-N-ferrocenylidenehydrazide (R=H, Ar=C_6H_4OH(o))	$Fe(C_{18}H_{16}N_2O_2)$	85	210	348	62.66 (62.09)	5.01 (4.63)	8.01 (8.04)
6.	α-N-Benzoyl-β-N-(methyl)-ferrocenylidenehydrazide (R=CH_3, Ar=C_6H_5)	$Fe(C_{19}H_{18}N_2O)$	65	165	346	67.18 (65.94)	5.59 (5.24)	8.59 (8.09)
7.	α-N-Isonicotinoyl-β-N-(methyl) ferrocenylidenehydrazide (R=CH_3, Ar=C_5H_4N)	$Fe(C_{18}H_{17}N_3O)$	80	140	347	63.35 (62.26)	5.35 (4.93)	11.47 (12.10)

Contd.

(TABLE -1 CONTD.]

S.No.	Compound	Composition	Yield %	m.p. °C	Mol.wt.	Elemental analysis(%)		
						C	H	N
8.	α-N-Salicyloyl-β-N-(methyl)-ferrocenylidenehydrazide (R = CH_3, Ar=C_6H_4OH(o)).	$Fe(C_{19}H_{18}N_2O_2)$	70	226	363	62.21 (63.00)	5.65 (5.05)	7.98 (7.73)

TABLE 2

COPPER(II) COMPLEXES OF FERROCENYLIDENE DERIVATIVES OF α-N-ACYLHYDRAZINES

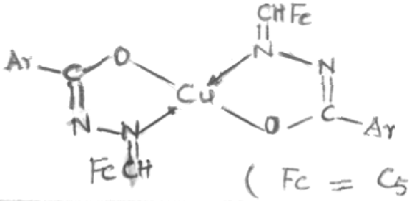

(Fc = $C_5H_5FeC_5H_4$)

S.No.	Compound	Composition	Yield %	Elemental analysis (%) C	H	N
1.	Bis(α-N-benzoyl-β-N-ferrocenylidene hydrazidato)copper(II) (R=H, Ar=C_6H_5).	$C_{36}H_{30}N_4O_2Fe_2Cu$	90	59.92 (59.56)	4.30 (4.16)	8.22 (7.72)
2.	Bis(α-N-Salicyloyl-β-N-ferrocenylidenehydrazidato)copper(II) (R=H, Ar=$C_6H_4OH(o)$).	$C_{36}H_{30}N_4O_4Fe_2Cu$	85	57.81 (57.23)	4.41 (3.71)	6.67 (7.47)
3.	Bis(α-N-Isonicotinoyl-β-N-ferrocenylidenehydrazidato)copper(II) (R=H, Ar=C_5H_4N)	$C_{34}H_{28}N_6O_2Fe_2Cu$	65	55.29 (56.10)	3.84 (3.88)	10.56 (11.54)
4.	Bis(α-N-Benzoyl-β-N-(methyl)-ferrocenylidenehydrazidato)-copper(II) (R=CH_3, Ar=C_6H_5).	$C_{38}H_{34}N_4O_2Fe_2Cu$	88	61.67 (60.52)	4.91 (4.54)	7.29 (7.42)
5.	Bis(α-N-Salicyloyl-β-N-(methyl)-ferrocenylidenehydrazidato)-copper(II) (R=CH_3, Ar=$C_6H_4OH(o)$).	$C_{38}H_{34}N_4O_4Fe_2Cu$	85	59.33 (58.07)	4.72 (4.36)	6.62 (7.12)

TABLE 3

TIN(IV) COMPLEXES OF FERROCENYLIDENE DERIVATIVES OF α-N-ACYLHYDRAZINES

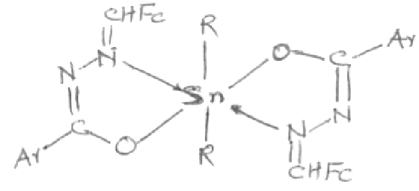

S.No.	Compound	Composition	m.p. °C	Elemental analysis %		
				C	H	N
1.	Dichlorobis(α-N-benzoyl-β-N-ferrocenylidenehydrazidato)tin(IV) (R = Cl, Ar = C_6H_5).	$C_{36}H_{30}N_4O_2Cl_2Fe_2Sn$	>300	50.30 (50.70)	3.85 (3.52)	6.45 (6.57)
2.	Dichlorobis(α-N-(p)-chlorobenzoyl-β-N-ferrocenylidenehydrazidato)-tin(IV) (R = Cl, Ar = C_6H_4Cl(p)	$C_{36}H_{28}N_4O_2Cl_4Fe_2Sn$	>300	47.25 (47.18)	3.21 (3.46)	6.01 (6.09)
3.	Dichlorobis(α-N-(o)-nitrobenzoyl-β-N-ferrocenylidenehydrazidato)-tin(IV) (R = Cl, Ar = $C_6H_4NO_2$(o))	$C_{36}H_{28}N_6O_6Cl_2Fe_2Sn$	>300	45.06 (45.85)	3.11 (2.97)	9.05 (8.92)
4.	Dichlorobis(α-N-isinicotinoyl-β-N-ferrocenylidenehydrazidato) tin(IV) (R = Cl, Ar = C_5H_4N)	$C_{34}H_{28}N_6O_2Cl_2Fe_2Sn$	>300	47.45 (47.30)	3.52 (3.31)	9.49 (9.90)
5.	Bis(α-N-benzoyl-β-N-ferrocenylidenehydrazidato)dibutyltin(IV) (R = C_4H_9, Ar = C_6H_5).	$C_{44}H_{48}N_4O_2Fe_2Sn$	125 (dec.)	59.49 (59.08)	5.67 (5.41)	6.06 (6.26)

TABLE 3 (CONTD.)

7.	Bis(α-N-(o)-Nitrobenzoyl-β-N-ferrocenylidenehydrazidato)dibutyltin(IV) (R = C_4H_9, Ar = $C_6H_4NO_2$(o)).	$C_{44}H_{46}N_6O_6Fe_2Sn$	208	53.57 (53.67)	5.11 (4.78)	8.67 (8.53)
8.	Bis(α-N-isonicotinoyl-β-N-ferrocenylidenehydrazidato)dibutyltin(IV) (R = C_4H_9, Ar = C_5H_4N).	$C_{42}H_{46}N_6O_2Fe_2Sn$	185 (dec.)	57.24 (56.26)	5.55 (5.17)	9.54 (9.37)
9.	Bis(α-N-Salicyloyl-β-N-ferrocenylidenehydrazidato)dibutyltin(IV) (R = C_4H_9, Ar = C_6H_4OH(o)).	$C_{44}H_{48}N_4O_4Fe_2Sn$	176	56.04 (57.04)	5.85 (5.22)	5.51 (6.05)
10.	Bis(α-N-Benzoyl-β-N-ferrocenylidenehydrazidato)dioctyltin(IV) (R = C_8H_{17}, Ar = C_6H_5)	$C_{52}H_{64}N_4O_2Fe_2Sn$	semi-solid	61.41 (62.03)	6.50 (6.40)	5.28 (5.26)
11.	Bis(α-N-(p)-Chlorobenzoyl-β-N-ferrocenylidenehydrazidato)-dioctyltin(IV) (R = C_8H_{17}), Ar = C_6H_4(Cl)(p))	$C_{52}H_{62}N_4O_2Cl_2Fe_2Sn$	145 (dec.)	57.00 (58.06)	6.41 (5.81)	4.73 (5.21)
12.	Bis-(α-N-(o)-nitrobenzoyl-β-N-ferrocenylidenehydrazidato)-dioctyltin(IV) (R = C_8H_{17}, Ar = $C_6H_4NO_2$(o)).	$C_{52}H_{62}N_6Fe_2Sn$	168 (dec.)	55.34 (56.95)	6.38 (5.70)	7.43 (7.66)
13.	Bis(α-N-Isonicotinoyl-β-N-ferrocenylidenehydrazidato)-dioctyltin(IV) (R = C_8H_{17}, Ar = C_5H_4N).	$C_{50}H_{62}N_6O_2Fe_2Sn$	semi-solid	59.15 (59.50)	6.55 (6.20)	8.51 (8.33)
14.	Bis(α-N-Salicyloyl-β-N-ferrocenylidenehydrazidato)dioctyltin(IV) (R = C_8H_{17}, Ar = C_6H_4OH(o)).	$C_{52}H_{64}N_4O_4Fe_2Sn$	semi-solid	62.03 (60.12)	6.47 (6.21)	6.55 (5.39)

TABLE 4

TIN(IV) COMPLEXES OF FERROCENYLIDENE DERIVATIVES OF α-N-ACYLHYDRAZINES

S.No.	Name of the complex	Composition	Yield	m.p. °C	Elemental analysis(%) C	H	N
1.	μ-Acetoxy-(α-N-(o)-nitrobenzoyl(β-N-ferrocenylidenehydrazidato)diphenyltin(IV)	$C_{32}H_{27}N_3O_5FeSn$	90	235	54.48 (54.30)	4.10 (3.85)	6.18 (5.94)
2.	μ-Acetoxy-(α-N-isonicotinoyl-β-N-ferrocenylidenehydrazidato)-diphenyltin(IV)	$C_{31}H_{24}N_3O_3FeSn$	80	232	57.56 (56.69)	4.47 (4.24)	6.11 (6.32)
3.	μ-Acetoxy-(α-N-salicyloyl-β-N-ferrocenylidenehydrazidato)-diphenyltin(IV)	$C_{32}H_{28}N_2O_4FeSn$	78	214	58.19 (58.65)	4.76 (4.16)	3.91 (4.13)
4.	Bis-(α-N-benzoyl-β-N-ferrocenylidene-hydrazidato)diphenyltin(IV)	$C_{48}H_{40}N_4O_2Fe_2Sn$	95	252	60.39 (61.67)	4.69 (4.31)	6.12 (5.99)
5.	α-N-(p)-Chlorobenzoyl-β-N-ferrocenylidenehydrazidato)-triphenyltin(IV)	$C_{36}H_{29}N_2OClFeSn$	85	255	61.39 (60.50)	4.96 (4.60)	4.40 (4.00)

CHAPTER -III

MASS SPECTRAL STUDIES ON SOME FERROCENYLIDENE DERIVATIVES OF α-N-ACYL HYDRAZINES : RESULTS AND DISCUSSION

	Page
Simple cleavage	42
Hydrogen rearrangement process	53
Skeletal rearrangement	54
Ortho effect	55

Mass spectral studies on some ferrocenylidene derivatives of α-N-acylhydrazine.

The mass spectra of compounds I-VIII (Chapter II, Table 1) have been recorded and the data are presented in Table 1 and Figures 1-8.

The molecular ion peaks are the base peaks in all these compounds as reported earlier in the case of many a ferrocenyl compounds[26,96]. Incidently Kingston and coworkers[97] have reported that the daughter ion peaks are the base peaks in the mass spectra of aroyl hydrazones of the formula $ArCONHN{=}C(R)Ar'$ (where Ar = substituted phenyl group, Ar' = C_6H_5 and R = H or CH_3). The compounds reported here are similar to aroyl hydrazones except the phenyl group. It appears therefore that the ferrocenyl moiety renders more stability to the common backbone of these molecules.

The mass spectral fragmentation of these compounds reveals simple cleavage, hydrogen rearrangement and skeletal rearrangement occuring under electron impact.

Simple Cleavage Reactions:

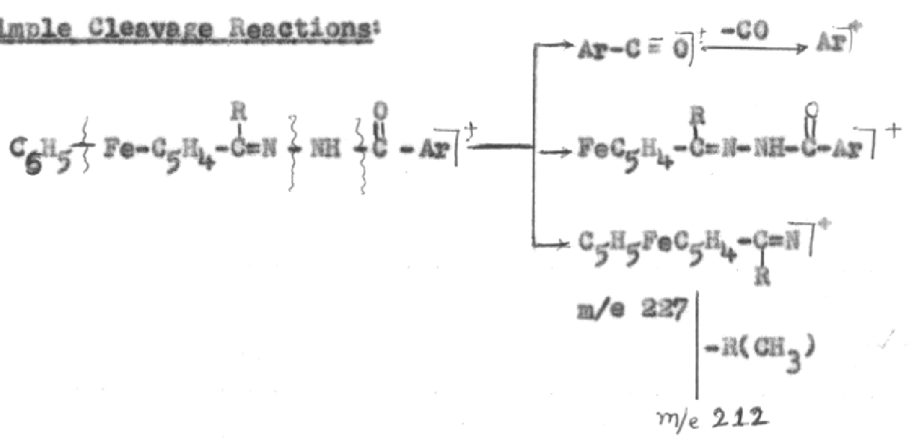

TABLE -1

MASS SPECTRAL DATA OF FERROCENYLIDENE DERIVATIVES OF

α-N-ACYLHYDRAZINES

m/e/(% intensity)

I	II	III	IV	V	VI	VII	VIII
332 (100)	366 (100)	377 (100)	348 (100)	333 (100)	346 (100)	362 (100)	347 (100)
		347 (9.52)				297 (30.00)	
267 (5.5)	301 (3.76)	312 (2.12)	283 (7.20)	268 (3.00)	281 (11.9)	279 (13.7)	282 (7.9)
	275 (6.45)	286 (7.41)	265 (5.70)			269 (1.5)	
			257 (3.50)			257 (6.7)	
241 (10.1)	232 (13.44)	213 (10.58)	239 (4.10)	242 (8.8)	241 (12.2)	242 (79.00)	242 (11.4)
					227 (5.2)	239 (13.7)	227 (6.4)
						227 (6.00)	
211 (34.7)	211 (40.86)	211 (42.86)	211 (30.12)	211 (29.7)	212 (4.9)	212 (6.9)	212 (4.3)
198 (18.3)	210 (5.35)	198 (4.23)	192 (5.19)	199 (14.1)	198 (10.9)	192 (7.3)	199 (10.00)
185 (3.00)	185 (3.76)	185 (6.88)	185 (3.00)	185 (4.6)	185 (6.1)	185 (3.7)	185 (4.00)
		178 (3.70)	174 (9.62)	177 (3.2)	178 (6.7)	178 (8.3)	178 (4.3)
		150 (11.64)	1		176 (4.3)	174 (11.00)	177 (2.2)
					162 (4.3)	162 (11.7)	

Contd.....

TABLE -1 (Contd.)

I	II	III	IV	V	VI	VII	VIII
146 (8.8)	146 (6.45)	146 (7.44)	146 (3.50)	146 (10.6)			
				134 (12.4)	133 (7.4)		134 (5.7)
129 (7.7)	129 (5.38)	129 (8.99)	129 (4.94)	129 (5.00)	129 (4.6)	129 (7.7)	129 (5.4)
121 (41.3)	121 (55.91)	121 (63.49)	121 (39.50)	121 (53.4)	121 (32.9)	121 (41.3)	121 (2.5)
		120 (19.05)					
105 (13.73)	111 (21.50)	104 (11.64)		106 (12.00)	105 (16.72)		106 (4.28)
95 (1.8)	95 (4.30)	95 (4.23)	95 (5.00)	95 (3.00)	95 (2.72)	95 (5.6)	95 (5.00)
94 (1.8)	94 (4.30)	94 (4.23)	94 (5.00)	94 (3.00)	94 (2.72)	94 (4.6)	94 (4.6)
81 (1.2)	81 (4.4)	81 (1.2)	81 (9.82)	81 (5.00)	81 (2.72)	81 (4.00)	81 (4.00)
77 (11.35)	77 (4.30)	77 (5.29)	77 (2.5)	78 (5.82)	77 (16.72)		77 (9.28)
	65 (3.70)	65 (6.00)	65 (30.61)	65 (1.00)		65 (21.66)	
56 (9.52)	56 (40.0)	56 (29.10)	56 (45.92)	56 (34.00)	56 (12.77)	56 (32.66)	56 (15.71)

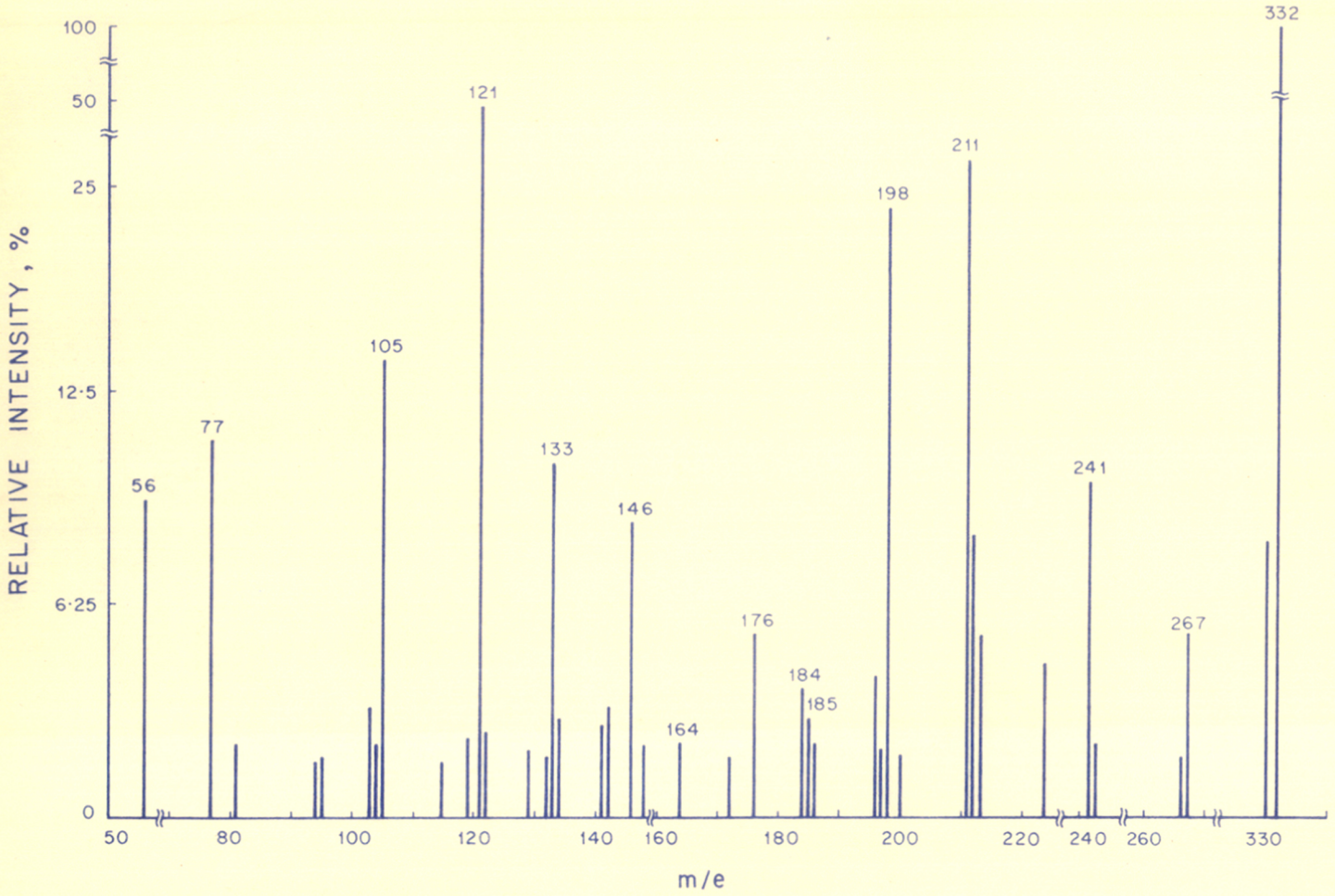

FIG. 1 : MASS SPECTRUM OF α -N-BENZOYL-β-N-FERROCENYLIDENEHYDRAZIDE.

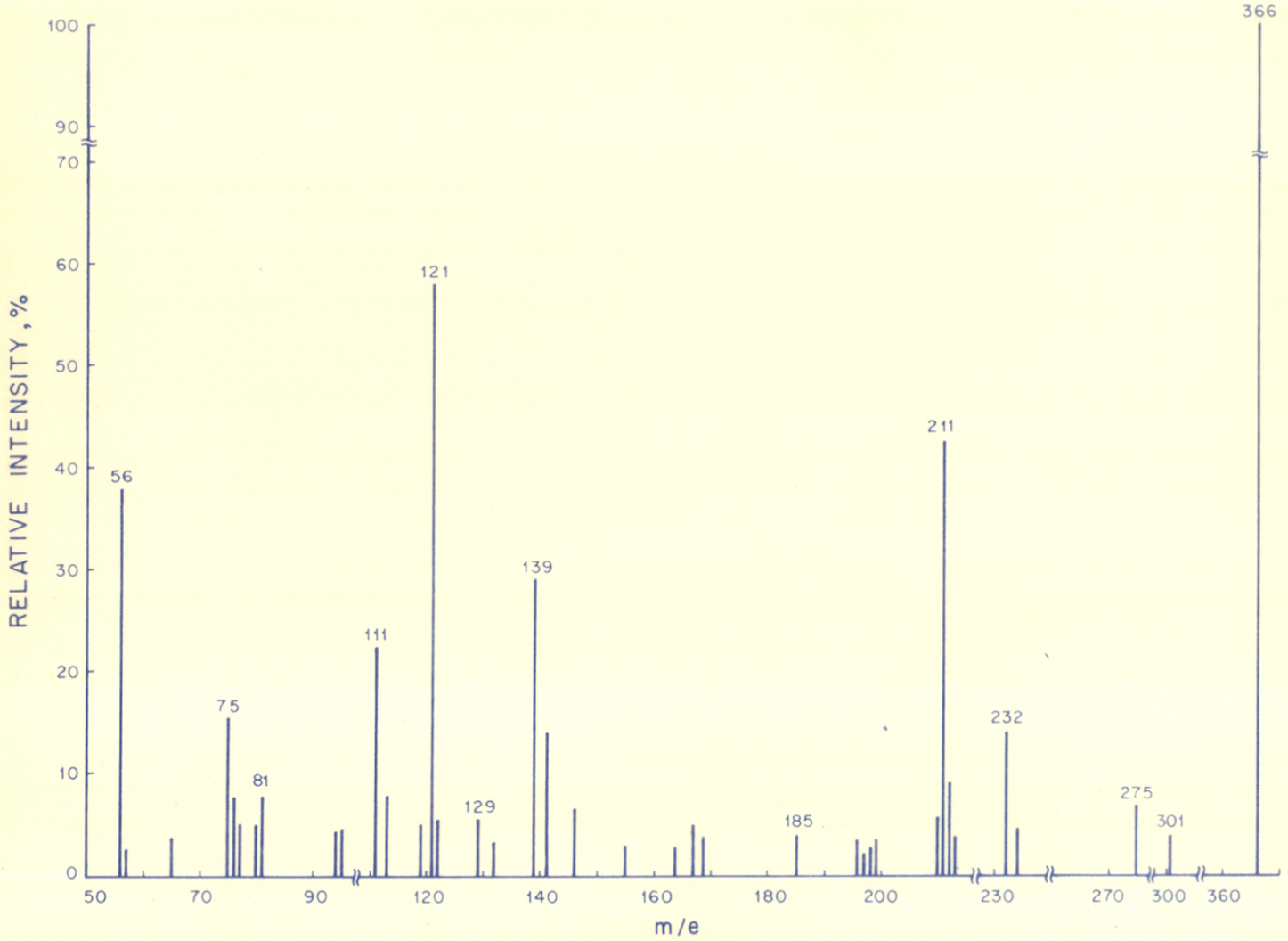

FIG. 2 : MASS SPECTRUM OF α-N-(p) CHLOROBENZOYL-β-N-FERROCENYLIDENEHYDRAZIDE.

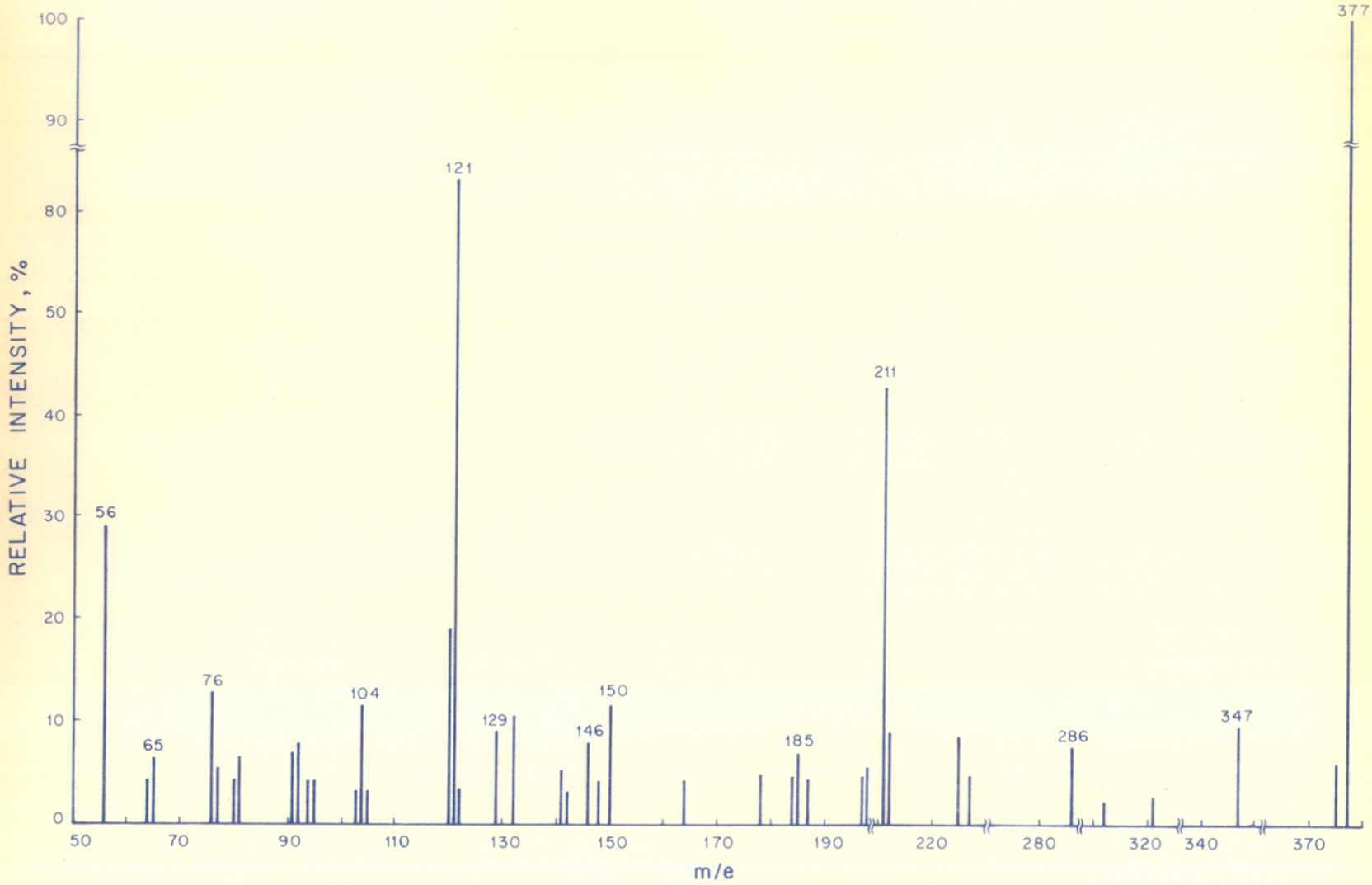

FIG. 3 : MASS SPECTRUM OF α-N-(o) NITROBENZOYL-β-N-FERROCENYLIDENEHYDRAZIDE.

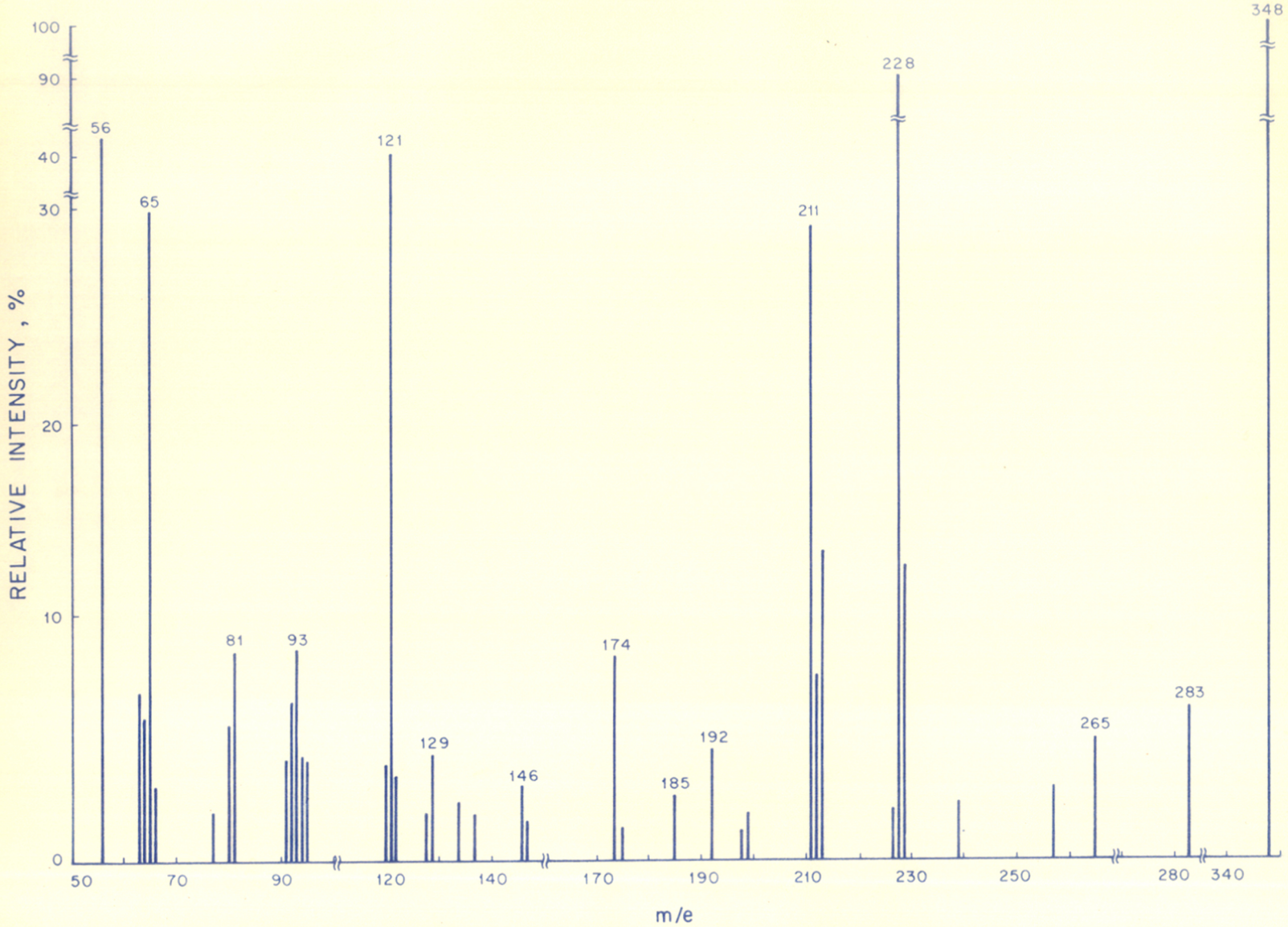

FIG. 4 : MASS SPECTRUM OF α-N-SALICYLOYL-β-N-FERROCENYLIDENEHYDRAZIDE.

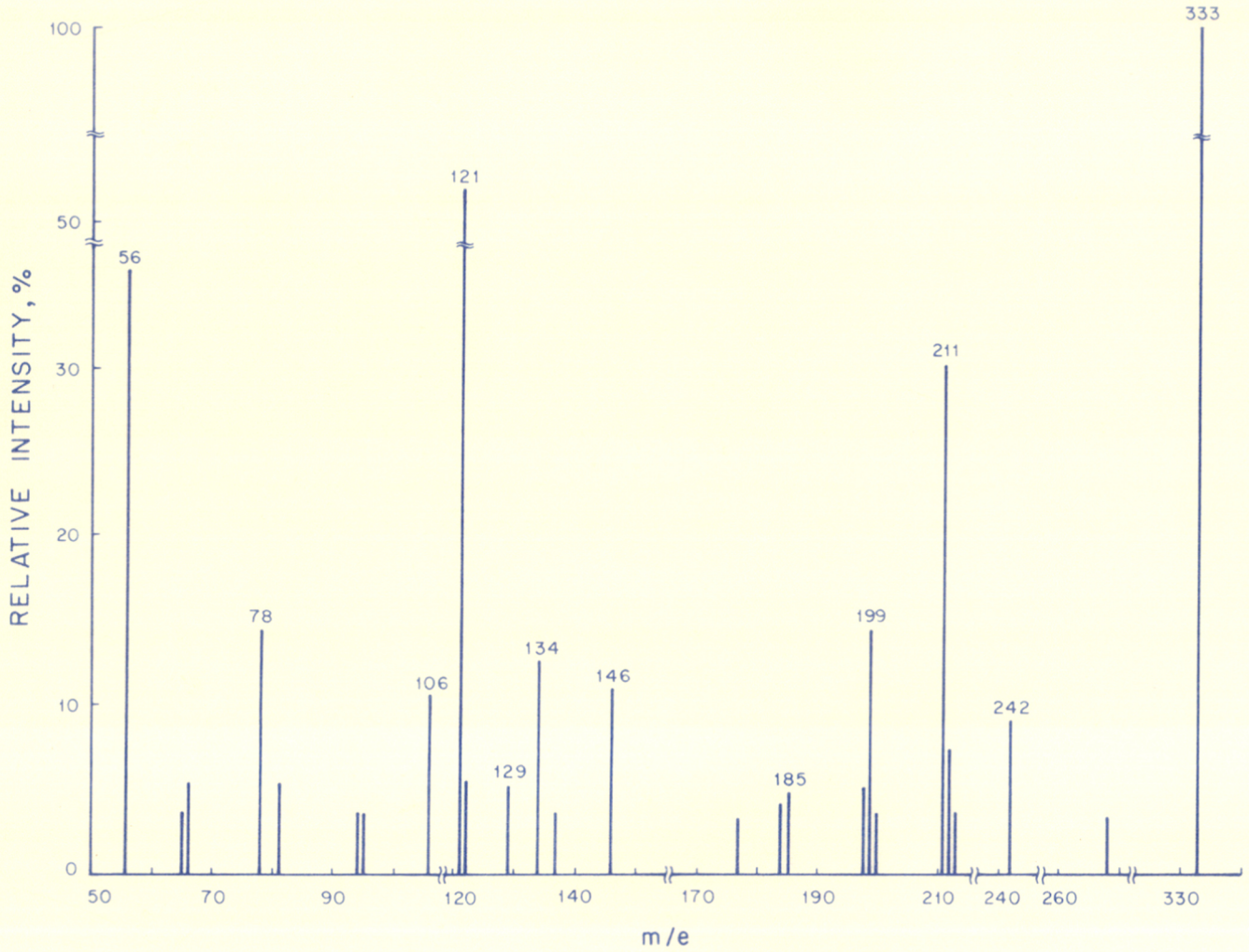

FIG. 5 : MASS SPECTRUM OF α-N-ISONICOTINOYL-β-N-FERROCENYLIDENEHYDRAZIDE.

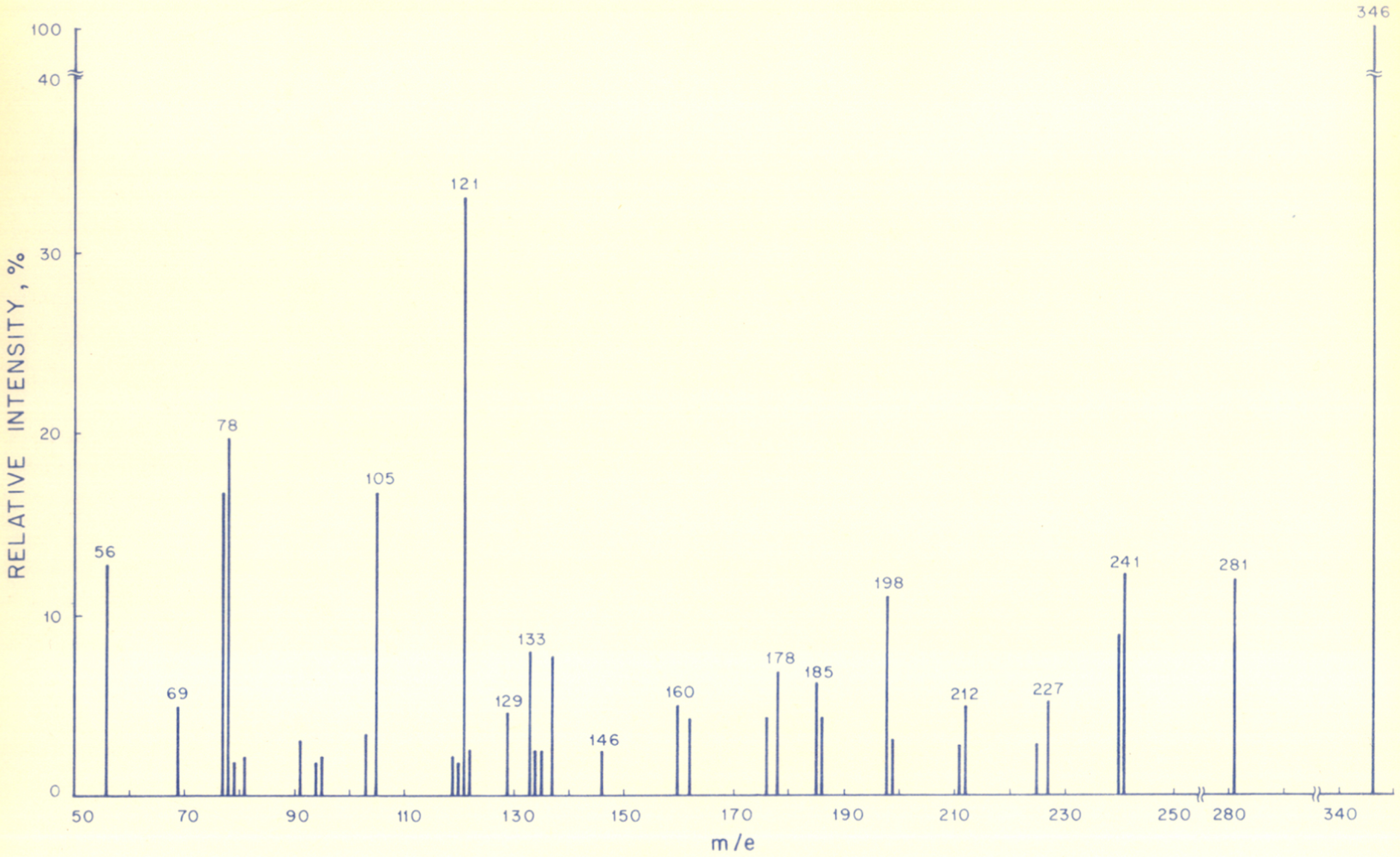

FIG.6 : MASS SPECTRUM OF α-N-BENZOYL-β-N-(METHYL) FERROCENYLIDENEHYDRAZIDE.

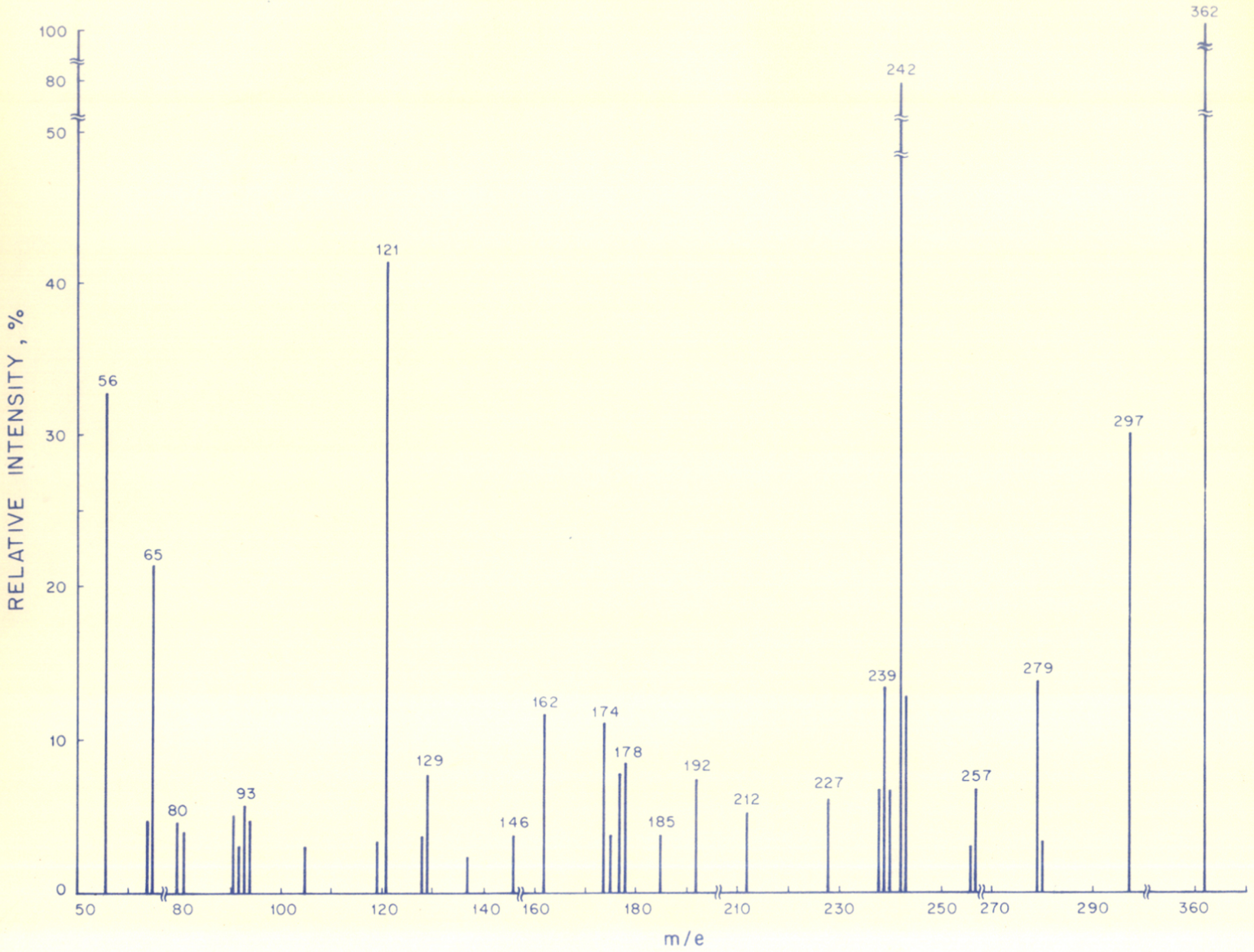

FIG. 7 : MASS SPECTRUM OF α-N-SALICYLOYL-β-N-(METHYL) FERROCENYLIDENEHYDRAZIDE.

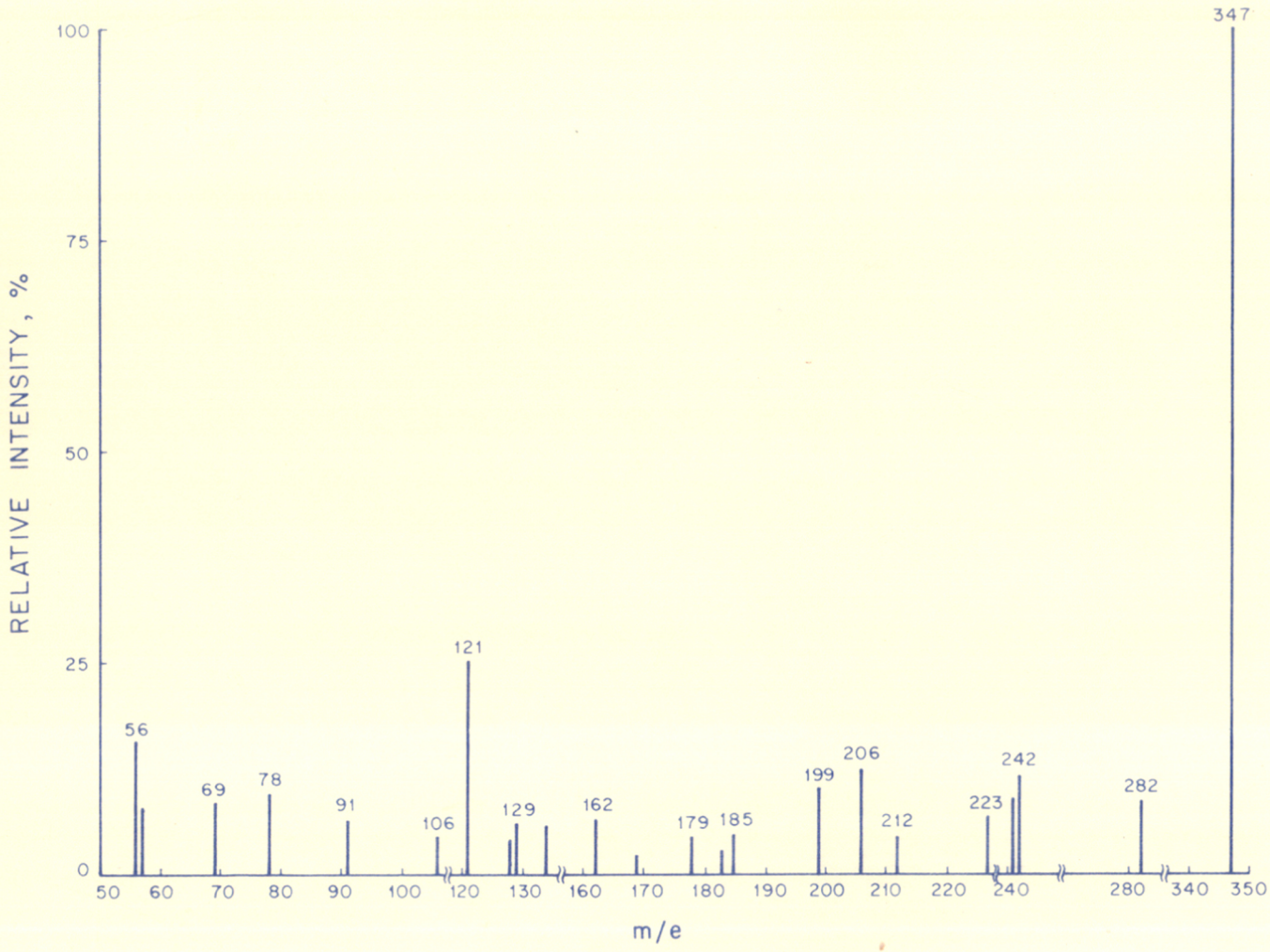

FIG. 8 : MASS SPECTRUM OF α-N-ISONICOTINOYL -β-N-(METHYL)-FERROCENYLIDENEHYDRAZIDE

Cleavage α- to the carbonyl function produces significant aroyl ions $(Ar-C\equiv O)^+$ which fragments further by loss of carbon monoxide producing another ion Ar^+.

Loss of unsubstituted cyclopentadienyl group from the parent ion is another significant simple cleavage process leading to $(M^+ - C_5H_5)^+$ in all the spectra.

The cleavage of N-N bond in aryl hydrazones has been reported in the spectra of carbonyl derivatives[101]. In the present study such a simple cleavage of weak N-N bond is observed to produce abundant ions in the spectra of compounds VI to VIII leading to fragment ion at m/e 227, which fragments further by loss of methyl radical to give another characteristic ion at m/e 212.

Hydrogen Rearrangement Process:

The characteristic peaks observed in the case of compounds I to V at m/e 211 is ascribed to hydrogen elimination process occuring via four membered transition state. The driving force for this rearrangement being the elimination of thermodynamically stable neutral molecule $ArCONH_2$ i.e. amide as shown below:

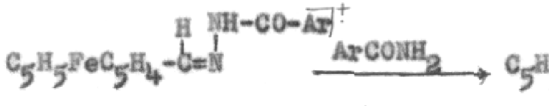

m/e 211

Skeletal Rearrangement:

The mass spectra of the compounds show ions arising due to skeletal rearrangement processes in the molecular ions and fragment ions.

The rearrangement leading to the formation of $C_5H_5Fe\text{-}NH\text{-}\overset{O}{\overset{\|}{C}}\text{-}Ar\rceil^+$ ion has been found to occur in all the compounds. The rearrangement occurs by the cleavage of N-N bond followed by transfer of C_5H_5Fe group to the nitrogen atom via six membered transition state. The rearranged product then loses another C_5H_5 group leading to the formation of $Fe\text{-}NH\text{-}\overset{O}{\overset{\|}{C}}\text{-}Ar^+$

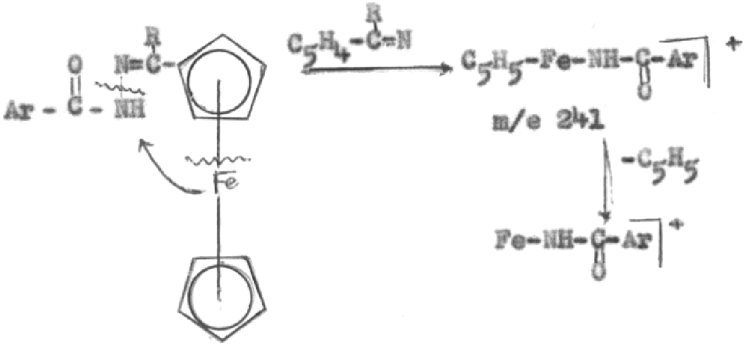

In the compounds IV and VII loss of $C_6H_4\text{-}OH$ from M^+ is followed by expulsion of HCN.

$$M^+ \xrightarrow{-C_6H_4OH} C_5H_5FeC_5H_4\text{-}C(R)=N\text{-}NH\text{-}C\equiv O\rceil^+$$

m/e 255 (IV)
m/e 269 (VII)
$\downarrow -HCN$

$$C_5H_5\text{-}Fe\text{-}C_5H_4\text{-}C(R)=N=O\rceil^+$$

m/e 228 (IV)
m/e 242 (VII)

The product of skeletal rearrangement reactions further undergoes another skeletal rearrangement as shown below:

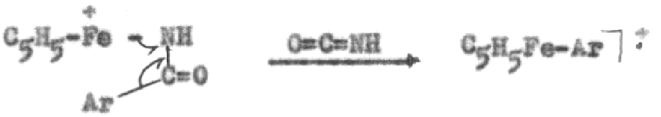

m/e 241 (I, VI)	m/e 198 (VI, I)
m/e 242 (V, VIII)	m/e 199 (V, VIII)
m/e 275 (II)	m/e 232 (II).
m/e 286 (III)	

Ortho Effect

In the mass spectra of the compounds IV and VII several frggment ions show elimination of water. This could be due to isomerization of 'keto' structure to 'enol' form and then elimination of water via six membered transition state as indicated below.

1)

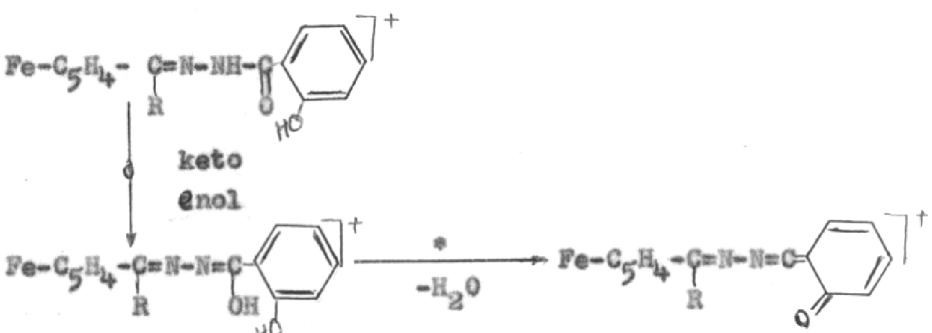

m/e 283 (IV)	m/e 265 (IV)
m/e 297 (VII)	m/e 279 (VII)

ii) 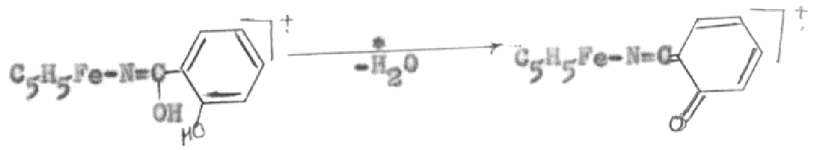

m/e 257 m/e 239

iii) 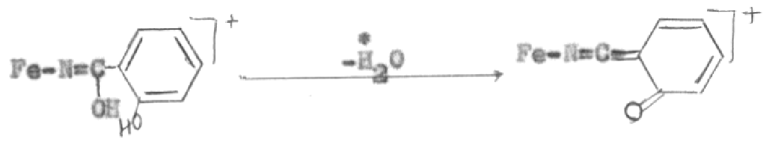

m/e 192 m/e 174

As expected, intense peaks corresponding to fragment ions $C_5H_5^+$ (m/e 65), $C_5H_5Fe^+$ (m/e 121), $C_5H_5.C_5H_4^+$ (m/e 129), $C_5H_5FeC_5H_4^+$ (m/e 185) and Fe^+ (m/e 56) are observed in the spectra of all the compounds. These are the characteristic fragmentation ions reported for ferrocene[25] and substituted ferrocenes[26,98]. Fragment ions at m/e 81, m/e 94 and m/e 95 which are observed in the mass spectra of all the compounds, normally observed for ferrocene compounds can be assigned to the ions FeC_2H^+, $FeC_3H_2^+$ and $FeC_3H_3^+$ respectively which result from fragmentation of cyclopentadienyl ring. Such type of fragmentation pattern has been reported by Schumacher and Taubenest[24] in the mass-spectral studies on ferrocene and nickelocene. In addition to this, these authors have observed ion peaks corresponding to $Fe_2CpC_3H_3$ (m/e 216), $Cp_2Fe_2^+$ (m/e 242), $Fe_2Cp_2C_3H_3$ (m/e 281) and $FeCp_3$ (m/e 307) (where $C_p = C_5H_5$) in the mass spectrum of ferrocene, whereas Friedman and coworkers[22] could not detect these ion peaks in the mass spectrum of ferrocene. We are are unable to detect these ions in the present study.

CHAPTER -IV

INFRARED SPECTRAL STUDIES - RESULTS AND DISCUSSION

		Page
4.1	Infrared spectra of ferrocenylidene hydrazides	57
4.2	Copper(II) complexes	72
4.3	Tin(IV) complexes	76
4.4	Hydrogen bonding	95
4.5	Complexes derived from triphenyltin acetate	97

4.1 Infrared spectra of ferrocenylidene hydrazides

The principal absorption frequencies observed in the infrared spectra of compounds one to eight (Chapter II, Table 1) in the region 4000-200 cm^{-1} in nujol mull (Figures 1-7) are presented in Tables 1 and 2. Infrared spectra of these compounds show a broad, strong composite band in the region 3260-3160 cm^{-1} which can be attributed to the NH stretching vibrations. Sahni and coworkers[102] have reported NH stretching frequencies in the range 3300-3200 cm^{-1} and Sayed and Iskander[103] have reported a band at 3220 cm^{-1} for NH stretching mode in the infrared spectra of aroylhydrazones. Several workers[104-106] have also reported the NH stretching band around 3270 cm^{-1} in the case of open-chain secondary amides.

Characteristic bands around 1640, 1535 and 1310 cm^{-1} due to amide-I, amide-II and amide-III respectively[108] are found in these compounds. The assignment of amide-I (mainly due to $\nu C{=}O$) at 1640 cm^{-1} is in conformity with several such assignments made for hydrazone type Schiff bases[107]. The bands at 1535 and 1285 cm^{-1} have been assigned for amide-II and amide-III respectively in the infrared spectrum of dibenzoylhydrazine[109].

The amide-II absorption band has been a subject of intensive investigation. Usually this band is observed in

the range 1570-1510 cm^{-1} in the solid state and between 1550-1500 cm^{-1} in dilute solution[104,110]. The position of this band is very sensitive to changes in the physical state of the compound. Amide-II band originates from the mixing between the N-H in-plane bending and C-N stretching vibration modes and the relative contribution of these modes is a matter of considerable controversy[111]. The intense bands of ~ 1310 cm^{-1} in these compounds can be attributed to the amide-III band. A broad medium band around 640 cm^{-1} and a strong band around 480 cm^{-1} in these compounds can be assigned to amide-IV (C=O in-plane) and amide-V (C=O out of-plane deformation) respectively. In the case of dipicolinic acid hydrazide, Sahni and coworkers[102] have reported the C=O in-plane and out-of-plane deformation at 640 and 470 cm^{-1} respectively. The presence of the NH stretching band, amide-I, II, III, IV and V bands clearly indicates that these compounds are predominantly in 'keto' form, in the solid state.

The strong intensity bands around 940 cm^{-1} can be attributed to the N-N stretching vibrations. Aggarwal and Narang[113] have assigned the bands in the range 950-930 cm^{-1} for N-N stretching vibrations in the spectra of diacetylhydrazines.

The strong bands around 1600, 1580, 1500 and 1450 cm^{-1} can be assigned for skeletal stretching vibrations as are

usually found in ordinary organic compounds[114]. The characteristic bands around 1000, 800, 720 and 400 cm^{-1} are observed and can be assigned to ring breathing mode, C-H out-of-plane deformation, skeletal mode and C-C out-of-plane deformation mode respectively. The bands around 3085, 1410, 1105, 1020, 830, 500 and 400 are also observed and are assigned for ferrocenyl group as ν C-H, ν C-C or ring deformation, ν C-C, δ C-H, π C-H, ring tilt and (Fe-ring) respectively. These assignments are based on the spectrum reported for ferrocene in the literature[115].

In the spectra of the compounds α-N-salicyloyl-β-N-(methyl)- and α-N-salicyloyl-β-N-ferrocenylidenehydrazides (Figs. 3 and 5), an additional broad and medium intensity band around 3200-2700 cm^{-1}, superimposed on C-H stretching vibrations is observed, which may be associated with an inter/intramolecularly bonded OH vibration. The stretching vibration of unbonded hydroxy group appears as a strong band in the 3620 cm^{-1} region. A shift of this band to the lower frequency is accepted as a criterian for the presence of hydrogen bonding[114]. The nature of hydrogen bonding in these compounds could not be studied because of their limited solubilities in carbon tetrachloride or chloroform, but such intramolecular hydrogen bonding could be studied in case of organotin(IV) complexes of these ligands.

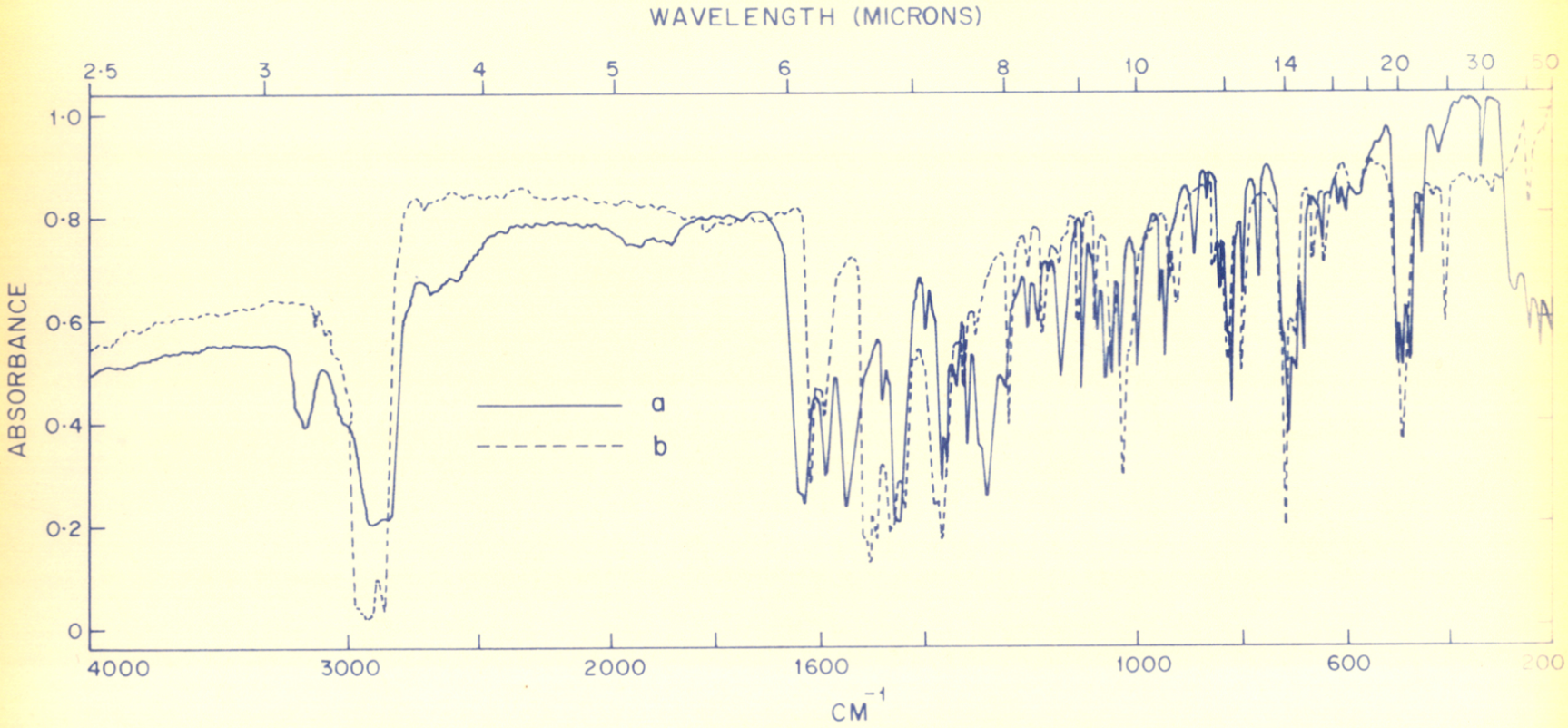

FIGURE 1 : IR SPECTRA OF :

a) α-N-BENZOYL-β-N-FERROCENYLIDENEHYDRAZIDE ,

b) BIS (α-N-BENZOYL-β-N-FERROCENYLIDENEHYDRAZIDATO) COPPER(II) IN NUJOL MULL.

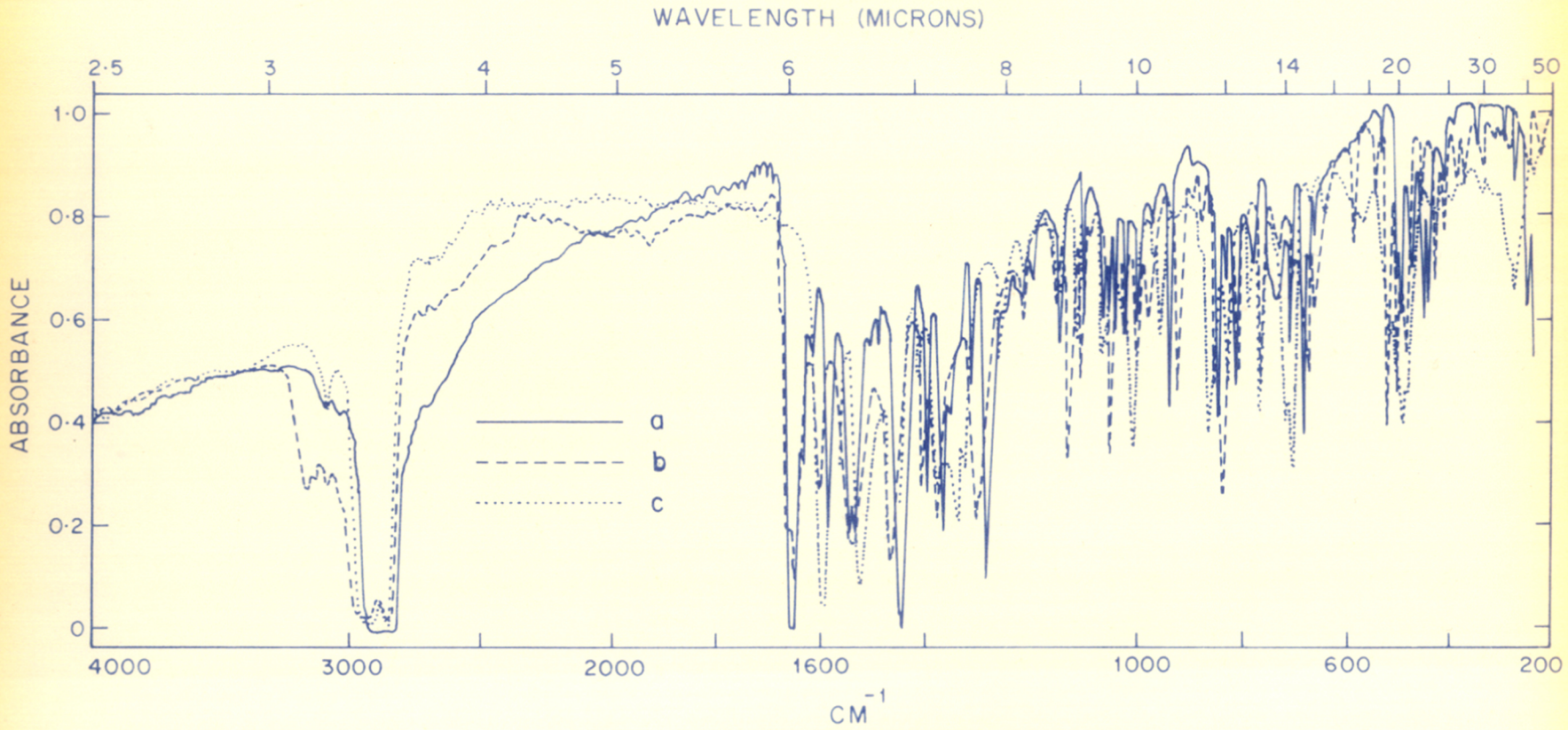

FIGURE 2 : IR SPECTRA OF :

a) α-N-ISONICOTINOYL-β-N-FERROCENYLIDENEHYDRAZIDE,

b) α-N-ISONICOTINOYL-β-N-(METHYL) FERROCENYLIDENEHYDRAZIDE,

c) BIS (α-N-ISONICOTINOYL-β-N-FERROCENYLIDENEHYDRAZIDATO)-COPPER (II) IN NUJOL MULL.

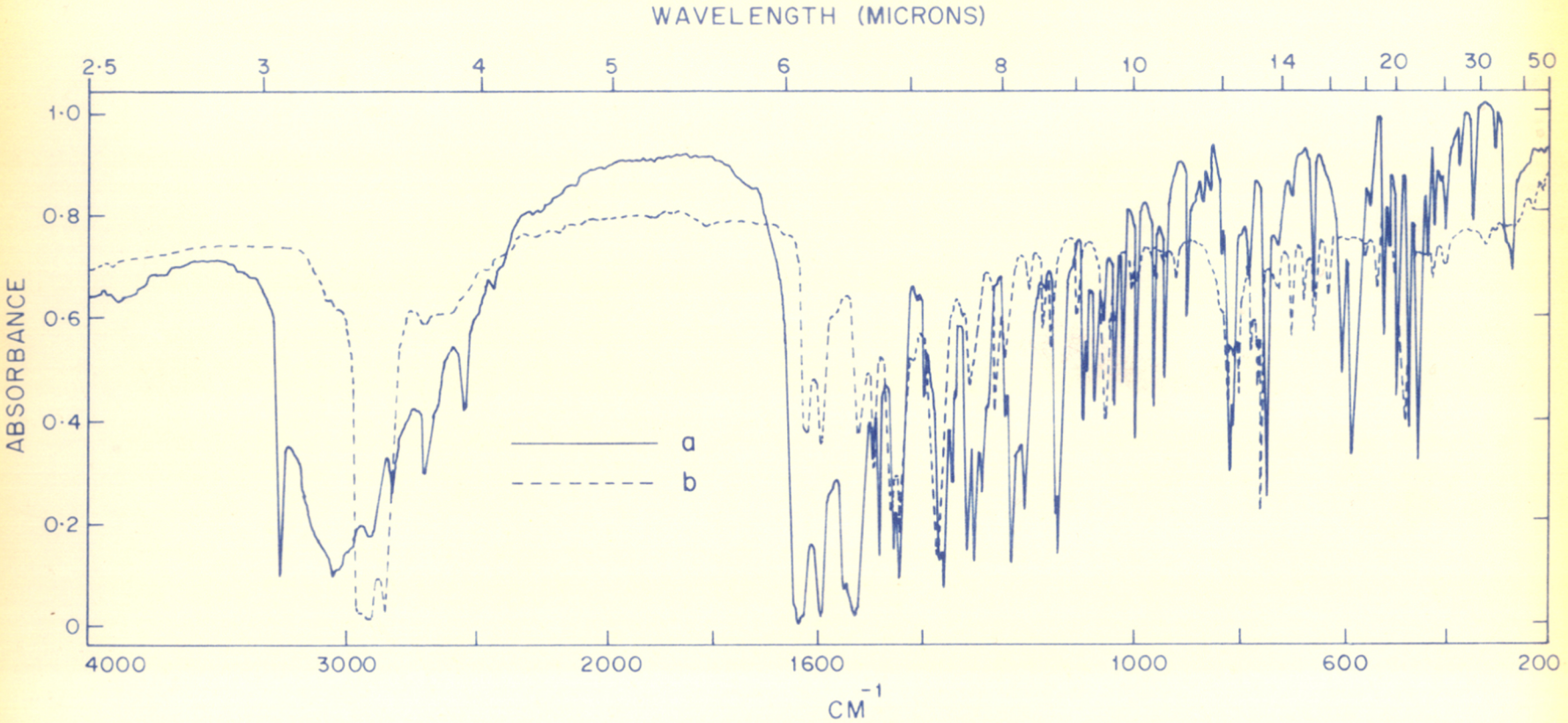

FIGURE 3 : IR SPECTRA OF :

a) α-N-SALICYLOYL-β-N-FERROCENYLIDENEHYDRAZIDE IN HCB/NUJOL

b) BIS(α-N-SALICYLOYL-β-N-FERROCENYLIDENEHYDRAZIDATO)-COPPER (II) IN NUJOL MULL.

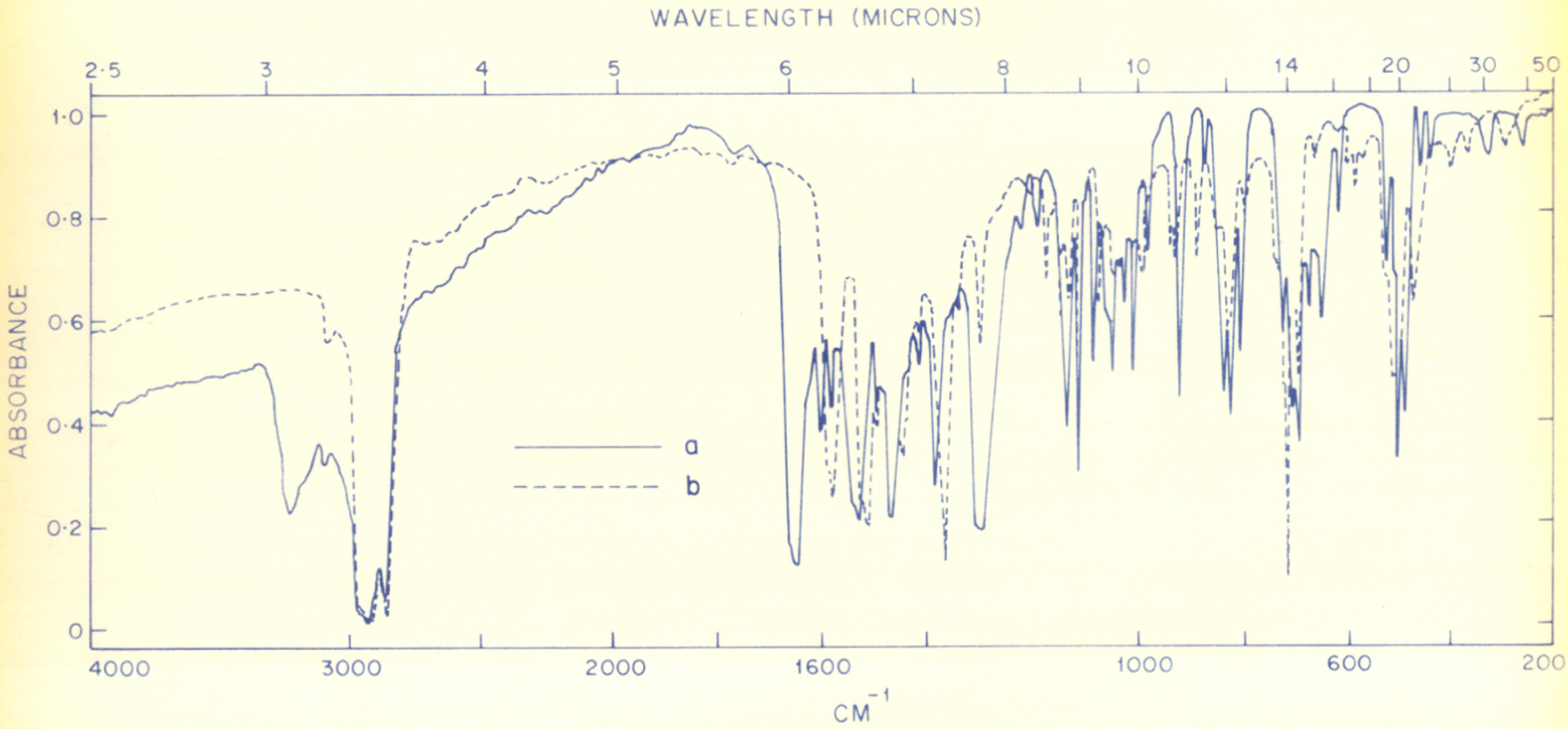

FIGURE 4 : IR SPECTRA OF :

a) α-N-BENZOYL-β-N-(METHYL)-FERROCENYLIDENEHYDRAZIDE,

b) BIS (α-N-BENZOYL-β-N-(METHYL)-FERROCENYLIDENEHYDRAZIDATO)-COPPER (II) IN NUJOL MULL.

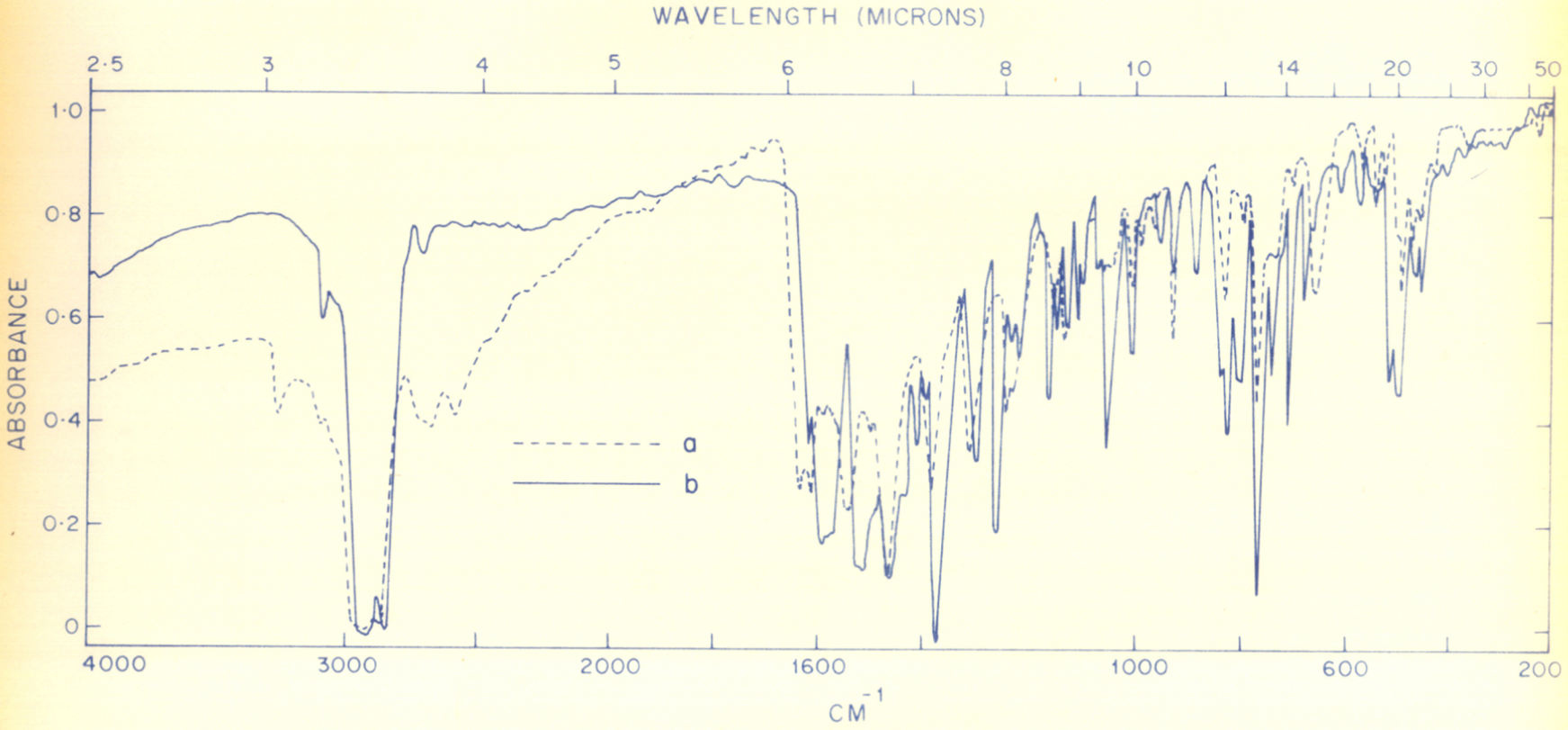

FIGURE 5 : IR SPECTRA OF :

a) α-N-SALICYLOYL-β-N-(METHYL) FERROCENYLIDENEHYDRAZIDE ,

b) BIS (α-N-SALICYLOYL-β-N-(METHYL) FERROCENYLIDENEHYDRAZIDATO)-COPPER (II) IN NUJOL MULL.

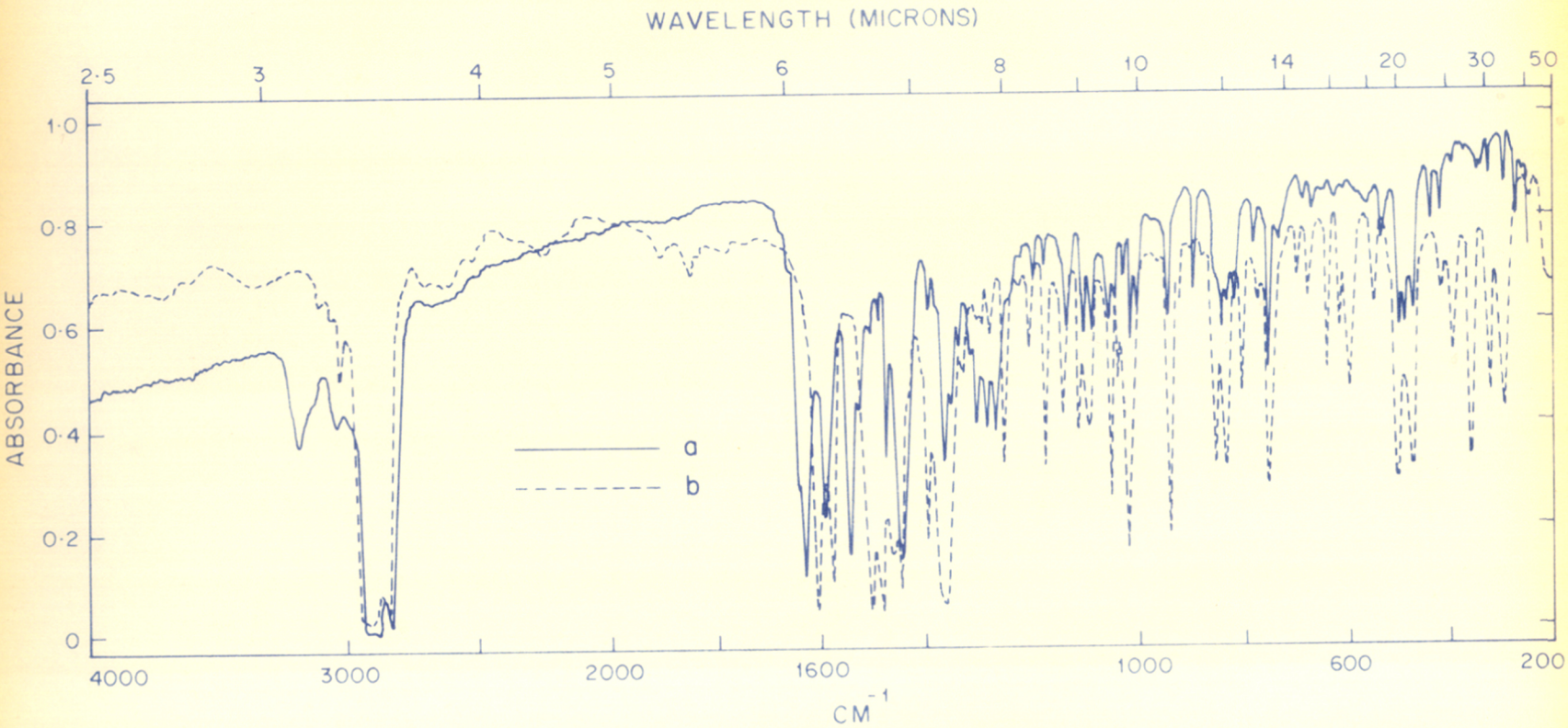

FIGURE 6 : IR SPECTRA OF :

a) α-N-CHLOROBENZOYL-β-N-FERROCENYLIDENEHYDRAZIDE,

b) DICHLORO BIS(α-N-(p) CHLOROBENZOYL-β-N-FERROCENYLIDENEHYDRAZIDATO)-TIN (IV) IN NUJOL MULL.

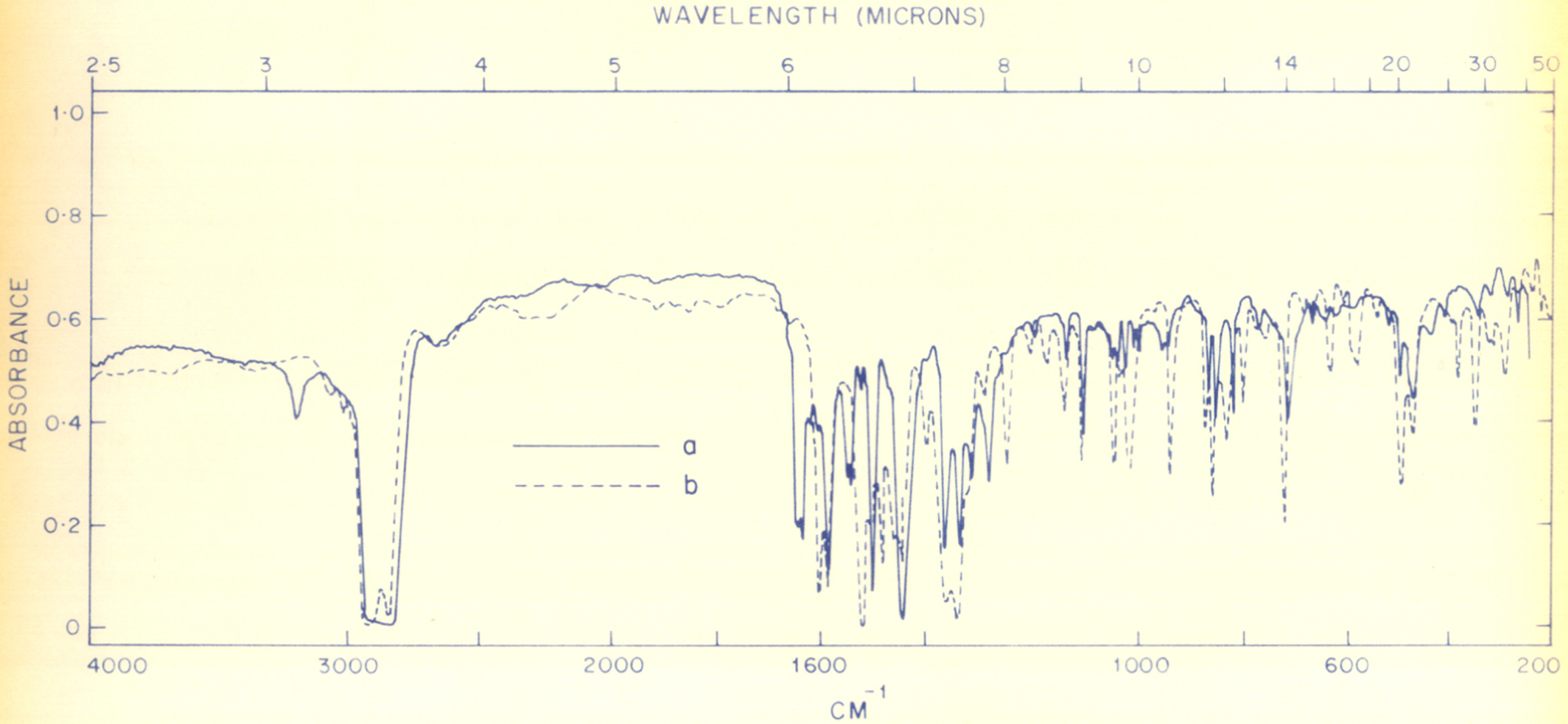

FIGURE 7 : IR SPECTRA OF :

a) α-N-NITROBENZOYL-β-N-FERROCENYLIDENEHYDRAZIDE ,

b) DICHLORO BIS(α-N-(o)-NITROBENZOYL-β-N-FERROCENYLIDENEHYDRAZIDATO)-TIN(IV) IN NUJOL MULL.

TABLE - 1

Infrared absorption frequencies (cm^{-1}) of A. α-N-benzoyl-β-N-ferrocenylidene hydrazide
B. α-N-p-chloro-benzoyl-β-N-ferrocenylidene-hydrazide.
C. α-N-(o)-nitrobenzoyl-β-N-ferrocenylidene-hydrazide.
D. α-N-isonicotinoyl-β-N-ferrocenylidene hydrazide
E. α-N-salicyloyl-β-N-ferrocenylidene hydrazide.

A	B	C	D	E	Possible assignment
3160(br,m)	3200(br,s)	3160(br,m)	3120(m)	3260(vs) 3060-2500(br)	ν NH ν OH
3040(w)	3060(w)	3030(w)			ν CH
2900(br,s)*	2910(s)*	2900(br,s)*	2900(br,s)*		
2830(br,s)*	2830(br,s)*	2830(br,s)*	2830(br,s)*		
1630(s)	1640(vs)	1650(s)	1655(vs)	1660(br,s)	Amide-I
	1620(sh)		1640(sh)		
1580(s)	1590(s)	1590(s)	1590(s)	1595(vs)	
1565(sh)		1560(m)			
1545(s)	1550(sh)	1550(m)	1545(s)	1550(sh) }	Amide-II
1525(sh)	1535(sh)	1525(w)	1535(s)	1530(s,d) }	
1480(m)	1495(vs)	1490(sh)	1490(w)	1480(s)*	ν C=C
1450(br,s)*		1450(vs)*	1456(vs)*	1460(s)	
				1440(s)	
1400(s)		1425(sh)	1400(s)	1400(m)	ν CC or ring def
1370(s)*	1370(s)*	1370(s)*	1370(s)	1370(sh)*	
1355(s)	1360(sh)	1355(sh)	1355(sh)	1360(vs) }	C-H out of plane def.
1340(m)	1340(w)	1340(s)	1340(sh)	1340(m) }	

contd....

TABLE -1 (contd.)

A	B	C	D	E	Possible assignment
1320(s)	1300(m)	1320(m)	1315(m)	1320(s)	
				1300(m)	Amide-III
1280(s)	1280(m)	1280(s)	1285(vs)	1285(m)	
1245(w)	1255(s)	1240(w)	1220(w)	1245(sh)	
				1230(s)	
1200(m)	1200(w)	1200(vw)	1200(w)	1200(m)	
1185(m)	1180(w)	-	-	-	C-H in plane def.
1165(w)	-	-	-	1150(s)	
1140(s)	1135(s)	1140(w)	1145(s)	1140(vs)	
1100(vs)	1100(s)	1100(s)	1100(m)	1100(s)	ν CC or ring def.
	1085(m)	-	-	1090(m)	
1070(m)	-	-	-	1070(m)	
1052(m)	1050(m)	1050(w)	1060(m)	-	
1040(s)	1035(m)	1040(w)	1040(s)	1040(m)	δ CH
1028(s)	1020(w)	1020(m)	1020(s)	1020(m)	
1000(s)	1010(m)	1010(w)	1000(m)	1000(s)	ring breathing
	995(m)	995(w)		965(s)	
950(m)	-	-	-	965(s)	
940(s)	940(s)	940(m)	935(w)	940(s)	ν -N-N
890(m)	890(s)	-	-	900(m)	
865(w)	850(sh)		855(sh)	860(w)	
840(m)	840(m)	840(m)	845(s)	835(w)	π-CH
820(vs)	825(m)		820(m)	820(s)	π-CH
	815(m)	815(m)		810(m)	
795(m)					
	775(w)	770(w)	780(m)	770(w)	ν C-O (phenyl)
	750(s)			750(vs)	

contd....

TABLE -1 (contd.)

A	B	C	D	E	Possible assignment
710(vs)	730(w)	715(s)	730(br,m)	720(w)	Skeletal mode
690(sh)			705(s)		
680(s)	680(w)	-	680(vs)	-	
	665(w)	665(w)	670(sh)	660(m) }	C=O out of plane def.
640(m)	-	-	-	640(s) }	
615(w)	620(w)	620(vw)	-	-	
600(w)				585(vs)	
	560(w)				
	530(m)	520(m)	530(w)	520(s) }	
500(s)	500(s)	500(m)	500(m)	500(s) }	ring tilt. out
490(s)	485(s)		490(s)	}	C=O in-plane def.
472(s)	470(m)	475(s)	470(m)	470(s) }	
450(m)			450(s)	455(s)	
	440(m)	435(w)	440(m)	440(m)	ν(Fe-ring)
425(w)		410(w)		425(m)	
		410(w)			
340(m)	350(w)	350(m)	350(m)	350(m)	
	300(m)		300(w)	310(w)	
260(m)	270(s)	250(m)	260(m)	275(m)	C-C mode

* Nujol peaks

VS = Very strong, s = strong, m = medium, w = weak, VW = Very weak, Sh = Shoulder

TABLE - 2

Infrared absorption frequencies (cm^{-1}) of

A. α-N-benzoyl-β-N-(methyl)ferrocenylidenehydrazide

B. α-N-isonicotinoyl-β-N-(methyl)ferrocenylidene hydrazide and

C. α-N-salicyloyl-β-N-(methyl)ferrocenylidene hydrazide

A	B	C	Possible assignment
3230(br,m)	3180(br,m)	3260(br,m)	ν NH
3100(w)	3090(w)	3100(w)	ν CH
		3060-2500(br,m)	ν OH
2920(br,s)*	2920(br,s)*	2920(br,s)*	
2860(br,s)*	2860(s)*	2850(br,s)*	
1640(br,s)	1640(s)	1625(br,s)	Amide-I
1600(m)	1600(s)	1605(s)	
1580(m)	1550(sh)	1580(vw)	
1525(br,s)	1540(br,s)	1535(br,s)	Amide-II
1480(w)		1490(w)	
1465(br,s)*	1460(br,s)*	1455(br,s)*	
1410(w)	1405(s)		ν CC or ring def.
1380(s)*	1380(s)*	1375(s)*	
1340(vw)	1340(sh,w)		
1300(s)	1305(s)	1305(br,s)	
1280(s)		1230(br,m)	Amide-III
1215(vw)	1215(m)		
1185(w)		1190(sh)	
1140(sh)	1150(m)	1150(m)	C-H in plane def.
1130(s)	1125(s)	1125(m)	
1105(vs)	1105(m)	1110(m)	ν CC or ring def.
1080(s)			
1040(s)	1045(s)	1050(w)	δ CH
1020(m)	1020(m)	1035(w)	
1000(s)	995(br,m)	1000(m)	ring breathing
975(m)	975(m)	980(w)	
920(s)	920(s)	920(s)	ν N-N
870(w)	890(w)	880(vw)	
830(s)	845(m)	870(vw)	π-CH
820(vs)	835(vs)	815(s)	
800(s)	800(m)	785(w)	
	760(s)	760(s)	
720(m)	720(w)	720(w)	Aromatic group vibrations.
700(s)	700(m)		

contd.....

(TABLE -2 contd.)

A	B	C	Possible assignment
690(vs)		690(vw)	
665(m)	670(s)		
640(br,m)	655(m)	645(br,s)	C=O out-of plane def.
	570(m)	580(w)	
610(m)			
	540(m)	530(m)	
520(m)	520(vs)	515(m)	ring tilt
500(s)	500(s)		
480(s)	480(m)	480(s)	C=O in plane def.
455(m)	450(m)	460(m)	ν(Fe-ring)
440(m)	425(s)	420(w)	
	405(m)	400(vw)	
	380(w)		
	370(w)		
330(w)	340(w)	340(w)	
260(w)	255(w)	240(w)	C-C mode

* Nujol peaks

4.2 Copper(II) complexes

The infrared spectra of copper(II) complexes of ferrocenyl ligands are presented in Figs. 1-5 and Table 3.

The infrared spectra of these compounds show significant changes as compared with those of the parent ligands. The bands due to N-H stretching, amide-I, III, IV and V are absent in the spectra of these compounds. Instead, a very sharp band is observed in the range 1620-1600 cm^{-1}. This band can be related to the stretching vibration mode of the conjugate -C=N-N=C grouping analogous to that for azines[116]. Disappearance of ν(N-H) and amide-I, III, IV and V bands and the formation of a neutral copper(II) complex molecule indicate that keto-enol tautomerization takes place in the solution in the presence of metal ion.

In the spectra of these complexes amide-II band shifts to lower frequency. This change in amide-II bands indicates the coordination of metal to amide oxygen of the ligand. A slight positive shift in the ν(N-N) frequency has also been observed on chelation which indicates the coordination of β-nitrogen to the metal ion (Fig.15). The positive shift in N-N stretching frequency suggests that the nitrogen of the azomethine group is coordinated to metal ion in the case of aroyl hydrazone complexes[117,118].

A new medium to strong intense band appearing at 1260-1220 cm^{-1} in the copper(II) complexes can be assigned for C-O stretching vibration. This clearly supports the deprotonation or removal of secondary amide hydrogen atom via the enol form as shown in Fig.14.

The infrared spectra of all these compounds show bands at 3085, 1411, 1108, 1002, 834, 492 and 478 cm^{-1} which are assigned for ferrocenyl group as in the case of ligand spectrum.

In the far infrared region two strong to medium intensity bands ~ 425 and 280 cm^{-1} are observed, which are not seen in the spectra of free ligands. These can be assigned to (Cu-N) and (Cu-O) stretching vibrations. The Cu-N stretching frequency is of particular interest and a subject of controversy. Because of the relatively heavy mass of the metal and the low bond order of the coordinate bond, the Cu-N stretching vibration appears in low frequency region. Powell and Sheppard[119] have assigned the band at 419 cm^{-1} to (Cu-N) stretching vibrations in the spectra of glycino-complexes. The copper-nitrogen stretching frequencies assigned in the literature for these compounds are always higher by 40-60 cm^{-1} than those for the corresponding tetramine complexes. In the spectra of glycineglycino copper(II) trihydrates and bis-(aminomethane sulfanato)copper(II), the bands

TABLE -3

Infrared absorption frequencies (cm^{-1}) of :

A. Bis(α-N-benzoyl-β-N-ferrocenylidene hydrazidato)copper(II), B. Bis(α-N-isonicotinyl)-β-N-ferrocenylidene hydrazidato)copper(II), C. Bis(α-N-salicyloyl-β-N-ferrocenylidene-hydrazidato)copper(II), D. Bis(α-N-benzoyl-β-N-(methyl)ferrocenylidenehydrazidato)-copper(II) and E. Bis(α-N-salicyloyl-β-N-(methyl)ferrocenylidenehydrazidato)copper(II).

A	B	C	D	E	Possible assignment
3080(w)	3090(w)	3100(vw)	3100(vw)	3100(w)	ν CH
2920(s)*	2920(br,s)*	2920(s,br)*	2920(br,s)*	2920(br,s)*	
2860(s)*	2850(s)*	2860(s)*	2850(s)*	2860(s)*	
		3100-2500 (br,m)		3100-2500(br,s)	OH
1615(s)		1620(m)		1620(w)	-C=N-N=C- mode
1600(m)	1590(br,s)	1595(m)	1600(sh)	1590(br,s)	
1590(m)	1570(m)		1580(vs)	1575(br,s)	ν C=C
1510(sh)	1515(br,s)	1525(m)	1525(s,sh)	1505(br,s)	Amide-II
1500(vs)	1500(sh)	1495(m)	1500(s)	1500(sh)	
1480(s)		1460(m)*	1460(br,s)*	1465(s)*	
1460(br,s)*	1460(br,s)*				
1440(s)		1440(s)	1440(w)	1435(sh)	
	1410(m)		1415(w)	1415(m)	
1385(sh)					
1375(sh)*	1375(m)*	1375(vs)*	1375(sh)*	1370(vs)*	
1365(s)	1335(s)		1365(vs)		C-H out of plane def.
1325(m)	1320(m)				
1300(w)	1310(w)	1310(m)	1300(m)	1300(s)	
1240(s)	1260(m)	1260(s)		1260(vs)	Amide-III
		1245(m)		1235(w)	ν C-O
1200(w)	1210(w)	1200(w)	1215(vw)	1220(m)	

contd...

(TABLE -3 contd.)

A	B	C	D	E	Possible assignment
1170(m)		1170(w)	1170(m)	1160(s)	
1140(w)	1150(m)	1160(m)	1140(w)	1150(m)	
			1130(m)	1130(m)	ν C-C or ring def.
1105(m)	1110(s)	1110(m)	1110(s)	1110(m)	
1070(m)	1090(vw)	1100(sh)	1070(m)	1100(w)	
	1060(m)				
1040(m)	1050(m)	1052(s)	1040(s)	1050(s)	CH
1020(vs)	1015(sh,w)	1030(w)			
1010(sh)	1005(s)	1005(w)	1010(m)	1005(m)	ring breathing
930(w)	950(m)	955(w)	990(m)	955(w)	ν N-N
920(m)		920(w)	920(m)	930(w)	
	870(sh)		880(m)		
850(w)	850(s)		845(sh)	855(m)	
820(s)	815(s)	820(s)	825(vs)	825(s)	π-CH
795(s)		795(s)	790(m)	800(m)	
	775(m)	775(m)			
	760(s)	760(ws)		760(m)	
705(vs)	705(s)	700(m)	710(vs)	705(s)	Skeletal mode
690(m)	695(vs)	670(w)	690(s)		
655(m)		655(m)	660(w)	670(m)	
630(m)	640(w)	630(m)		660(sh)	
580(w)	590(vw)		595(w)	600(w)	
	560(br,w)	560(w)	580(w)	565(w)	
	520(sh)	535(w)		535(w)	
500(w)	510(m)		505(br,s)	505(s)	
490(vs)	495(sh)				
	480(vs)	480(br,s)	495(s)	485(s,br)	ring tilt
455(sh)	470(sh)	465(sh)	470(s)	460(m)	C-C out of plane def.
405(s)	425(m)	430(w)		440(m)	
	380(w)	405(w)	405(w)	400(w)	ν Cu-N
320(w)	340(w)	330(vw)	365(w)		
285(w)	270(br,m)	290(w)	295(br,w)	290(w)	ν Cu-O
240(m)	240(w)	270(w)	230(w)	230(w)	

* Nujol peaks

at 445 and 440 cm^{-1} are assigned to Cu-N stretching modes[120]. Nakamoto and Martell[121] studied the spectrum (in the far infrared region) of the compound bis-(acetylacetonato)-copper(II) and bands at 455 cm^{-1} and 320 cm^{-1} are assigned for Cu-O asymmetric and Cu-O symmetric stretching modes.

4.3. Tin(IV) complexes

The infrared spectra of the dialkyl and dichlorotin(IV) complexes of substituted α-N-benzoyl-β-N-ferrocenylidene-hydrazides in the region 4000-200 cm^{-1} are presented in Figs. 6-13. The observed frequencies along with possible assignments are given in Tables 4-6.

As observed in the case of copper(II) complexes, the bands due to N-H stretching, >C=O stretching, >C=O out-of-plane and in-plane deformation vibrations are not observed in the spectra of these compounds. Also a new band around 1230 cm^{-1} appears and may be assigned to C-O stretching vibration. The disappearance of ν(NH), ν(C=O) bands and appearance of new bands due to ν(C-O), ν(Sn-N) and ν(Sn-O) indicate that ligands enolize in solution and then react with metal ions forming the metal-complexes.

A strong band observed in the spectra around 1605 cm^{-1} can be ascribed to the stretching vibration mode of conjugate -C=N-N=C- grouping. Such type of stretching vibration mode has also been observed in the case of copper(II) complexes

of the same ligands. In the spectra of these compounds amide-II band shifts to the lower frequency by ca.40 cm^{-1}. This negative shift in amide-II band indicates the coordination of metal to amide oxygen of the ligand. A new medium to strong intense band appearing around 1260-1220 cm^{-1} in the spectra of all these compounds can be assigned to C-O stretching vibration. This clearly indicates the removal of secondary amide hydrogen atom via an enol form as shown in Fig. 14.

The characteristic bands of ferrocenyl moiety are also observed and assigned as reported in the previous sections.

Far infrared spectroscopy

Some new bands presumably due to ν Sn-O, ν Sn-N, ν Sn-C and ν Sn-Cl are observed in the infrared spectra of dichloro-, dibutyl- and dioctyltin(IV) chelates in the region 700-200 cm^{-1} (Figs. 6-13 and Tables 4-6).

Sn-C stretching vibrations

In the spectra of organotin(IV) compounds, strong-medium intense bands around 610 cm^{-1}, characteristic of Sn-alkyl groups, which are not observed in the spectra of ligands and dichlorotin(IV) chelates, are observed and can be assigned to (Sn-C) stretching mode. The appearance of a single band due to (Sn-C) stretching mode suggests

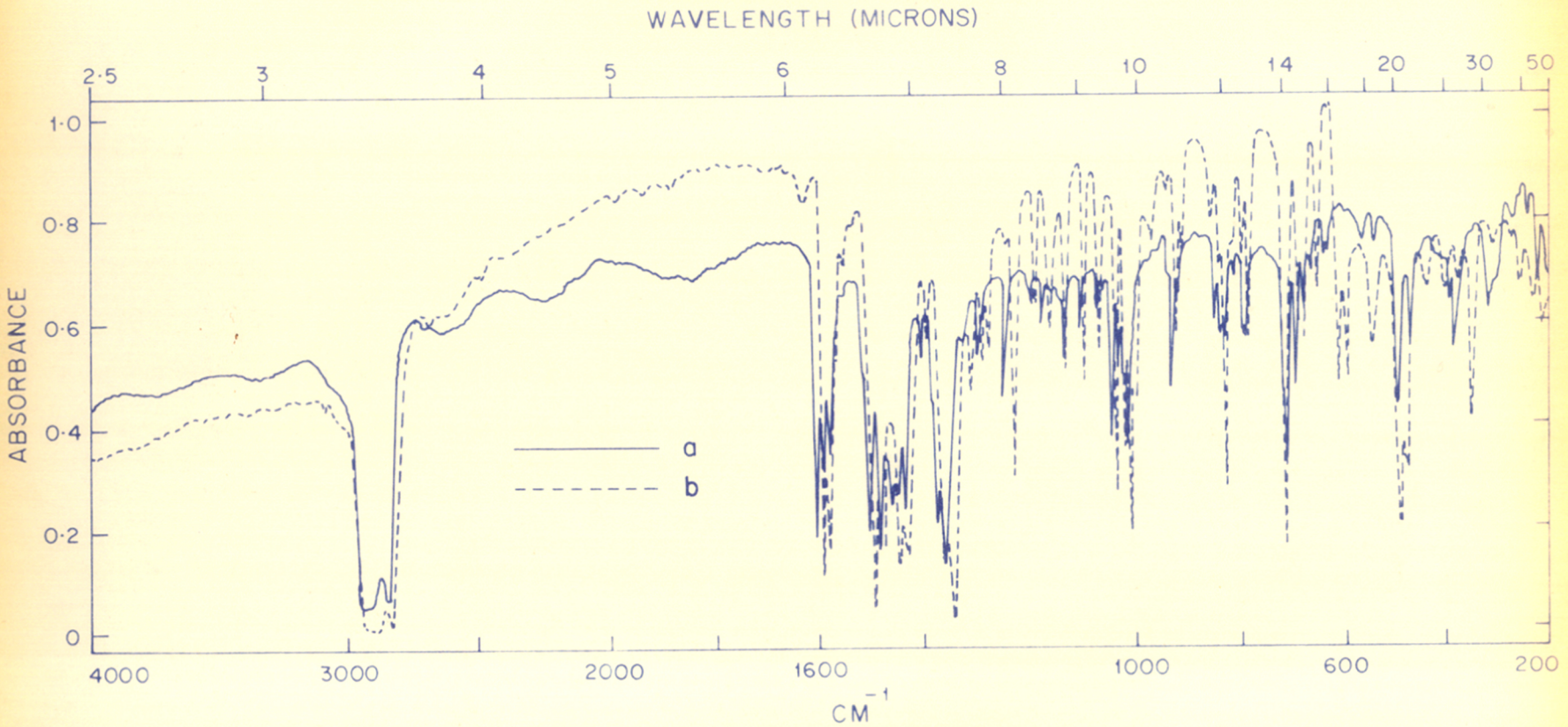

FIGURE 8 : IR SPECTRA OF :

a) DICHLORO BIS(α-N-BENZOYL-β-N-FERROCENYLIDENEHYDRAZIDATO) TIN (IV),

b) BIS(α-N-BENZOYL-β-N-FERROCENYLIDENEHYDRAZIDATO) DIBUTYL TIN (IV) IN NUJOL MULL.

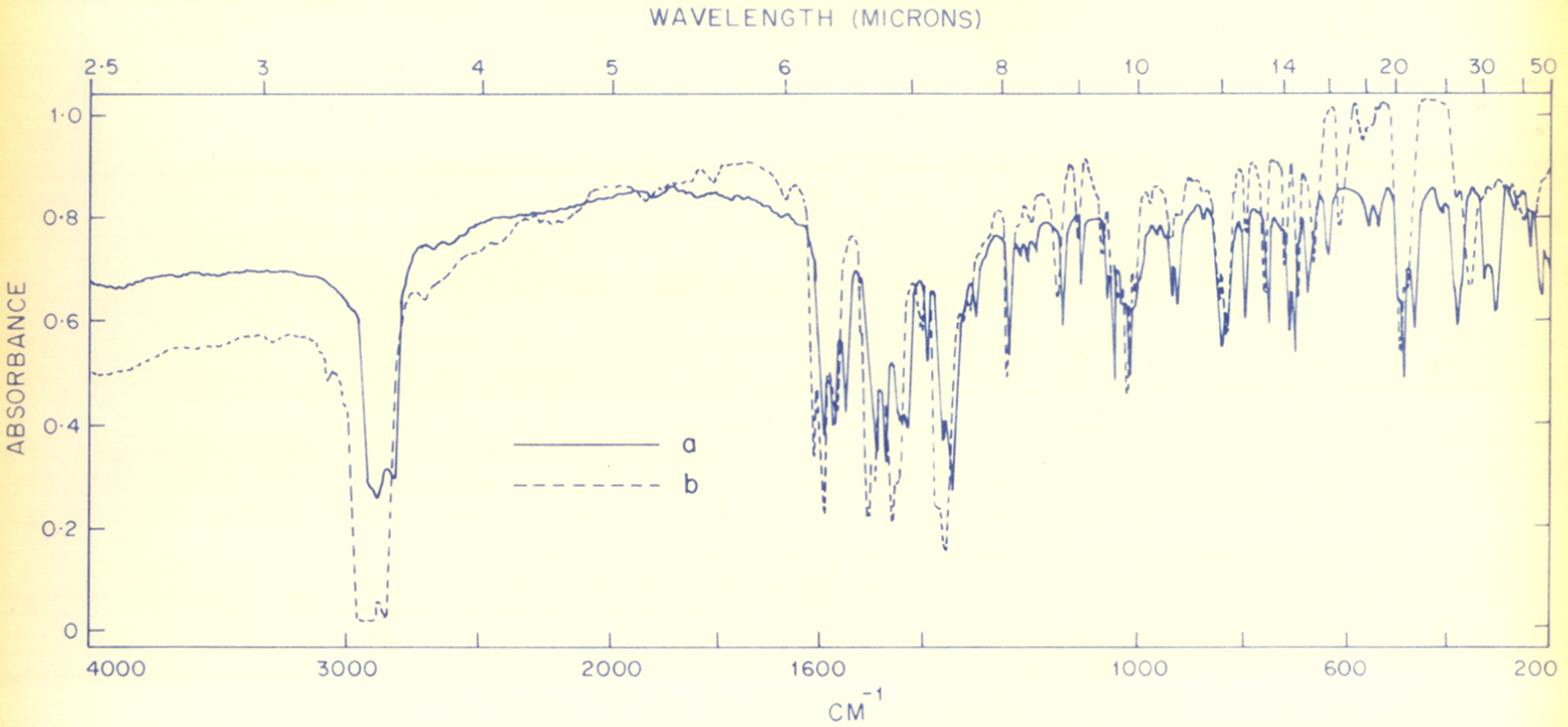

FIGURE 9 : IR SPECTRA OF :

a) DICHLORO BIS (α-N-ISONICOTINOYL-β-N-FERROCENYLIDENEHYDRAZIDATO)-TIN (IV),

b) BIS (α-N-ISONICOTINOYL-β-N-FERROCENYLIDENEHYDRAZIDATO) DIBUTYLTIN(IV) IN NUJOL MULL.

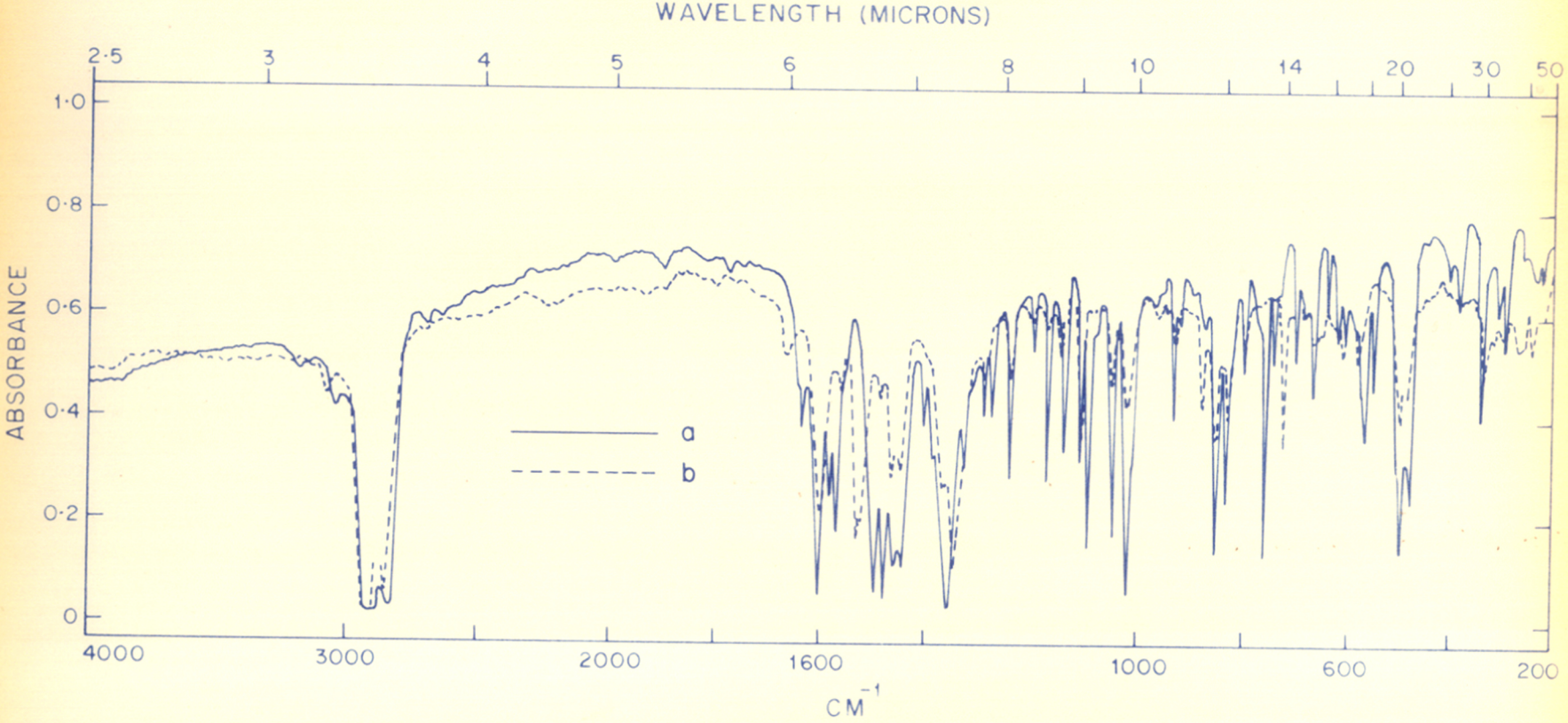

FIGURE 10 : IR SPECTRA OF : BENZOYL

a) BIS(α-N-(p) CHLORO-β-N-FERROCENYLIDENEHYDRAZIDATO) DIBUTYLTIN (IV),

b) BIS (α-N-(o) NITROBENZOYL-β-N-FERROCENYLIDENEHYDRAZIDATO)-DIBUTYLTIN(IV) IN NUJOL MULL.

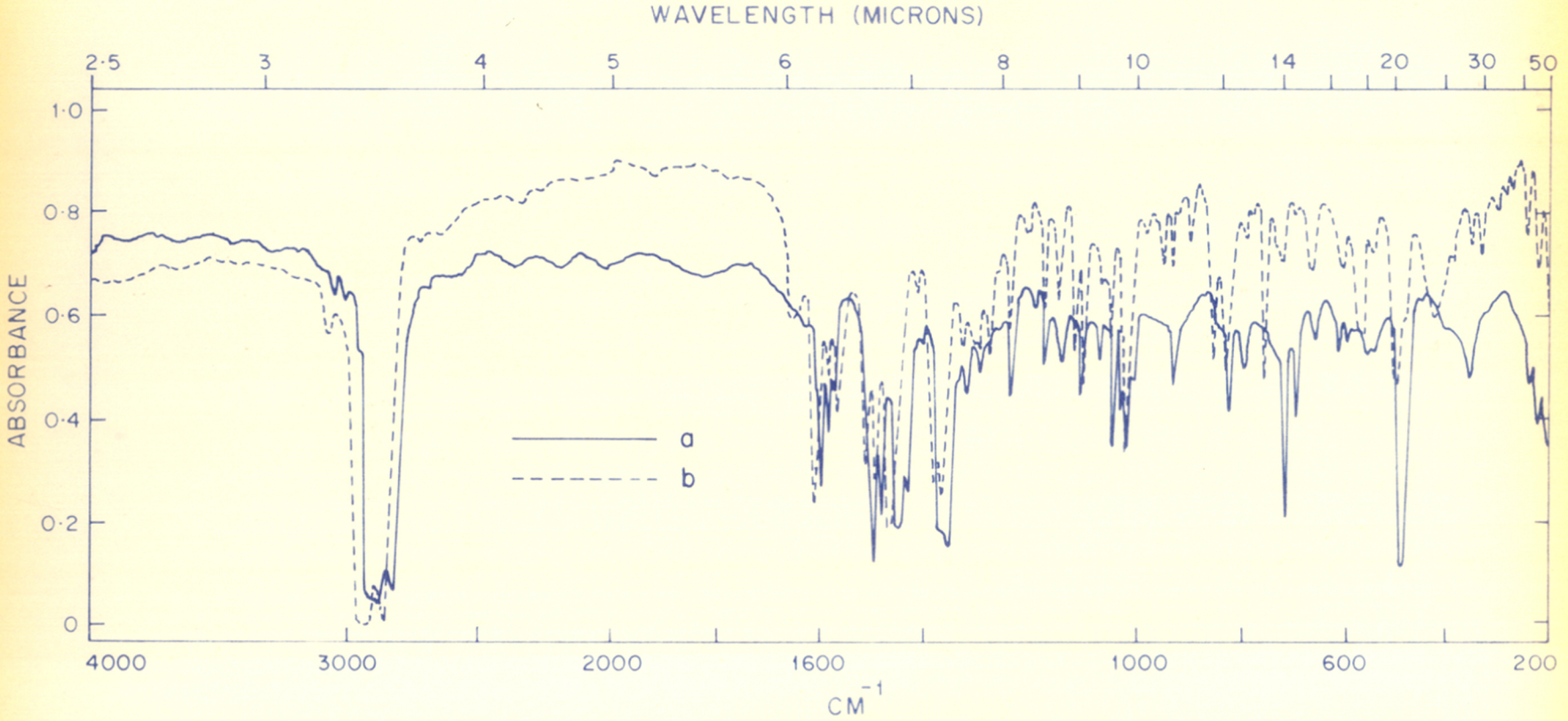

FIGURE 11 : IR SPECTRA OF :

a) BIS(α-N-BENZOYL-β-N-FERROCENYLIDENEHYDRAZIDATO) DIOCTYLTIN (IV),

b) BIS(α-N-(p) CHLOROBENZOYL-β-N-FERROCENYLIDENEHYDRAZIDATO)-DIOCTYLTIN(IV) IN NUJOL MULL.

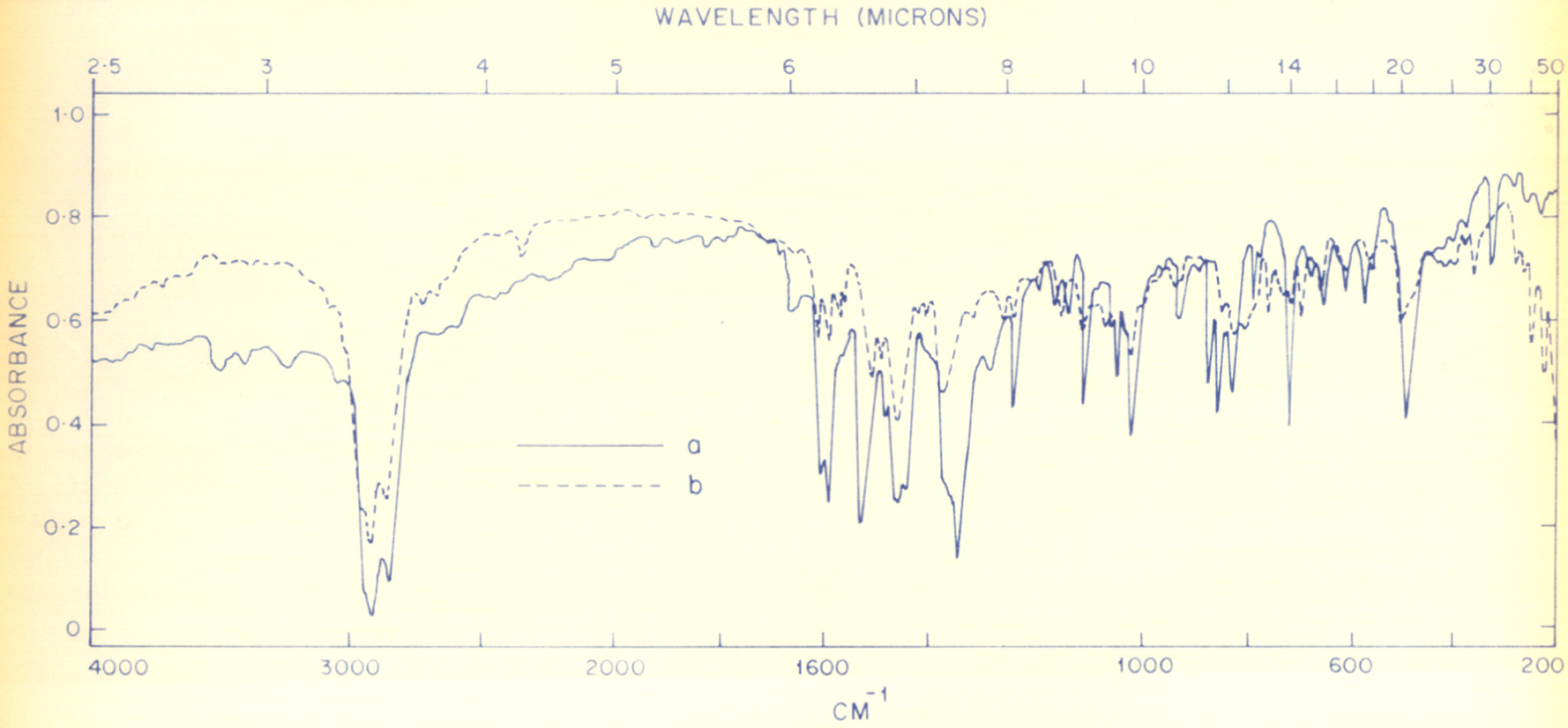

FIGURE 12 : IR SPECTRA OF :

a) BIS(α-N-(o)-NITROBENZOYL-β-N-FERROCENYLIDENEHYDRAZIDATO)-DIOCTYLTIN(IV),

b) BIS(α-N-ISONICOTINOYL-β-N-FERROCENYLIDENEHYDRAZIDATO)-DIOCTYLTIN(IV) IN NUJOL MULL.

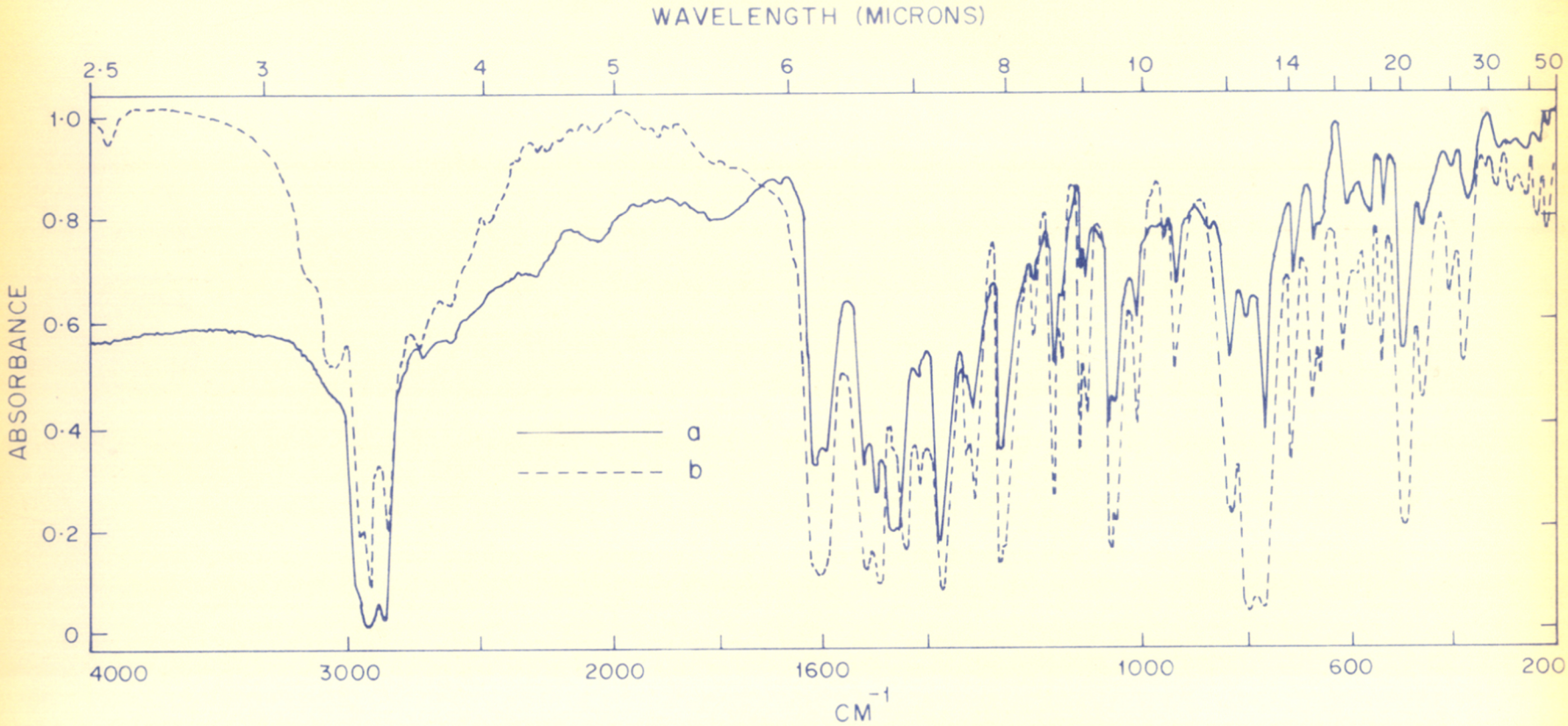

FIGURE 13 : IR SPECTRA OF :

a) BIS(α-N-SALICYLOYL-β-N-FERROCENYLIDENEHYDRAZIDATO) DIBUTYLTIN (IV) IN NUJOL MULL,

b) BIS(α-N-SALICYLOYL-β-N-FERROCENYLIDENEHYDRAZIDATO) DIBUTYLTIN(IV) IN CCl_4.

TABLE -4

Infrared absorption frequencies (cm^{-1}) of A. bis(α-N-benzoyl-β-N-ferrocenylidene-hydrazidato)tin(IV)-dichloride, B. bis-(α-N-p-chlorobenzoyl-β-N-ferrocenylidene-hydrazidato)tin(IV)dichloride, C. bis(α-N-(o)-nitrobenzoyl-β-N-ferrocenylidene-hydrazidato)tin(IV)dichloride and D. bis(α-N-isonicotinoyl-β-N-ferrocenylidene-hydrazidato)tin(IV)dichloride.

A	B	C	D	Possible assignment
3025(w)	3025(w)	3020(w)	3020(w)	ν CH
2960(br,s)*	2930(br,s)*	2930(br,s)*	2920(br,s)*	
2840(br,s)*	2840(br,s)*	2840(br,s)*	2820(br,s)*	
1605(s)	1610(vs)	1605(vs)	1600(s)	-C=N-N=C mode
1590(m)	1585(sh)	1590(s)	1570(s)	
1580(m)	1575(s)	1525(vs)	1550(s)	
1500(s)	1498(s)	1500(w)	1490(s)	Amide-II
1480(s)	1478(s)	1482(m)	1475(s)	
1455(m)*	1460(m)*	1460(m)*		
1430(m)	1440(s)	1440(s)	1450(sh)	
1370(s)*	1390(s)*	1400(m)	1400(m)	ν CC or ring def.
1360(vs)*	1360(s,d)*	1360(s)*	1365(m)*	
	1325(w)	1340(s)	1350(s)	
1300(m)	1300(w)	1315(sh)	1300(w)	C-H out of plane def.
	1280(w)	1290(w)		
1250(s)	1250(s)	1250(m)	1240(s)	ν C-O
1200(w)	1200(m)	1200(w)	1220(w)	

contd....

(TABLE -4 contd.)

A	B	C	D	Possible assignment
1170(m)	1170(s)	1170(w)	1190(w)	C-H in-plane def.
1135(m)	1135(s)	1135(m)	1135(s)	
1105(w)	1105(s)	1105(s)	1100(m)	ν CC or ring def.
1070(w)	1085(m)		1055(m)	
1040(s)	1045(s)	1045(s)	1040(s)	δ CH
1030(w)	1030(w)	1030(w)	1025(w)	
1000(sh)	1010(vs)	1020(s)	1010(m)	ring breathing
930(s)	932(vs)	935(s)	930(m)	ν N-N
915(w)	910(w)	865(m)	920(m)	
845(w)	845(s)	850(s)	870(w)	
835(w)	830(s)	830(m)	830(s)	π-CH
			820(m)	
825(m)	800(m)	800(m)	800(s)	
785(m)	760(w)	760(w)	770(s)	
			765(m)	Skeletal mode
712(sh)	742(s)	715(vs)	730(m)	
690(m)	690(w)	680(w)	690(m)	
675(w)	670(m)	665(w)	670(m)	Skeletal mode
630(w)	632(m)	630(m)	630(m)	
560(w)	580(s)	580(m)	550(w)	
540(w)	540(m)	540(w)	530(w)	ν Sn-O
500(m,sh)	500(vs)	490(vs)	485(vs)	ring tilt
490(s)			465(s)	C-C out of plane def.
470(m)	470(vs)	470(s)	410(w)	
395(w)	410(w)		380(s,d)	ν -Sn -SnN
385(s)	390(m)	385(m)		
	358(s)	350(s)	330(m)	ν -Sn-Cl
325(m)	320(s)	330(w)	310(s)	
305(m)	300(sh)	295(m)		
	290(s)	270(w)		
240(w)	240(w)	240(w)	260(w)	C-C mode

* Nujol peaks

TABLE -5

Infrared absorption frequencies (cm^{-1}) of A. Bis(α-N-benzoyl-β-N-ferrocenylidene-hydrazidato)dibutyltin(IV), B. Bis(α-N-p-chlorobenzoyl-β-N-ferrocenylidene-hydrazidato)dibutyltin(IV), C. Bis(α-N-(o)-nitrobenzoyl-β-N-ferrocenylidene-hydrazidato)dibutyltin(IV), D. Bis(α-N-isonicotinoyl-β-N-ferrocenylidene-hydrazidato)dibutyltin(IV) and E. Bis(α-N-salicyloyl-β-N-ferrocenylidene-hydrazidato)dibutyltin(IV).

A	B	C	D	E	Possible assignment
				3200 - 2500 (br, m)	ν OH
3060(w)	3060(w)	3090(w)	3040(w)	[illegible]	ν C=C
2900(br,s)*	2920(br,s)*	2930(s)*	2940(br,s)*		
2840(s)*	2840(br,s)*	2860(br,s)*	2840(br,s)*		
	1630(w)	1670(w)			
1590(vs)	1600(s)	1610(s)	1610(s)	1610(s)	-C=N-N=C- mode
1580(vs)	1580(m)	1595(s)	1590(vs)	1590(s)	
	1565(s)	1570(w)	1570(m)		
		1530(s)			
1500(vs)	1500(sh)	1520(sh)	1520(vs)	1515(s)	Amide-II
1480(s)	1490(s)	1490(w)	1480(s)	1490(s)	
	1470(s)	1470(m)		1460(s)*	
1450(s)*	1450(m)*	1450(m)*	1450(sh)*	↓	
1430(s)	1440(m)				
1400(w)	1400(m)		1410(w)	1415(w)	
1365(s)*	1380(m)*		1380(s,sh)*	1380(s)*	
1350(vs)	1350(br,s)	1330(sh)	1360(vs)	1340(sh)	C-H out of plane def.
1325(m)	1320(m)	1320(sh)	1315(w)	1310(m)	

contd...

(TABLE -5 contd.)

A	B	C	D	E	Possible assignment
1295(m)	1288(m)	1295(s)		1300(sh)	
1280(m)	1270(m)	1260(w)		1260(s)	
1230(s)	1235(s)	1240(m)	1240(m)	1250(s)	ν C-O
1190(m)	1190(m)	1200(w)	1200(w)	1200(w)	
1165(s)	1160(s)	1170(w)			C-H in-plane def.
1130(s)	1130(s)	1140(m)	1150(m)	1160(s)	
		1110(s)	1110(m)	1110(m)	ν CC or ring def.
1100(s)	1100(s)			1100(m)	
1070(s)	1085(vs)	1045(m)	1060(m)		
1035(vs)	1035(s)	1030(m)	1040(s)	1050(s)	
			1030(m)	1040(s)	δ CH
1020(s)	1010(vs)	1015(s)	1015(vs)		
1005(vs)	1000(sh)	1000(sh)	990(m)	1000(m)	ring breathing
1000(s)					
	925(m)		930(w)	930(m)	ν N-N
920(s)	920(m)	920(m)	910(w)		
910(m)	910(w)				
860(m)	865(w)	870(s)		860(w)	
835(m)	840(s)	850(s)	840(m)		π-CH
825(vs)	820(s)	825(m)	825(s)	820(s)	
795(m)	790(m)	785(w)	790(m)	790(m)	
780(s)	750(vs)		750(s)	760(vs)	
710(vs)	730(m)	720(vs)	710(m)	700(m)	Skeletal mode
690(s)	690(m)		690(s)		
680(s)				665(m)	

contd....

(TABLE -5 contd)

A	B	C	D	E	Possible assignment
650(s)	655(s)	650(w)	655(m)	650(sh)	
	630(w)				
605(s)	610(m)	605(m)	605(s)	605(m)	νSn-C
595(s)	595(w)		590(sh)		
	560(s)	580(m)	570(w)	560(w)	νSn-O
545(m)	540(m)			540(m)	
490(vs)	490(vs)	495(s)	495(vs)	490(vs)	
475(s)	470(s)	480(s)	480(sh)		
405(w)	400(w)				
380(w)	380(m)	380(br,w)	380(m)	370(m)	νSn-N
355(s)	330(s)	330(m)	360(s)		
315(w)	300(w)	300(w)		310(w)	
	280(m)				
260(m)	250(w)	260(m)	250(w)	260(w)	C-C mode

* Nujol peaks

TABLE - 6

Infrared absorption frequencies (cm^{-1}) of A. Bis(α-N-benzoyl-β-N-ferrocenylidenehydrazidato)dioctyltin(IV), B. Bis(α-N-p-chlorobenzoyl-β-N-ferrocenylidenehydrazidato)dioctyltin(IV), C. Bis(α-N-(o)nitrobenzoyl-β-N-ferrocenylidenehydrazidato)dioctyltin(IV), D. Bis(α-N-isonicotinoyl-β-N-ferrocenylidenehydrazidato)-dioctyltin(IV) in Nujol and E. Bis(α-N-salicyloyl-β-N-ferrocenylidenehydrazidato) dioctyltin(IV) in CCl_4.

A	B	C	D	E	Possible assignment
				3100-2500(br,m)	ν OH (bonded)
3040(br,w)	3090(br,w)	3100(br,w)	3080(w,br)	3060(w)	ν CH
2900(br,s)*	2940(br,s)*	2930(s)*	2920(br,s)*	2930(s)*	
2830(s)*	2860(br,s)*	2860(br,s)*	2860(br,s)*	2860(s)*	
	1650(ws)	1670(w)			
1600(vs)	1610(vs)	1610(s)	1610(s)	1605(br,s)	-C=N-N=C mode
1580(vs)	1590(sh)	1595(vs)	1590(vs)		
1572(m)	1580(m)	1560(vs)	1570(m)		
1500(vs)	1505(s)	1500(sh)	1510(s)	1515(s)	Amide-II
	1490(s)		1490(m)	1490(s)	
1480(s)	1465(vs)*	1460(br,s)*	1460(vs)*	1460(sh)*	
1450(s)*	1450(sh)*	1450(sh)	1450(br,s)	1440(s)	ν C=C or
1430(s)				1410(w)	ν C-C
1365(s)*	1380(vs)*	1380(sh)*	1370(vs)*	1370(br,s)*	
1350(vs)	1360(s)	1350(vs)			
1325(m)			1320(w)	1310(m)	C-H out-of plane
1295(m)	1290(br,w)	1290(w)			def.
1280(m)	1280(m)		1260(m)		

contd...

(TABLE-6 contd.)

A	B	C	D	E	Possible assignment
1230(s)	1240(s)	1240(s)	1240(m)	1250(vs)	ν C-O
1190(m)		1200(w)	1200(w)	1200(m)	
1165(s)	1170(s)	1170(w)		1160(s)	C-H in plane def.
1130(s)	1140(s)	1140(m)	1150(s)	1145(m)	
1100(s)	1110(s)	1110(s)	1110(s)	1110(s)	ν CC or ring def.
1070(s)	1090(vs)	1055(sh)	1060(m)	1050(s)	
1035(vs)	1040(m)	1045(m)	1040(s)	1040(sh)	δ CH
1020(s)	1015(vs)	1025(s)	1015(s)		ring breathing
1005(vs)	945(m)		990(w)	1000(m)	
1000(s)					
980(s)	930(m)	930(m)	930(m)	930(s)	ν N-N
			920(m)		
860(m)	890(m)	870(s)			
835(m)	845(s)	850(vs)	840(m)	840(sh)	π-CH
825(vs)	820(vs)	830(s)	820(s)	820(s)	π-CH
795(m)	785(w)	785(m)	790(s)		
780(s)	750(vs)		750(s)		
710(vs)	720(w)	720(vs)	710(m)		
690(s)				705(s)	
680(s)	660(m)	680(w)	685(s)	665(m)	Skeletal mode
650(s)	655(m)	650(m)	650(m)	650(w)	
605(s)	600(w)	610(m)	610(m)	605(m)	ν Sn-C
595(s)		580(m)		580(w)	

contd...

(TABLE-6 contd.)

A	B	C	D	E	Possible assignment
545(m)	560(s)	560(sh)	560(m)	560(m)	νSn-O
	540(w)	500(vs)	495(vs)	535(m)	ring tilt.
490(vs)	490(s)	480(sh)	480(sh)	490(br,s)	
475(s)	420(br,s)			435(m)	
380(w)	380(br,w)	380(w)	410(w)	405(w)	
335(s)	330(m)	330(s)	360(s)	380(m)	νSn-N
315(w)	300(m)	290(w)	275(m)	285(w)	
260(m)	275(w)		260(m)	260(w)	C-C mode.
230(m)	240(m)	245(w)	245(s)	240(w)	

* Nujol peaks

that these compounds may have a symmetrical structure with two alkyl groups in trans-position. This assignment of (Sn-C) stretching mode for bands around 610 cm^{-1} is in accordance with the work of Poller[122] and Lohmann[123]. These authors have reported a single, strong band in the region 580-550 cm^{-1} attributable to ν(Sn-C) mode in the spectra of dialkyltin(IV) oxinates.

Sn-N stretching vibrations

The strong intense bands in the range 390-355 cm^{-1} in the spectra of these compounds can be assigned to a tin-nitrogen stretching mode. This band is not observed in the spectra of ligands and also in organotin(IV) chelates of β-diketones. Tanaka and coworkers[52] and Kawakami and coworkers[52b] have indicated that Sn-N stretching frequencies in organotin oxinates occur at ca. 395 cm^{-1}.

Sn-O stretching vibrations

The strong bands observed in the region 580-540 cm^{-1} in the spectra of all the tin(IV) compounds can be assigned to asymmetric (OSnO) stretching vibration on the basis of corresponding assignment reported for organotin(IV) acetylacetonates[124] and organotin(IV) oxinates[122]. The frequency of the tin-oxygen band is rather lower compared to those in alkyltin alkoxides, which are

covalent[125]. This may be due to the variation in the magnitude of interaction between the $d_{\pi}p_{\pi}$ ligand oxygen and tin atom.

Sn-Cl stretching vibrations

The overall range of the tin-chlorine stretching frequencies[126] (Sn-Cl) is 398-385 cm^{-1}. The tin-halogen stretching frequencies are highly sensitive to changes in coordination number of the tin atom and also vary with physical states of the compounds. In the spectra of dichlorotin(IV) compounds, the strong to medium intense bands in the range 350-320 cm^{-1} can be assigned to Sn-Cl stretching modes. These bands are not observed in the spectra of ligands as well as in the spectra of dialkyltin(IV) chelates.

Poller and Toley[127] assigned the bands in the range 360-340 cm^{-1} for ν(Sn-Cl) to the simple di-organotin(IV) dichloride compounds. The conversion of a four coordinate di-organotin dichloride to a six coordinate adduct with Lewis bases causes a reduction in frequency of the ν(Sn-Cl) band by 100 cm^{-1} with respect to free dichloride[54]. However, in the spectra of these compounds such type of reduction is not observed and ν(Sn-Cl) frequencies are observed in the range 360-340 cm^{-1}. Very recently, Das and Ghosh[128] also reported ν(Sn-Cl) frequency for the tin(IV) complexes of monohydroxamic acids in the range of 350-325 cm^{-1}.

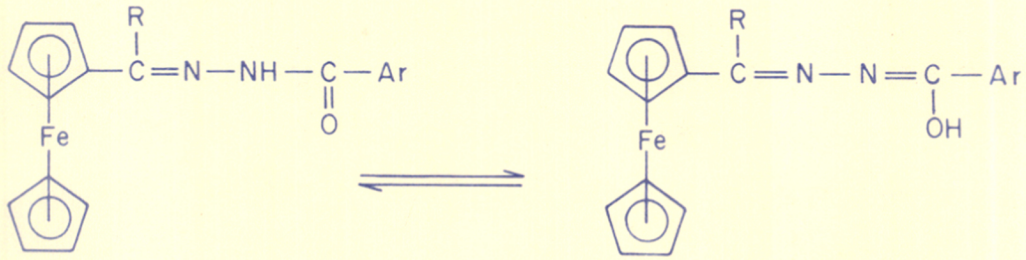

'KETO' 'ENOL'

FIG. 14

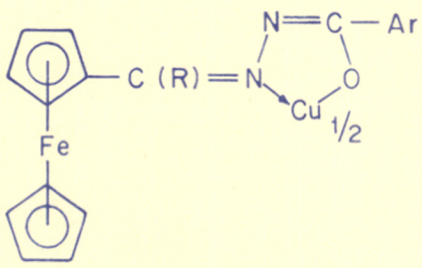

FIG. 15

R = H or CH_3

Ar = C_6H_5 , C_6H_4OH , C_5H_4N

4.4 Hydrogen bonding

In the spectra of dibutyl- and dioctyltin(IV) chelates with α-N-salicyloyl-β-N-ferrocenylidene hydrazide ligand a broad medium intensity band at 3200-2700 cm^{-1} with a series of maxima are observed, while CH stretching vibrations which are sharp occur in this region, the broad nature of the absorption indicates an underlying hydrogen bonded hydroxyl or amino group. In order to find out the nature of hydrogen bonding in these compounds, dilution studies were carried out in carbon tetrachloride. The infrared spectra of dibutyl tin(IV) compound in carbon tetrachloride in the region 3300-2600 cm^{-1} are shown in Fig.16 for three different concentrations. In spite of the large change in concentration, (10^{-4}M) the nature of the bands did not alter, establishing the presence of an underlying intramolecular broad band in the region near 2900 cm^{-1}. Henricks and coworkers[129] and Sen and coworkers[130] have carried out hydrogen bonding studies with respect to some hydrazones, e.g. salicylaldehyde-α-methyl-α-phenylhydrazone [$(2\text{-}HOC_6H_4CH{=}N\text{-}N{=}CCH_3)C_6H_5$], salicylaldehyde dimethyl hydrazone [$2\text{-}HOC_6H_4CH{=}N\text{-}N\text{-}(CH_3)_2$] and salicylaldehyde hydrazone respectively. They observed that intramolecular hydrogen bond formation in these compounds takes place between phenolic hydroxy group and the α-nitrogen atom.

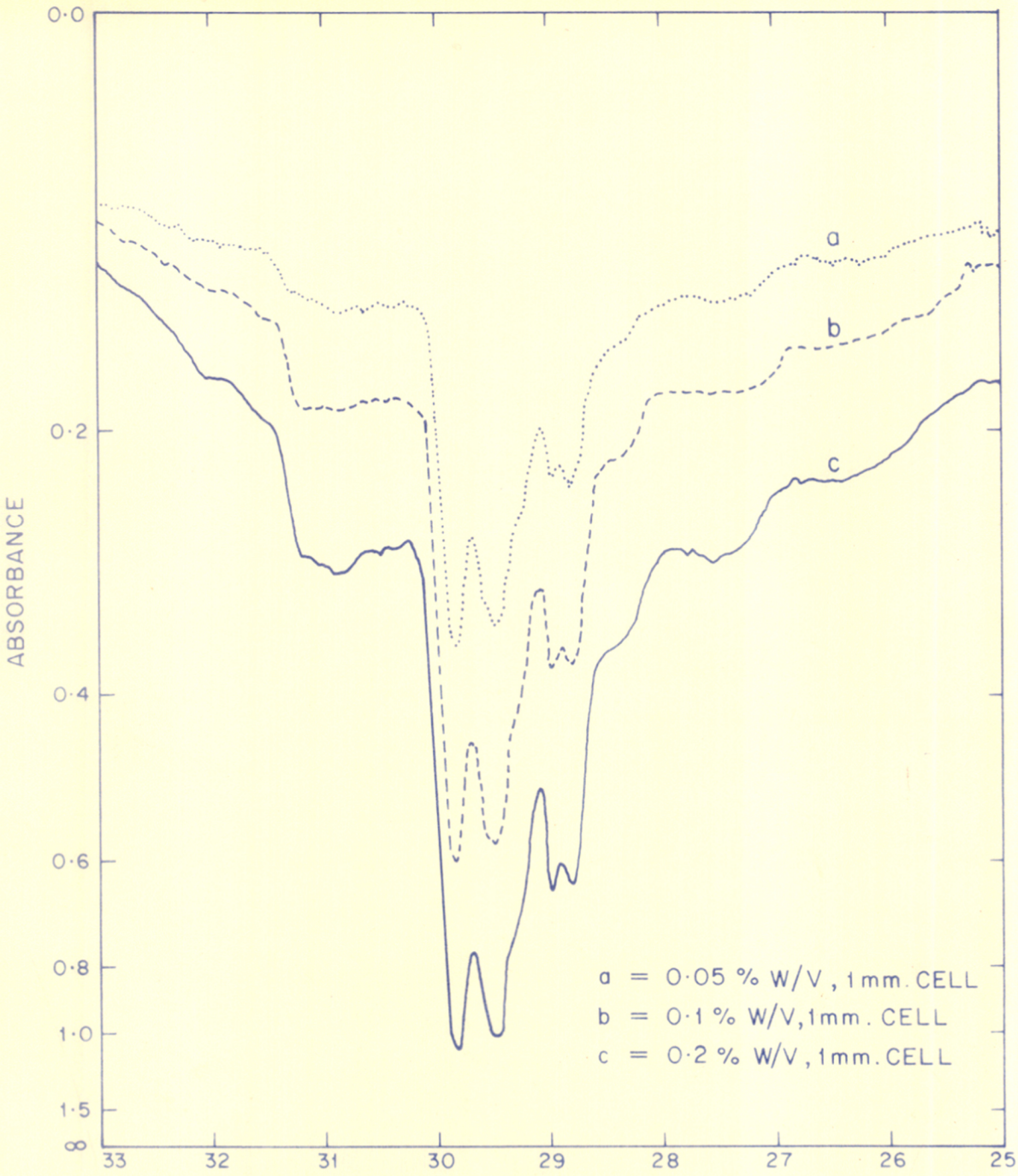

FIG. 16 : IR SPECTRA OF BIS (α-N-SALICYLOYL-β-N-FERROCENYLIDENEHYDRAZIDATO) DIBUTYLTIN(IV) IN CCl_4.

4.5 Complexes derived from triphenyltin acetate

The infrared spectral data of the compounds I–V (Chapter II, Table 4) prepared by reacting triphenyltin acetate with ferrocenyl ligands are presented in Figs. 17-19 and Table 7.

The disappearance of the infrared absorption bands due to νNH as well as due to amide-I, III, IV and V, the negative shift in the position of amide-II band and appearance of a new band around 1240 cm^{-1} indicate the formation of chelates of the type shown earlier (Fig.15).

The spectra in the region 1600-1450 cm^{-1} is complex in all these compounds due to the overlapping of several absorption bands. Although acetoxy group frequencies are difficult to locate due to superimposition by aromatic group frequencies, the presence of acetoxy group in the compounds I-III has been indicated by elemental analysis and supported by ^{1}H n.m.r. spectral data as discussed in Chapter V.

In general, organotin carboxylates have been shown to exist in two forms, either polymeric 5-coordinate complexes in the solid state or monomeric 4-coordinate species in solution[131] (Fig.7, Chapter I). The different structures are readily identified from their infrared spectral studies. In the solid form these compounds are dimeric in nature (Fig.20a). In the case of dialkyltin

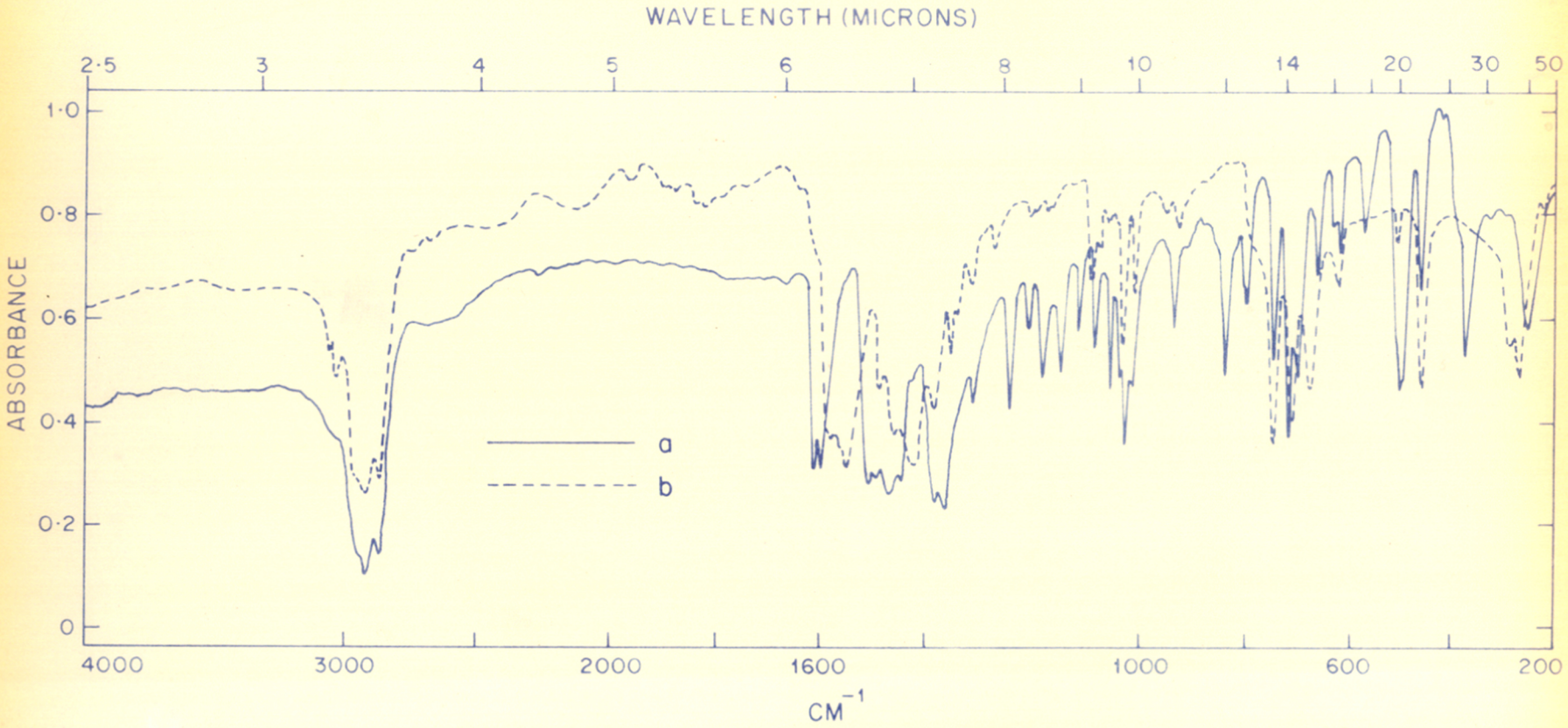

FIG. 17 : IR SPECTRA OF

a) BIS (α-N-BENZOYL-β-N-FERROCENYLIDENEHYDRAZIDATO) DIPHENYLTIN (IV),

b) TRIPHENYLTIN ACETATE IN NUJOL MULL.

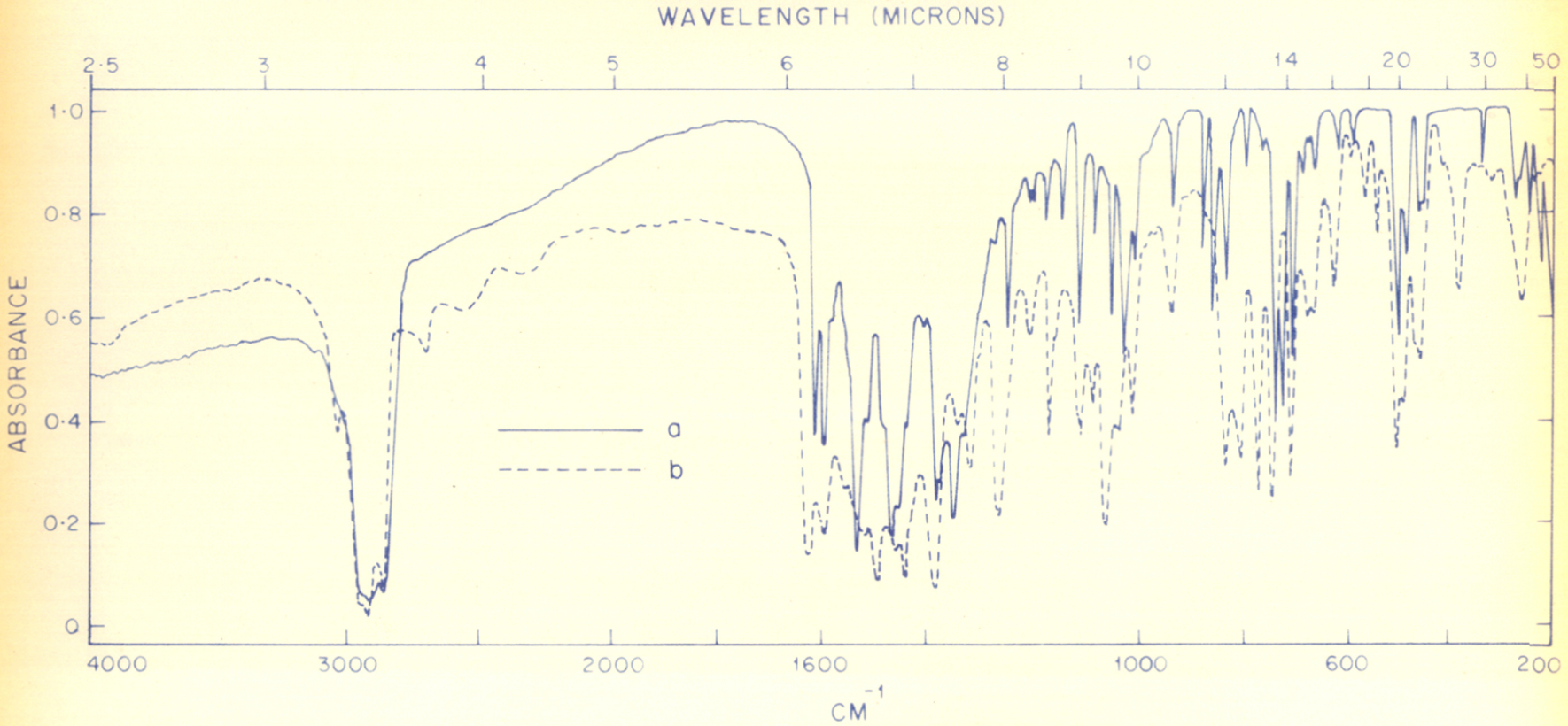

FIGURE 18 : IR SPECTRA OF :

a) μ-ACETOXY(α-N-(o)-NITROBENZOYL-β-N-FERROCENYLIDENEHYDRAZIDATO)-DIPHENYLTIN(IV) ,

b) μ-ACETOXY(α-N-SALICYLOYL-β-N-FERROCENYLIDENEHYDRAZIDATO)-DIPHENYLTIN(IV) IN NUJOL MULL.

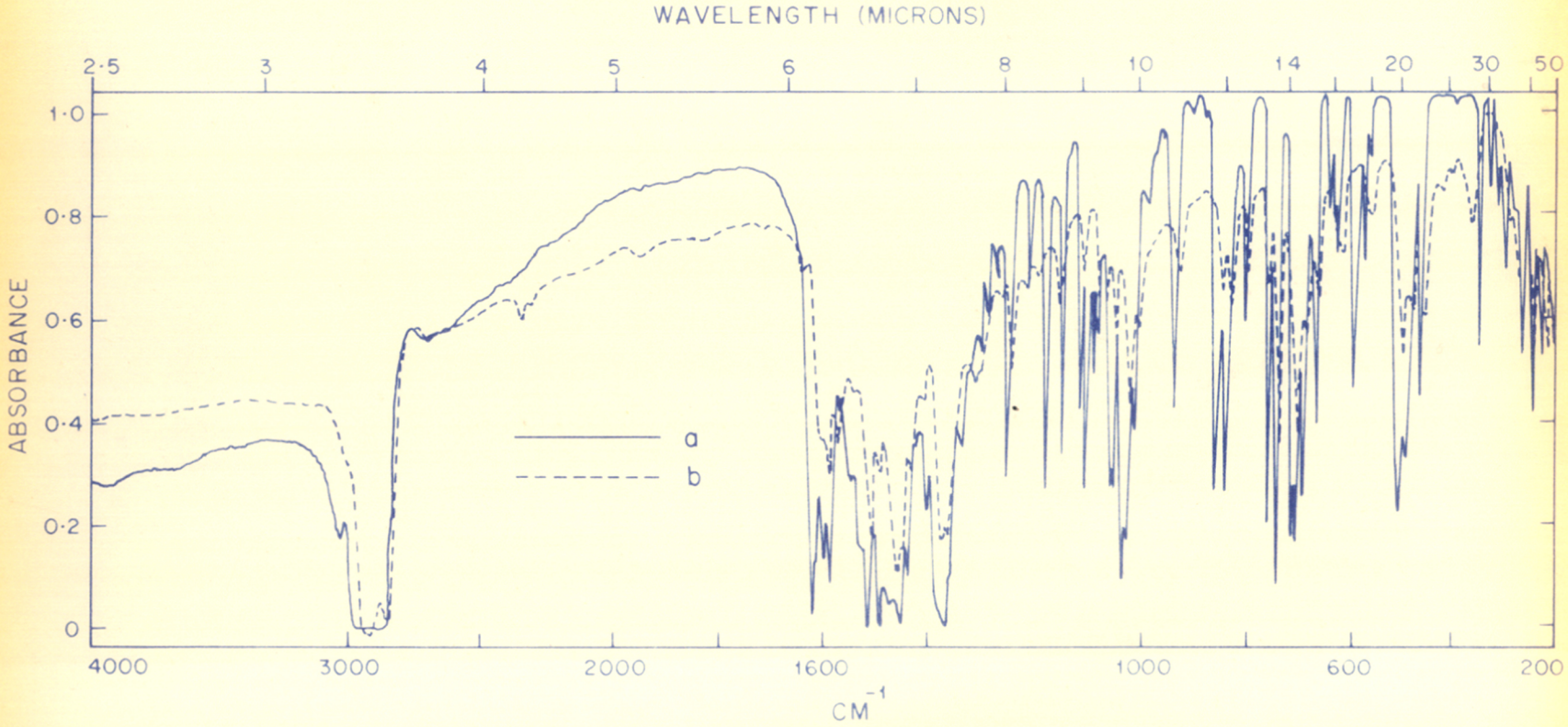

FIGURE 19 : IR SPECTRA OF :

a) α-N-(p)-CHLOROBENZOYL-β-N-FERROCENYLIDENEHYDRAZIDATO-DIPHENYLTIN(IV),

b) μ-ACETOXY (α-N-ISONICOTINOYL-β-N-FERROCENYLIDENEHYDRAZIDATO)-DIPHENYLTIN(IV) IN NUJOL MULL.

TABLE - 7

Infrared absorption frequencies (cm^{-1}) of A. Bis(α-N-benzoyl-β-N-ferrocenylidene — hydrazidato)diphenyltin(IV), B. (α-N-p-chloro-benzoyl-β-N-ferrocenylidene-hydrazidato)triphenyltin(IV), C. μ-acetoxy(α-N-o-nitrobenzoyl-β-N-ferrocenylidene-hydrazidato)diphenyltin(IV), D. μ-acetoxy(α-N-isonicotinoyl-β-N-ferrocenylidene-hydrazidato)diphenyltin(IV), E. μ-acetoxy-(α-N-salicyloyl-β-N-ferrocenylidene-hydrazidato)diphenyltin(IV), in Nujol.

A	B	C	D	E	Possible assignment
3040(br,w)	3040(w)	3040(w)	3050(w)	3050(w)	ν CH
2930(br,s)*	2910(br,s)*	2920(br,s)*	2940(br,s)*	2920(br,s)*	
2860(br,s)*		2860(br,s)*	2860(br,s)*	2860(s)*	
1610(s)	1610(s)	1610(s)	1600(w)	1615(s)	-C=N-N=C- mode
1595(s)	1595(m)	1590(m)	1590(br,s)	1590(br,s)	
	1580(s)		1570(m)		
1510(s)	1510(br,s)	1530(s)	1510(s)	1515(m)	
1490(m)	1485(s,d)		1490(m)	1490(s)	
1460(w)*	1450(s)*	1460(s)*	1455(br,s)	1450(w)	
1440(m)	1430(m)	1440(sh)	1430(w)	1435(m)	
1380(sh)	1395(m)	1400(w)			
1355(br,s)*	1360(br,s)*	1375(s)*	1375(s)*	1375(s)*	
1330(sh)	1330(w)	1340(s)	1365(s)		
1300(m)	1290(w)	1320(sh)	1315(br,s)	1310(s)	
	1280(w)				
1260(m)	1260(w)	1260(w)	1260(w)	1260(s)	ν C-O
1240(s)	1245(s)	1240(s)	1240(m)		
1200(m)	1200(m)	1195(w)	1210(w)		
1175(s)	1170(s)	1170(m)	1190(w)	1195(m)	

contd....

(TABLE -7 contd.)

A	B	C	D	E	Possible assignment
1140(s)	1135(s)	1140(m)	1145(m)	1160(s)	
1105(s)	1105(s)	1105(s)	1105(m)	1100(s)	
	1095(s)				
1075(s)	1075(m)	1075(m)	1075(m)	1080(m)	Ph-Sn
	1070(m)		1060(m)		
1045(s)	1045(s)	1040(s)	1040(m)	1050(s)	
	1040(s)				CH in-plane def.
1025(m)	1020(s)	1020(s)	1015(s)		
1015(s)	1015(m)				
1000(m)	1000(m)	1000(m)	995(w)	1000(m)	ring breathing
	975(w)				
930(m)	925(s)	930(m)	920(m)	930(m)	N-N
		870(s)			
	845(s)	850(s)	840(m)		
825(s)	825(s)	825(s)	820(m)	825(s)	ω-CH
785(m)	790(s)	790(m)	790(m)	795(s)	
	750(s)	755(m)	750(m)	760(s)	
735(s)	730(s)	730(s)	730(s)	730(s)	
700(s)	700(s)	715(s)			
690(s)	690(s)	695(s)	695(s)	700(s)	
	680(s)	680(w)	675(m)	665(m)	C-H out-of plane
650(m)	655(s)	655(m)	655(m)	650(m)	def.
	630(m)				
610(m)	610(m)	610(w)	610(m)	615(s)	Sn-C
	580(s)	580(s)		585(w)	
560(br,m)	560(m)		555(m)	560(m)	
				530(m)	Sn-O
490(s)	495(s)	495(s)	495(s)	495(s)	
480(sh)	480(s)	480(m)	475(m)	480(sh)	

contd....

(TABLE - 7 contd.)

A	B	C	D	E	Possible assignment
450(s)	455(s)	455(m,d)	455(s)	450(s)	ν Sn-C
370(s)	340(s)	335(m)	360(m)	380(s)	ν Sn-H
	320(m)			320(w)	
	305(m)				
	295(m)		290(sh)		
	260(s)		260(m)	260(d,s)	C-C mode
250(s)	240(s)	245(m)	245(m)		
	220(m)	220(m)	220(m)		

* Nujol peaks

chloride carboxylates, the bands at 1540-1565 cm^{-1} have been assigned to acetoxy group and get shifted to 1605 cm^{-1} in solution where the compound has been reported to be monomeric (Fig.20b). Although it is not possible to assign unequivocally bands in this region of the compounds I-III, the appearance of a new band at ca 1610-1620 cm^{-1} shows structural changes that take place in solution. Due to the position of this new band at 1610-1620 cm^{-1} suggesting the presence of a non-ester type of acetoxy group, tentatively the following structures of the compounds (Fig. 20c) where tin is hexacoordinated is being suggested and this is further substantiated by the determination of molecular weight.

The molecular weight determination in chloroform using vapour-pressure osmometric method shows the molecular weight to be in between the monomeric and dimeric form, which suggests that in chloroform these compounds may dissociate to monomer and an equilibrium between monomer-dimer may exists. On the basis of infrared spectral data and molecular weight determination it can be said that these compounds are dimeric in nature (Fig. 20a) in the solid form and monomeric in nature in chloroform solution (Fig. 20c).

Elemental analysis and spectral studies indicate that compound IV may have the six coordinate, octahedral

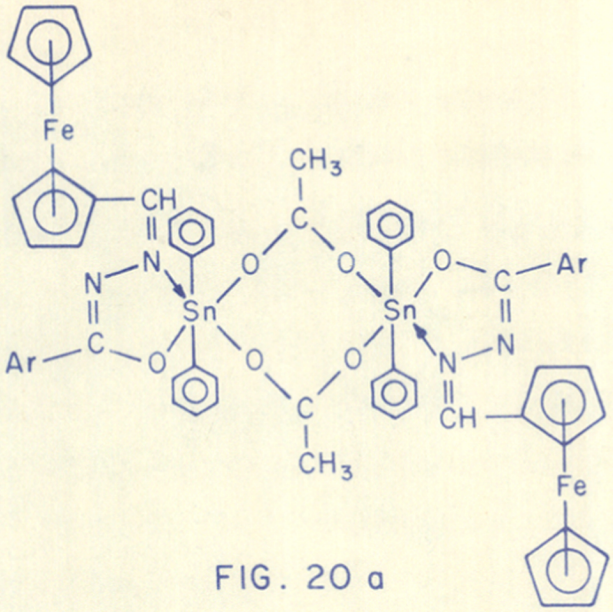

FIG. 20 a

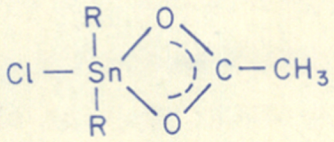

(R = ALKYL GROUP)

FIG. 20 b

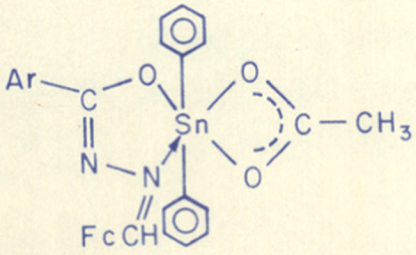

(Fc = FERROCENYL GROUP, Ar = $C_6H_4NO_2$ (p), C_6H_4OH (o), AND C_5H_4N)

FIG. 20 c

structure as shown in Fig. 21 and compound V may have 5-coordinate trigonal bipyramidal structure (Fig. 22).

In the spectra of all tin(IV) chelates, an additional strong medium intense band around 1075 cm^{-1} is observed which can be assigned for phenyl-tin vibration. Poller[49] has studied the infrared spectra of a number of phenyl-tin carboxylates and the strong intensity band occuring in the range 1076-1062 cm^{-1} has been assigned to phenyl-tin stretching vibration.

Characteristic bands of ferrocenyl group are also observed in the spectra of all these compounds. Bands in the range 1210-1150 cm^{-1} and strong bands around 1020 cm^{-1} can be assigned for C-H in-plane deformation vibration. The bands around 1100 cm^{-1} and below are much more complicated due to the presence of phenyl group vibrations.

The strong bands observed around 495 cm^{-1} in the spectra of all the tin(IV) chelates can be assigned to asymmetric (OSnO) stretching vibration. The bands in the range 380-335 cm^{-1} and 610-600 cm^{-1} can be assigned for Sn-N and Sn-C stretching vibrations respectively.

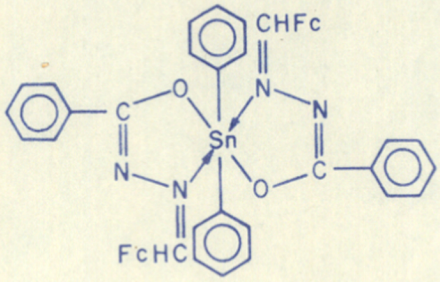

(Fc = FERROCENYL GROUP)

FIG. 21

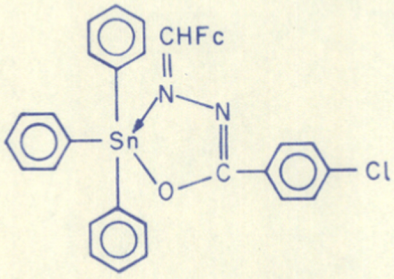

(Fc = FERROCENYL GROUP)

FIG. 22

CHAPTER -V

^1H NMR STUDIES ON TIN(IV) COMPLEXES OF FERROCENYLIDENE DERIVATIVES OF α-N-ACYL HYDRAZINES

	Page
Results and Discussion	108

^{1}H n.m.r. spectra of organotin(IV) and dichlorotin(IV) compounds of α-N-aroyl-β-N-ferrocenylidenehydrazide.

The ^{1}H n.m.r. spectra of some tin compounds synthesized for the first time, are recorded either in carbon tetrachloride or deuterated chloroform. Fig.I gives the structural formula of the compounds studied and the proton chemical shifts are listed in Table 1.

From Figs. 1-6, it can be seen that the protons from unsubstituted and substituted cyclopentadienyl rings in ferrocene moiety appear (respectively) at 3.8 - 4.3 δ as singlet and as two broad peaks at 4.0 - 4.4 δ and 4.4 - 5.23 δ (as triplets for 2,5 and 3,4 protons in the substituted ring). This broadening of peaks for ferrocenyl derivatives can be interpreted in terms of the slowing down of the motion of cyclopentadienyl rings resulting from substitution. This observation is in good agreement with the observations made by Rausch and Siegel[77] in the spectra of formyl and acetyl ferrocenes which suggest that there is no remarkable influence on the chemical shift of ferrocenyl protons on chelation. Kamezawa[73] and Slocum and coworkers[78] have reported the ^{1}H n.m.r. spectra of several ferrocenyl derivatives showing a singlet for unsubstituted cyclopentadienyl ring protons and splitting into two triplets for substituted cyclopentadienyl ring protons.

Figure I

Structural formula of the dichloro- and dialkyl bis(α-N-aroyl-β-N-ferrocenylidenehydrazidato)tin(IV) compounds

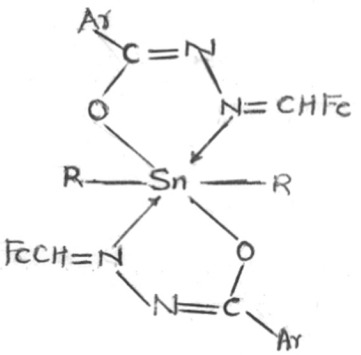

where FC = ferrocenyl group

Compound	R	Ar
I	C_4H_9	C_6H_5
II	C_4H_9	$C_6H_4Cl(p)$
III	C_4H_9	$C_6H_4NO_2(o)$
IV	C_4H_9	C_5H_4N
V	C_4H_9	$C_6H_4OH(o)$
VI	C_8H_{17}	C_6H_5
VII	C_8H_{17}	$C_6H_4NO_2(o)$
VIII	C_8H_{17}	C_5H_4N
IX	C_8H_{17}	$C_6H_4OH(o)$
X	Cl	$C_6H_4Cl(p)$
XI	Cl	$C_6H_4NO_2(o)$

TABLE -1

PROTON CHEMICAL SHIFTS (τ) OF DICHLORO- AND DIALKYL-BIS(α-N-AROYL-β-N-FERROCENYLIDENEHYDRAZIDATO)TIN(IV) COMPLEXES

Compound	Ferrocenyl group		Azomethine proton	Aromatic group					R	OH	Solvent
	Unsubstituted (C_5H_5)	Substituted (C_5H_5)		2-H	3-H	4-H	5-H	6-H			
I	3.9(s)	4.26 4.83	7.01(s)	7.33	8.16	7.33	8.16	7.33	1.26(m)	-	$CDCl_3$
II	3.93(s)	4.09 4.46	7.01(s)	7.23 (J=8 Hz)	8.03 (J=8 Hz)	-	8.03	7.23	1.16(m)	-	$CDCl_3$
III	4.03(s)	4.26 4.60	7.23(s)			8.33			1.5(m)	-	$CDCl_3$
IV	3.93(s)	4.37 4.86	7.23(s)	7.93 (J=6 Hz)	8.66 (J=6 Hz)	-	8.66	7.93	1.23(m)	-	$CDCl_4$
V	3.93(s)	4.33 4.56	7.16(s)	6.76	7.26	-	7.26	6.76	1.2(m)	7.86	CCl_4
VI	3.8(s)	4.16 4.76	7.00(s)	7.20	8.00	7.20	8.00	7.20	1.01(m)	-	CCl_4
VII	4.00(s)	4.43 4.90	7.33(s)			8.33			1.16(m)	-	CCl_4
VIII	4.00(s)	4.40 4.93	7.26(s)	8.40 (J=5 Hz)	8.00 (J=5 Hz)	-	8.40	8.00	1.2(m)	-	CCl_4
IX	3.9(s)	4.16 4.50	7.01(s)			7.00			1.16(m)	12.30	CCl_4
X	4.3(s)	4.76 5.2	7.23(s)	7.9	8.01	-	8.01	7.9	-	-	$CDCl_3$
XI	4.33(s)	4.86 5.23	8.01(s)			8.33			-	-	-

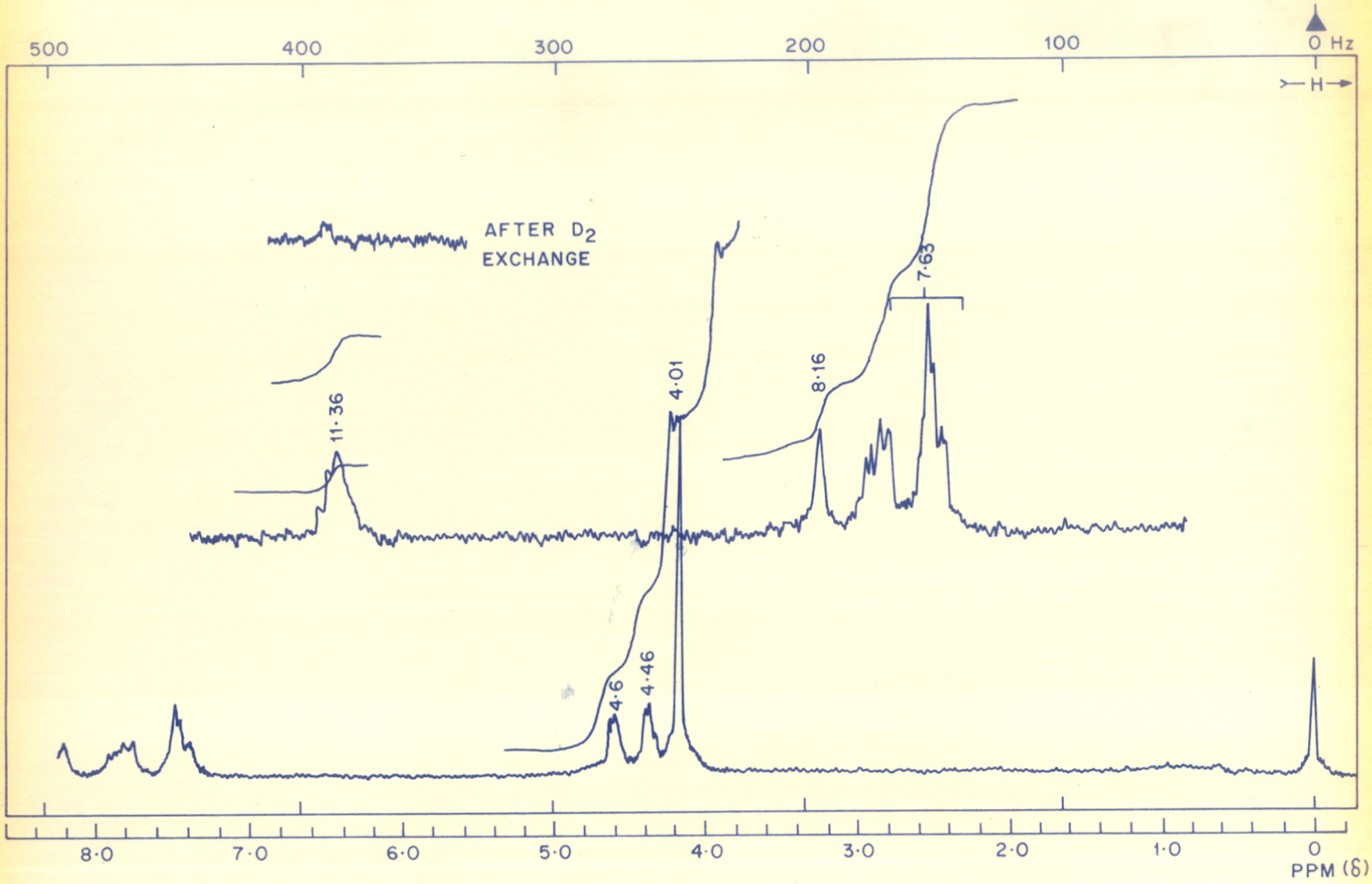

FIG. 1 : NMR SPECTRUM OF α-N-BENZOYL-β-N-FERROCENYLIDENEHYDRAZIDE IN DMSO.

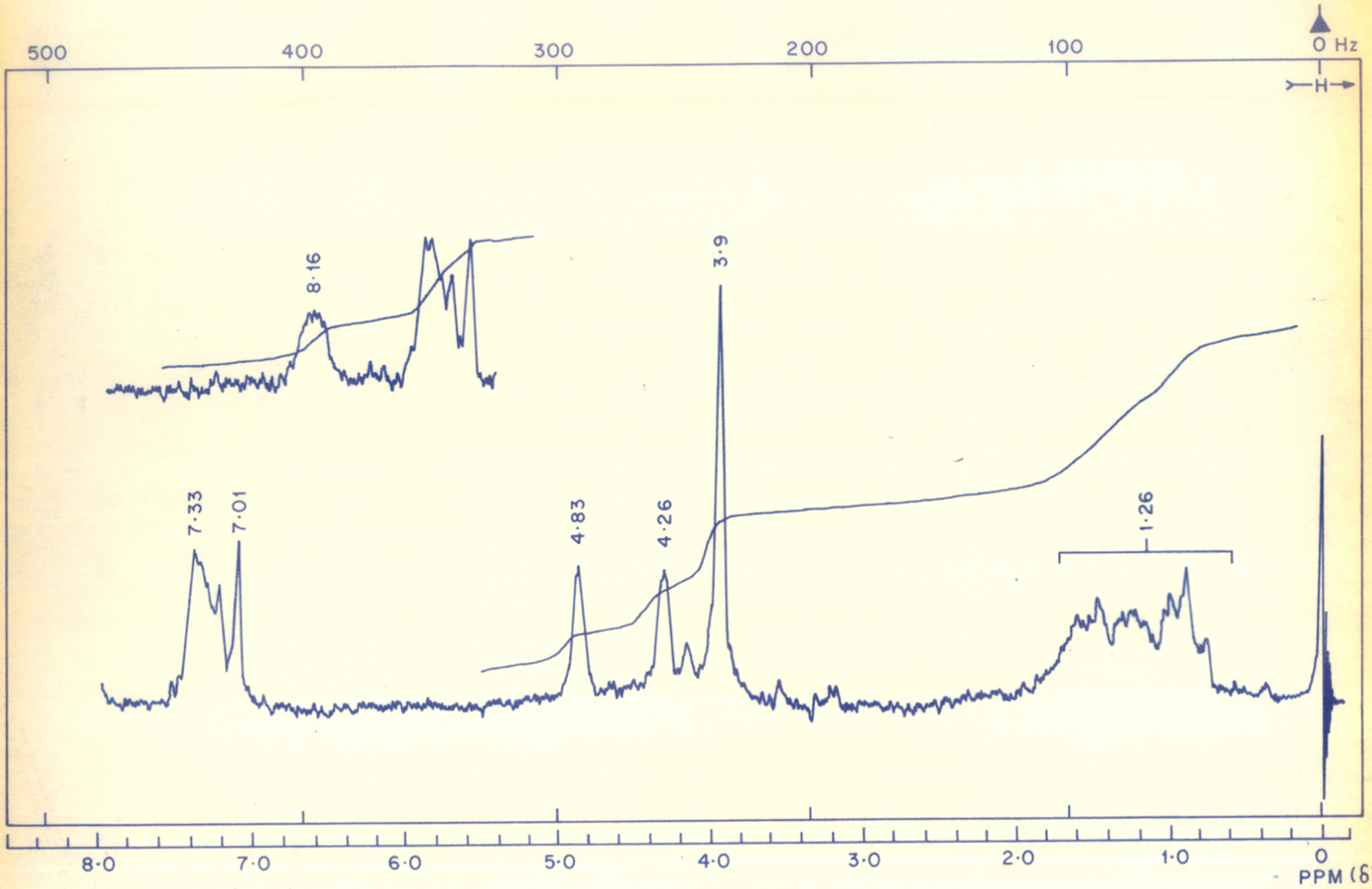

FIG. 2 : NMR SPECTRUM OF BIS(α-N-BENZOYL-β-N-FERROCENYLIDENEHYDRAZIDATO) DIBUTYLTIN (IV) IN $CDCl_3$.

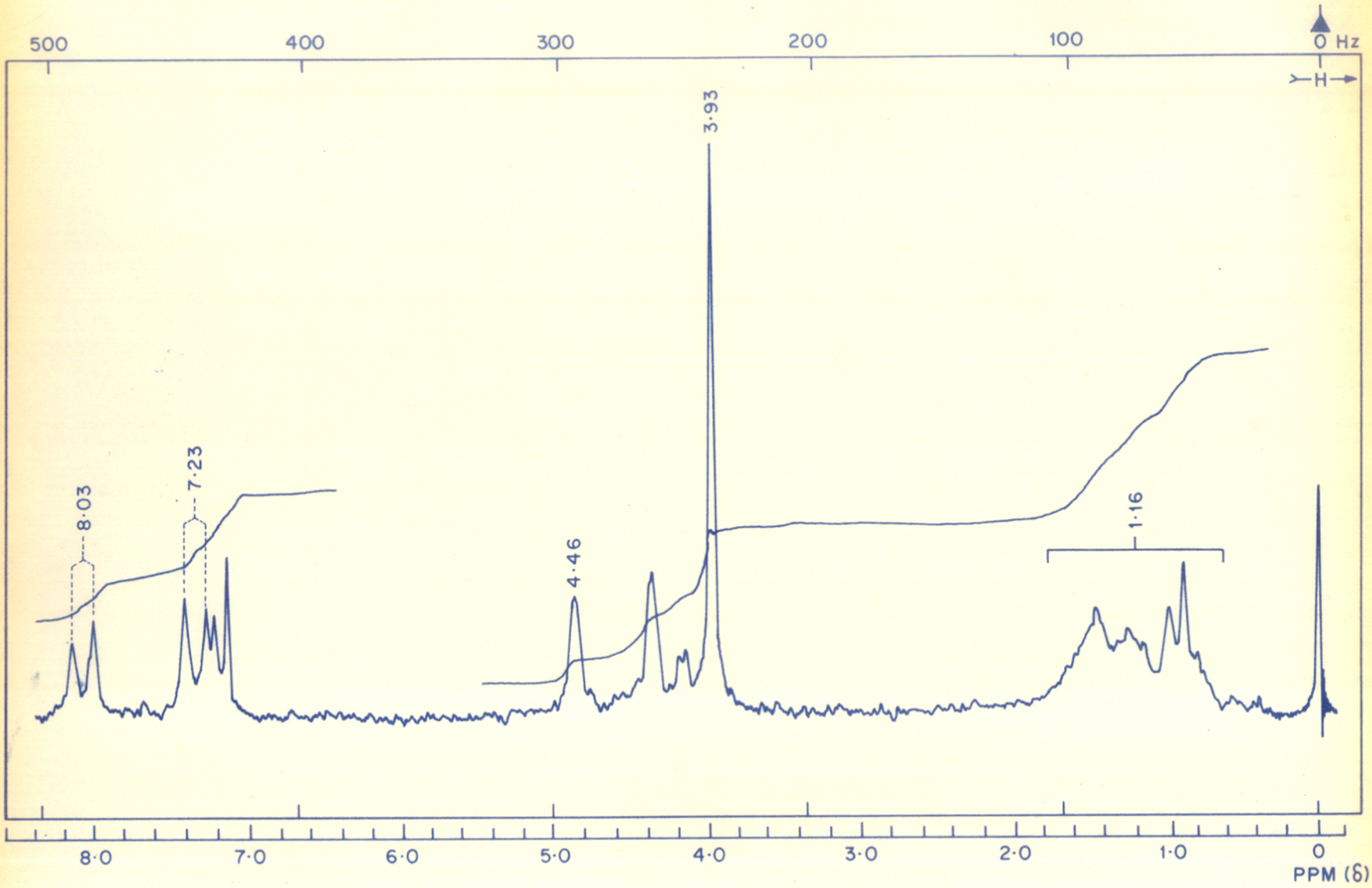

FIG. 3 : NMR SPECTRUM OF BIS (α-N-(p)-CHLOROBENZOYL-β-N-FERROCENYLIDENE-HYDRAZIDATO) DIBUTYLTIN (IV) IN $CDCl_3$.

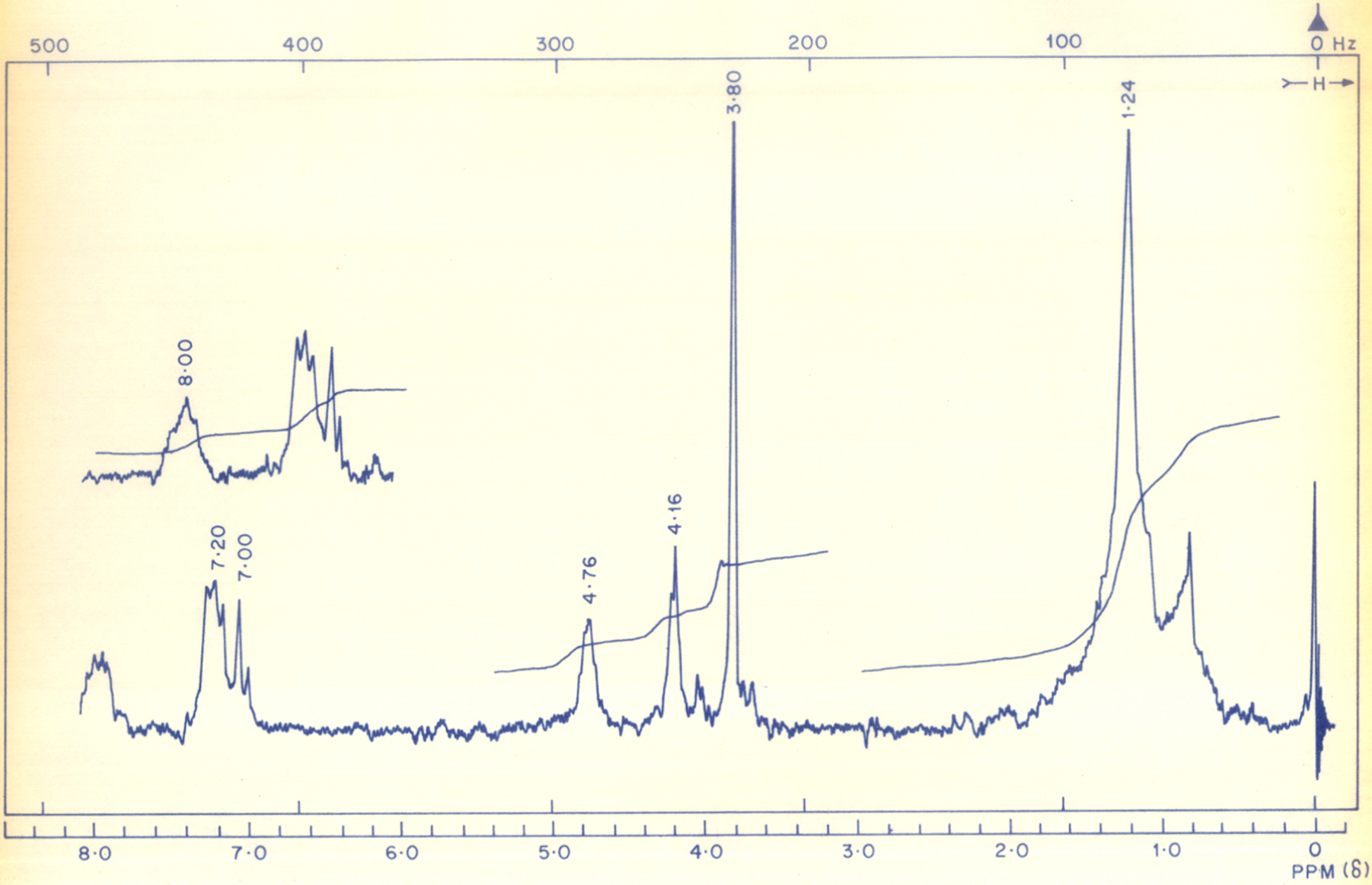

FIG. 4 : NMR SPECTRUM OF BIS (α-N-BENZOYL-β-N-FERROCENYLIDENEHYDRAZIDATO) DIOCTYLTIN (IV) IN CCl_4.

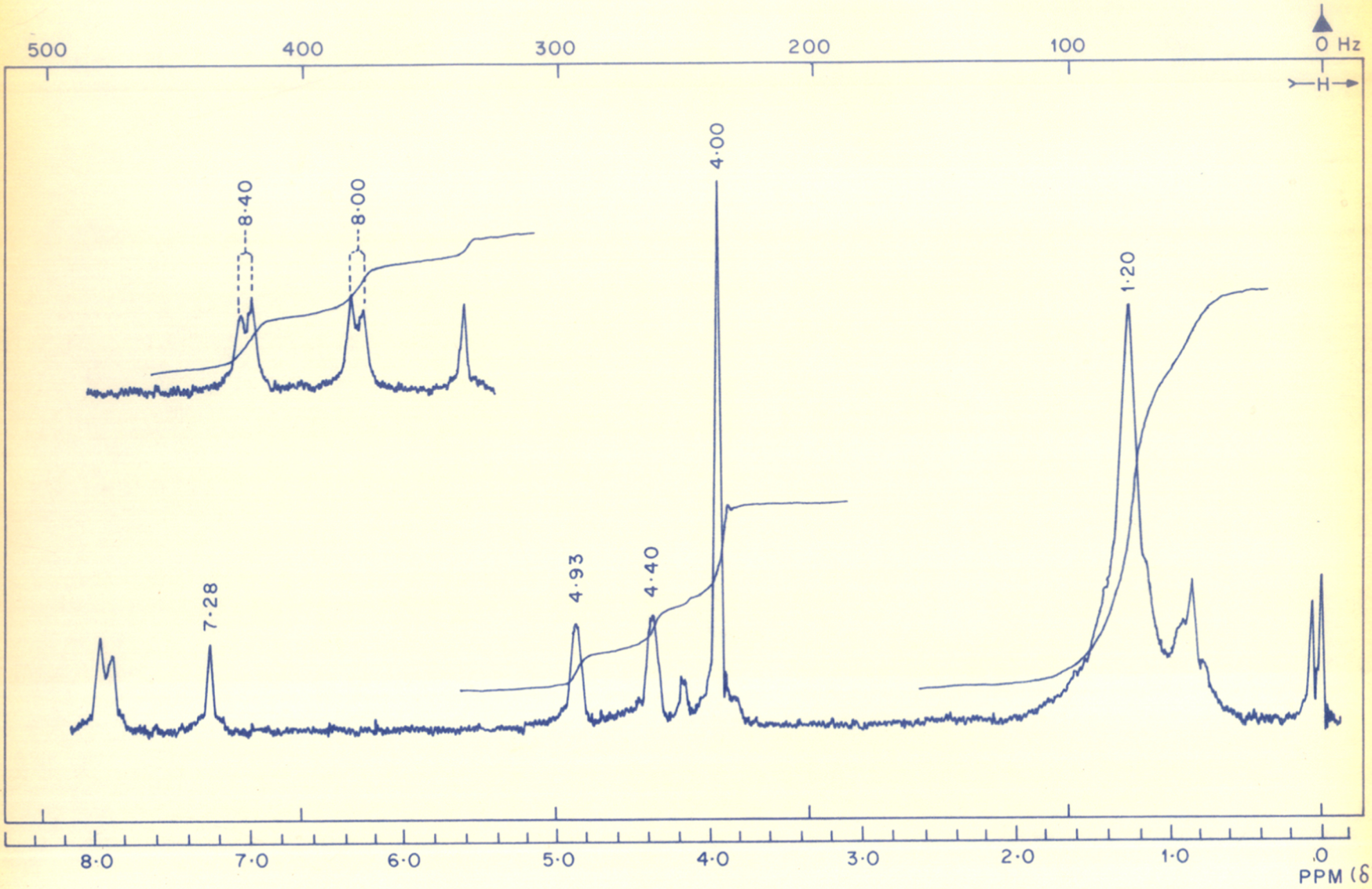

FIG. 5 : NMR SPECTRUM OF BIS (α-N-ISONICOTINOYL-β-N-FERROCENYLIDENE - HYDRAZIDATO) DIOCTYLTIN (IV) IN CCl_4.

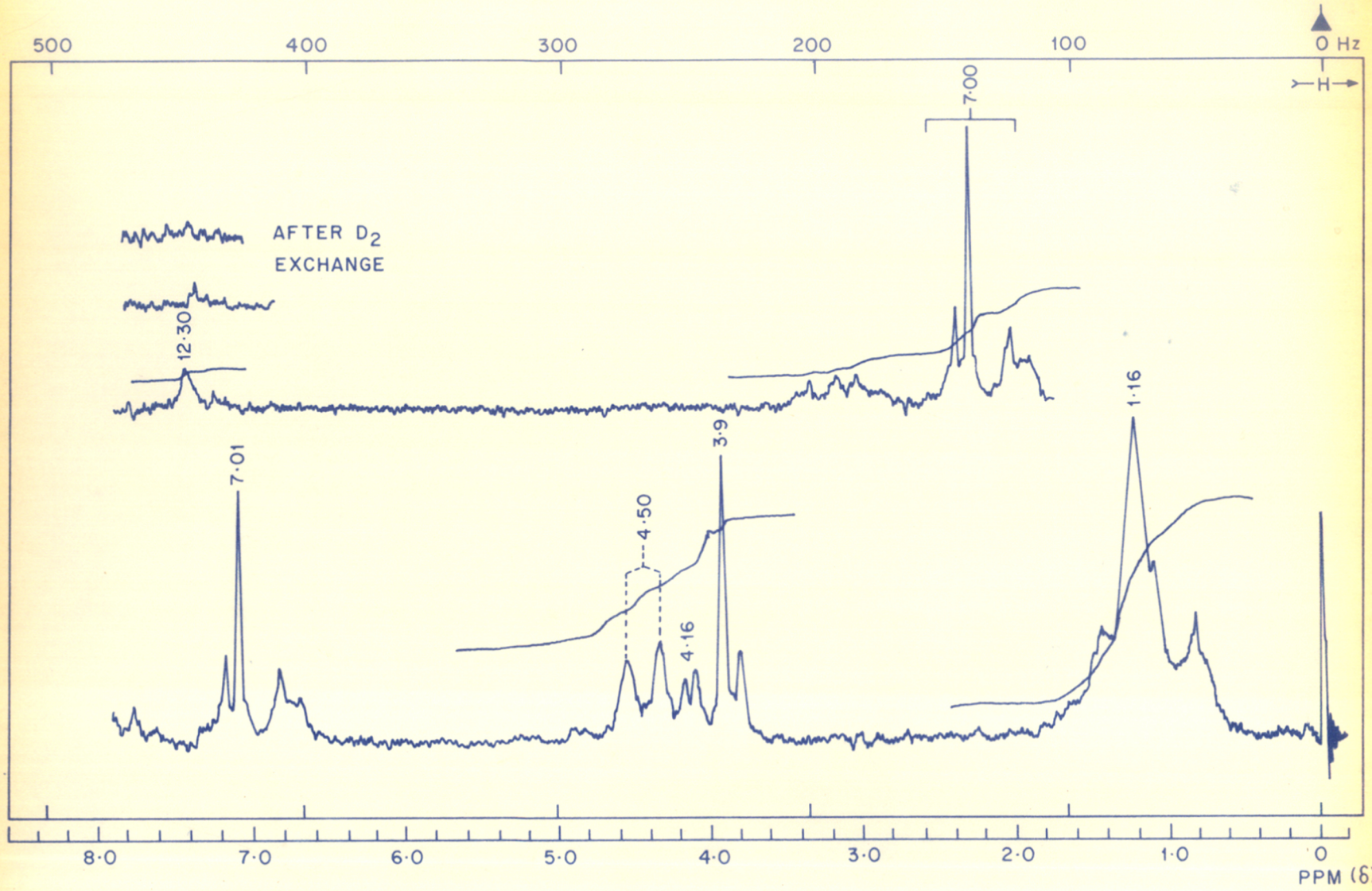

FIG. 6 : NMR SPECTRUM OF BIS(α-N-SALICYLOYL-β-N-FERROCENYLIDENE-HYDRAZIDATO) DIOCTYLTIN (IV) IN CCl_4.

Although the protons of the ferrocenyl group are not involved in metal chelation, consideration of changes in the chemical shifts for the ferrocenyl protons and aromatic protons upon chelation relative to their positions for the free ligands gives an insight into the nature of the metal-ligand bonds.

The dibutyl and dioctyltin(IV) complexes (Figs. 2-6) show complex resonance patterns for the alkyl groups which are similar to those observed in the spectra of uncomplexed dialkyltin dichlorides[132]. A slight chemical shift has been observed for the alkyl protons in different substituted bis(α-N-aroyl-β-N-ferrocenylidenehydrazidato)dibutyl- and dioctyltin(IV) chelates.

The azomethine proton appears at 7.01-8.01 δ as singlet in the spectra of complexes (Figs. 2-9) whereas in the spectra of free ligand α-N-benzoyl-β-N-ferrocenylidene-hydrazide it appears at 8.16 δ (Fig.1). The downfield chemical shift of the azomethine proton indicates deshielding on chelation, chelation being taking place through azomethine nitrogen atom. In general on complex formation, the alkyl groups attached to the tin in chelates exhibit shielding which is in agreement with an increased electron density on the tin via ligand donation. On the other hand, methylene protons are shifted to the down field indicating deshielding on chelation.

The aromatic protons appear in the range of 7.00-8.40 δ. The introduction of the halogen substituent at para-position in the aromatic ring results in the redistribution of electron-density in the molecule, and influences the availability of electrons at oxygen donar atom for chelate formation and this is reflected in the spectrum of bis-(α-N-p-chlorobenzoyl-β-N-ferrocenylidenehydrazidato)-dibutyltin(IV) (Fig.3). In the spectrum of this compound aromatic protons 2H, 3H, 4H and 5H are shifted to the downfield, indicating deshielding effect due to chloro group substitution as compared to the spectrum of bis-(α-N-benzoyl-β-N-ferrocenylidenehydrazidato)dibututyltin(IV) complex (Fig. 2). The aromatic protons at position 2 and 6 are coupled with each other with coupling constant, J = 8 Hz, while protons at position 3 and 5 are coupled with each other with coupling constant, J = 8 Hz. The same coupling constants for both kind of protons in the aromatic ring show that they are also coupled with each other. Similar kind of spliting has also been observed in the spectra of compounds dibutyl/diacetyl bis(α-N-isonicotinoyl-β-N-ferrocenylidenehydrazidato)tin(IV).

The inductive effects of hydroxy and nitro groups show opposite effect on the chemical shifts of aromatic protons. This effect is transferred predominantly through π-electron system. Thus shielding and deshielding due to

electron withdraving and electron-donating substituents have been observed in the spectra of substituted bis-(α-N-benzoyl-β-N-ferrocenylidenehydrazidato)-dialkyltin(IV) chelates. Similar trend has been observed in the case of dialkyltin(IV) complexes with substituted 8-quinolinols[132].

In the spectra of bis-(α-N-salicyloyl-β-N-ferrocenylidenehydrazidato)dibutyl and dioctyltin(IV) chelates, additional peaks at 7.86 τ and 12.30 τ respectively are observed and assigned for the hydroxy groups, which confirms the presence of OH group showing that the phenolic OH group is not involved in the chelate formation.

The ^{1}H n.m.r. spectra of compounds I to V (Chapter II, Table 4) are presented in Figs. 7-9. The chemical shifts of unsubstituted and substituted cyclopentadienyl rings, aromatic group, azomethine and methyl group protons are given in Table 2. It is interesting to note that in compounds I-III, acetoxy groups can be confirmed by the presence of methyl group protons at ~ 2.10 τ. It can be seen from Fig.10 that the methyl protons of acetoxy group appear at 2.10 τ in the spectrum of triphenyltin acetate. The integration ratios of aromatic protons in the ^{1}H n.m.r. spectra of these compounds show the presence of two phenyl groups. In case of compound III, integration ratio for methyl

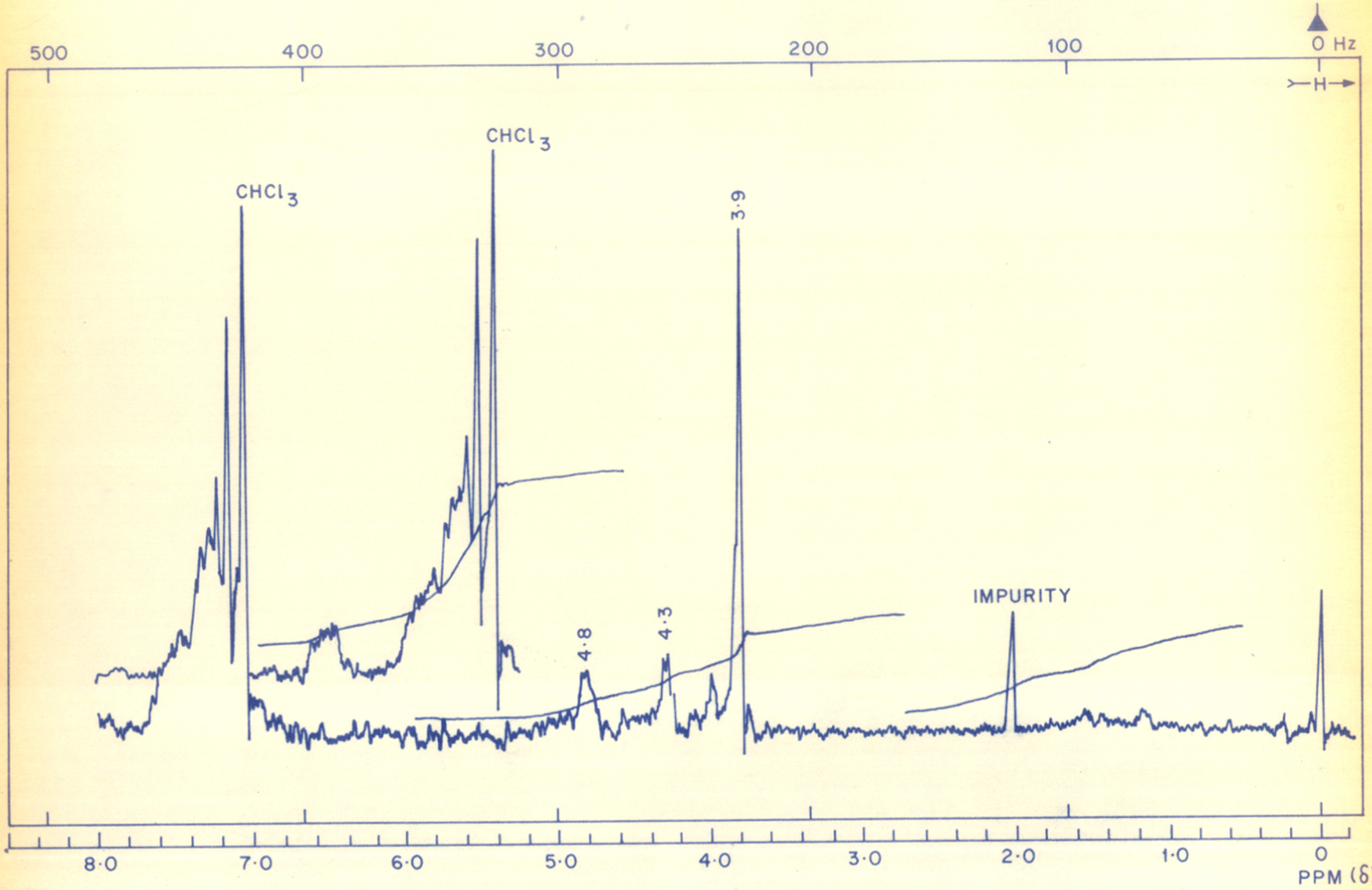

FIG. 7 : NMR SPECTRUM OF BIS (α-N-BENZOYL-β-N-FERROCENYLIDENEHYDRAZIDATO) DIPHENYLTIN (IV) IN $CDCl_3$.

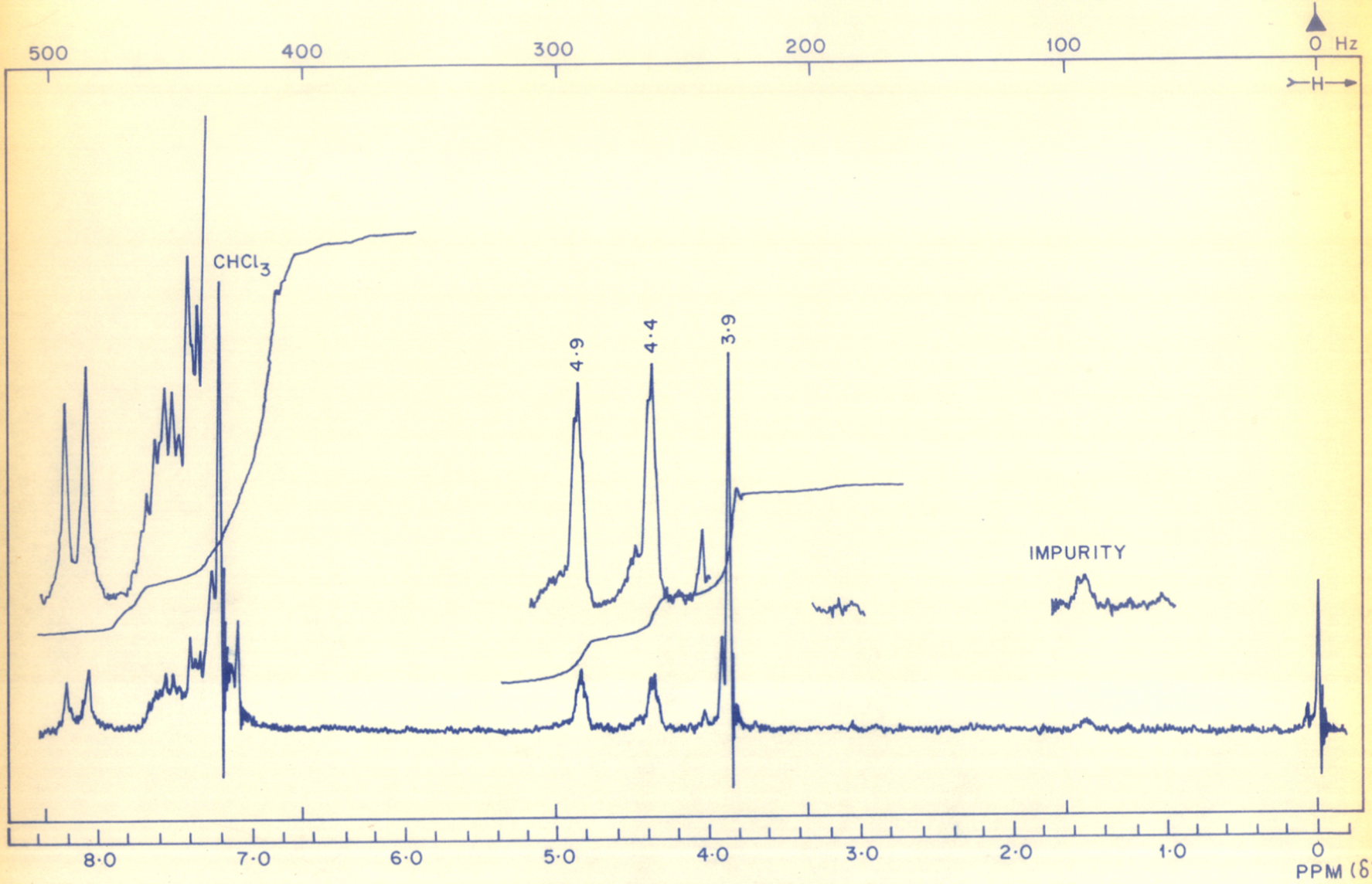

FIG. 8 : NMR SPECTRUM OF (α-N-p-CHLOROBENZOYL-β-N-FERROCENYLIDENE-HYDRAZIDATO) TRIPHENYLTIN (IV) IN $CDCl_3$.

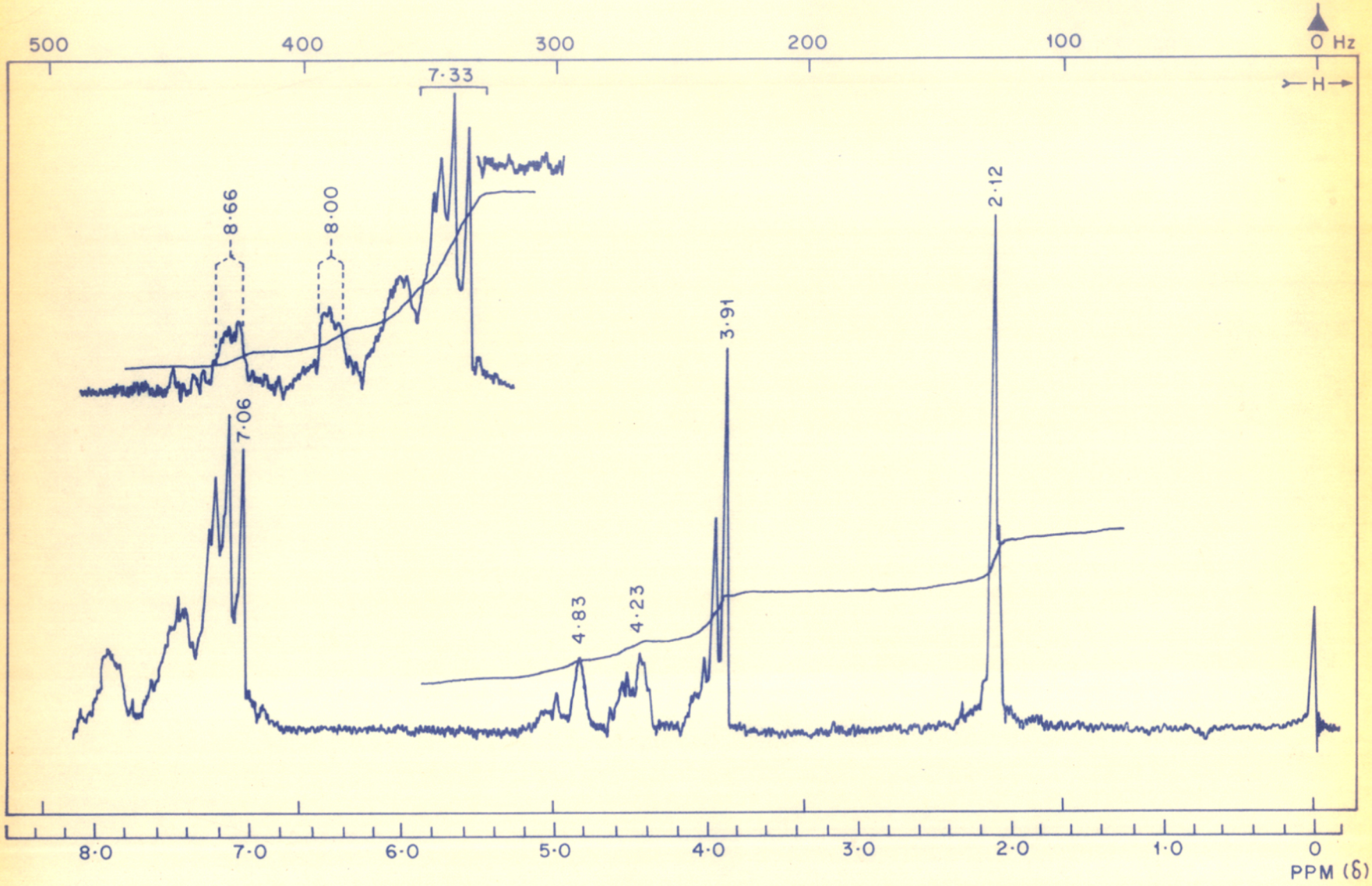

FIG. 9 : NMR SPECTRUM OF μ-ACETOXY (α-N-ISONICOTINOYL-β-N-FERROCENYLIDENE-HYDRAZIDATO) DIPHENYLTIN (IV) IN $CDCl_3$.

TABLE -2

PROTON CHEMICAL SHIFTS (τ) OF COMPLEXES DERIVED FROM TRIPHENYLTIN ACETATE

S.No.	Compound	Ferrocenyl group		Azomethine proton	Aromatic	phenyl group	$OCCH_3$ protons
		Unsubstituted C_5H_5	Substituted C_5H_5				
1.	μ-Acetoxy-α-N-(p)nitrobenzoyl-β-N-ferrocenylidenehydrazidato)-diphenyltin(IV)	3.93	4.40 5.00	*	8.06	7.16	2.06
2.	μ-Acetoxy-α-N-isonicotinoyl-β-N-ferrocenylidenehydrazidato)-diphenyltin(IV).	3.91	4.23 4.83	7.06	8.00 8.66	7.33	2.12
3.	Bis-(α-N-benzoyl-β-N-ferrocenylidenehydrazidato)diphenyltin(IV)	3.9	4.33 4.86	*	8.23	7.4	-
4.	(α-N-(p)chlorobenzoyl-β-N-ferrocenylidenehydrazidato)-triphenyltin(IV)	3.9	4.4 4.9	7.16	8.23	7.4	-
5.	Triphenyltin acetate	-	-	-	-	7.43	2.00

* superimposed by peaks due to aromatic protons

protons, ferrocenyl protons, azomethine proton, protons from phenyl groups and protons from aromatic group is 3:9:1:10:4 which accounts for all the protons present in the molecule and also shows the presence of two phenyl rings. Though it has been reported that phenyltin cleavage is favoured at temperatures above 100°C, in our studies we found that phenyltin cleavage can occur at comparatively mild conditions. But such type of phenyltin cleavage appears to be not important in the case of ligands, α-N-benzoyl- and α-N-p-chlorobenzyl-β-N-ferrocenylidene-hydrazides where cleavage of acetoxy group takes place more readily. The nmr spectra of these compounds (Figs.7,8) show that the acetoxybridged compounds are probably present in small amounts as impurities.

In the spectrum of triphenyltin acetate (Fig.10) phenyl group protons appear at 7.43 δ as multiplet, whereas in the spectra of chelates these protons appear around 7.16-7.33 δ. Thus on chelation phenyl ring protons are shifted to downfield by an order of 0.26-0.10 δ. Azomethine proton appears in the range 7.06-7.01 δ which is also shifted to downfield by an order of 1.00 δ. This downfield chemical shift may be due to the deshielding on chelation via an azomethine nitrogen atom.

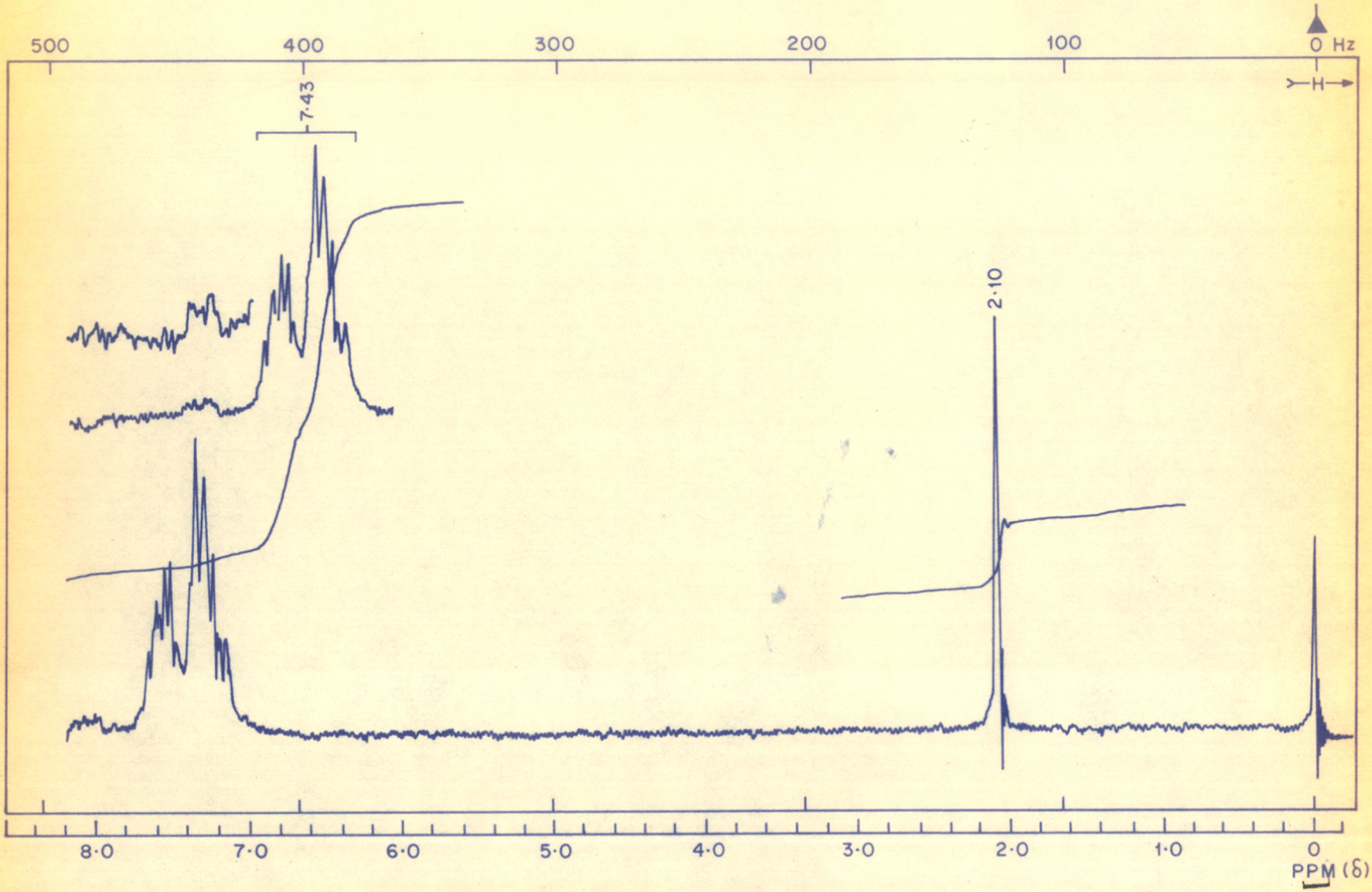

FIG. 10 : NMR SPECTRUM OF TRIPHENYLTIN ACETATE IN CCl_4.

REFERENCES

REFERENCES

1. Anderson, W.F., Inorganic Chemistry in Biology and Medicine, A.C.S. Symposium series, No.140 (1980), 251.

2. Guchton, R.R., Struct.Bonding (Berlin), 17 (1973), 67.

3. Gill, T.J. III and Mann, L.T. Jr., J.Immunology, 96 (1966), 906.

4. Edwards, E.I., J.Organometal Chem., 85 (1975), C-23.

5. Rockett, G.W. and Marr, G., J.Organometal.Chem., 123 (1976), 205.

6. Albert, A., Nature, 177 (1956), 525.

7. Brit.Patent, 841,151; CA: 54 (1960), 126007.

8. Knowles, D.G., Plastic technol., 6 (1960), 35,42.

9. Caldwell, J.R., U.S. Patent 2,720,507, Octo.11,1955; CA: 50 (1956), 2205.

10. Horn, C.F. and Vineyard, R., Brit.Patent 899,896, June 27, 1962; CA: 57 (1962), 11391.

11. Hiroshi, K., Jap.Patent,74,119,879 Nov.15, 1974; CA: 83 (1975), 11466w.

12. Kalemnikov, E.A. Vesti Akad.Nauk, B SSR, Ser.Khim.Nauk (1975), 57.

13. Omote, Y., Kobayashi, R. and Sugigama, N., Bull.Chem.Soc.Japan, 46 (1973), 2896.

14. Casellato, U., Vidali, M., Vigato, P.A., Bandoli, G. and Clemente, D.A., Inorg.Nucl.Chem.Lett., 9 (1973), 299.

15. Imai, H. and Ota, T., Bull.Chem.Soc.Japan, 47 (1974), 2497.

16. Sherchik, A.M., Losov Yu.P. and Paushkin Ya.M., Chem.Abstr., 91 (1979), 157858.

17. Bruce, M.I., Advan.Organometal Chem., 6 (1968), 273.

18. Cais, M. and Lupin, M.S., Advan.Organometal.Chem., 8 (1970), 211.

19. Margrave, J.L., "Mass-spectroscopy in Inorganic Chemistry" Advan.Chem.Ser. Vol. 72, A.C.S. Washington, D.C., 1968.

20. Spalding, T.R., "Spectroscopic methods in organometallic chemistry", Ed. George, W.O., Butterworths, 1970, p.95.

21. Litzov, M.R. and Spalding, T.R., Mass-spectrometry of Inorganic and Organometallic Compounds, Elsevier Scientific Publishing Company, 1973.

22. Friedman, H.L., Irsa, A.P. and Wilkinson, G., J.Am.Chem.Soc., 77 (1955), 3689.

23. Muller, J. and D'Or, L., J.Organometal.Chem., 10 (1967), 313.

24. Schumacher, E. and Taubenest, R., Helv.Chim.Acta, 47 (1964), 1525.

25. Denning, R.G. and Wentworth, R.A.D., J.Am.Chem.Soc., 88 (1966), 4619.

26. Mendelbaum, A. and Cais, M., Tetrahedron Lett., 51 (1964), 3847.

27. Seel, F. and Sperber, V., J.Organometal Chem., 14 (1968), 405.

28. Egger, H., Monotsh.Chem., 97 (1966), 602.

29. Cais, M., Lupin, M.S., Maoz, N. and Sharvit, J., J.Chem.Soc. A. (1968), 3086.

30. Maoz, N., Mendelbaum, A. and Cais, M., Tetrahedron Lett., (1965), 2087.

31. Rosenblum, M. and Woodward, R.B., J.Am.Chem.Soc., 80 (1958), 5453.

32. Imai, H., Bull.Chem.Soc.Japan, 45 (1972), 1264.

33. King, R.B., Appl.Spectr., 23 (1969), 148.

34. Nesmeyanov, A.N., Zagorevskii, D.V., Nekrasov Yu, S., Sizoi, V.F., Postnov, V.M., Baran, A.M. and Klimova, E.I., J.Organometal.Chem., 169 (1979), 77.

35. Charalambous, J. (Ed.) "Mass-spectrometry of metal compounds", Butterworths, London (1975), page 47.

36. Popp, F.D. and Moynaham, E.B., J.Heterocycl.Chem., 7 (1970), 351.

37. Rockett, B.W. and Marr, G., J.Organometal.Chem., 211 (1981), 215.

38. Marr, G. and Rockett, B.W., J.Organometal.Chem., 189 (1980), 163.

39. Rockett, B.W. and Marr, G., J.Organometal.Chem., 167 (1979), 53.

40. Marr, G. and Rockett, B.W., J.Organometal.Chem., 147 (1978), 273.

41. Lippincott, E.R. and Nelson, R.D., J.Chem.Phys., 21 (1953), 1307.

42. Rosenblum, M., Chem. and Ind. (1958), 953.

43. Rosenblum, M. and Woodward, R.B., J.Am.Chem.Soc., 80 (1958), 5443.

44. Toma, S. and Per'Jessy, A., Chem.Zwesti, 23 (1969), 533.

45. Dvoryanstsera, G.G., Doklady.Akad.Nauk.SSSR, 152 (3) (1963), 617.

46. Nesmeyanov, A.N., Doklady.Akad.Nauk SSSR, 112 (1957), 433.

47. Beattie, J.R. and McQuillan, G.R., J.Chem.Soc. (1963), 1519.

48i) Taimsalu, P. and Wood, J.L., Spectrochim.Acta, 20 (1964), 1943.

ii) ibid, 20 (1964), 1357.

iii) Taimsalu, P. and Wood, J.L., Trans.Faraday Soc., 59 (1963), 1754.

49. Poller, R.C., J.Inorg.Nucl.Chem., 24 (1962), 593.

50. Cummins, R.A., Austra.J.Chem., 18 (1965), 98.

51. Kawasaki, Y., Hari, M. and Uneka, K., Bull.Chem.Soc.Japan, 40 (1967), 2463.

521) Tanaka, T., Komura, M., Kawasaki, Y. and Okawara, R., J.Organomet.Chem. 1 (1964), 484.

11) Kawakami, K. and Okawara, R., J.Organomet.Chem., 6 (1966), 249.

53. Nakamoto, K. and Martell, A.E., J.Chem.Phys., 32 (1960), 588.

54. Clark, R.J.H. and Williams, C.S., Spectrochim.Acta, 21 (1965), 1861.

55. Beattie, I.R., and McQuillan, G.R., J.Chem.Soc., (1963), 1519.

56. Taimsalu, P. and Wood, J.A., Spectrochim.Acta, 20 (1964), 1043.

57. Clark, R.J.H. and Williams, C.S., Spectrochim.Acta, 21 (1965), 1861.

58. Beattie, I.R. and McQuillan, G.R., J.Chem.Soc., (1963), 113.

59. Sawyer, A.K., "Organotin Compounds", Vol.1 to 3, 1971, New York.

60. Janssen, M.J., Rec.trav.chim., 82 (1962), 90.

61. Cummins, R.A. and Dunn, P., Aust.J.Chem., 17 (1964), 185.

62. Okawara, R. and Ohara, M., Bull.Chem.Soc.,Japan, 36 (1963), 624.

63. Sato, H. and Okawara, R., Int.Symp.Mol.Struc. Spectro., Tokyo, Japan, Sept.1962.

64. Newman, R., J.Chem.Phys., 20 (1952), 1663.

65. Okawara, R., Webster, D.E. and Rochow, E.G., J.Am.Chem.Soc., 82 (1960), 3287.

66. Crecely, R.W., Crecely, K.M. and Goldstein, J.H., Inorg.Chem., 8 (1969), 252.

67. Benkeser, R.A., Nagai, Y. and Hooz,J., Bull.Chem.Soc., Japan, 36 (1963), 482.

68. Dvoryanstseva, G.G., Portnova, S.L., Sheinker, Yu.N, Yureva, L.P. and Nesmeyanov, A.N., Dokl.Akad.Nauk. SSSR, 169 (1966), 1083.

69. Dvoryanstsera, G.G., Portnova, S.L., Grandberg, K.I., Gubin, S.P. and Sheinker, Yu.N., Dokl.Akad.Nauk SSSR, 160 (1965), 1075.

70. Levenberg, M.I. and Richards, J.H., J.Am.Chem.Soc., 86 (1964), 2634.

71. Nagai, K., Hooz, J. and Benkeser, R.A., Bull.Chem.Soc. Japan, 37 (1964), 53.

72. Raush, M.D. and Mark, V., J.Org.Chem., 28 (1968), 3225.

73. Kamezawa, N., J.Magn.Res., 11 (1978), 88.

74. Curpey, T.J., Sonter, J.O., Rosenblum, M. and Richards, J.H., J.Am.Chem.Soc., 82 (1960), 5249.

75. Frankel, G., Carter, R.E., McLachlan, A. and Richards, J.H., ibid, 82 (1960), 5846.

76. Bublitz, D.E., McEwen, W.E. and Keinberg, J., ibid, 84 (1962), 1845.

77. Raush, M.D. and Siegel, A., J.Organometal.Chem., 17 (1969), 117.

78. Slocum, D.W., Engelmann, T.R., Lewis, R. and Kurland, P.J., J.Chem.Eng.Data, 13 (1968), 378.

79. Raush, M.D. and Siegel, A., J.Organometal.Chem., 11 (1968), 317.

80. Poller, R.C., "The chemistry of organotin compounds", (1970), pp.315; Lagos Press Ltd., London.

81. Sawyer, A.K., "Organotin Compounds", Vol.1 to 3, 1971, Inc. New York.

82. Maddox, M.L., Stafford, S.L. and Kaesz, H.D., Adv.Organometal.Chem., 3 (1965), 1.

83. Boue, S., Gielens, M. and Nasielski, J., Bull.Soc.Chim.Belges, 76 (1967), 559.

84. Considine, W.J., Baum, G.A. and Jones, R.C., J.Organometal.Chem., 3 (1965), 308.

85. Kawasaki, Y., Tanaka, T. and Okawara, R., Bull.Chem.Soc.Japan, 40 (1967), 1562.

86. Kawasaki, Y., Tanaka, T. and Okawara, R., Spectrochim.Acta, 22 (1966), 1571.

87. Serpone, N. and Hersh, K.A., Inorg.Chem. 13 (12), (1974), 2901.

88. Duffy, D.J. and Pignolet, L.H., Inorg.Chem., 11 (1972), 2843 and references therein.

89. Bater, S.S., Hutchison, J.R., Holm, R.H. and Muetterties, E.L., J.Am.Chem.Soc., 94 (1972), 6411.

90. Komura, M., Tanaka, T. and Okawara, R., Inorg.Chim.Acta, 2 (1968), 321.

91. Otero, J., Kawasaki, Y. and Tanaka, T., Inorg.Chim.Acta, 1 (1967), 294.

92. Jolly, W.L., Inorg.Synthesis, 11 (1968), 120.

93. Graham, P.J., Lindsay, R.V., Parshall, G.W., Peterson, M.L. and Whitman, G.M., J.Am.Chem.Soc., 79 (1957), 3416.

94. Struve, O., J.Prakt.Chemie, 52 (1895), 170.

95. Vogel, A.I., A Textbook of Practical Organic Chemistry, Fourth Edn. ELBS, London, 1978, p.264.

96. Spilners, I.J. and Larson, J.G., Org.Mass.Spectrom., 3 (1970), 915.

97. Kingston, D.G.I., Tannenbaum, H.P., Baker, G.B., Dimmock, J.R. and Taylor, W.G., J.Chem.Soc., (1970), 2574.

98. King, R.B., Cand.J.Chem., 47 (1969), 559.

99. Goldsmith, D. and Djerassi, C., J.Org.Chem., 31 (1966), 3611.

100. Budzikiewiez, H., Djerassi, C. and Williams, D.H., "Mass-spectrometry of Organic Compounds", Holden-Day, San-Francisco, 1967, pp. 158-159.

101. Budzikiewiez, H., Djerassi, C. and Williams, D.H., "Interpretation of Mass-Spectra of Organic Compounds", Holden-Day, Inc. (1964), San-Francisco, p.205.

102. Sahni, S.K., Sangal, S.K., Gupta, S.P. and Rana, V.B., J.Inorg.Nucl.Chem., 39 (1977), 1093.

103. Sayed, L.EL. and Iskander, M.F., J.Inorg.Nucl.Chem., 33 (1971), 435.

104. Richards, R.E. and Thomson, H.W., J.Chem.Soc., (1947), 1248.

105. Dorman, S.E. and Sutherland, G.B.B.M., Nature, 164 (1949), 440.

106. Letaw, H.(Jr) and Gropp, A.H., J.Chem.Phys., 21 (1953), 1621.

107.i) Dutta, R.L. and Banerjee, S.P., J.Indian Chem.Soc., 51 (1974), 497.

ii) Mashima, M., Bull.Chem.Soc.Japan, 35 (1962), 1882.

108. Monoyama, M. and Yamasaki, K., Inorg.Chim.Acta, 3 (1969), 585.

109. Mashima, M., Bull.Chem.Soc.Japan, 35 (1962), 332.

110. Clarke, H.T., Ed. "The Chemistry of Penicillin" Princeton Univ.Press, Prinston, New Jersey, 1949.

111. Miyazawa, T., Shimanouchi, T. and Mizushima, S., J.Chem.Phys., 24 (1956), 408.

112. Bhasin, S.K., Ph.D. Thesis, Poona University, Poona, India (1970).

113. Aggarwal, R.C. and Narang, K.K., Ind.J.Chem., 9 (1971), 1413.

114. Bellamy, L.J., "The Infrared Spectra of Complex Molecules", 1954.

115. Nakamoto, K., "Infrared Spectra of Inorganic and Coordination Compounds", Second Edn. (1970), Wiley-Interscience, N.Y., page 268.

116. Bacon, R.G.R. and Lindsay, W.S., J.Chem.Soc., (1958), 1382.

117. Giguere, P.A. and Liu, I.D., J.Chem.Phys., 20 (1952), 136.

118. Nicholls, D., Rowley, M. and Swindells, R., J.Chem.Soc. A, (1966), 950.

119. Powell, D.B. and Sheppard, N., J.Chem.Soc., (1956), 3108.

120. Condrate, R.A. and Nakamoto, K., J.Chem.Phys., 42 (1965), 2590.

121. Nakamoto, K. and Martell, A.E., J.Chem.Phys., 32 (1960), 588.

122. Poller, R.C. and Ruddick, J.N.R., J.Chem.Soc.A, (1969), 2273.

123. Lohmann, D.H., J.Organometal.Chem., 4 (1965), 382.

124. Domasetis, G., Magee, R.J. and James, B.D., J.Inorg.Nucl.Chem., 41 (1979), 1547.

125. Bucher, F.K., Gerrard, W., Mooney, E.F., Rees, R.G. and Willis, H.A., Spectrochim.Acta, 20 (1964), 51.

126. Taimsalu, P. and Wood, J.L., Spectrochim.Acta, 20 (1964), 1043.

127. Poller, R.C. and Toley, D.L.B., J.Chem.Soc.A (1967), 1578.

128. Dash, M.K. and Ghosh, M.R., J.Ind.Chem.Soc. Vol.LXII (1980), 678.

129. Henricks, S.B., Wulf, O.R., Hilbert, G.E. and Liddel, U., J.Am.Chem.Soc., 58 (1936), 1991.

130. Bhasin, S.K., Ph.D. Thesis, Poona University, Poona, India, (1970), p.189.

131. Sawyer, A.K., "Organotin Compounds", Vol.2, (1971), Marcel Dekker Inc., New York, page 254.

132. Barsode, C.D., Ph.D. thesis, Poona University, Poona, India (1976).

PART - II

CHAPTER -I GENERAL INTRODUCTION

		Page
1.1	Introduction	135
1.2	Ruthenium complexes as homogeneous catalysts	137
1.2.1	Hydrogenation of olefins	137
1.2.2	Hydrogenation of polyenes/ acetylenes	141
1.2.3	Hydrogenation of unsaturated acids	142
1.2.4	Hydrogenation of allylic compounds	143
1.2.5	Other hydrogenation reactions	143
1.3	Reaction mechanism and kinetic studies	145
1.4	Scope and objective of the present work	150

1.1. Introduction

Homogeneous catalysts consisting of transition metal complexes are known to be active for a variety of reactions such as isomerization[1], carbonylation[2], oxidation[3], hydroformylation[4], polymerization[5] and hydrogenation[6-11]. Though most of the commercial processes today are employing heterogeneous catalysts - a well known example being the iron oxide catalyst for ammonia synthesis, recently soluble transition metal complexes as homogeneous catalysts have gained much importance, because the homogeneous catalysts are active at relatively mild operating conditions and are also highly selective. In contrast to this, the heterogeneous catalysts require severe operating conditions and often pose serious problems of selectivity. Another attractive feature of the transition metal complexes is that they are able to activate substrates such as hydrogen, oxygen, carbon monoxide, olefins, acetylenes and dienes which are commonly involved in petrochemical processes. A large number of patents and research publications have appeared in the literature and now more than twenty important industrial processes use homogeneous catalysts. The reactions involving hydrogenation, carbonylation and oxidation of organic substrates have been most widely studied. Hydrogenation of a variety of organic

substrates (e.g. olefins, acetylenes, dienes, polyenes, nitro-compounds, etc.) can be carried out under mild operating conditions and with high selectivity using homogeneous catalysts. Complexes of Group VIII transition metals, particularly the platinum metals (ruthenium, rhodium, palladium, platinum, osmium and iridium) are known to be active for these reactions. Several reviews on hydrogenation by homogeneous catalysts have already been published[6-11].

The most widely studied catalysts for hydrogenation reactions are: Wilkinson catalyst - chlorotris(triphenylphosphine)rhodium(I) and Vaska catalyst - chlorocarbonyl bis(triphenylphosphine)iridium(I). The complexes of ruthenium have also been found to be active for homogeneous hydrogenation reactions. Since the present work is mainly concerned with hydrogenation reactions using ruthenium complex catalysts, the literature background on various aspects of these catalysts is discussed in the following sections.

The literature on this subject upto 1973 has been covered by James, B.R. and the same author published another review in 1978 covering the new developments in the area.[6a,6b] These reports indicate that the catalytic

activity of ruthenium complexes has not been thoroughly investigated.

1.2. Ruthenium complexes as hydrogenation catalysts

In one of the earlier studies Halpern[12] has reported that ruthenium complexes are effective catalysts for hydrogenation reactions. Later a large number of publications[13-22] dealing with ruthenium complexes as hydrogenation catalysts have appeared in the literature. A summary of investigations on these catalysts is presented in Table 1. Of the various catalysts listed, the complexes such as $RuCl_4^{2-}$, $RuCl_2(bipy)_2$, $RuCl_2(L_3)$ (where L = PPh_3, $AsPh_3$), $Ru_2(CO_2Me)_4$ etc. have been found to be active at mild operating conditions (1 atm H_2; 25-80°C). The major studies using ruthenium complex catalysts are concerned with the hydrogenation of unsaturated acids and terminal olefins.

1.2.1. Hydrogenation of olefins

Wilkinson and coworkers[14-17] have investigated the hydrogenation of linear olefins using several ruthenium(II) phosphine complexes as catalysts. They have found that the hydrido complex of ruthenium(II) is an extremely efficient catalyst for the reduction of olefins at 25°C and 1 atm H_2 pressure. Many other groups

have also reported the activation of hydrogen using dichlorotris(triphenylphosphine)ruthenium(II)[16-18]. A summary of hydrogenation reactions studied using $RuCl_2(PPh_3)_3$ catalyst is presented in Table 2.

Jardine and McQuillin[19] have reported that ruthenium trichloride (10^{-2}M) with triphenylphosphine ($6x10^{-2}$M) in methanol solution catalyzes hydrogenation of cycloalkenes to cycloalkanes at room temperature and 1 atm pressure of hydrogen. However, Hallman, McGarvey and Wilkinson have studied the hydrogenation of cyclic as well as terminal and internal olefins using $HRuCl(PPh_3)_3$ catalyst which is formed <u>in situ</u> by reaction of hydrogen with dichlorotris(triphenylphosphine)ruthenium(II) complex[17]. No isomerization of alkenes during hydrogenation has been observed in this study. Internal, cyclic and substituted alkenes are hydrogenated slowly in comparison to terminal alkenes. Horner and coworkers[20] have used benzene:ethanol (2:1) solutions of rutheniumtrichloride/triphenylphosphine in the presence of basic amines for the hydrogenation of pent-1-ene. In this study it is presumed that $HRuCl(PPh_3)_3$ is the catalytically active species.

Hydrogenation of pent-1-ene using π-arene-ruthenium complex catalyst has also been studied by Ogata and coworkers[21] at 30 atm H_2 pressure and 30°C. They have

found that during hydrogenation, isomerization of pent-1-ene to pent-2-ene is significant. These authors also have reported that the catalytic behaviour of this complex is similar to that of dichlorotris(triphenylphosphine)ruthenium(II).

Later, Abley and McQuillin[22] have shown that some chloride-bridged complexes of ruthenium also catalyze the hydrogenation of terminal olefins under mild operating conditions. They have studied hydrogenation of oct-1-ene using $[(PPh_3)_3RuCl_3Ru(PPh_3)_3]Cl$ as a catalyst and benzene as a solvent. Quantitative hydrogenation takes place at 20°C and 1 atm H_2 pressure. Isomerization of oct-1-ene to oct-2-ene has also been observed under these conditions but the rate was very slow compared to hydrogenation.

Ruthenium(III) acetylacetonate with triisobutylaluminium has been found to be active for hydrogenation of oct-1-ene at 40° and 3.5 atm H_2 in n-heptane solution[23]. Triisobutylaluminium acts as a reducing agent in the preparation of the catalytically active ruthenium(II) complex.

Wilkinson[14] has claimed that $RuCl_2(PPh_3)_4$ and $[Ru_2Cl_3(PPh_2PEt)_6]Cl$ are efficient catalysts for the hydrogenation of hex-1-ene at ambient conditions. Wilkinson and coworkers[15] have studied the hydrogenation

of alkenes using complexes of the type $[HRu(COOR)(PPh_3)_3]$ as catalysts. The effect of different carboxyl groups on the hydrogenation activity has been investigated. These authors have also reported[16,17] that the hydrogenation of hept-1-ene using $RuCl_2(PPh_3)_3$ complex catalyst in benzene solution is very slow but in benzene:ethanol (1:1), the rate of hydrogenation becomes very rapid after a short initial induction period. The initial induction period has been explained as the time required for the activation of hydrogen to form the catalytically active hydridochlororuthenium(II) species. During this process the colour of the catalyst solution changes from brown to violet. It has also been reported that the bases, for example ethanol, triethylamine, potassium hydroxide, etc. act as promoters for the hydrogenation reactions with $RuCl_2(PPh_3)_3$ catalyst.

Hui and Rampel[24] have used $Ru_2(CO_2Me)_4$ as a catalyst in dimethylformamide solution for the hydrogenation of terminal olefins and dienes at 80°C and 1 atm H_2 pressure. These metal carboxylates have the ability to activate olefins and hydrogen. The catalyst consisting of irradiated trans-$Ru(CO)_3(PPh_3)_2$ has been found to be active for hydrogenation of cyclohexene[25]. In this work it has been shown that the oxidative addition of hydrogen to the

coordinatively unsaturated species $Ru(CO)_2(PPh_3)_2$ forms the catalytically active species.

1.2.2. Hydrogenation of polyenes/acetylenes

In one of the earlier studies, Jardine and McQuillin[19] have shown that ruthenium complexes can be used for the reduction of acetylene to olefin and dienes to monoenes. They have studied the hydrogenation of diphenylacetylene to cis-stilbene and 3,5-dimethylhex-1-yn-3-ol to 3,5-dimethylhexane-1-ol at room temperature and 1 atm pressure. Furthermore, Candlin and coworkers[26] have studied the selective hydrogenation of acetylenes to olefins using $RuCl_3.3H_2O$ and $RuCl_3(SEt_2)_3$ compounds as catalysts in the presence of lithium aluminium hydride in different solvents. Research group in Imperial Chemical Industries has studied hydrogenation of a mixture of acetylene and olefin using ruthenium(II) complex catalysts containing tertiary phosphines as ligands and in this system acetylene is selectively hydrogenated to olefin.

Since the report of Jardine and McQuillin[19] on the selective hydrogenation of norbornadiene to norbornene using ruthenium trichloride trihydrate and triphenyl phosphine in methanol solution, several reports have appeared on the use of ruthenium complex catalysts for the selective reduction of polyenes to monoenes.

Takahashi and coworkers[27] have used a benzene:ethanol solution of $RuCl_2(PPh_3)_3$ to reduce 1-methoxy-octa-2,7-diene to 1-methoxy-oct-2-ene selectively. Nashimura and Tsuneda[28] have used similar catalyst to hydrogenate 1,4-androstadiene-3,17-diene to 4-androene-3,17-diene using benzene as a solvent at H_2 pressure of 125 atm. Later studies of Fahey[29] and Tsuji[30] have showed that $RuCl_2(PPh_3)_3$ complex catalyst is selective for the reduction of cyclododecatriene to cyclododecene and 1,5,9-cyclooctatriene to cyclooctene at room temperature.

1.2.3. Hydrogenation of unsaturated acids

Halpern and coworkers[12] are the first to report hydrogenation of maleic acid and fumaric acid using $RuCl_4^{2-}$ catalyst. James and Rhui[31] have also studied hydrogenation of maleic acid to succinic acid using $[RuCl_4(bipy)]^{2-}$ complex catalyst at 1 atm H_2 pressure and 80°C. In this study it has been shown that the activation of olefins results in the formation of a π-complex of moderate stability while with excess of olefin, the hydrogenation follows autocatalysis. In this study the colour of the catalyst solution changes from red to yellow and at the end of the reaction, precipitation of ruthenium metal takes place.

Using a 3M HCl solution of $RuCl_4^{2-}$ as catalyst, hydrogenation of acrylamide, acrylic acid, crotonic acid, ethylene and propylene has also been studied.[32] Hydrogenations of acrylamide, acrylic and crotonic acid are feasible at 1 atm pressure and 25°C whereas ethylene and propylene are not hydrogenated at all. This can be explained on the basis that carboxyl group adjacent to the double bond is essential to activate the double bond for the hydrogenation to proceed.

1.2.4. Hydrogenation of allylic compounds

The only references in the literature on hydrogenation of allylic compounds, such as allyl alcohol, allyl bromide and allyl cyanide using various rhodium[33-35] and ruthenium[15] phosphine complex catalysts are due to Wilkinson and coworkers. These authors have found that under identical conditions the rate of hydrogenation for allyl alcohol is faster than that of allyl bromide or allyl cyanide. This difference in the rates may be due to substituted functional groups which may alter the dielectric or other properties of the solvent medium or may coordinate strongly to the metal complex so that the rate of one or more steps in the hydrogenation process are retarded.

1.2.5. Other hydrogenation reactions

It has been claimed in a patent by Dewhurst[36] that

the reductions of unsaturated moieties, such as keto-, formyl- and nitrile as well as non-aromatic carbon-carbon double and triple bonds are feasible using the catalysts $RuCl_2(PPh_3)_3$, $HRuCl(CO)(PPh_3)_3$, $H_2Ru(Ph_2PMe)_4$ and $H_2Ru(CO)(Ph_2PMe)_3$ at 100 atm H_2 pressure and 20-130°C temperature.

Dichlorotris(triphenylphosphine)ruthenium(II) in the presence of a base also appears to be useful for catalytic hydrogenation of saturated aldehydes to alcohols[37], aliphatic and aromatic nitro-compounds to amines at hydrogen pressure of 90 atm and at 120°C[38,39]. Fahey[40] has studied the partial hydrogenation of multiunsaturated organic compounds, α-β-unsaturated ketones and esters, nitro-aromatics and aldehydes using a stable and easily prepared $RuCl_2(CO)_2(PPh_3)_2$ complex catalyst in a wide variety of solvents between 110-200°C and under 1-1200 psig hydrogen pressure.

Catalytic hydrogenation of acrylonitrile to 1,4-adiponitrile using ruthenium complex catalyst has been investigated by Strohmeier and Kaiser[41]. In this reaction only 2% of 1,4-dicyanobut-1-ene is obtained as a side product. The selective hydrogenation of cyclic carboxylic acid anhydrides to γ-lactones is achieved using $RuCl_2(PPh_3)_3$ complex catalyst and a tentative

reaction mechanism[42,43] has been proposed.

More recently, Toth and coworkers[44] have reported the hydrogenation of carbohydrates (e.g. fructose) using sulphonated ruthenium-phosphine complex catalyst in aqueous solution under mild operating conditions (20-70°C) and 1 atm H_2. Hydrogenation of carbon monoxide to methanol has been carried out using a soluble ruthenium complex catalyst, tris(2,4-pentanediono)ruthenium(III) under high pressure of 1300 atm. of carbonmonoxide and hydrogen (60:40) and at 268°C using tetrahydrofuran as a solvent[45].

1.3. Reaction mechanism and kinetic studies

In the catalytic hydrogenation by metal complexes, an important aspect is to investigate the reaction mechanism and the rate determining steps. This calls for a detailed study on the kinetics of the reactions. As the homogeneously catalyzed reactions involve a number of steps, the mechanism and kinetics are often very complex. In this section, the mechanisms of olefin hydrogenation using ruthenium(II) complexes as catalysts along with a brief account of kinetic studies has been presented.

Though many reports indicating the feasibility of hydrogenation of olefins with ruthenium catalysts have been published, only limited information is available

on the reaction mechanisms and the kinetics. James and Hui[46] have studied the kinetics of hydrogenation of maleic acid using $HRuCl(PPh_3)_3$ catalyst in dimethyl acetamide solution. The catalyst is prepared *in situ* by the reaction of H_2 with $RuCl_2(PPh_3)_3$ complex. They have found from the spectroscopic studies that the active catalytic species is the hydrido complex of ruthenium $[HRuCl(PPh_3)_3]$.

The following mechanism has been proposed:

$$RuCl_2(PPh_3)_3 + H_2 \xrightleftharpoons{\text{base}} HRuCl(PPh_3)_3 + HCl \text{ base} \quad (1)$$

$$HRuCl(PPh_3)_3 \xrightleftharpoons{K_1} HRuCl(PPh_3)_2 + PPh_3 \quad (2)$$

$$HRuCl(PPh_3)_2 + \text{olefin} \xrightleftharpoons{K_2} RuCl(PPh_3)_2(\text{alkyl}) \quad (3)$$

$$RuCl(PPh_3)_2(\text{alkyl}) + H_2 \xrightarrow{k} HRuCl(PPh_3)_3 + \text{alkane} \quad (4)$$

The following rate equation represent the experimental data of James and Hui.

$$\frac{-d[H_2]}{dt} = \frac{kK_2[Ru^{II}]T\,[\text{olefin}][H_2]}{1 + K_2[\text{olefin}] + [PPh_3]/K_1} \quad \ldots (i)$$

where [olefin] and $[PPh_3]$ refer to the free concentration of these species.

This is consistent with the above reaction mechanism, where the step (4) is assumed to be rate determining. Under certain conditions, some limiting forms of the above equation can also be used. The kinetics have been studied at 35° and the rate has been found to be first order in hydrogen and between zero and first order in olefin. The rate is inversely proportional to the concentration of triphenyl phosphine. The dependence of the reaction rate on catalyst concentration is found to be complex. James and Hui[31] have also studied detailed kinetics and mechanism of hydrogenation of maleic acid using tetrachloro(bipyridyl) ruthenate(II) anion $[RuCl_4(bipy)]^{2-}$ as catalysts at 80° and 1 atm H_2 pressure. The following reaction mechanism has been proposed.

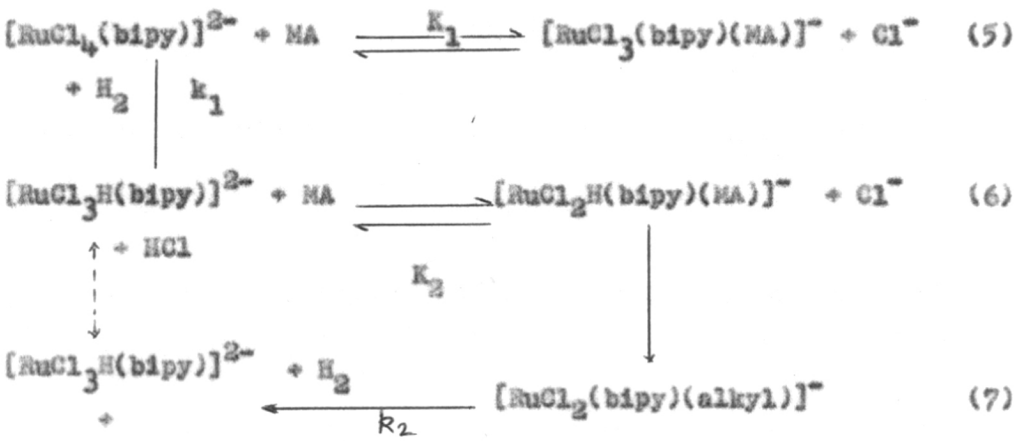

where MA = maleic acid, bipy = bipyridyl.

The rate data have been correlated using the following equation which is derived based on the above reaction mechanism.

$$\frac{-d[H_2]}{dt} = \frac{k_2 K_2 [H_2][\text{olefin}]\,[Ru^{II}]_T}{1 + K_2\,[\text{olefin}]} \qquad .. \quad (ii)$$

In this system, rate of reaction has been found to be first order in catalyst and hydrogen and zero- and first order in maleic acid concentrations. At catalyst concentrations of ~ 10^{-3}M, with a ten-fold excess of olefin, autocatalysis has been observed. The initial red solution of $[RuCl_4(bipy)]^{2-}$ turns yellow in the presence of excess substrate and spectrophotometric measurements have indicated a 1:1 Ru-olefin complex. Under certain conditions precipitation of metallic ruthenium has also been observed in this study.

More recently James and Wang[47] have studied the hydrogenation of acrylamide catalyzed by hydridobis(triphenylphosphine)ruthenium(II) chloride in N,N'-dimethylacetamide (DMA) and proposed the following reaction mechanism.

$$HRuCl(PPh_3)_2 + A \underset{}{\overset{\text{Fast}}{\rightleftharpoons}} RuCl(PPh_3)_2(alkyl) \qquad (8)$$

$$RuCl(pph_3)_2(alkyl) + HRuCl(PPh_3)_2 \underset{}{\overset{K_1}{\rightleftharpoons}} RuCl(PPh_3)_2 + AH_2 \qquad (9)$$

$$RuCl(PPh_3)_2 + H_2 \xrightarrow{k_2} 2HRuCl(PPh_3)_2 \qquad (10)$$

where A = acrylamide and AH_2 = propionamide.

The following rate equation have been proposed based on the above mechanism, in which the rate controlling step is represented by equation (10).

$$\frac{-d[H_2]}{dt} = \frac{Kk_1k_2\,[Ru_{total}]^2\,[H_2][olefin]}{(1+K[olefin]^2)\,(k_2[H_2] + K\text{-}1\,[sat.product]} \qquad .. (iii)$$

The kinetic data obtained for the hydrogenation of acrylamide using $[HRuCl(PPh_3)_2.DMA]_2$ in dimethylacetamide solvent is in agreement with the proposed mechanism. The kinetics have been determined at 35°C from the region of maximum rate of hydrogenation and it has been found that catalyst dependence is second order upto $4x10^{-3}$M,

hydrogen dependence is first order upto ca.100 mm Hg and then the rate decreases towards zero order at pressure > 500 mm Hg. An unusual inverse dependence on acrylamide has also been observed.

Jardine and coworkers[13] have studied the mechanism and kinetics of hydrogenation of norbornadiene using $RuCl_2(PPh_3)_3$ catalyst (prepared *in situ*) and also reported some unusual observations. In this, they have found that the effect of substrate concentration on the rate is highly complex as shown in the diagram. The explanation of this type of behaviour remains uncertain, but the maximum and minimum at 1:1 and 2:1 diene to ruthenium ratios respectively have been presumed to be related to the presence of one and two moles of coordinated diene moieties in reactions such as metal alkyl formation and oxidative addition of hydrogen molecule in the rate determining steps.

From the reported kinetic studies on ruthenium-complex catalyzed hydrogenation, it appears that the effect of catalyst and olefin concentrations on the rate is rather complex and there is much scope for further investigations.

1.4. Scope and objective of the present work

It can be seen from the literature published on ruthenium catalyzed hydrogenation of unsaturated compounds

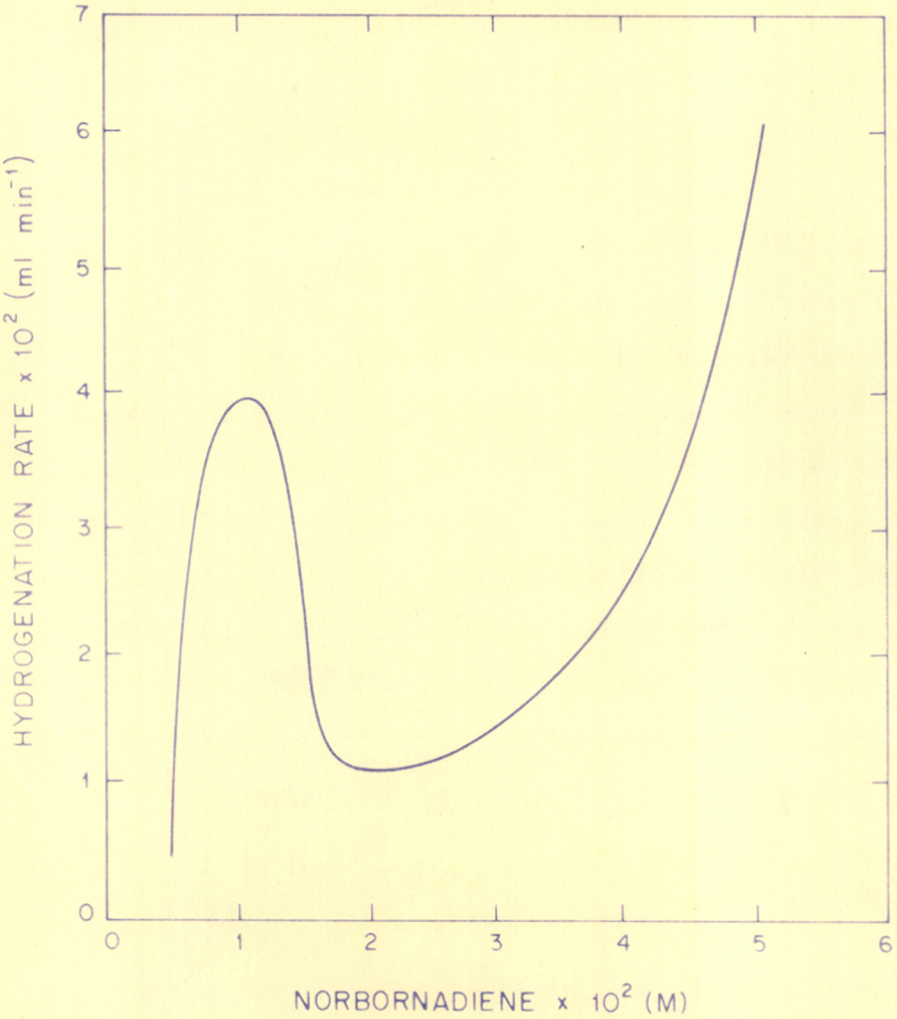

EFFECT OF NORBORNADIENE CONCENTRATION ON RATE OF HYDROGENATION BY $RuCl_3$ (10^{-2} M) AND PPh_3 (6×10^{-2} M) IN 50ml METHANOL.

that most of the work is qualitative in nature and only a few studies on important aspects such as kinetics and reaction mechanism have been reported. Particularly, the investigations on the hydrogenation of olefins such as cyclohexene, hex-1-ene and allylic compounds are very limited. Since a number of steps are involved in a catalytic cycle, it is likely that for different substrates, the rate determining steps and hence, the rate equations may be different. Therefore, it is necessary to undertake systematic studies on the kinetics of hydrogenation of different olefinic compounds. Furthermore, due to the growing importance of the area of homogeneous catalysis, such a study would be extremely useful in our understanding of the reaction mechanism and catalyst development. The objective of the present work is to investigate the following reactions:

1. Hydrogenation of cyclohexene with $RuCl_2(PPh_3)_3$ as a catalyst.
2. Hydrogenation of allyl alcohol and allyl bromide using $RuCl_2(PPh_3)_3$ as a catalyst.

While in choosing the first system, the objective is mainly to develop rate equation, the second system is chosen to investigate the complex effects such as carbonmonoxide abstraction from alcohol leading to the catalyst deactivation.

TABLE -1

A SUMMARY OF RUTHENIUM COMPLEXES AS HYDROGENATION CATALYSTS

S.No.	Catalytic complex	Substrate	Product	Conditions	References
1.	$[RuCl_4]^{2-}$	Fumaric acid	Succinic acid	25°C, 1 atm. H_2	12, 48
		Maleic acid	Succinic acid		
		Acrylamide	Propionamide	25°C, 1 atm H_2	32
		Acrylic acid	Propionic acid	25°C; 1 atm H_2	33
		Crotonic acid	Butyric acid		
2.	$[RuCl_4(bipy)]^{2-}$	Maleic acid	Succinic acid	80°C, 1 atm H_2	31
3.	$RuCl_3.3H_2O$ + PPh_3	Norbornadiene	Norboranane		
		Cyclohexene	Cyclohexane	25°C, 1 atm H_2	19
		Diphenyl acetylene	cis-Stilbene		
4.	$Ru(acac)_3$ + $(t\text{-}Bu)_3Al$	Octene	Octane		23
5.	trans-$Ru(CO)_3(PPh_3)_2$	Cyclohexene	Cyclohexane	Irradiated at 365 nm	25
6.	$Ru_3(CO)_{10}(NO)_2$	Hex-1-ene	Hexane	25°C, 4 atm H_2	49
7.	$HRuCl(CO)(PPh_3)_3$; $H_2Ru(CO)(Ph_2PMe)_3$; $H_2Ru(Ph_2PMe)_4$	Hex-1-ene	Hexane	20 to 130°C; 10-100 atm H_2	36
8.	$Ru_2(CO_2Me)_4Cl$ + HBF_4	Hexa-1,4-diene	Hexane	25°C, 1 atm H_2	50,51
	+ PPh_3	Hex-1-ene	Hexane		

contd....

S.No.	Catalytic complex	Substrate	Product	Conditions	References
9.	$Ru_2(CO_2Me)_4$	Oct-1-ene	Octane		
		Dec-1-ene	Decane	80°C, 1 atm H_2	24
		Cycloocta-1,3-diene	Cyclooctane		
10.	$(C_6H_6RuCl_2)_n$	Pent-1-ene	Pentane	30°C, 1 atm H_2	21
11.	$Ru_3(CO)_{12}$ $Ru(CO)_5$ $Ru(acac)_3$	Nitrobenzene	Aniline	(H_2 + CO mixture 200 atm), 100°C	52
12.	$HRu(CF_3CO_2)(PPh_3)_3$	Hex-1-ene	Not mentioned	50 cm, H_2, 25°C	15
		Hept-1-ene			
		Allyl benzene			
		Hexa-1,5-diene			
		1-Methyl cyclohexene			
		trans-hexa-1,4-diene			
		Cyclohexene			
		Penta-1,3-diene			
		Cyclooctene			
		Allyl alcohol			
13.	$Cis\text{-}RuCl_2(CO)_2(PPh_3)_2$	1,5,9-Cyclododecatriene	Cyclododecene	125-160°C	29
		1,5,9-Cyclooctatriene	Cyclooctene	100-200 psig H_2	

TABLE - 2

A SUMMARY OF HYDROGENATION REACTIONS USING $RuCl_2(PPh_3)_3$ COMPLEX CATALYST

S.No.	Substrate	Product	Conditions	Reference
I.	MONOENES			
	Pent-1-ene	Pentane	p_{H_2} 50 cm, 25°C	16
	Hex-1-ene	Hexane		
	Hept-1-ene	Heptane		
	Dec-1-ene	Decane		
	Cyclohexene	-		
II.	POLYENES AND ACETYLENS			
	Penta-1,3-diene	Pent-2-ene	p_{H_2} 50 cm, Temp.25°C	16
	Trans-hexa-1,4-diene	Trans-hex-2-ene, cis-hex-2-ene	p_{H_2} 60 cm, Temp.25°C	17
	Cis-hexa-1,4-diene	Trans-hex-2-ene cis-hex-2-ene	-do-	17
	2-Methyl-hexa-1,5-diene	2-Methylhex-1-ene	-do-	17
	Norboranadiene	Norbornane	1 atm H_2; 25°C	19
	1,4-Androstadiene-3,17-dione	4-Androene-3,17-dione	125 atm. H_2	28

contd...

Cyclododecatriene	Cyclododecene	-	29
1,5,9-Cyclooctatriene	Cyclooctene	-	30
Phenyl acetylene	Cis-stilbene	-	19
3,5-Dimethylhex-1-yn-3-ol	3,5-Dimethylhexane-1-ol	-	19
<u>Other substrates</u>			
Nitrobenzene	Aniline	Temp. 25-100°C, 100 atm. H_2	38
Benzaldehyde	Benzal alcohol	80°C, 20 atm H_2	37
Acrylonitrile	1,4-Adiponitrile	-	41
Cyclic carboxylic acid anhydrides	-Lactones	-	42-43

CHAPTER - II EXPERIMENTAL

		Page
2.1	Catalyst preparation	157
2.2	Kinetic studies	158
2.2.1	Apparatus	158
2.2.2	Procedure	158
2.3	Materials	161

2.1. Catalyst preparation

The catalyst precursor, tris(triphenylphosphine)-ruthenium(II) chloride, $RuCl_2(PPh_3)_3$, was prepared by the procedure reported by Wilkinson and Stephenson[53]. In this procedure ruthenium(III) chloride trihydrate, $RuCl_3.3H_2O$ was dissolved in methanol and to this solution a six-fold excess of triphenylphosphine was added. This mixture was filtered and the resulting deep-brown coloured solution was refluxed under nitrogen for six hours. The precipitated complex was filtered, washed several times with methanol and ether, dried and stored in a desiccator. The yield of the complex obtained was 75% of the theoretical. This complex, $[RuCl_2(PPh_3)_3]$ was analyzed for C, H and Cl and the results are given below:

Analysis (%)

Element	Found	Calc. for $C_{54}H_{45}Cl_2P_3Ru$
C	67.58	67.6
H	4.56	4.7
Cl	7.6	7.4

The i.r. spectrum of the complex showed characteristic bands at 310 cm^{-1}, 240 cm^{-1}, 250 cm^{-1} and 270 cm^{-1} which can be assigned for Ru-Cl and Ru-P bonds respectively.

2.2. Kinetic studies

2.2.1. Apparatus

The kinetic studies were carried out in an apparatus designed in such a way that the hydrogen uptake could be monitored continuously. This apparatus had a provision to vary the pressure in the system. A schematic diagram of the experimental set-up is shown in Fig. 1 .

A glass reaction vessel A with 4.5 cm diameter and 9.00 cm height was provided with an outer jacket for circulation of water at a constant temperature. The connecting tube T and the graduated glass burrette B were also jacketed. A magnetic stirrer device M was used for agitation of the reaction mixture and bypass trap G was used to fill the hydrogen gas in the system.

2.2.2. Procedure

The experimental procedure used for the measurement of reaction rates was as follows:

The entire system consisting of the reaction vessel, burrette, reservoirs and the surge tank was first evacuated using a high vacuum pump. The hydrogen x gas was introduced into the system carefully until one atm pressure. This evacuation filling cycle was repeated for a number of times. The reservoir liquid saturated with hydrogen was then

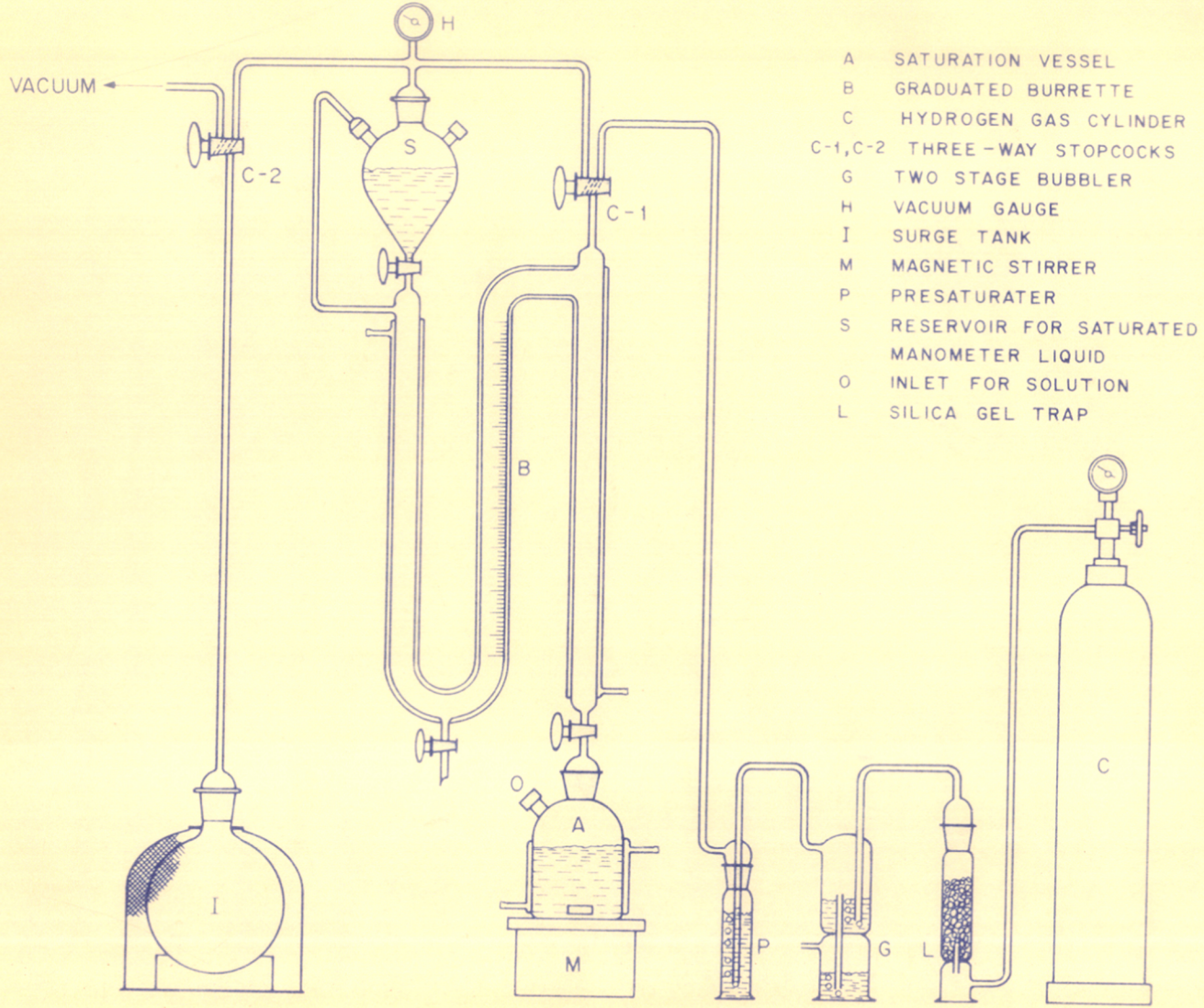

A SATURATION VESSEL
B GRADUATED BURRETTE
C HYDROGEN GAS CYLINDER
C-1,C-2 THREE-WAY STOPCOCKS
G TWO STAGE BUBBLER
H VACUUM GAUGE
I SURGE TANK
M MAGNETIC STIRRER
P PRESATURATER
S RESERVOIR FOR SATURATED MANOMETER LIQUID
O INLET FOR SOLUTION
L SILICA GEL TRAP

FIG. 1 : SCHEMATIC DIAGRAM OF THE EXPERIMENTAL SETUP.

introduced into the burrette to adjust the zero time reading, while a positive flow of hydrogen was maintained through the reaction vessel. In a typical experiment, a sample of the catalyst, $RuCl_2(PPh_3)_3$ was weighed accurately and charged into the reactor along with freshly distilled (under nitrogen) degassed solvents (benzene: ethanol, 1:1). The solution was stirred for 30 minutes to ensure the complete dissolution of catalyst after which freshly distilled cyclohexene of known quantity was added. In order to adjust a desired temperature, thermostatic water was circulated through the outer jacket of the reactor. After the desired temperature was attained the reaction was started by switching the stirring on. The volume of hydrogen absorbed was measured by movement of the liquid in the graduated burrette. After this the hydrogen uptake was continuously measured by equalising the pressure in the system by adjusting the water level in the manometer tube. The same procedure was repeated under different operating conditions to observe the volume of hydrogen absorbed vs time. In a few runs the concentration of unreacted olefins was also analysed.

For low pressure experiments the procedure followed was the same as given above, except that after charging the reactants into reaction vessel the system was set to

a desired pressure by controlled evacuation. The pressure in the system was recorded by a pressure guage.

2.3. Materials

2.3.1. Ruthenium trichloride trihydrate ($RuCl_3.3H_2O$) : Ruthenium trichloride trihydrate Fluka, A.G. Switzerland was used without further purification.

2.3.2. Triphenylphosphine (PPh_3) : Triphenylphosphine supplied by Fluka A.G. Switzerland was used without further purification.

2.3.3. Cyclohexene : Cyclohexene was obtained from M/s SD's chemicals, Bombay purified and distilled under nitrogen before use.

2.3.4. Allyl alcohol
2.3.5. Allyl bromide : Allyl alcohol and allyl bromide supplied by SD's Chemicals, Bombay, were purified and distilled under nitrogen before use.

2.3.6. Hydrogen gas : Hydrogen gas was supplied in cylinders by M/s. Indian Oxygen Co. (Bombay).

2.3.7. Solvents : Commercially available solvents were used after purification by standard procedures.

CHAPTER -III

HYDROGENATION OF CYCLOHEXENE - RESULTS AND DISCUSSION

		Page
3.1	Experimental results	162
3.1.1	Calculations of reaction rates	162
3.2	Solubility of hydrogen	164
3.3	Effect of solvents	167
3.4	Effect of agitation speed	171
3.5	Effect of hydrogen pressure	171
3.6	Effect of cyclohexene concentration	174
3.7	Effect of catalyst loading	174
3.8	Effect of temperature	179
3.9	Effect of triphenylphosphine	179
3.10	Discussion	182
3.10.1	Kinetic modelling	187
3.10.2	Unusual dependence of reaction rate on catalyst concentration	197

Hydrogenation of cyclohexene

3.1. Experimental results:

Hydrogenation experiments are carried out under different operating conditions as per the procedure described in Chapter II. As the purpose of this work is to study the kinetics of the reaction, only initial rates are observed such that the change in the substrate concentration is not large (< 10%) during an experiment.

3.1.1. Calculation of the reaction rates

In each experimental run, the volume of hydrogen absorbed is recorded as a function of time. A typical plot for different temperatures is shown in Fig.1. The reaction rate is calculated from the slope of this plot which is in the units cm^{-3}/min. This is converted into mole/cm^3/sec. It has been assumed in this calculation that the hydrogen uptake rate is also stoichiometrically proportional to the cyclohexene reaction rate. The overall reaction is as follows:-

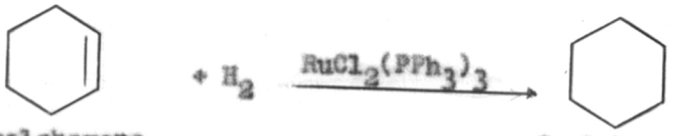

Cyclohexene Cyclohexane .. (i)

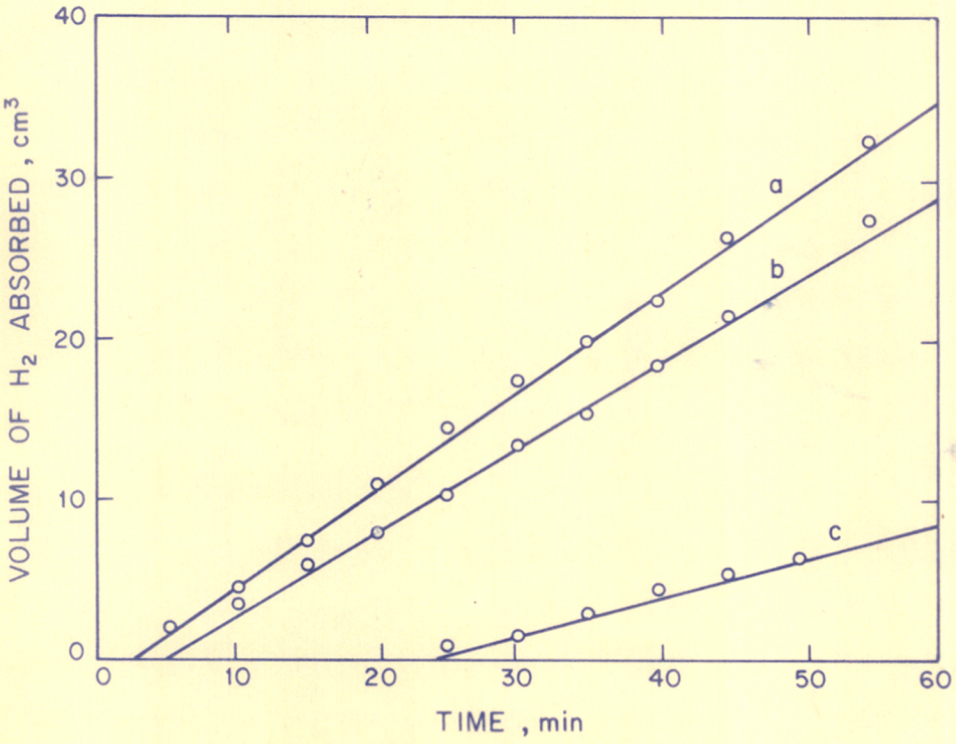

FIGURE 1 : EFFECT OF TEMPERATURE ON H_2 UPTAKE vs TIME PLOT.

CONCENTRATION OF $RuCl_2(PPh_3)_3$: $4{\cdot}184 \times 10^{-7}$ mole/cm^3, CYCLOHEXENE CONCENTRATION : $9{\cdot}8624 \times 10^{-4}$ mole/cm^3, H_2 PRESSURE : 1 atm, TEMPERATURES : a) 15° b) 35° c) 45° C.

In order to confirm this assumption, in a few experiments, the reaction is allowed to continue for longer durations (upto 20 hrs) and the volume of H_2 absorbed is compared with the cyclohexene converted (as calculated based on unreacted cyclohexene analysis). In all these experiments these data are in agreement with the equation (i). Hence for all the kinetic runs, the reaction rates are based on the measurement of hydrogen uptake. The reaction rates are observed under different operating conditions and the range of variables studied is presented in Table 1.

3.2. Solubility of hydrogen

Hydrogenation of cyclohexene is a gas-liquid reaction system using a dissolved catalyst. For such reactions dissolution of hydrogen is an important step. The concentration of the dissolved hydrogen will depend on the solubility at the operating temperature and partial pressure of H_2. For the interpretation of kinetic data, it is essential to have a knowledge of the solubility of hydrogen in the solvent system used (benzene + ethanol, 1:1). Solubility of hydrogen in pure benzene and ethanol has been reported in the literature[54,55]. The difference in solubility values (for pure benzene and pure ethanol) is not very large (~ 10%). However, to be more precise

TABLE -1

RANGE OF VARIABLES STUDIED

Parameter		Range
Catalyst concentration	:	1.459×10^{-7} to 1.60×10^{-6}, mole/cm^3
Hydrogen pressure	:	0.59 - 1.00 atm.
Cyclohexene concentration	:	7.889×10^{-4} to 1.972×10^{-3}, mole/cm^3
Temperature	:	15-45°C
Triphenylphosphine concentration	:	1.526×10^{-8} to 3.816×10^{-7}, mole/cm^3

TABLE -2

HENRY'S LAW CONSTANT AT VARIOUS TEMPERATURE

Temperature ($^{\circ}$C)	Henry's law constant (mole/cm^3/atm)$\times 10^6$
10	2.9762
15	3.0799
20	3.1800
25	3.2767
30	3.3703
35	3.4608
40	3.5485
45	3.6334
50	3.7156

the solubility of hydrogen in benzene:ethanol (1:1) mixture is calculated from these data using the theory proposed by Prausnet and coworkers[56]. According to this theory the solubility in a mixture can be calculated using the following equation.

$$(\text{Solubility})_{\text{mix}} = \sum_{1}^{2} \bar{\nu} S_1 \qquad (2)$$

where ν is the volume fraction and S is the solubility in mole/cm^3/atm.

In case of 1:1 mixture the volume fraction is 0.5. Therefore

$$(\text{Solubility})_{\text{mix}} = \nu_1 \; S_1 + \nu_2 \; S_2 \qquad (3)$$

$$= 0.5 \; (S_1 + S_2) \qquad (4)$$

where S_1 and S_2 are the solubilities of hydrogen (mole/cm^3/atm) in benzene and ethanol respectively. Solubility of H_2 in benzene:ethanol (1:1) mixture is expressed in terms of Henry's coefficient i.e., solubility of H_2 in solvents at atmospheric pressure.

The values of the Henry's coefficient calculated using Equation (4) is presented in Table 2.

In order to predict the actual concentration of dissolved hydrogen, it is also essential to know the partial pressure of hydrogen and the vapour-pressure of the solvent system. Vapour-pressure of the solvent system (benzene:ethanol, 1:1) is calculated using the following equation:

$$(P)_{mix} = \sum_{t=1}^{n} x_1 p_1 \gamma_1 \qquad (5)$$

where x_1 = mole fraction of the solvent

p_1 = vapour-pressure of pure component, mm.Hg

γ_1 = activity coefficient constant

P = vapour-pressure of the mixture, mm.Hg.

Vapour-pressure equilibrium data for individual components is taken from the literature[56]. The values of the vapour-pressure data calculated using equation (5) are presented in Table 3.

3.3. Effect of solvents

In homogeneously catalyzed reactions the solvents used play an important role in two ways:

(a) Different solvents will have different solubilities for gaseous reactants (such as hydrogen) and thus would result in different concentrations.

TABLE -3

VAPOUR-PRESSURE DATA FOR BENZENE:ETHANOL (1:1) MIXTURE

Temperature (^{o}C)	Vapour-pressure of a mixture (mm.Hg)
15	61.16
25	116.46
35	185.04
45	290.52

(b) The solvents can have coordinating ability with the metal-complex catalysts and hence can influence the reactivity of the catalytic complex.

Therefore, the effect of various solvents on hydrogenation of cyclohexene has been studied. The initial rates of hydrogenation is measured by the procedure described earlier (Chapter II) and the initial rate data are presented in Table 4.

It can be seen from Table 4 that no hydrogenation occured in DMF and DMSO solvents. When benzene was used as a solvent the hydrogenation rates are rather slow, though at higher catalyst concentrations, appreciable rates are observed. The solvent systems consisting of benzene or toluene and alcohol are found to be effective for this reaction. For example, 1:1 mixtures of benzene and ethanol, benzene and butanol, toluene and ethanol give the highest initial rates of hydrogenation. When pure ethanol is used the catalyst solubility being very low, most of the catalyst is not dissolved and hence very low hydrogenation rates are observed. Therefore, for the kinetic studies 1:1, benzene:ethanol solvent system is chosen.

TABLE -4

INITIAL RATES OF HYDROGENATION OF CYCLOHEXENE USING $RuCl_2(PPh_3)_3$ IN VARIOUS SOLVENTS

	Solvent	Initial rate of reaction ($mole/cm^3/sec$)
1.	Benzene	0.3260×10^{-9}
2.	Benzene:methanol (1:1)	0.1293×10^{-8}
3.	Benzene:ethanol (1:1)	0.3388×10^{-8}
4.	Benzene:n-propanol (1:1)	0.1601×10^{-8}
5.	Benzene:n-butanol (1:1)	0.3573×10^{-8}
6.	Toluene:ethanol (1:1)	0.3326×10^{-8}
7.	Xylene:ethanol (1:1)	No absorption
8.	Dimethyl formamide (DMF)	No absorption
9.	Dimethyl sulphoxide (DMSO)	No absorption

Conditions: Catalyst concentration 4.184×10^{-7}, $mole/cm^3$; cyclohexene concentration 9.8624×10^{-4}, $mole/cm^3$; temperature $35^{\circ}C$ and H_2 pressure 1 atm.

3.4. Effect of agitation speed

In gas-liquid reactions, it is necessary to ensure that dissolution of the gaseous species is not rate controlling. This can be achieved by studying the influence of stirring speed on the rate of hydrogenation. If stirring speed has no influence on the rate of reaction, it suggests that the transport limitations are not important and the reaction is kinetically controlled.

The effect of stirring speed on the initial rates of hydrogenation has been studied at two catalyst concentrations (0.2092×10^{-6} mole/cm^3 and 0.4184×10^{-6} mole/cm^3) and at 35° and 45°C. The rates are found to be independent of stirring speed under these conditions, which indicates the absence of diffusional resistance.

3.5. Effect of hydrogen pressure

In order to determine the order of reaction with respect to hydrogen pressure, hydrogenation rates are observed in a pressure range of 370 to 710 mm. Hg. A typical plot of hydrogen uptake vs time at 35°C and a catalyst concentration of 0.418×10^{-6} mole/cm^3 is shown in Fig.2. The effect of H_2 partial pressure on the rate of hydrogenation is shown in Fig. 3, which is a straight line passing through the origin. This suggests that the reaction rate is first order with respect to hydrogen.

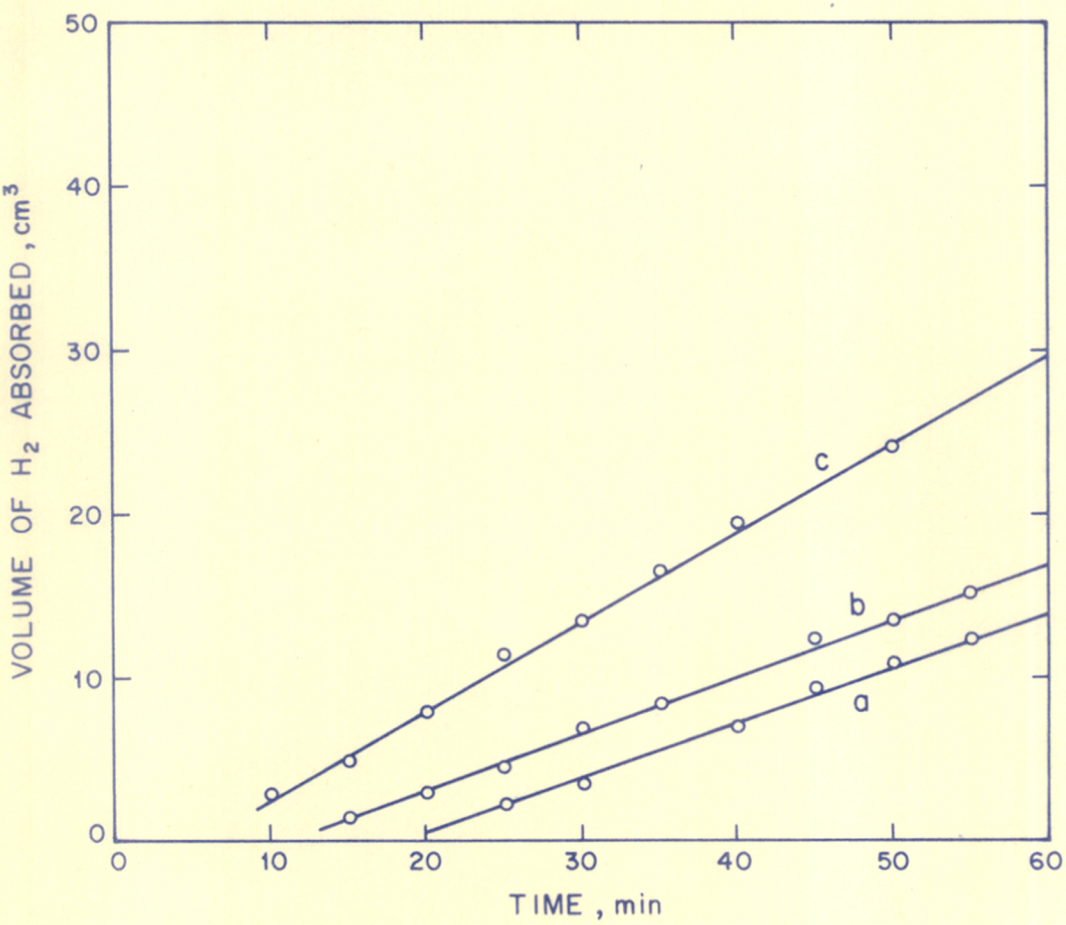

FIGURE 2 : EFFECT OF HYDROGEN PRESSURE ON H_2 UPTAKE vs TIME PLOT.

CONCENTRATION OF $RuCl_2(PPh_3)_3$: $4{\cdot}184 \times 10^{-7}$ mole/cm^3,
CYCLOHEXENE CONCENTRATION : $9{\cdot}8624 \times 10^{-4}$ mole/cm^3,
TEMP. 35°C , H_2 PRESSURE : a) 0·48 b) 0·59 c) 1·0 atm.

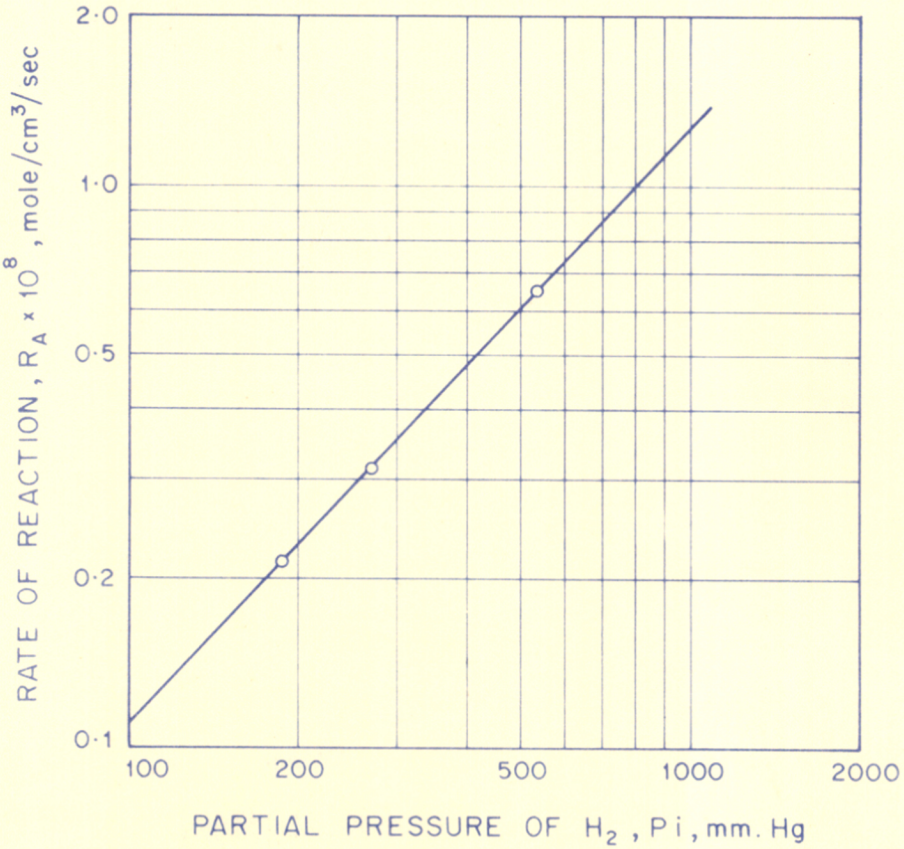

FIGURE 3 : EFFECT OF H_2 PARTIAL PRESSURE ON THE RATE OF HYDROGENATION.

CONCENTRATION OF $RuCl_2(PPh_3)_3$: $4{\cdot}184 \times 10^{-7}$ mole/cm³,
CYCLOHEXENE CONCENTRATION : $9{\cdot}862 \times 10^{-4}$ mole/cm³,
TEMP. 35 °C.

3.6. Effect of cyclohexene concentration

The effect of cyclohexene concentration on the rate of reaction has been studied by varying the cyclohexene concentration from 7.8899×10^{-4} to 19.7248×10^{-4} mole/cm^3. A typical plot of hydrogen uptake vs time at 35°C and a catalyst concentration of 0.418×10^{-6} mole/cm^3 is shown in Fig.4.

In order to determine the order of reaction with respect to cyclohexene concentration, a log-log graph of rate of reaction vs cyclohexene concentration is plotted and is shown in Fig.5. The order of reaction with respect to cyclohexene is found to be 0.741.

3.7. Effect of catalyst loading

The effect of catalyst ($RuCl_2(PPh_3)_3$) concentration on the rate of reaction has been studied in the concentration range of 1.459×10^{-7} to 1.6×10^{-6} mole/cm^3. In these experiments, all other conditions are kept constant. Fig.6 shows a plot of hydrogen absorbed vs time at different catalyst concentrations at 35°C and 1 atm H_2 pressure. Similar data have been obtained at different concentrations of cyclohexene and Fig. 7 shows a plot of rate of reaction vs catalyst concentration. It can be noticed that the rate vs catalyst concentration plot goes through a maximum.

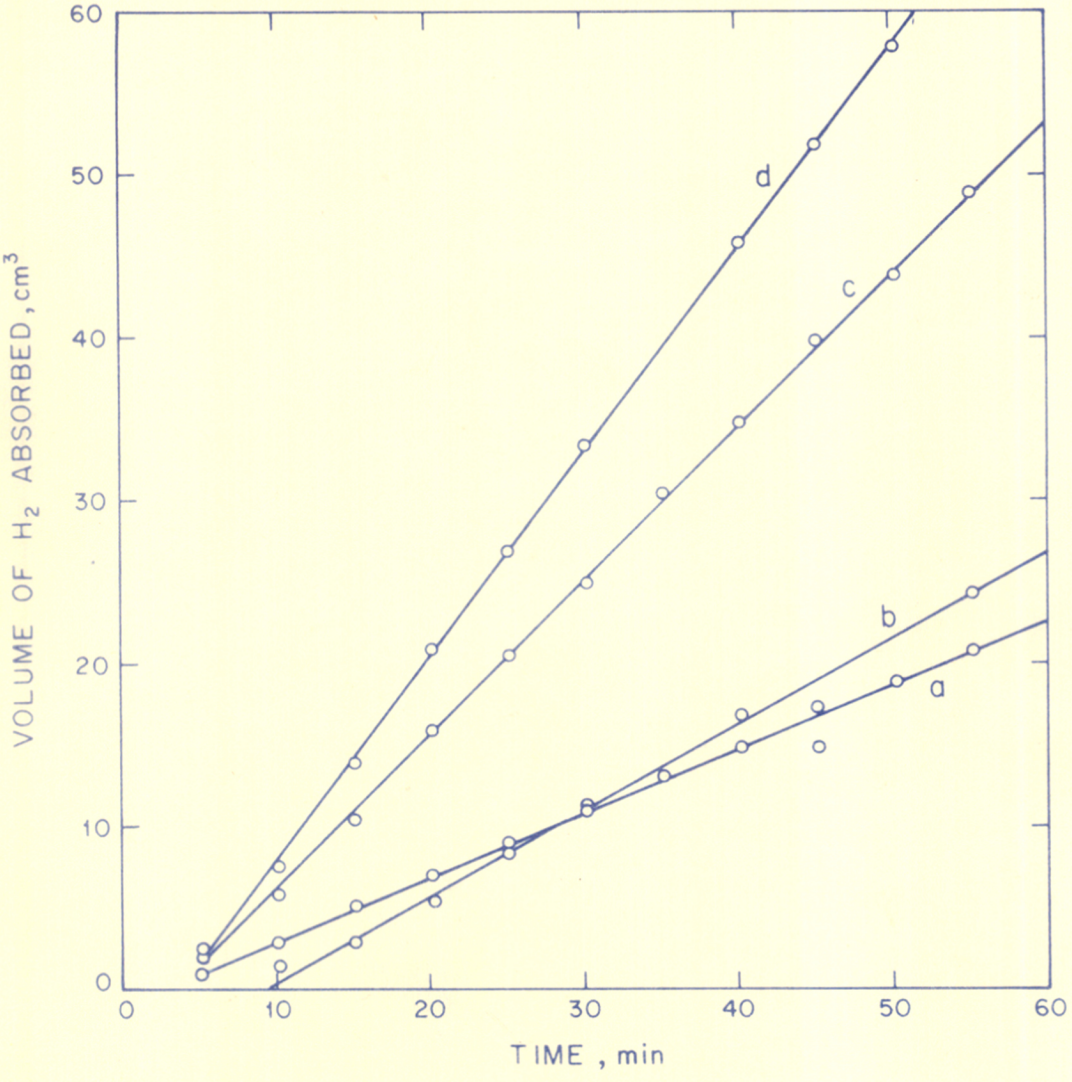

FIGURE 4 : EFFECT OF CYCLOHEXENE CONCENTRATION ON H_2 UPTAKE vs TIME PLOT.
CONCENTRATION OF $RuCl_2(PPh_3)_3$: $4{\cdot}184 \times 10^{-7}$ mole/cm^3, H_2 PRESSURE : 1 atm, TEMP. 35 °C, CYCLOHEXENE CONCENTRATION : a) $4{\cdot}8818 \times 10^{-4}$ mole/cm^3 b) $9{\cdot}8624 \times 10^{-4}$ mole/cm^3 c) $13{\cdot}807 \times 10^{-4}$ mole/cm^3.

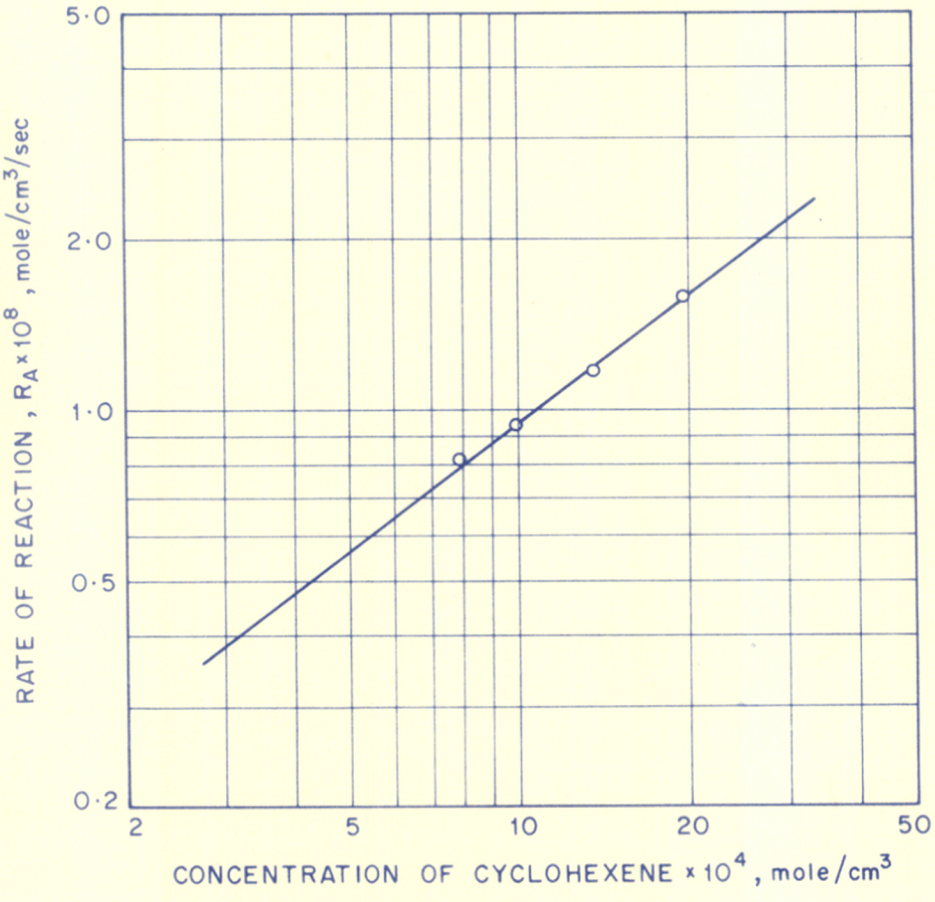

FIGURE 5 : EFFECT OF CYCLOHEXENE CONCENTRATION ON THE RATE OF HYDROGENATION.

CONCENTRATION OF $RuCl_2(PPh_3)_3$: $4{\cdot}184 \times 10^{-7}$ mole/cm^3, TEMP. 35 °C , H_2 PRESSURE : 1 atm.

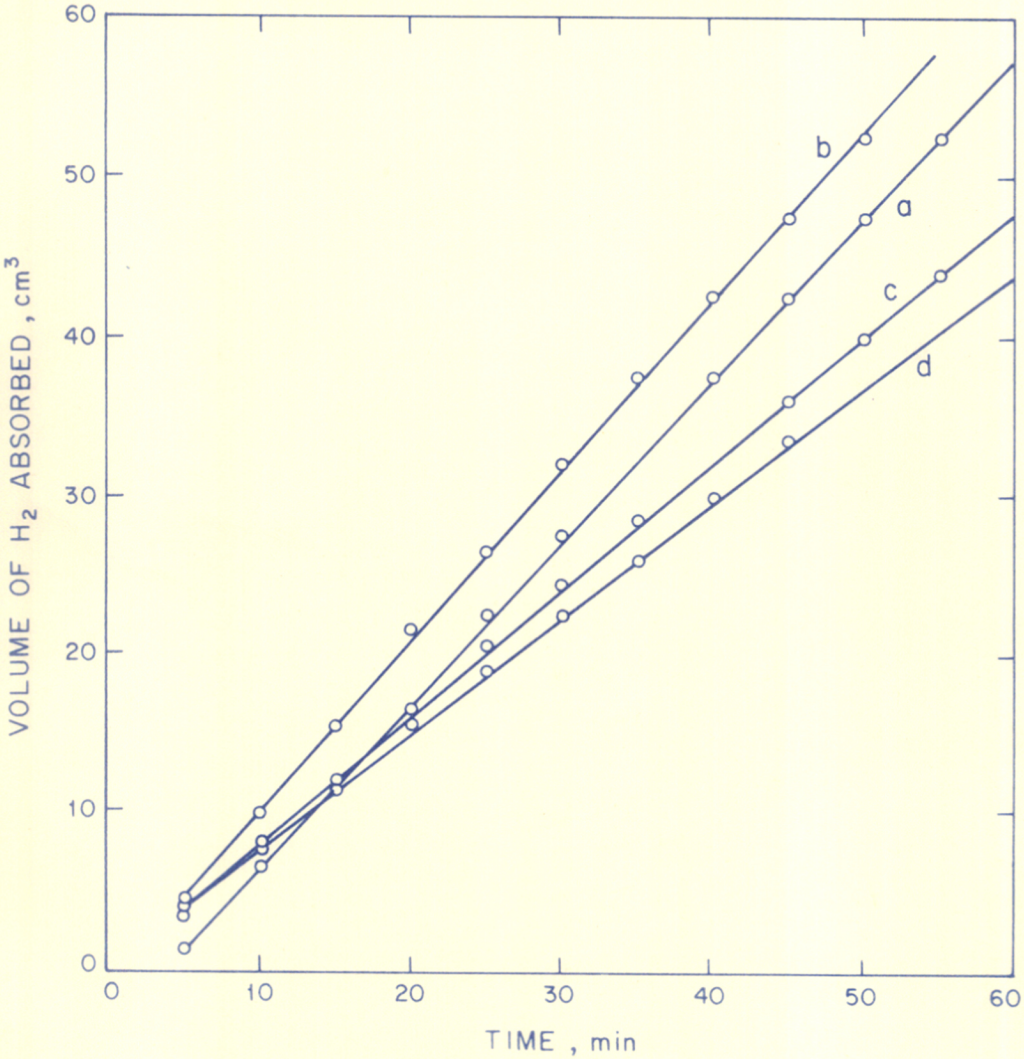

FIGURE 6 : EFFECT OF CATALYST CONCENTRATION ON H_2 UPTAKE vs TIME PLOT.
CONCENTRATION OF CYCLOHEXENE : $13 \cdot 807 \times 10^{-4}$ mole/cm^3, TEMP. 35°C , H_2 PRESSURE : 1 atm , CONCENTRATION OF $RuCl_2(PPh_3)_3$: a) $4 \cdot 184 \times 10^{-7}$ mole/cm^3, b) $8 \cdot 368 \times 10^{-7}$ mole/cm^3, c) $12 \cdot 552 \times 10^{-7}$ mole/cm^3, d) $16 \cdot 684 \times 10^{-7}$ mole/cm^3.

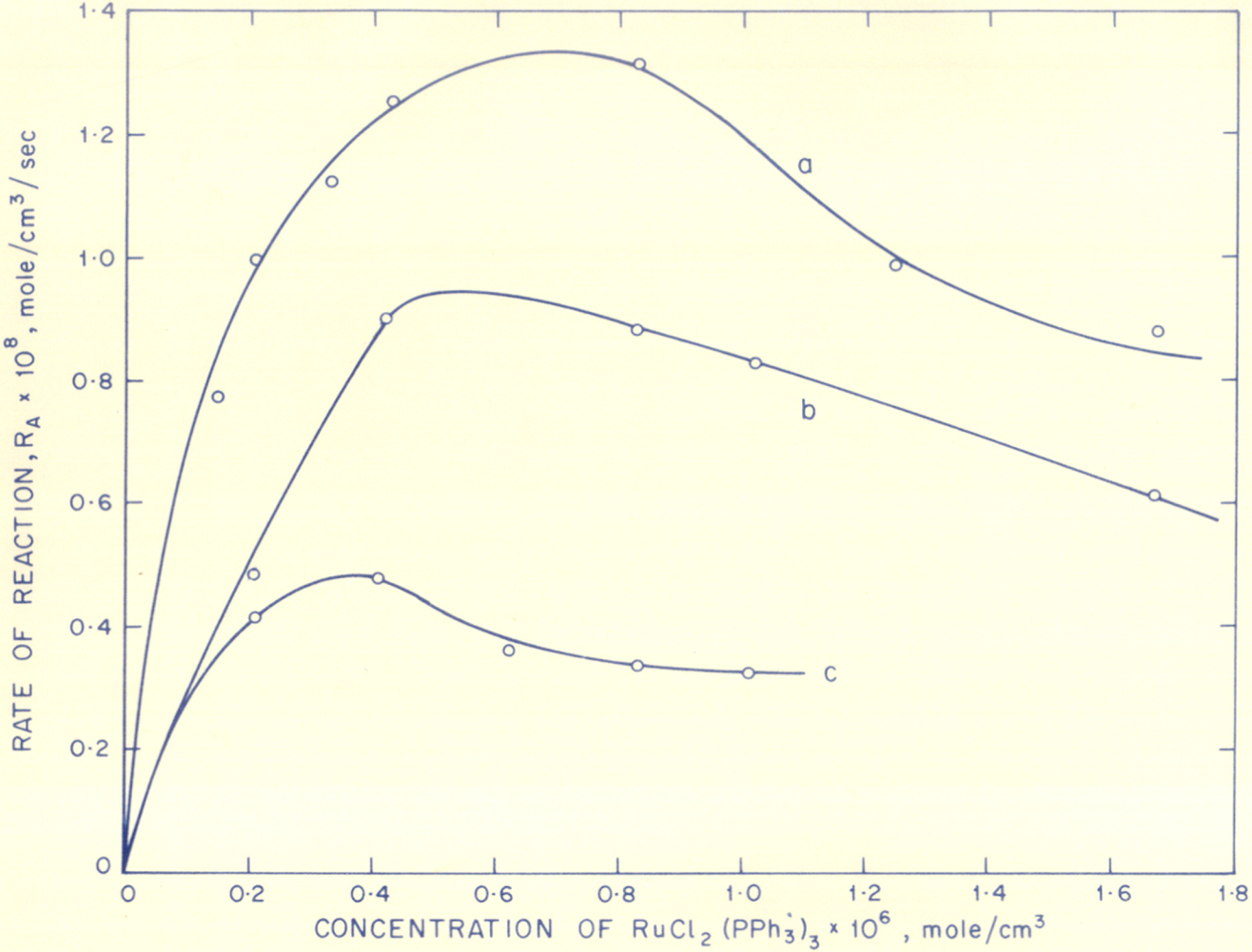

FIGURE 7 : EFFECT OF CATALYST CONCENTRATION ON THE RATE OF HYDROGENATION.

CYCLOHEXENE CONCENTRATION : a) $13{\cdot}807 \times 10^{-4}$ mole/cm^3, b) $9{\cdot}8624 \times 10^{-4}$ mole/cm^3, c) $4{\cdot}9312 \times 10^{-4}$ mole/cm^3, TEMP. 35 °C , H_2 PRESSURE : 1 atm.

The rates are found to increase with increase in catalyst concentration in the lower concentration range, while at higher catalyst concentrations the rates decrease with increase in concentration.

3.8. Effect of temperature

The effect of temperature on the overall rate of reaction has been studied between 15-45°C at a catalyst loading of 0.4184×10^{-6} mole/cm^3 cyclohexene concentration of 9.832×10^{-4} mole/cm^3 and 1 atm H_2 pressure. It is observed that increase in temperature increased the reaction rates significantly. Fig. 1 shows H_2 uptake vs time for different temperatures. The reaction rates calculated from these results are presented in Table 5.

3.9 Effect of added triphenylphosphine

In order to study the effect of triphenylphosphine on the reaction rate, experiments are carried out with various concentrations of added triphenylphosphine in a range of 0.01526×10^{-6} to 0.3816×10^{-6} mole/cm^3. During these experiments, other conditions are kept constant. It is found that triphenylphosphine retards the rate of reaction. The results are shown in Fig. 8 as a plot of rate of reaction vs concentration of added triphenylphosphine. This indicates that the reaction is retarded significantly in the presence of excess triphenylphosphine.

TABLE -5

SUMMARY OF KINETIC DATA FOR HYDROGENATION OF CYCLOHEXENE IN BENZENE:ETHANOL (1:1) AT 35°C.

S.No.	$[RuCl_2(PPh_3)]$ moles/cm^3 [A] x 10^7	[Cyclohexene] moles/cm^3 [B] x 10^4	$[H_2]$ moles/cm^3 x 10^6	$[PPh_3]$ added moles/cm^3 x10^8	Rate of reaction moles/cm^3/sec x10^8
1.	1.459	13.807	2.42	-	0.7762
2.	2.092	13.807	2.42	-	1.0227
3.	3.138	13.807	2.42	-	1.1294
4.	4.184	13.807	2.42	-	1.2568
5.	4.184	7.8899	2.42	-	0.8132
6.	4.184	9.8624	2.42	-	0.9488
7.	4.184	13.8074	2.42	-	1.1582
8.	4.184	19.7248	2.42	-	1.6018
9.	4.184	9.8624	0.83	-	0.2119
10.	4.184	9.8624	1.21	-	0.3151
11.	4.184	9.8624	2.42	-	0.6653
12.	4.184	9.8624	2.42	1.5267	0.6777
13.	4.184	9.8624	2.42	7.6335	0.6161
14.	4.184	9.8624	2.42	15.2671	0.4928
15.	4.184	9.8624	2.42	22.900	0.4312
16.	4.184	9.8624	2.42	38.1679	0.2464

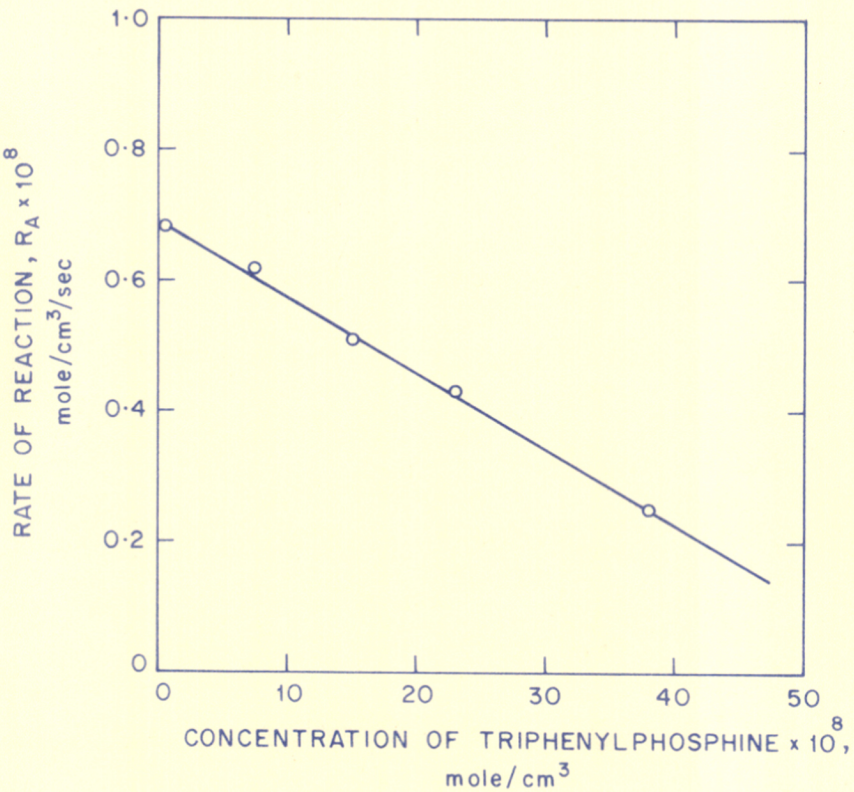

FIGURE 8: DEPENDENCE OF THE RATE OF HYDROGENATION ON THE CONCENTRATION OF TRIPHENYLPHOSPHINE.
CONCENTRATION OF $RuCl_2(PPh_3)_3$: $4{\cdot}184 \times 10^{-7}$ mole/cm³,
CYCLOHEXENE CONCENTRATION : $9{\cdot}862 \times 10^{-4}$ mole/cm³,
H_2 PRESSURE : 1 atm.

3.10. Discussion

The results presented in earlier section indicate that hydrogenation of olefins using $RuCl_2(PPh_3)_3$ catalyst is a complex reaction system and hence a discussion on the mechanism of the reaction is necessary. Hallman and coworkers[17] have suggested the following mechanism for hydrogenation of olefins using dichlorotris(triphenylphosphine)ruthenium(II) complex catalyst.

$$RuCl_2(PPh_3)_3 + H_2 \xrightleftharpoons{\text{base}} HRuCl(PPh_3)_3 + \text{base.HCl} \qquad (6)$$

$$HRuCl(PPh_3)_3 \xrightleftharpoons{K_1} HRuCl(PPh_3)_3 + PPh_3 \qquad (7)$$

$$HRuCl(PPh_3)_2 + \text{olefin} \xrightleftharpoons{K_2} RuCl(PPh_3)_2(\text{allyl}) \qquad (8)$$

$$RuCl(PPh_3)_2(\text{alkyl}) + H_2 \xrightarrow{k} HRuCl(PPh_3)_3 + \text{alkane} \qquad (9)$$

(rate determining step)

It is reported[17] that the hydrido-complex of the type $HRuCl(PPh_3)_3$ is the active species in hydrogenation and not the complex $RuCl_2(PPh_3)_3$. The hydrido-complex is formed *in situ* from $RuCl_2(PPh_3)_3$ and H_2. This is normally noticed by a change in the colour from brown to violet. Also, the initial induction period observed in the

hydrogenation reaction suggests that this is the time required for the formation of hydrido species. In the present work, it has been observed that the basic compounds such as triethyl amine act as promoters in the hydrogenation reaction. A plot of rate of reaction vs triethyl amine concentration is shown in Fig. 9. It is interesting to note that the rate increases with increase in triethylamine concentration upto a certain limit beyond which the rate decreases with increase in triethylamine concentration. This is because the function of this promoter is to react with HCl produced in the reaction (6), thus favouring the equilibrium towards formation of hydrido-species. Therefore, only the stoichiometric quantities of triethylamine, equivalent to the HCl produced is required. At higher concentrations, triethylamine may act as a coordinating ligand and thus inhibit the reaction due to the formation of coordinatively saturated species.

The other interesting feature of this reaction is the retardation of rates in the presence of triphenyl-phosphine (Fig. 8). This inhibitive effect of triphenyl-phosphine appears to be consistent with the above mechanism, the excess PPh_3 shifts the equilibrium in reaction to the left hand side thus lowering the concentration of hydrido species, $HRuCl(PPh_3)_2$ and hence the rate of hydrogenation.

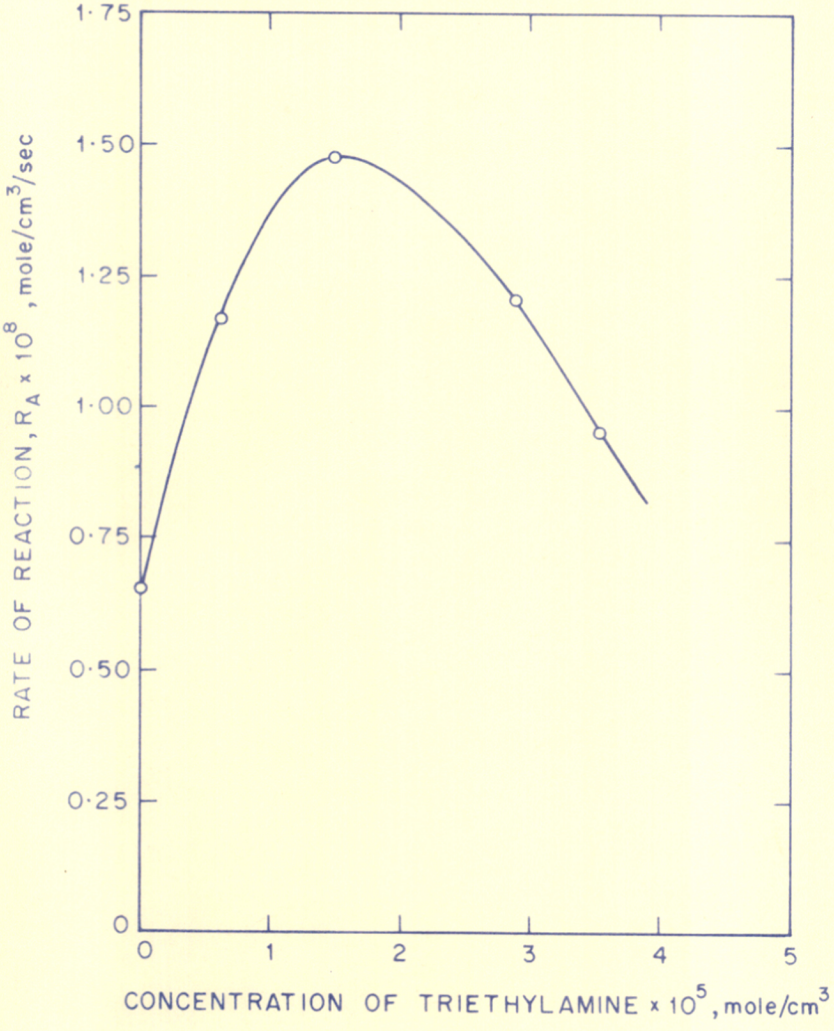

FIGURE 9 : EFFECT OF TRIETHYLAMINE CONCENTRATION ON THE RATE OF HYDROGENATION.
CONCENTRATION OF $RuCl_2(PPh_3)_3$: $4{\cdot}184 \times 10^{-7}$ mole/cm^3,
CYCLOHEXENE CONCENTRATION : $9{\cdot}8624 \times 10^{-4}$ mole/cm^3,
TEMP. 35 °C , H_2 PRESSURE : 1 atm .

Coordination of alkene is thought to take place before the hydrogen transfer step (reaction 8) which is considered to proceed to a four-centred transition state. The lower rates of hydrogenation observed for internal alkenes (e.g. hex-2-ene, hept-2-ene etc) are attributed to the difficulties in hydride transfer to the coordinated alkene caused by steric interaction of the triphenylphosphine groups. This conclusion is predominantly based on a comparative study with $HRh(CO)(PPh_3)_3$ system.

The rate determining step in the hydrogenation reaction catalyzed by the ruthenium(II) hydrido complexes (reaction 9) is thought to involve the reactions shown in the following scheme.

Either the oxidative addition of molecular hydrogen to the square planar alkyl complex to form the octahedral ruthenium(IV) species (ii), or the reductive elimination of alkane by hydrogen transfer (II → III → IV) could be rate controlling. The former is considered to be more likely.

The solvents play an important role in homogeneously catalyzed reactions, because the solvents can also coordinate with the metal complex and occupy the vacant sites in the coordination sphere. Therefore depending on the solvent used, different reaction rates can be observed. From the

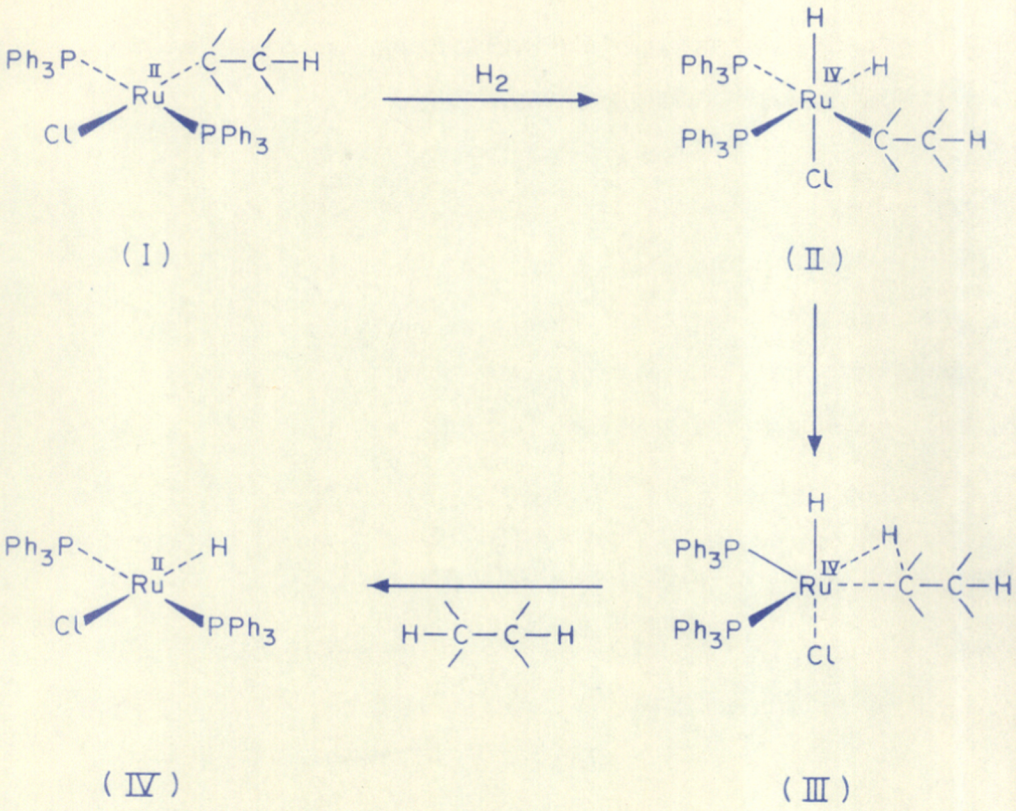
Ph3P
II
Ru
C—C—H
Cl
PPh3
H2
H
IV
H
Ph3P
Ru
Ph3P
C—C—H
Cl
(I)
(II)
H
IV
H
Ph3P
Ru
C—C—H
Ph3P
Cl
Ph3P
II
H
Ru
Cl
PPh3
H—C—C—H
(IV)
(III)

SCHEME – I

results presented in earlier section on the solvent effects, it can be noted that the hydrogenation rates are lower in solvents such as benzene, toluene and xylene. However, in mixtures like benzene:ethanol, toluene:ethanol, appreciable hydrogenation rates have been observed. This is because alcohol being a base it reacts with the HCl produced in reaction (6) and favours the formation of hydrido-species. Pure alcohol can not be used in this case as the solubility of the catalyst precursor $RuCl_2(PPh_3)_3$ is very low in alcohol. It is interesting to note that in the presence of solvents such as dimethylformamide and dimethylsulphoxide no hydrogenation occurs. This is obviously because these solvents have strong coordinating ability to form catalytically inactive complexes.

3.10.1. Kinetic modelling

In order to propose a suitable rate equation, two approaches were followed. In one, a rate model is derived based on the mechanism given in reactions (6-9). In the other, a power-law model is proposed and the results are correlated with the mechanism. If we assume that the reaction (9) is the rate determining step, the following rate equation can be derived using the principles of the steady state approximation.

$$R_A = \frac{kK_2[A][B][C]}{1+K_2[B] + [D]/K_1} \qquad (10)$$

where R_A = rate of hydrogenation in mole/cc/sec.

[A] = concentration of dissolved H_2, mole/cm^3;

[B] = concentration of olefin, mole/cm^3;

[C] = concentration of $RuCl_2(PPh_3)_3$, mole/cm^3;

[D] = concentration of triphenylphosphine, mole/cm^3.

K_1 and K_2 are the equilibrium constants of reactions (7) and (8) respectively and k is a rate constant for the rate controlling step (9).

In order to evaluate the various parameters of the kinetic model the experimental data in the catalyst concentration range of 1.459×10^{-7} to 4.184×10^{-7} mole/cm^3 are only considered, since beyond 4.184×10^{-7} mole/cm^3 concentration of the catalyst, the mechanism given in equations (6-9) is not applicable presumably due to the formation of dimeric species.

The following procedure was used to evaluate the reaction rate and equilibrium constants.

Rearranging equation (10), we get

$$\frac{1}{R} = \frac{1 + [D]/K_1}{kK_2[C][A]} \quad \frac{1}{[B]} + \frac{1}{k[C][A]} \qquad (11)$$

A plot of 1/R vs 1/[B] should be a straight line as per Equation (11). For the present work, such a plot is shown in Fig. 10. As can be noted from Equation (11), the slope and intercept of this plot will be equal to:

$$\text{Slope} = \frac{1 + [D]/K_1}{kK_2\,[C][A]} \qquad (12)$$

$$\text{Intercept} = \frac{1}{k[C][A]} \qquad (13)$$

From the intercept and the known concentrations A and C, the value of k can be calculated as 3.9505×10^4, $cm^3/mole.s$.

Similarly Equation (10) can be rearranged as

$$\frac{1}{R} = \frac{[D]}{kK_1K_2[A][B][C]} + \frac{1 + K_2[B]}{kK_2[A][B][C]} \qquad (14)$$

According to Equation (14) a plot of 1/R vs [D] should be a straight line as shown in Fig. 11. The slope intercept of this plot are as follows:

$$\text{Slope} = \frac{1}{kK_1K_2[A][B][C]} \qquad (15)$$

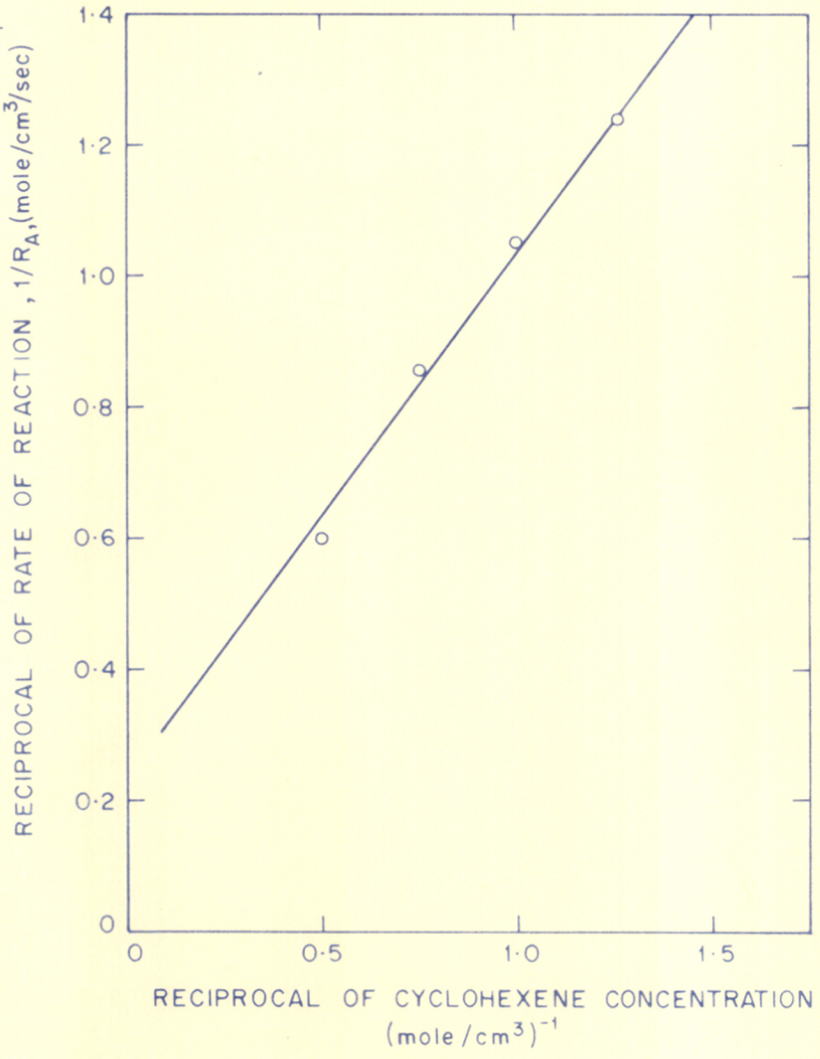

FIGURE 10 : PLOT OF RECIPROCAL OF RATE OF REACTION vs RECIPROCAL OF CYCLOHEXENE CONCENTRATION.
CONCENTRATION OF $RuCl_2(PPh_3)_3$: $4{\cdot}184 \times 10^{-7}$ mole/cm^3,
TEMP. 35 °C , H_2 PRESSURE : 1 atm .

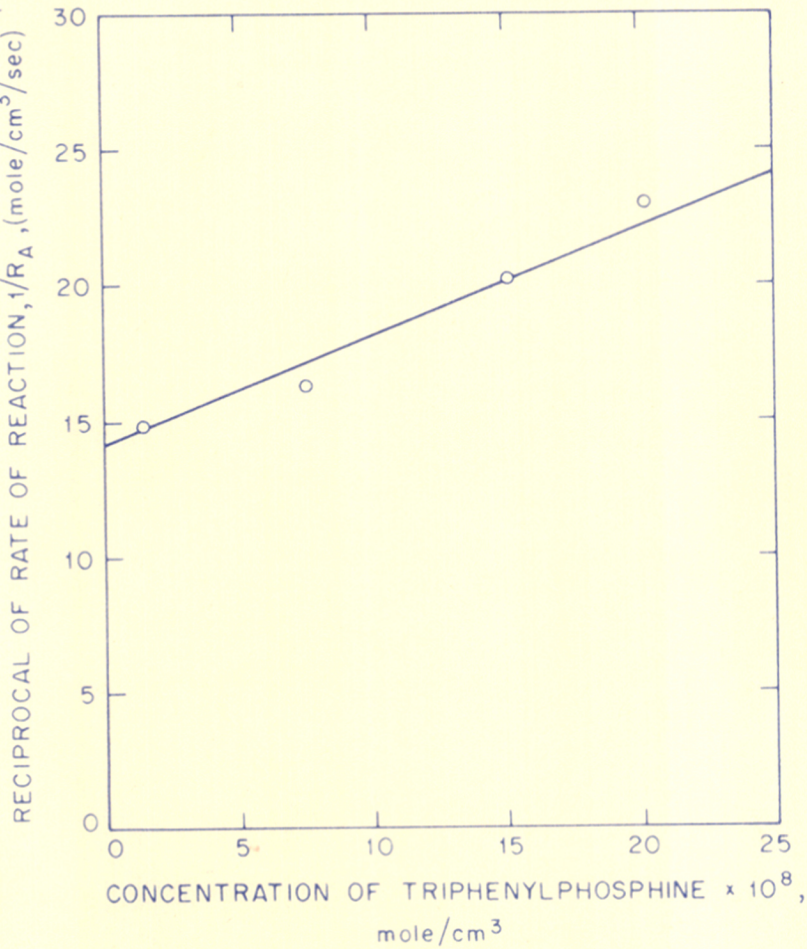

FIGURE 11 : PLOT OF RECIPROCAL OF RATE OF REACTION vs TRIPHENYLPHOSPHINE CONCENTRATION.
CONCENTRATION OF $RuCl_2(PPh_3)_3$: $4{\cdot}184 \times 10^{-7}$ mole/cm^3,
CYCLOHEXENE CONCENTRATION : $9{\cdot}8624 \times 10^{-4}$ mole/cm^3,
TEMP. 35°C, H_2 PRESSURE : 1 atm.

$$\text{Intercept} = \frac{1 + K_2[B]}{kK_2[A][B][C]} \qquad (16)$$

Knowing k, and the concentrations, A, B and C, a value of K_1K_2 can be calculated as 1.6197×10^4.

From the intercept of the plot in Fig. 11, K_2 can be calculated as:

$$K_2 = \frac{1}{(\text{intercept})\, k[A][B][C] - [B]} \qquad (17)$$

The value of K_2 obtained in this case is 225.123, cm^3/mole.

Knowing the value of K_2, the value of K_1 can be calculated as 71.95, mole/cm^3.

Thus the values of k, K_1 and K_2 obtained for 35°C are as follows:

$k = 3.9505 \times 10^4$ cm^3/mole, s

$K_1 = 71.95$ mole/cm^3

$K_2 = 225.12$ cm^3/mole

The kinetic data have also been fitted to a power law model:

$$R_A = k\,[A]^m[B]^n[C]^p \qquad (18)$$

where R_A = rate of reaction of hydrogen, mole/cm^3/sec.

[A] = concentration of dissolved hydrogen, mole/cm^3

[B] = concentration of cyclohexene, mole/cm^3

[C] = concentration of $RuCl_2(PPh_3)_3$, mole/cm^3

k = reaction rate constant with m, n and p as the reaction orders with respect to A, B and C.

In order to obtain the reaction orders and the rate constant the following procedure has been followed.

Taking logarithms on both the sides of Equation (18) we get:

$$\ln R_A = \ln k + m \ln A + n \ln B + p \ln C \qquad (19)$$

As can be seen from Equation (19), that a plot of $\ln R_A$ vs ln A at constant concentration of species B and C will have a slope = m; similarly the plots of $\ln R_A$ vs ln B and $\ln R_A$ vs ln C can give the reaction orders n and p respectively. Such plots are shown in Figs. 3, 5 and 12. The values of m, n and p obtained from these plots are as follows:

m = 1.06

n = 0.74

p = 0.53

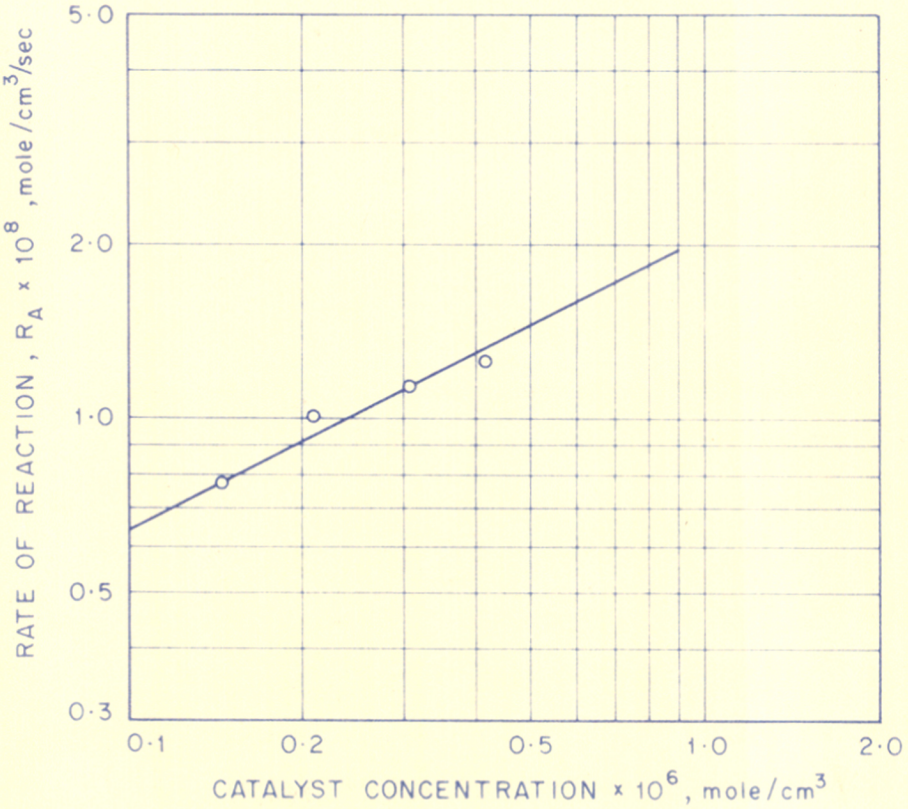

FIG. 12 : EFFECT OF CATALYST CONCENTRATION ON THE RATE OF REACTION.

CYCLOHEXENE CONCENTRATION : $13{\cdot}807 \times 10^{-4}$ mole/cm^3, TEMP. 35 °C , H_2 PRESSURE : 1 atm.

Knowing m, n and p the reaction rate constant k has been calculated for all the data points.

The effect of temperature on the reaction rate constant k is also shown in Fig. 13 which is a plot of ln k vs 1/T. According to Arrhenious law, the slope of this plot is equal to -E/R. From this, the activation energy has been calculated as 7.84 kcal/mole.

The comparison of the power law model suggests that the reaction orders observed with respect to hydrogen and olefin concentrations are consistent with the mechanism discussed earlier, but the observation of 0.5^{th} order with respect to catalyst concentration is not indicated from the rate model. This is because the term C in the rate model truly represents the concentration of the hydrido species, $HRuCl(PPh_3)_3$, while the order of 0.5 has been determined from the data on rate vs concentration of catalyst precursor $RuCl_2(PPh_3)_3$. Considering reaction (6) in the mechanism it can be realized that if the equilibrium constant is not very large, the concentration of hydrido-species will not always be directly proportional to the concentration of $RuCl_2(PPh_3)_3$.

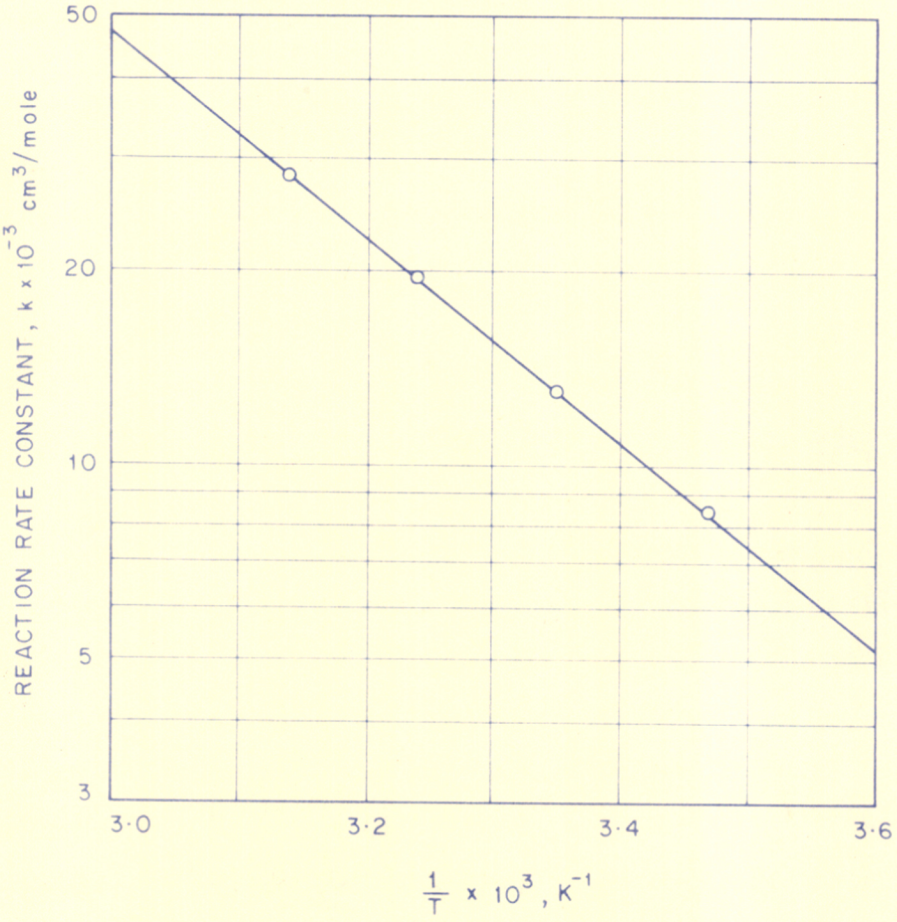

FIG. 13 : TEMPERATURE DEPENDANCE OF REACTION RATE CONSTANT.

CONCENTRATION OF $RuCl_2(PPh_3)_3$: $4 \cdot 184 \times 10^{-7}$ mole/cm^3,
CYCLOHEXENE CONCENTRATION : $9 \cdot 832 \times 10^{-4}$ mole/cm^3,
H_2 PRESSURE : 1 atm.

3.10.2. Unusual dependence of reaction rate on catalyst concentration.

From Fig. 7 it can be seen that the rates are found to increase with increase in catalyst concentration in the lower concentration range, while at higher catalyst concentration the rates decrease with increase in catalyst concentration.

This unusual observation is presumably due to dimerization of the catalytic species. On the basis of ^{31}P n.m.r. studies, Hoffman and Caulton[60] have pointed out that dichlorotris(triphenylphosphine)ruthenium(II), dissociates to triphenylphosphine to certain extent, forming a dimeric species of the type $[RuCl_2(PPh_3)_2]_2$. Hydrido species $HRuCl(PPh_3)_2$ also undergoes intramolecular rearrangement in order to form the dimeric species. However, at lower catalyst concentration, James and Markham[61] have been unable to detect any dimeric species. On the basis of visible spectral studies, the latter authors have found that dichlorotris(triphenylphosphine)ruthenium(II) dissociates to the extent of about 80% at 25°C in benzene solution. These two reports can perhaps, explain these unusual observation reported here. Thus at lower catalyst concentrations dimer formation is negligible whereas at higher catalyst concentration, the catalyst precursor tends to dissociate in benzene:ethanol (1:1) solution to $RuCl_2(PPh_3)_2$ which readily dimerizes to form $[RuCl_2(PPh_3)_2]_2$ a catalytically inactive species. Hence, the rates are retarted at higher catalyst concentration.

CHAPTER - IV HYDROGENATION OF ALLYLIC COMPOUNDS - RESULTS AND DISCUSSION

		Page
4.1	Hydrogenation of allyl alcohol	198
4.2	Hydrogenation of allyl bromide	206
4.2.1	Effect of hydrogen pressure	207
4.2.2	Effect of olefin concentration.	207
4.2.3	Effect of catalyst concentration	207
4.2.4	Effect of temperature	210
4.2.5	Kinetic modelling	210
4.2.6	Reaction mechanism	214

4. Hydrogenation of allylic compounds

In this Chapter, the results of hydrogenation of allylic compounds using dichlorotris(triphenylphosphine)-ruthenium(II) complex catalyst have been discussed. The hydrogenation experiments are carried out by the procedure described in Chapter II. The substrates investigated are allyl alcohol and allyl bromide. Allyl alcohol is chosen to study the change in the nature of catalytically active species due to the abstraction of carbon monoxide from allyl alcohol during the reaction. Such phenomenon often leads to deactivation of catalyst and hence it is thought to be an important problem. Allyl bromide hydrogenation has been studied with the objective of investigation of the reaction kinetics.

As described in Chapter III in this study also the reaction rates have been obtained from the measurement of volumetric uptake of hydrogen at different time intervals. For kinetic purposes only the initial rate data are taken, while for the deactivation studies the reactions are carried out for longer durations. The results obtained for both the substrates are shown in Tables 1 and 2.

4.1. Hydrogenation of allyl alcohol

Allyl alcohol hydrogenates to propyl alcohol in the

TABLE -1

SUMMARY OF KINETICS STUDY OF HYDROGENATION OF ALLYL ALCOHOL USING DICHLOROTRIS(TRIPHENYLPHOSPHINE)RUTHENIUM(II) IN BENZENE:ETHANOL (1:1) AT 35°C.

S.No.	Catalyst concentration, mole/cm^3 x10^6.	Allyl alcohol concentration, mole/cm^3 x10^4	Hydrogen pressure mm.Hg	Rate of reaction, mole/cm^3/sec. x10^7
1.	0.4171	14.721	710	1.7251
2.	0.6256	14.721	710	1.9715
3.	0.8342	14.721	710	2.7108
4.	1.2513	14.721	710	4.1895
5.	1.6684	14.721	710	3.0805
6.	0.4171	7.360	710	3.0805
7.	0.4171	14.721	710	2.5876
8.	0.4171	22.093	710	2.2179
9.	0.4171	29.442	710	1.9715

TABLE - 2

A SUMMARY OF KINETIC RESULTS OF HYDROGENATION OF ALLYL BROMIDE USING DICHLOROTRIS(TRIPHENYLPHOSPHINE)RUTHENIUM(II) COMPLEX IN BENZENE:ETHANOL (1:1).

S.No.	Catalyst concentration, mole/cm^3 x10^6	Allyl bromide concentration, mole/cm^3 x10^4	Hydrogen concentration, mole/cm^3 x10^6	Temp. (^oC)	Rate of reaction moles/cm^3/sec. x10^8	Rate constant, k sec^{-1} x10^4
1.	0.4171	5.7772	2.42	35	0.88718	2.2420
2.	0.8342	5.7772	2.42	35	1.6388	2.4777
3.	1.2513	5.7772	2.42	35	2.2426	2.5105
4.	1.6684	5.7772	2.42	35	2.2426	2.0285
5.	0.4171	5.7772	2.42	35	1.0104	2.5534
6.	0.4171	11.5556	2.42	35	0.9734	2.4828
7.	0.4171	17.3334	2.42	35	0.9734	2.4964
8.	0.4171	23.1112	2.42	35	0.9734	2.5061
9.	0.4171	5.7772	2.42	35	1.0227	2.5844
10.	0.4171	5.7772	1.68	35	1.0720	2.5376
11.	0.4171	5.7772	1.24	35	1.0227	2.4994
12.	0.4171	5.7772	0.80	35	1.0227	2.4454
13.	0.4171	5.7772	2.42	15	0.2635	0.6580
14.	0.4171	5.7722	2.42	25	0.6367	1.6090
15.	0.4171	5.7772	2.42	35	0.8871	2.2420
16.	0.4171	5.7772	2.42	45	1.7901	4.5236

presence of the catalyst dichlorotris(triphenylphosphine)-ruthenium(II) in benzene:ethanol (1:1) at 35°C and 1 atm hydrogen. Solutions of the catalyst in benzene:ethanol (1:1) are reddish brown and change to violet after stirring for 30 minutes which indicates the formation of hydridospecies,hydridochlorotris(triphenylphosphine)-ruthenium((I) [$HRuCl(PPh_3)_3$]. On addition of allyl alcohol this violet colour changes to red and starts becoming yellow. These yellow coloured solutions are stable towards air. The hydrogen absorption experiments carried out for longer durations indicate that the reactions stops before complete conversion of allyl alcohol. Fig. 1 shows a plot of volume of H_2 absorbed vs time for different catalyst concentrations at 35°C and Fig. 2 shows such a plot for different allyl alcohol concentrations. This shows that the catalyst is deactivated during the course of the reaction.

In order to investigate the change in the nature of the catalytic species, the complex has been isolated from the air stable yellow coloured reaction mixture and this complex has the following analysis. C, 62.06%; H, 3.79%; Cl, 9.40%. This is consistent with the formula dichlorocarbonyl-bis(triphenylphosphine)ruthenium(II), $RuCl_2(CO)(PPh_3)_2$. Infrared spectrum of an intermediate product (Fig. 3) shows a strong band at 1930 cm^{-1} which

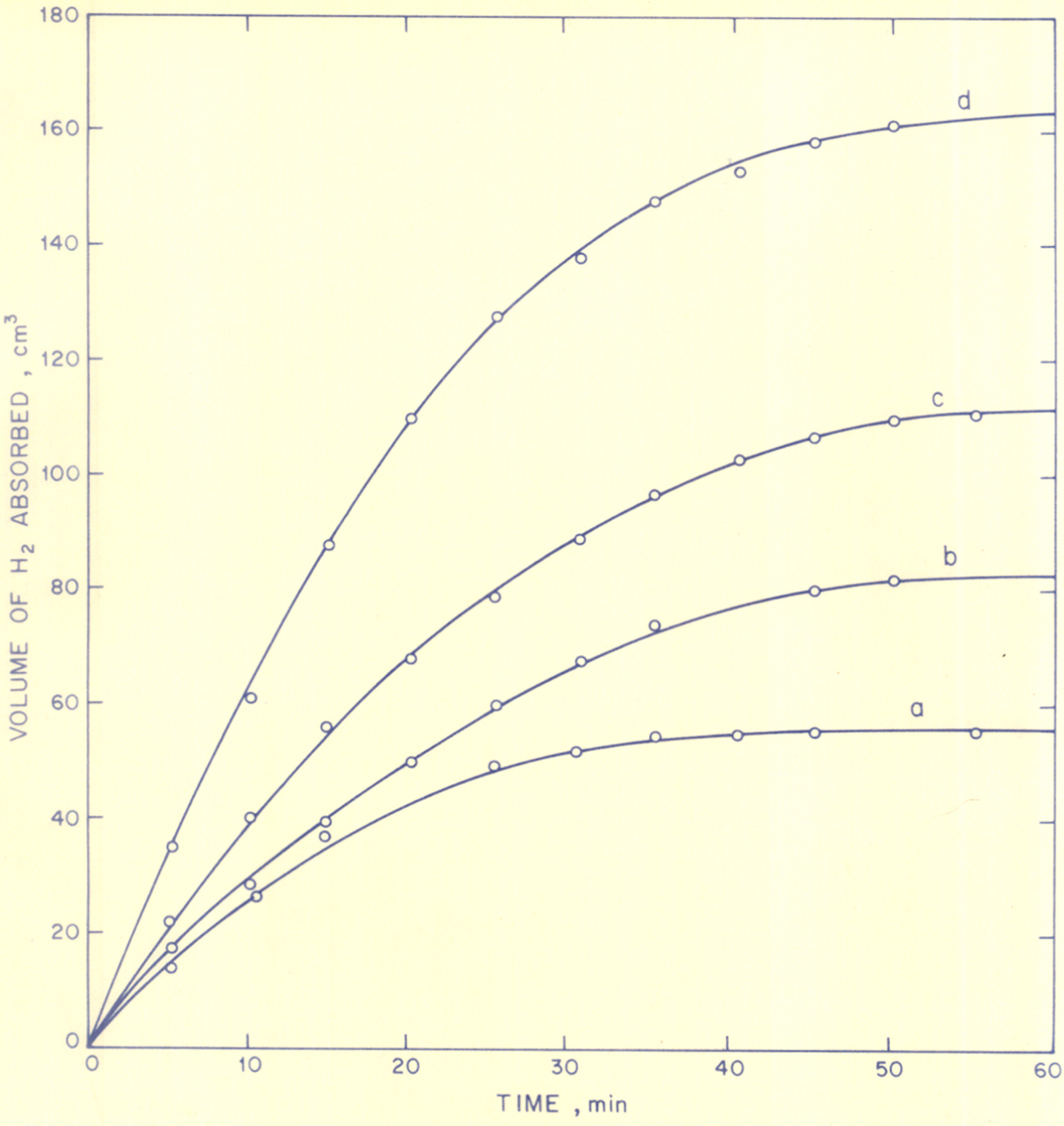

FIGURE 1: A PLOT OF VOLUME OF HYDROGEN ABSORBED vs TIME FOR DIFFERENT CATALYST CONCENTRATION.

CONCENTRATION OF $RuCl_2(PPh_3)_3$: a) $3{\cdot}1282 \times 10^{-7}$ mole/cm^3, b) $8{\cdot}3420 \times 10^{-7}$ mole/cm^3, c) $10{\cdot}427 \times 10^{-7}$ mole/cm^3, d) $12{\cdot}513 \times 10^{-7}$ mole/cm^3, ALLYL ALCOHOL CONCENTRATION : $14{\cdot}721 \times 10^{-4}$ mole/cm^3, TEMP. 35°C, H_2 PRESSURE : 1 atm.

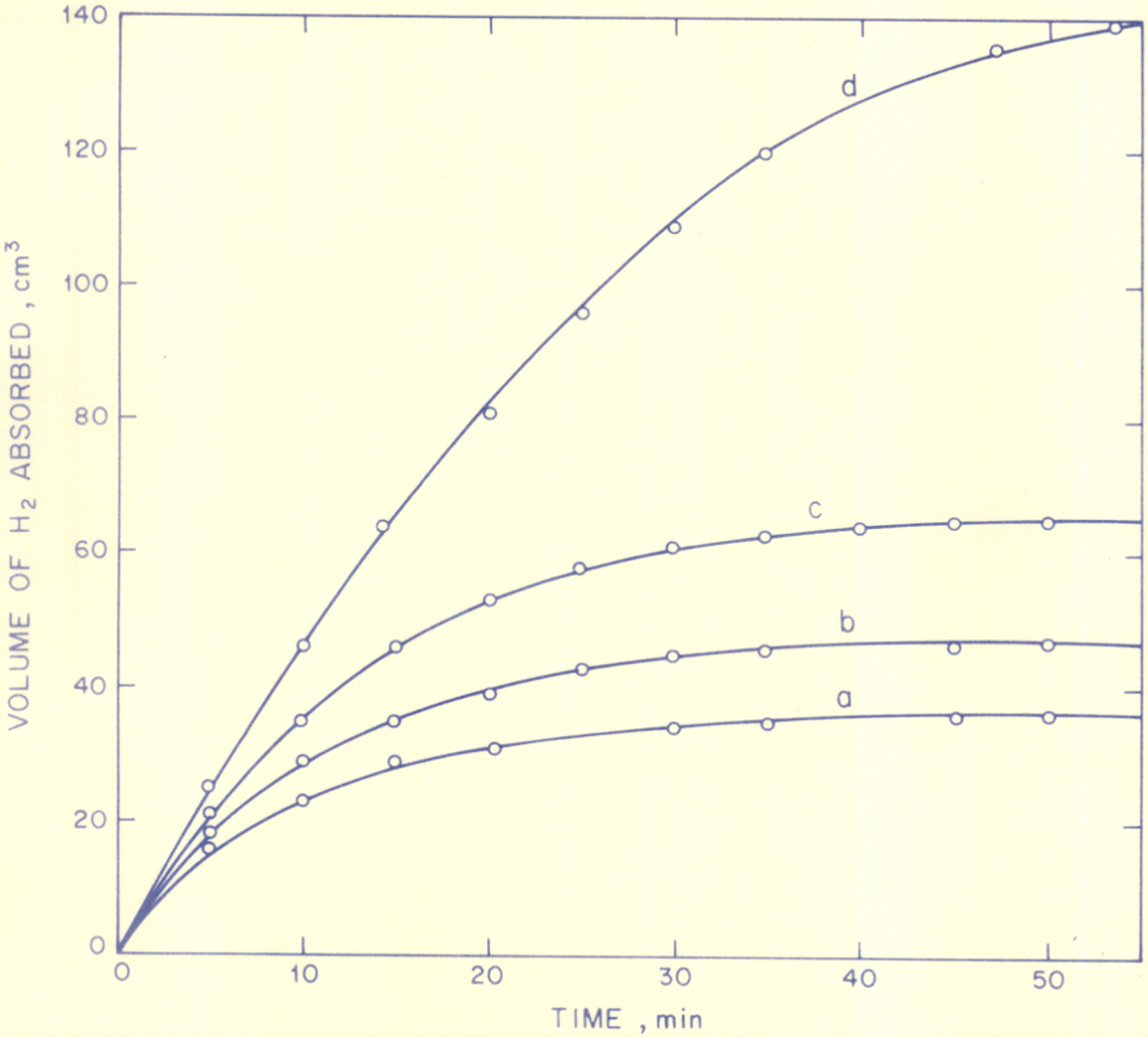

FIGURE 2 : A PLOT OF H_2 ABSORBED vs TIME FOR DIFFERENT ALLYL ALCOHOL CONCENTRATION.
CONCENTRATION OF $RuCl_2(PPh_3)_3$: $4{\cdot}171 \times 10^{-7}$ mole/cm^3, TEMP. 35 °C , H_2 PRESSURE : 1 atm , ALLYL ALCOHOL CONCENTRATION : a) $29{\cdot}442 \times 10^{-4}$ mole/cm^3, b) $22{\cdot}093 \times 10^{-4}$ mole/cm^3, c) $14{\cdot}721 \times 10^{-4}$ mole/cm^3, d) $7{\cdot}3605 \times 10^{-4}$ mole/cm^3.

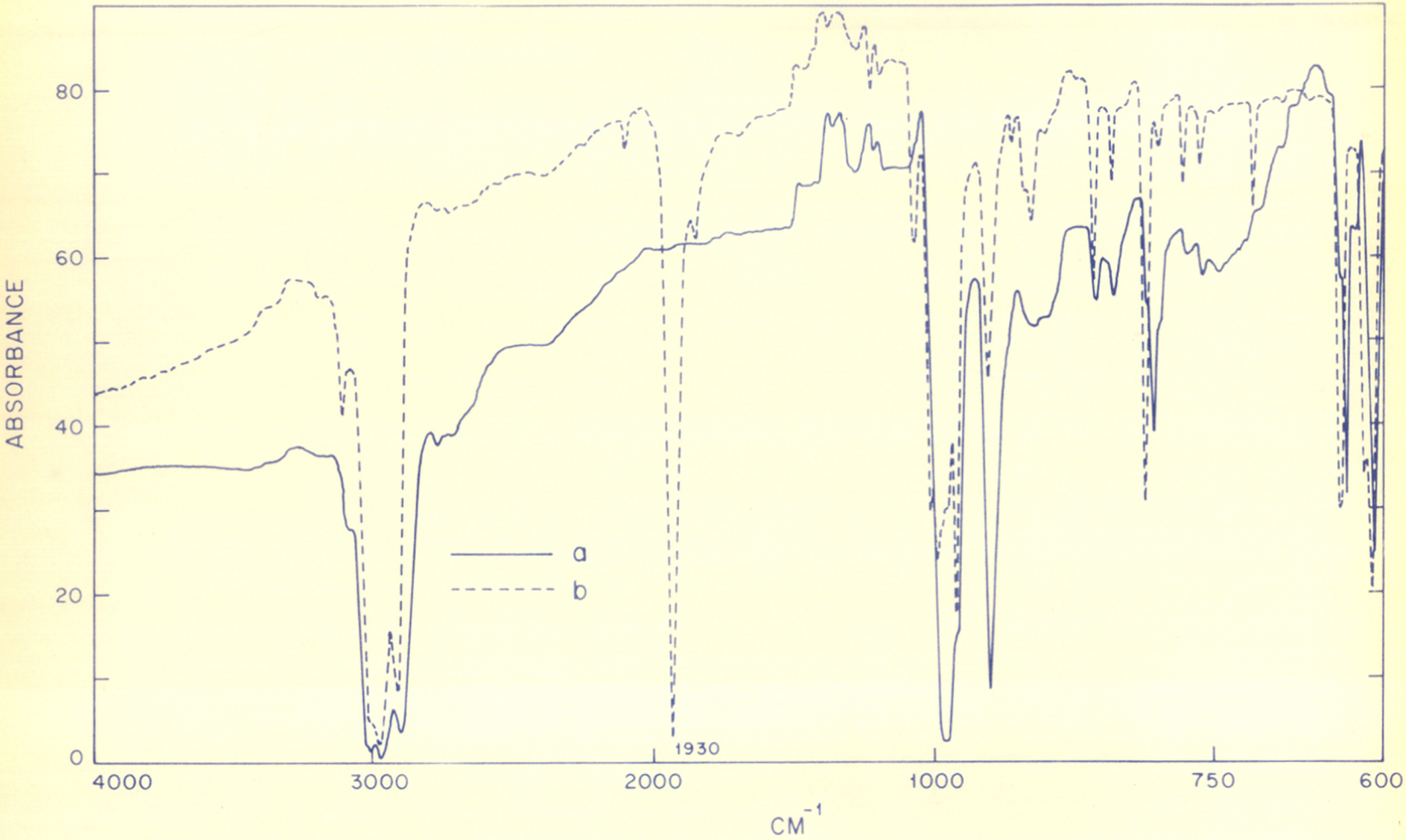

FIG. 3 : IR SPECTRA OF

a) DICHLOROTRIS (TRIPHENYLPHOSPHINE) RUTHENIUM(II) AND

b) DICHLORO CARBORNYL BIS(TRIPHENYLPHOSPHINE) RUTHENIUM(II) IN NUJOL MULL.

can be assigned for the C=O stretching frequency. ^{1}H nuclear magnetic resonance spectrum of this compound shows the presence of triphenylphosphine groups at 7.2 δ. Thus, on the basis of infrared, ^{1}H n.m.r. spectra and elemental analysis, this intermediate product has been characterized as dichlorocarbonylbis(triphenylphosphine)-ruthenium(II), $RuCl_2(CO)(PPh_3)_2$.

It has already been reported that ruthenium carbonyl species of the type $RuCl_2(CO)(PPh_3)_2$ are not active hydrogenation catalysts[57] and hence the deactivation is likely to be occuring due to the abstraction of carbon monoxide from allyl alcohol. An analogous study with Wilkinson complex, $RhCl(PPh_3)_3$ has also shown that the catalyst deactivation occurs during hydrogenation of allyl alcohol due to the formation of catalytically inactive carbonyl species[58].

Prince and Raspin[59] have studied decarbonylation reactions in detail and proposed a mechanism for carbon monoxide abstraction from aldehydes in the presence of phosphine complexes. Since carbon monoxide abstraction from alcohol may proceed via aldehyde formation, the following reaction mechanism can be suggested for carbon monoxide abstraction from allyl alcohol.

$$CH_2 = CH.CH_2OH \xrightarrow{[cat]} CH_2=CH.CHO + H_2$$

(allyl alcohol) acrylaldehyde

$$\downarrow -CO$$

$$CH_2=CH_2$$

In the first step dehydrogenation of allyl alcohol to acrylaldehyde takes place. Aldehydes behave as an electron-donor rather than acceptor and aldehydes form π-complexes with an active ruthenium(II) species which further decomposes into carbon monoxide and ethylene. Formation of ethylene may also poison the reaction during the reaction period.

4.2. Hydrogenation of allyl bromide

The hydrogenation of allyl bromide can be described by the following reaction.

$$CH_2 = CH.CH_2Br + H_2 \xrightarrow{\text{catalyst}} CH_3.CH_2.CH_2Br.$$

The preliminary experiments on the system show that the main product is propylbromide and no deactivation of catalyst occurs during the experiment. The effect of several parameters on the initial rates has been studied

and the rate data obtained are presented in Table 2. The effects of individual parameters are discussed below.

4.2.1. Effect of hydrogen pressure

In order to determine the order of reaction with respect to hydrogen pressure the hydrogenation rates have been observed in a pressure range of 350-710 mm Hg at a catalyst concentration 0.4171×10^{-6} mole/cm^3 and allyl bromide concentration 5.7772×10^{-4} mole/cm^3. A log-log plot of rate of reaction vs partial pressure of hydrogen is shown in Fig. 4 which suggests that the rate of reaction is independent of the hydrogen pressure.

4.2.2. Effect of olefin concentration

Effect of allyl bromide concentration on the rate of reaction has been studied by varying the allyl bromide concentration in a range from 5.7772×10^{-4} - 23.1112×10^{-4} mole/cm^3, and at a catalyst concentration 0.4171×10^{-6} mole/cm^3 at 35°C and 1 atm hydrogen pressure. A log-log graph of rate of reaction vs olefin concentration is shown in Fig. 5. Interestingly, the reaction rate has been found to be independent of the allyl bromide concentration, thus suggesting a zero order with respect to this species.

4.2.3. Effect of catalyst concentration

In a few experiments only the catalyst concentration

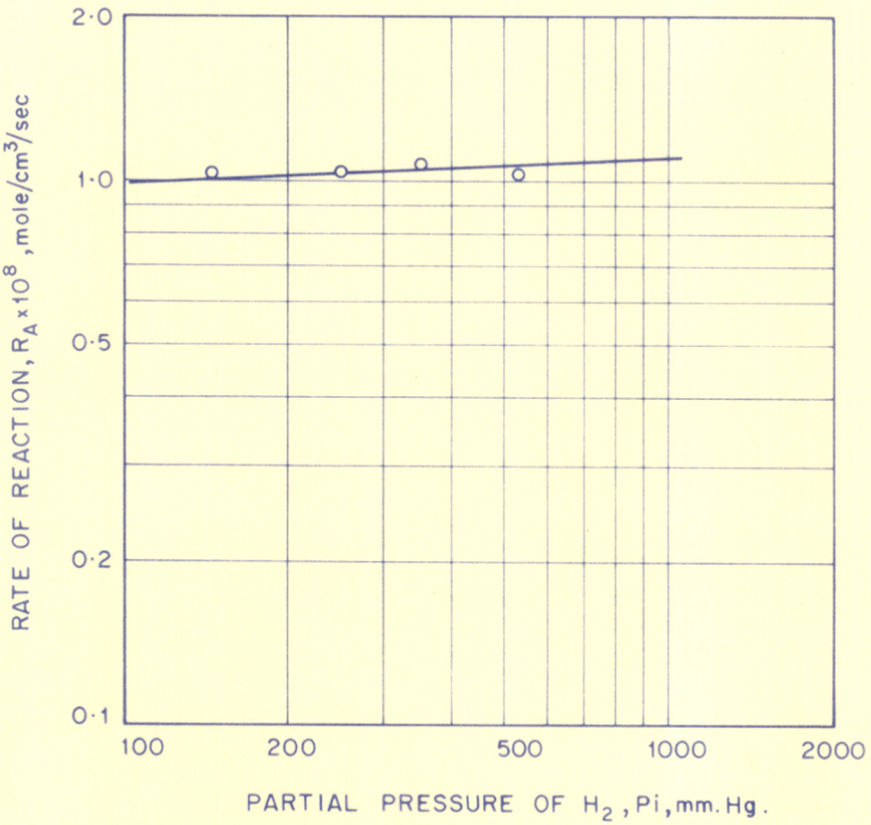

FIGURE 4 : EFFECT OF H_2 PARTIAL PRESSURE ON THE RATE OF HYDROGENATION.

CONCENTRATION OF $RuCl_2(PPh_3)_3$: $4{\cdot}171 \times 10^{-7}$ mole/cm³,
ALLYL BROMIDE CONCENTRATION : $5{\cdot}7772 \times 10^{-4}$ mole/cm³,
TEMP. 35 °C.

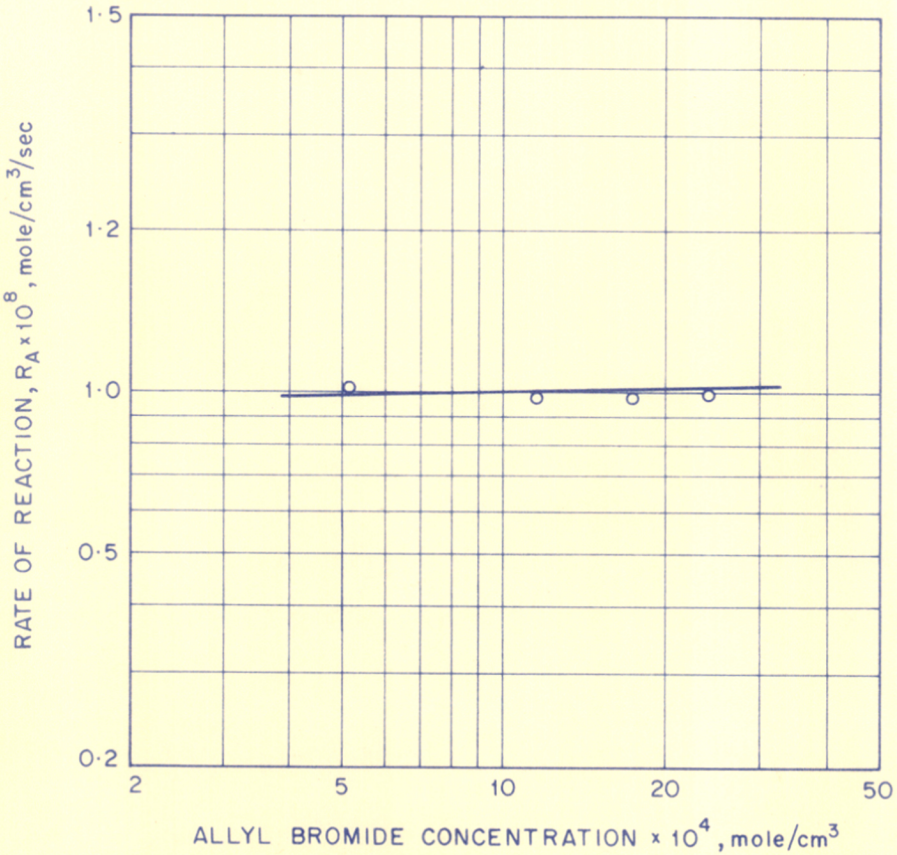

FIGURE 5 : EFFECT OF ALLYL BROMIDE CONCENTRATION ON THE RATE OF HYDROGENATION.
CONCENTRATION OF $RuCl_2(PPh_3)_3$: $4{\cdot}171 \times 10^{-7}$ mole/cm^3,
TEMP. 35 °C , H_2 PRESSURE : 1 atm.

has been varied keeping other conditions constant. The rates are observed in a catalyst concentration range of 0.4171×10^{-6} - 1.6684×10^{-6} mole/cm^3 and at allyl bromide concentration of 5.7772×10^{-4} mole/cm^3. Fig. 6 shows the influence of catalyst concentration on the initial rate of hydrogenation. It can be seen that the rate of reaction is proportional to the catalyst concentration with an approximate order of 0.85.

4.2.4. Effect of temperature

The effect of temperature on the initial rate has been studied in a range of 15-45°C and at a catalyst concentration of 0.4171×10^{-6} mole/cm^3 and 5.7772×10^{-4} mole/cm^3 allyl bromide. It is found that the reaction rate increases significantly with temperature.

4.2.5. Kinetic modelling

The following kind of rate equation has been used to correlate the experimental rate data.

$$R_A = k [A]^m [B]^n [C]^p \quad \text{- - - - - - (1)}$$

where

R_A = Rate of reaction, mole/cm^3/sec.

[A] = Concentration of dissolved hydrogen, mole/cm^3

[B] = Concentration of allyl bromide, mole/cm^3

[C] = Concentration of $RuCl_2(PPh_3)_3$, mole/cm^3

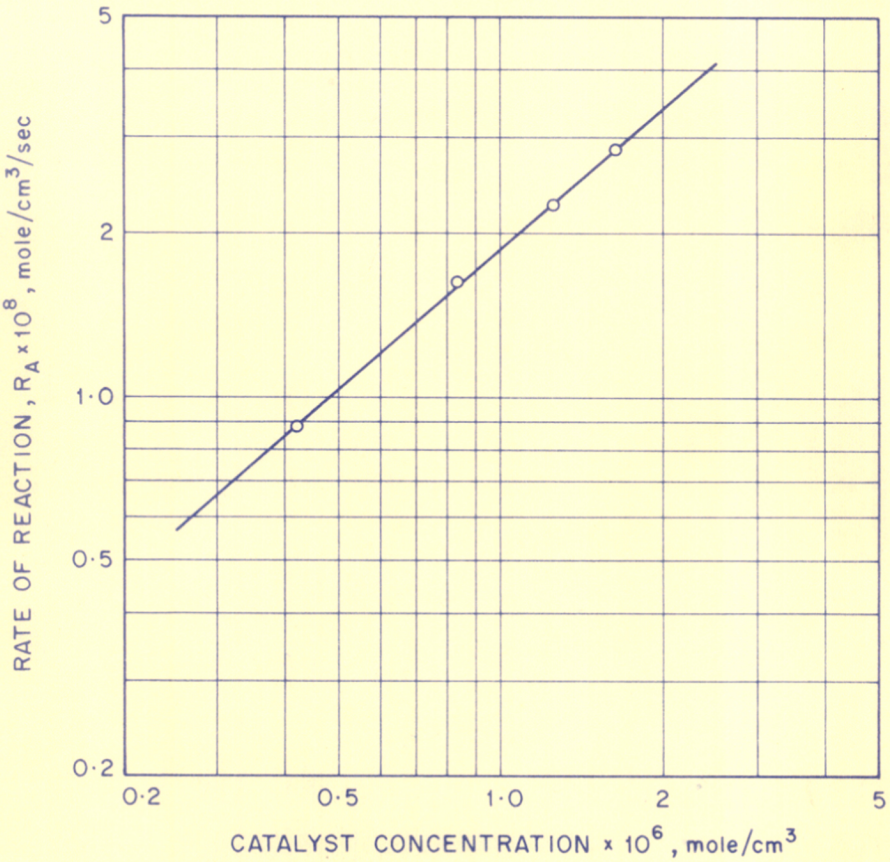

FIGURE 6 : EFFECT OF CATALYST CONCENTRATION ON THE RATE OF HYDROGENATION.

ALLYL BROMIDE CONCENTRATION : $5{\cdot}7772 \times 10^{-4}$ mole/cm^3, TEMP. 35 °C, H_2 PRESSURE : 1 atm.

k = reaction rate constant, $sec.^{-1}$ and m, n and p are the reaction orders with respect to [A], [B] and [C].

As can be seen from Figs. 4, 5 and 6 the rate of hydrogenation of allyl bromide is zero order with respect to olefin and hydrogen concentration and the order with respect to catalyst concentration is 0.85. This simplifies Equation (1) as:

$$R_A = k [C]^{0.85} \qquad (2)$$

Using Equation (2) the reaction rate constants are calculated at different temperatures. According to Arrhenius law, rate constant k can be expressed as:

$$k = \alpha \, e^{-E_a/RT} \qquad (3)$$

where E_a = activation energy, cal/mole; R = gas constant, $cal.deg^{-1}\ mole^{-1}$; T = temperature, ^{o}K; α = frequency factor, $sec.^{-1}$ k = reaction rate constant, $sec.^{-1}$.

The temperature dependence of the reaction rate constants is shown in Fig. 7 as a plot of ln k vs 1/T. As can be realized from Equation (3) the values of activation energy and the frequency factor can be calculated from the slope and intercept of this plot. These are given below:

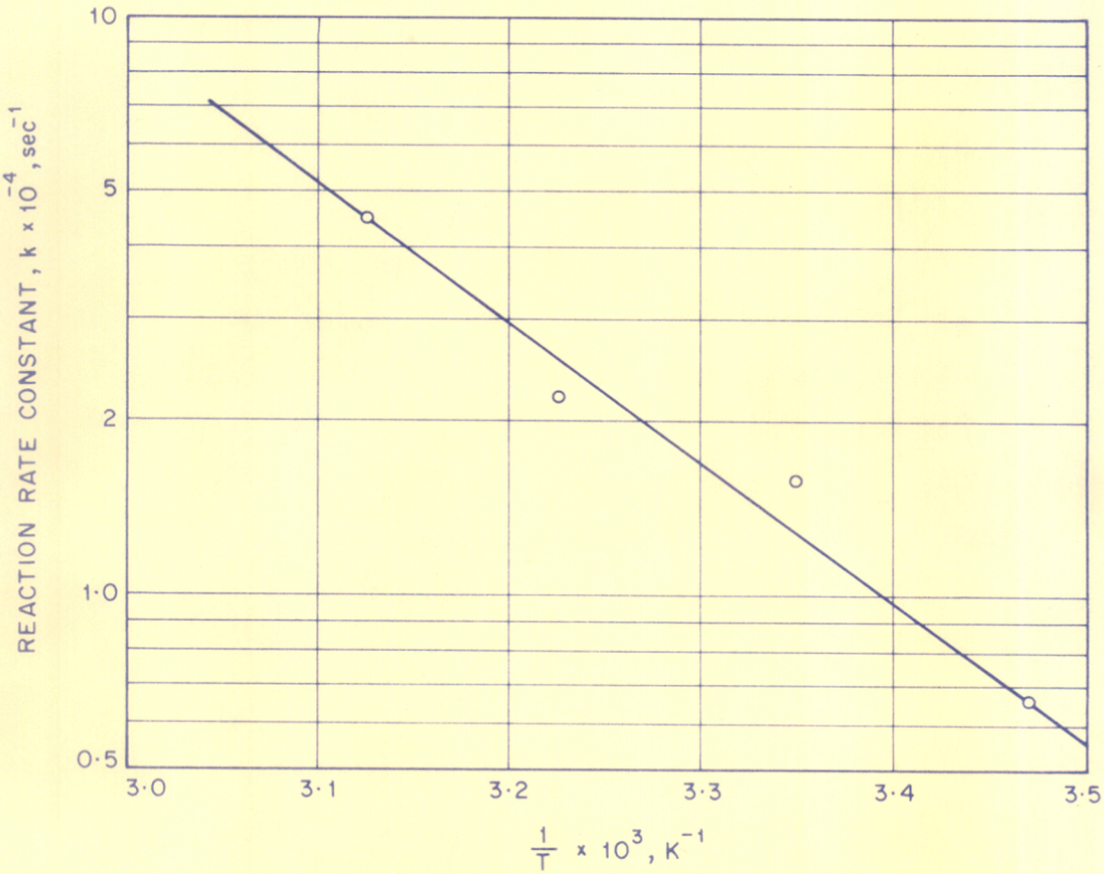

FIGURE 7 : TEMPERATURE DEPENDENCE OF THE REACTION RATE CONSTANT.

CONCENTRATION OF $RuCl_2(PPh_3)_3$: $4{\cdot}171 \times 10^{-7}$ mole/cm^3,
ALLYL BROMIDE CONCENTRATION : $5{\cdot}7772 \times 10^{-4}$ mole/cm^3,
H_2 PRESSURE : 1 atm.

E_a = 11.13 kcal/mole

α = 9.766 sec.$^{-1}$

4.2.6. Reaction mechanism

It is important to correlate the observed kinetics with the reaction mechanism. Hydrogenation of allyl bromide with dichlorotris(triphenylphosphine)ruthenium(II), $RuCl_2(PPh_3)_3$ complex catalyst can be explained by the following mechanism. A well known mechanism, proposed by several authors for the homogeneous hydrogenation of olefins using dichlorotris(triphenylphosphine)ruthenium(II) complex catalyst has been considered and discussed here.

$$RuCl_2(PPh_3)_3 + H_2 \xrightleftharpoons{\text{base}} HRuCl(PPh_3)_3 + \text{base.HCl} \quad \text{---(1)}$$

$$HRuCl(PPh_3)_3 \xrightarrow{K_1} HRuCl(PPh_3)_2 + PPh_3 \quad \text{---(2)}$$

$$HRuCl(PPh_3)_2 + \text{olefin} \xrightleftharpoons[K_2]{} RuCl(\text{alkyl})(PPh_3)_2 \quad \text{---(3)}$$

$$RuCl(\text{alkyl})(PPh_3)_2 + H_2 \xrightleftharpoons{K_3} HRuCl(PPh_3)_2 + \text{alkane} \quad \text{---(4)}$$

If we examine this mechanism, it can be noticed that the step (2) can be the rate controlling step, the reaction rate will be zero order with both allyl bromide (olefin) and hydrogen. The dependence of the rate on the

catalyst concentration also supports this. This indicates that the rate controlling step in this reaction is the dissociation of hydrido species, tris(triphenylphosphine)ruthenium(II) complex to hydrido bis(triphenylphosphine)ruthenium(II) complex.

REFERENCES

References

1.a. Orchin, M., Adv. in Catalysis, 16 (1966), 1.

b. Hartley, R.F., Chem.Rev., 69 (1969), 799.

2. Organic synthesis with metal carbonyls, Vol.II, Eds. Wender and Pino, Interscience (1977).

3. Lyons, J.E., Fundamental research in homogeneous catalysis, Eds. Tsutshi, M. and Ugo, R., Plenum Press, N.Y. (1976).

4. Prutt, R.L., in Advances in Organometal.Chem. Vol.17, Eds. F.G.A. Stone and West, R., Academic Press, N.Y. (1979), p.1.

5. Reich, L.S. and Schindler, A., "Polymerization of Organometallic Compounds", Interscience-Wiley, 1966.

6a. James, B.R., "Homogeneous hydrogenation", John-Wiley and Sons,Inc. (1973).

b. James, B.R., in "Advances in Organometallic Chemistry", Vol.17, Ed. by Stone, F.G.A. and West, R., Academic Press, (1979) p.319.

7. Harman, R.E., Gupta, S.K. and Brown, D.J., Chem.Revs., 73 (1973), 21.

8. Dolcetti, G. and Hoffman, N.W., Inorg.Chim.Acta., 9 (1974), 269.

9. Coffey, R.S., in "Aspects of homogeneous catalysis" Vol.1, Ed. by Ugo, R., Carlo Manfredi, Milan, (1970), p.3.

10. James, B.R., Inorg.Chim.Acta,Revs., 4 (1970), 73.

11. Jewar, S.S., Rajaram, J. and Kuriacose, J.C., J.Sci.Ind.Res., 33 (1974), 651.

12. Halpern, J., Nerrod, J.N. and James, B.R., J.Am.Chem.Soc., 83 (1961), 753.

13. Jardine, I., Howsam, R.W. and McQuillin, F.J., J.Chem.Soc. C (1969), 260.

14. Wilkinson, G., Fr.Patent 1,538,700; Chem.Abstr., 72 (1970), 3056.

15. Rose, D., Gilbert, J.D., Richardson, R.P. and Wilkinson, G., J.Chem.Soc.A, (1969), 2610.

16. Hallman, P.S., Evans, D., Osborn, J.A. and Wilkinson, G., Chem.Commun., (1967), 305.

17. Hallman, P.S., McGarvey, B.R. and Wilkinson, G., J.Chem.Soc.A, (1968), 3143.

18. Evans, D., Osborn, J.A., Jardine, F.H. and Wilkinson, G., Nature, 208 (1965), 1203.

19. Jardine, F.H. and McQuillin, F.J., Tetrahedron Lett., (1966), 4871.

20. Horner, L., Buthe, H. and Siegel, H., Tetrahedron Lett., (1968), 4023.

21. Ogata, I., Iwata, R. and Ikeda, Y., Tetrahedron Lett., (1970), 3011.

22. Abley, P. and McQuillin, F.J., Diss.Faraday Soc., 46 (1968), 31.

23. Sloan, M.F., Matlock, A.S. and Breslow, D.S., J.Am.Chem.Soc., 85 (1963), 4014.

24. Hui, B.C. and Rampel, G.L., Chem.Commun., (1970), 1195.

25. Velentine, D. and Collman, J.P., Unpublished results quoted in ref.6.

26. Candlin, J.P., Fr.Patent 1,548,700 (Imperial Chem.Ind.Ltd.) Chem.Abstr., 71, 833174.

27. Takahashi, S., Yamazaki, H. and Nagihara, N., Bull.Chem.Soc.Japan, 41 (1968), 254.

28. Nashimura, S. and Tsuneda, K., Bull.Chem.Soc.Japan, 42 (1969), 852.

29. Fahey, D.R., J.Org.Chem., 38 (1973), 80.

30. Tsuiji, J. and Suzuki, H., Chem.Lett., 1083, (1977).

31. Hui, B.C. and James, B.R., Inorg.Nucl.Chem.Lett., 6 (1970), 367.

32. Louie, J., M.Sc. Thesis, British Columbia University, Canada.

33. Candlin, J.P. and Oldhom, A.R., Discuss.Faraday Soc., 46 (1968), 60.

34. Jardine, F.H., Osborn, J.A. and Wilkinson, G., J.Chem.Soc.A. (1967), 1574.

35. Conner, C. and Wilkinson, G., J.Chem.Soc.A., (1968), 2665.

36. Dewhurst, K.C., U.S. Patent, 3,454,644, Chem.Abstr., 71 (1969), 91647.

37. Tsuji, J. and Suzuki, H., Chem.Lett., (1977), 1085.

38. Knifton, J.F., J.Org.Chem., 40 (1975), 579; 41 (1976), 1200.

39. Knifton, J.F., Tetrahedron Lett., (1975), 2163.

40. Fahey, D.R., in 'Catalysis in Organic Synthesis' Ed. by Rylander and Greenfield, H., Academic Press, (1976), p.287.

41. Strohmeier, W. and Kaiser, A., J.Organometal.Chem., 114 (1976), 273.

42. Lyons, J.E., J.Chem.Soc., Chem.Commun., (1975), 412.

43. Morand, P. and Kayser, M., J.Chem.Soc., Chem.Commun. (1976), 314.

44. Toth, Z., Joo, F. and Beck, M.T., Inorg.Chim.Acta., 42 (1980), 153.

45. Bradley, J.S., J.Am.Chem.Soc., 101 (1979), 7419.

46. Refs. 221 and 222 cited in "Homogeneous hydrogenation" by James, B.R., John-Wiley (1973), p.86-87.

47. James, B.R. and Wang, K.W., in "Fundamental Research in Homogeneous Catalysis", Vol.2, Ed. by Ishii, Y. and Tsutsui, M., Plenum Press, N.Y. (1978) p.35.

48. Halpern, J., Harrod, J.F. and James, B.R., J.Am.Chem.Soc., 88 (1966), 5150.

49. Norton, J., Valentine, D. and Collman, J.P., J.Am.Chem.Soc., 91 (1969), 7537.

50. Legzdins, P., Mitchell, R.W., Rempel, G.L., Ruddick, J.D. and Wilkinson, G., J.Chem.Soc.A, (1970), 3322.

51. Legzdins, P., Rempel, G.L. and Wilkinson, G., J.Chem.Soc., Chem.Commun., (1969), 825.

52. L'Eplattenier, F., Matthys, P. and Calderazzo, F., Inorg.Chem., 9 (1970), 342.

53. Stephenson, T.A. and Wilkinson, G., J.Inorg.Nucl.Chem., 28 (1966), 945.

54. Cook, M.W., Hanson, D.N. and Alder, B.J., J.Chem.Phys.,26 (1957), 748.

55. Solubility of Inorganic and Organic Compounds, Vol.I, Table 1712, Ed. Stephen, H. and Stephen, T.

56. Prausnitz, J.M. and Shair, F.H., A.I.Ch.E.J., (1961), 682.

57. Jardine, F.H. and Wilkinson, G., J.Chem.Soc., C (1967), 270.

58. Bennett, M.A. and Longstaff, P.A., Chem. and Ind., (1965), 846.

59. Prince, R.H. and Raspin, K.A., J.Chem.Soc. A., (1969), 612.

60. Hoffman, P.R. and Caulton, K.G., J.Am.Chem.Soc., 97 (1975), 4221.

61. James, B.R. and Markham, L.D., Inorg.Chem., 13 (1974), 97.

ACKNOWLEDGEMENT

I wish to record my deep sense of gratitude to Dr. D.N. Sen, Scientist, National Chemical Laboratory, for his inspiring guidance. I am grateful to Dr. R.V. Chaudhari for his inspiring guidance during the work on kinetics of homogeneously catalyzed reactions.

My sincere thanks are due to Drs. C.I. Jose and P.S. Kulkarni for useful discussions on spectral data. I acknowledge with gratitude the liberal help I received from Dr.U.N. Kantak.

I am also thankful to the staff of the Microanalytical section and other sections for microanalysis, recording of IR, NMR and mass spectra. Thanks are also due to my other colleagues working in the area "Coordination and Organometallic Compounds" for their generous cooperation.

I wish to record my sincere thanks to Mr. T. Koshy for typing the thesis and to the library staff for their help.

I especially thank the Director, National Chemical Laboratory, Poona, for giving me permission to submit this thesis and to the Council of Scientific and Industrial Research, New Delhi, for the award of a research fellowship.

[S.R. PATIL]

N.C.L.
Poona-8